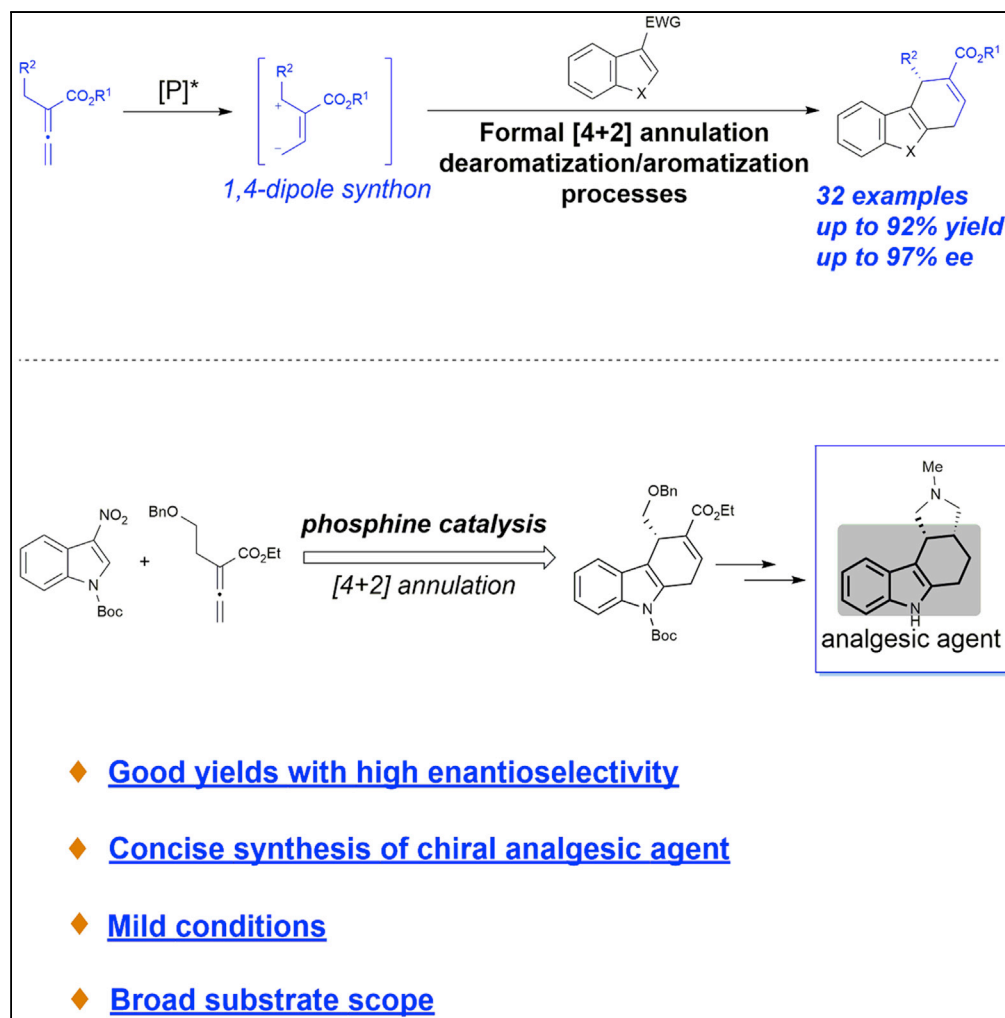


## Article

## Enantioselective [4+2] Annulation to the Concise Synthesis of Chiral Dihydrocarbazoles



Haiyang Wang,  
Qingdong Hu,  
Mingxu Wang,  
Chang Guo

guochang@ustc.edu.cn

**HIGHLIGHTS**

High regio-, chemo-, and enantioselectivity

Broad substrate scope

Dearomatization/  
aromatization steps  
proceed under mild  
conditions

Concise synthesis of chiral  
analgesic agent

Wang et al., iScience 23,  
100840  
February 21, 2020 © 2020 The  
Author(s).  
<https://doi.org/10.1016/j.isci.2020.100840>



## Article

# Enantioselective [4+2] Annulation to the Concise Synthesis of Chiral Dihydrocarbazoles

Haiyang Wang,<sup>1</sup> Qingdong Hu,<sup>1</sup> Mingxu Wang,<sup>1</sup> and Chang Guo<sup>1,2,\*</sup>

## SUMMARY

A highly efficient phosphine-catalyzed enantioselective [4 + 2] annulation of allenotes with 3-nitroindoles or 3-nitrobenzothiophenes has been developed. The protocol represents a unique dearomatization-aromatization process to access functionalized dihydrocarbazoles or dihydronaphthalenethiophenes with high optical purity (up to 97% ee) under mild reaction conditions. The synthetic utility of the highly enantioselective [4 + 2] annulation enables a concise synthesis of analgesic agent.

## INTRODUCTION

Fused polycyclic indoles are common structural motifs found in a vast array of natural and biologically active molecules (Saxton, 1996; Knölker and Reddy, 2002; Schmidt et al., 2012; Tan and Cheng, 2019), such as kopsihainanine A, isoelliptixin, and analgesic agents (Scheme 1A) (Madalengoitia and Macdonald, 1993; Carmosin et al., 2000; Chen et al., 2011). In this regard, the development of efficient methods for enantioselective construction of hydrocarbazole skeleton is still highly demanded (Sings et al., 2001; Lu et al., 2012; Zhou et al., 2015; Gu et al., 2016). The group of Jørgensen disclosed a novel [4 + 2] annulation by trienamine catalysis, thus obtaining dihydrocarbazoles in good yields and enantioselectivities (Li et al., 2016b). In this context, we hypothesized that the development of new methods through the enantioselective phosphine-catalyzed [4 + 2] dearomatization would provide practical and efficient approach to this class of enantioenriched heterocycles (Scheme 1B).

Phosphine catalysis has been recognized as a reliable tool for the development of unique transformations of allenotes, allowing for the discovery of novel asymmetric synthetic methodology (Lu et al., 2001; Methot and Roush, 2004; Ye et al., 2008; Cowen and Miller, 2009; Wei and Shi, 2010, 2017; Fan and Kwon, 2013; Wang et al., 2014, 2016; López and Mascareñas, 2014; Xie and Huang, 2015; Li and Zhang, 2016a; Li and Lu, 2017; Ni et al., 2018; Guo et al., 2018). Considerable research efforts have been devoted to the development of new methods for the phosphine-catalyzed enantioselective reactions. The use of phosphine catalysts has introduced a set of elementary steps that operate via discrete reactive species, allowing access to natural products and pharmaceuticals (Tran and Kwon, 2005; Andrews and Kwon, 2012; Han et al., 2012; Wang and Krische, 2003; Cai et al., 2016). One particularly versatile and reactive species is the phosphine-mediated 1,4-dipole generated upon addition of the phosphine catalyst to an allenote substrate, thus providing a concise approach for accessing enantioselective annulations. Specially, Kwon group reported the result of their pioneering studies toward the development of a novel [4 + 2] annulation reaction of allenotes and N-tosylimines in the presence of phosphine catalyst (Zhu et al., 2003). Later, Fu group reported the phosphine-catalyzed highly enantioselective [4 + 2] annulation of N-tosylimines with allenotes (Wurz and Fu, 2005). Although great achievements have been made, concise syntheses of useful heterocycles involving phosphine-catalyzed [4 + 2] annulations in asymmetric versions were still rare (Tran and Kwon, 2007; Wang and Ye, 2010; Tran et al., 2011; Xiao et al., 2011; Baskar et al., 2011; Yu and Ma, 2012; Zhong et al., 2012; Takizawa et al., 2014; Yu et al., 2014; Liu et al., 2016; Wang and Guo, 2019a). Moreover, the development of an enantioselective phosphine-catalyzed [4 + 2] dearomatization reaction would provide an attractive and complementary approach for construction of privileged motifs, which will be of great value for the synthesis of bioactive molecules (Scheme 1C).

Enantioselective dearomatization reactions of heteroaromatic compounds are very powerful transformations because they provide direct access to a wide variety of chiral heterocycles (You, 2016; Roche and Porco, 2011; Zhuo et al., 2012; Zhuo et al., 2014; Zheng and You, 2016; Sun et al., 2016; Wu et al., 2016). In recent years, 3-nitroindole was demonstrated to be a good substrate for various dearomatization

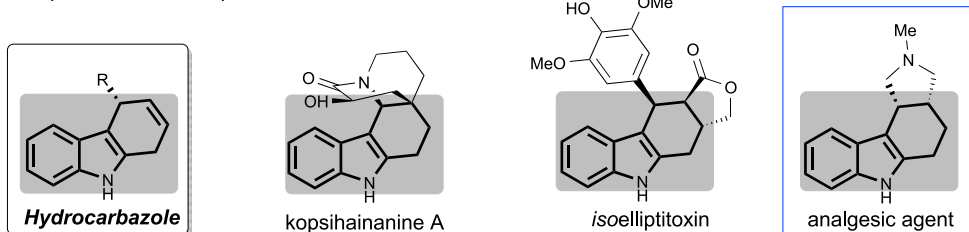
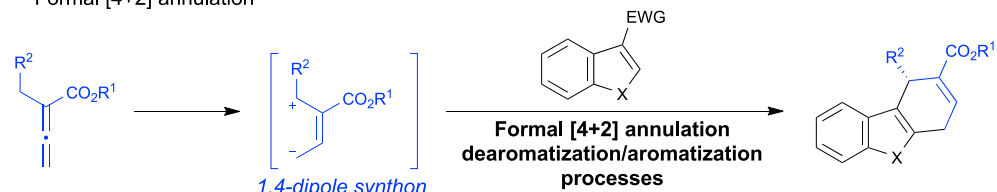
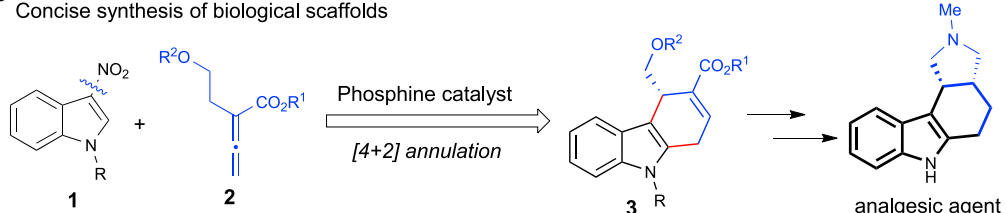
<sup>1</sup>Hefei National Laboratory for Physical Sciences at the Microscale, University of Science and Technology of China, Hefei 230026, China

<sup>2</sup>Lead Contact

\*Correspondence:  
guochang@ustc.edu.cn

<https://doi.org/10.1016/j.isci.2020.100840>



**A** Representative examples**B** Formal [4+2] annulation**C** Concise synthesis of biological scaffolds

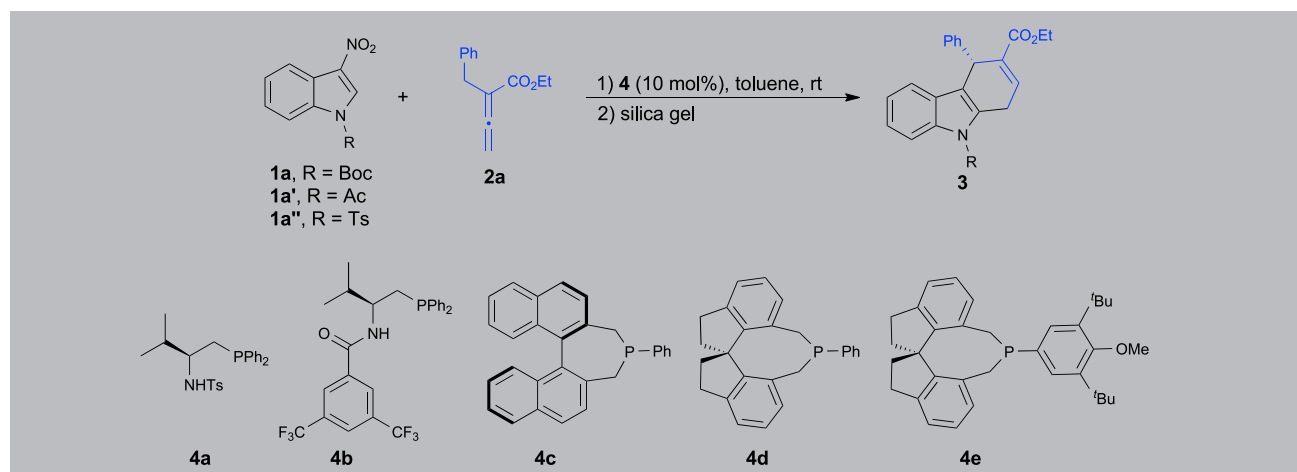
**Scheme 1. Phosphine-catalyzed [4 + 2] Dearomatization/Aromatization Reactions for the Formation of Enantioenriched Heterocycles**

- (A) Representative examples of chiral hydrocarbazole derivatives.  
 (B) Formal [4 + 2] annulation for the preparation of hydrocarbazole.  
 (C) Concise approach to the enantioselective synthesis of analgesic agent.

processes, and a number of enantioselective approaches have been reported (Awata and Arai, 2014; Zhao et al., 2015a, 2015b, 2018, 2019; Gerten and Stanley, 2016; Trost et al., 2014; Cheng et al., 2018; Zhang et al., 2018; Sun et al., 2018; Yue et al., 2017; Yang et al., 2019). Importantly, Lu group (Li et al., 2019) and Zhang group (Wang et al., 2019b) independently reported the efficient phosphine-catalyzed enantioselective [3 + 2] annulation of 3-nitroindoles with allenoates to afford cyclopentenindoline products in high yields and excellent enantioselectivities. We envisaged that heteroaromatic systems bearing an electron-withdrawing group could react with phosphine-mediated zwitterionic intermediate in a process involving the [4 + 2] reaction to achieve the chiral dihydrocarbazole scaffold (Scheme 1C). With this objective in mind, a readily available 3-nitroindole derivative was selected as a model substrate to investigate the optimum reaction condition for the enantioselective [4 + 2] dearomatization reaction using a phosphine catalyst.

## RESULTS AND DISCUSSION

Based on our previous work on phosphine chemistry (Wang and Guo, 2019a), we initiated the study by investigating the reaction between **1a** and **2a** in the presence of the phosphine **4a** (Table 1, entry 1). Initially, diverse chiral phosphine catalysts were examined (entries 1–5). However, the catalyst **4a** to **4c** did not work for this reaction (entries 1–3). To our great delight, the desired dihydrocarbozole **3a** could be obtained when the chiral phosphine **4d** was employed (entry 4). After surveying an array of additives, we determined that silica gel can promote elimination of  $\text{HNO}_2$  for the aromatization process to afford the corresponding adduct in 92% yield with 94% ee (entry 4) (So and Mattson, 2012; Long et al., 2016). Other additives, such as  $\text{Sc}(\text{OTf})_3$ ,  $\text{Et}_3\text{N}$ , and  $\text{SnCl}_2$  led to byproducts (for further details, see Table S1 in the *Supplemental Information*). Furthermore, the ee values of the **3a** decreased to 80% with low yield in the presence of **4e** as catalyst (entry 5). Varying the solvents led to no improvement in the reaction, and toluene was proven to be the best choice (entries 4 vs 6–8). Further optimization studies revealed that the protection group of the 3-nitroindole was also sensitive to the reaction, and the variation of the N-substituent of the 3-nitroindole **1a'** or **1a''** generated no product at all (entries 9 and 10) (Rivinoja et al., 2017; Suo et al., 2018).



Entry	1	4	Solvent	Yield (%) <sup>a</sup>	ee (%) <sup>b</sup>
1	1a	4a	Toluene	nr	—
2	1a	4b	Toluene	nr	—
3	1a	4c	Toluene	nr	—
4	1a	4d	Toluene	92	94
5	1a	4e	Toluene	26	80
6	1a	4d	CH <sub>2</sub> Cl <sub>2</sub>	23	73
7	1a	4d	THF	73	84
8	1a	4d	Dioxane	57	90
9	1a'	4d	Toluene	nr	—
10	1a''	4d	Toluene	nr	—

**Table 1. Optimization of Reaction Conditions**

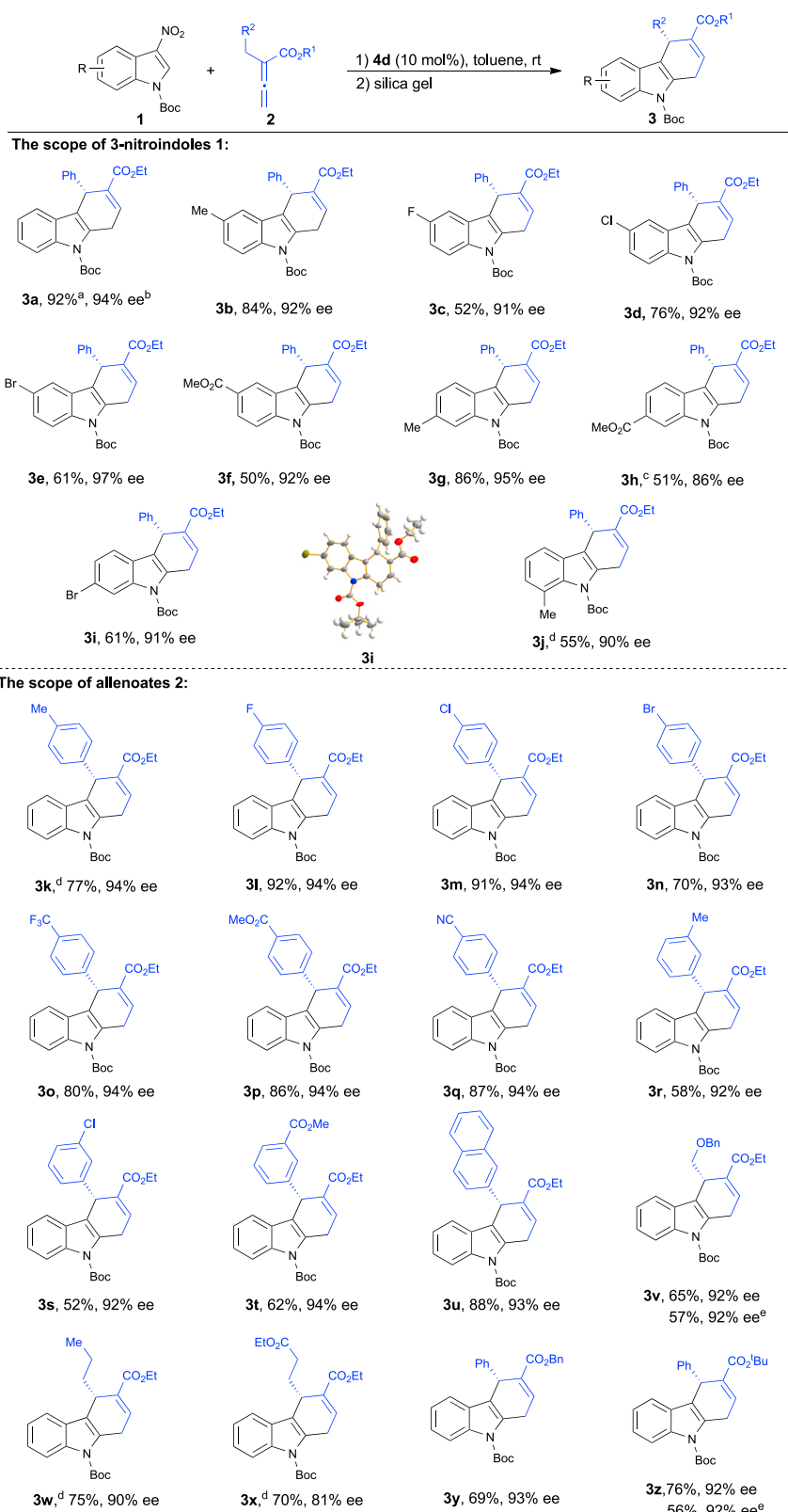
Unless indicated otherwise, the reaction were conducted with 1 (0.1 mmol), 2a (0.15 mmol), and 4 (0.01 mmol) in toluene (1.0 mL) at room temperature for 18 h. Then silica gel (200 mg) was added to the reaction mixture to complete elimination of HNO<sub>2</sub>. nr = no reaction.

<sup>a</sup>Yield of isolated product.

<sup>b</sup>Determined by HPLC analysis.

With the optimal reaction conditions in hand, we set out to explore the substrate scope of the procedure. As shown in **Scheme 2**, various electron-withdrawing or donating groups on the indole ring were well tolerated and resulted in excellent levels of enantioselectivities ranging from 86% to 97% ee (**3a–3j**). The extension of the protocol to the 3-nitroindole with a variety of substitution patterns at the 5-position was successful to afford corresponding adducts with excellent enantioselectivities (**3b–3f**). To our delight, substrates bearing substituents on different positions of the indole ring also facilitate the annulation with high yields and ee values (**3b**, **3g**, and **3j**). The absolute configuration of the enantiopure **3i**, recrystallized from ethyl acetate and petroleum ether, was assigned by single-crystal X-ray diffraction analysis.

The generality of the reaction with respect to the scope of the allenoates **2** was also investigated using 3-nitroindole **1a** as the reaction partner under the optimized conditions. A diverse array of allenoates (**2**) with a variety of functional groups (methyl, fluoro, chloro, bromo, ester, trifluoromethyl, and cyano) performed well in this annulation reaction, and the corresponding products were isolated in good yields with high ee values (**3k–3q**). Remarkably, this method was compatible with alkyl allenoate, affording the desired products in good yields with good enantioselectivity (**3v–3x**). Additionally, all reactions with different esters attached to the allenoates proceeded smoothly, giving the corresponding products in good yields and excellent ee (**3y** and **3z**). To test the synthetic utility of the current annulation, we performed the reaction on a 1 mmol scale with the formation of **3z** in 56% yield and 92% ee.



**Scheme 2. Substrate Scope of Enantioselective [4 + 2] Annulation**

Unless indicated otherwise, the reactions were conducted with **1** (0.1 mmol), **2** (0.15 mmol), and catalyst **4d** (0.01 mmol) in toluene at room temperature for 12–48 h. Then silica gel was added to the reaction mixture to complete elimination of  $\text{HNO}_2$ .

<sup>a</sup>Yield of the isolated product after purification by chromatography on silica gel.

<sup>b</sup>Enantiomeric excess determined by HPLC analysis.

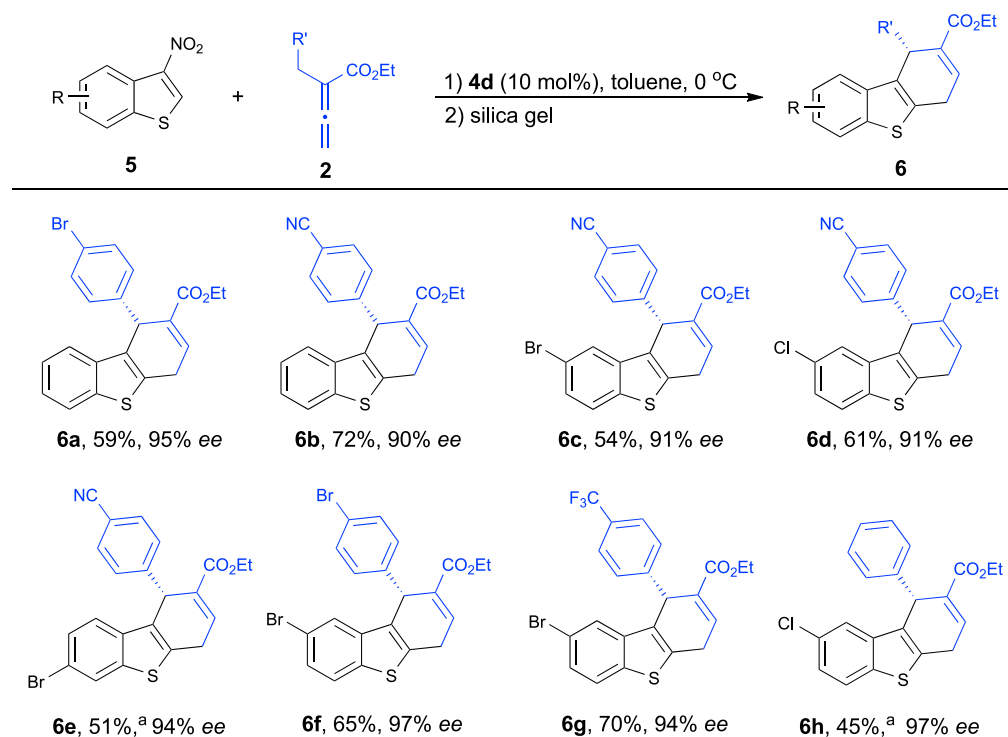
<sup>c</sup>Aromatization process was performed at 50°C.

<sup>d</sup>20 mol% of **4d**.

<sup>e</sup>The reaction was performed on 1 mmol scale.

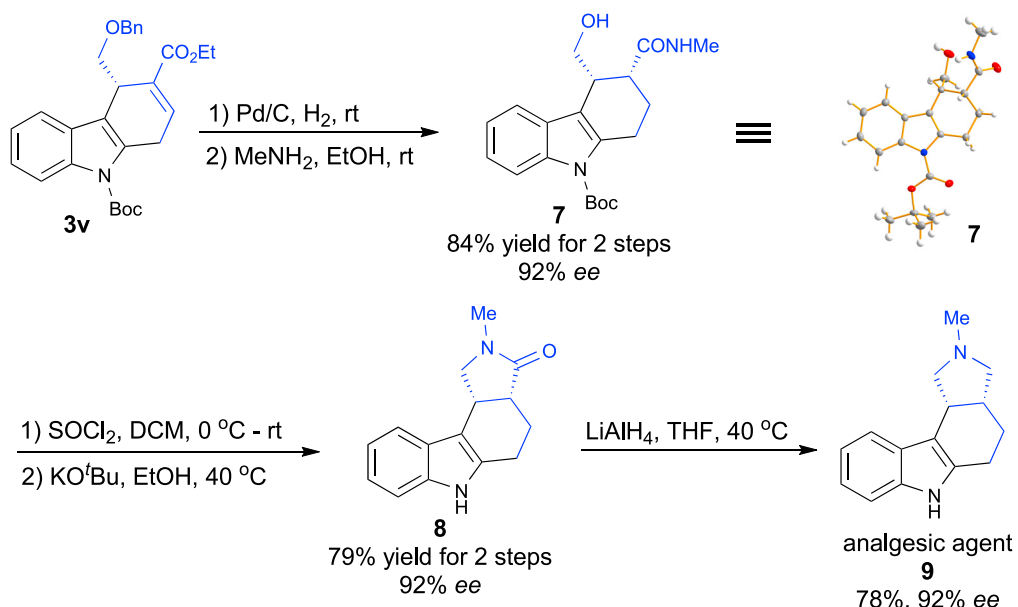
Encouraged by the excellent results with various 3-nitroindoles, we then investigated the [4 + 2] annulation reaction with a range of 3-nitrobenzothiophenes (**5**). Remarkably, process where the 3-nitrobenzothiophene as a reactive partner for asymmetric annulation has been much less studied (Tran and Kwon, 2007; Wang and Ye, 2010; Tran et al., 2011; Xiao et al., 2011; Baskar et al., 2011; Yu and Ma, 2012; Zhong et al., 2012; Takizawa et al., 2014; Yu et al., 2014; Liu et al., 2016; Wang and Guo, 2019a; Cheng et al., 2000; Cheng et al., 2017; Suo et al., 2018; Yue et al., 2018; Chen et al., 2019). Using phosphine **4d** in toluene at 0°C, we were able to access dihydron dibenzothiophene products **6** (Scheme 3). Under the optimized reaction condition (for further details, see Table S2 in the Supplemental Information), a broad range of allenotes **2** and 3-nitrobenzothiophenes **5** were investigated. Allenotes with different substituents on the aromatic ring underwent this catalytic transformation smoothly in good yields with excellent ee (**6a** and **6b**). Furthermore, various substitutions of 3-nitrobenzothiophenes **5** at the aromatic ring had little impact on the reactions (**6c–h**, 91%–97% ee).

To highlight the synthetic potential of the present method, the dihydrocabazole **3v**, which was obtained from the enantioselective [4 + 2] annulation, can be easily converted into analgesic agent **9** (Scheme 4). In 2000, Carmosin and co-workers obtained the racemic analgesic agent **9** via the Diels-Alder reaction,

**Scheme 3. Enantioselective [4 + 2] Annulation of 3-Nitrobenzothiophene 5**

Unless indicated otherwise, the reactions were conducted with **5** (0.1 mmol), **2** (0.15 mmol), and catalyst **4d** (0.01 mmol) in toluene (1.0 mL) at 0°C for 48–60 h. Then silica gel was added to the reaction mixture to complete elimination of  $\text{HNO}_2$ . Yield of the isolated product after purification by chromatography on silica gel. Enantiomeric excess determined by HPLC analysis.

<sup>a</sup>0.02 mmol of **4d** was used.



**Scheme 4. Enantioselective Synthesis of Analgesic Agent 9**

and the optical product was obtained by using preparative chromatography (Carmosin et al., 2000). Taking advantage of our current phosphine-catalyzed enantioselective [4 + 2] reaction, we can easily obtain the analgesic agent **9** with excellent enantioselectivity. Hydrogenation of **3v** in the presence of a catalytic amount of Pd/C, followed by amidation with MeNH<sub>2</sub> gave rise to the desired amide **7** in 84% yield over two steps. The configuration of compound **7** was assigned by X-ray analysis. The subsequent chlorination of alcohol, deprotection of the N-Boc group and cyclization furnished **8** in good yield. Finally, the amide **8** was reduced to generate the corresponding analgesic agent **9** in 78% yield and 92% ee.

The proposed catalytic cycle for the enantioselective [4 + 2] annulation is illustrated in Figure 1. The addition of phosphine catalyst **4d** to the allenolate **2** gives the intermediate **A**, which could react with the 3-nitroindole **1** or 3-nitrobenzothiophenes **5** to form the intermediate **B**. Following migration and intramolecular conjugate addition give rise to the intermediate **D** and regenerate the phosphine **4d**. This species **D** then undergoes elimination of HNO<sub>2</sub> through the aromatization process to furnish the final dihydrocarbozole **3** or dihydronitrobenzothiophene **6**.

In summary, we have developed simple and efficient synthetic routes to highly enriched hydrocarbozoles through chiral phosphine-catalyzed [4 + 2] annulation utilizing 3-nitroindole and allenotes as starting materials. This phosphine-catalyzed enantioselective [4 + 2] annulation procedure involving tandem dearomatization and aromatization steps proceeds under mild conditions. This reaction displays a broad substrate scope with respect to the substituents. Additionally, the obtained dihydrocarbozole could be efficiently transformed to an analgesic agent containing polycyclic indole frameworks.

### Limitations of the Study

The synthesis of the products needs two steps in one pot. No product was formed with the initial addition of silica gel.

### METHODS

All methods can be found in the accompanying *Transparent Methods supplemental file*.

### DATA AND CODE AVAILABILITY

Crystallographic data for the structures reported in this article have been deposited at the Cambridge Crystallographic Data Center (CCDC) under accession numbers CCDC 1938371 (**3i**) and CCDC 1955757 (**7**). Copies of the data can be obtained free of charge from [www.ccdc.cam.ac.uk/structures/](http://www.ccdc.cam.ac.uk/structures/).

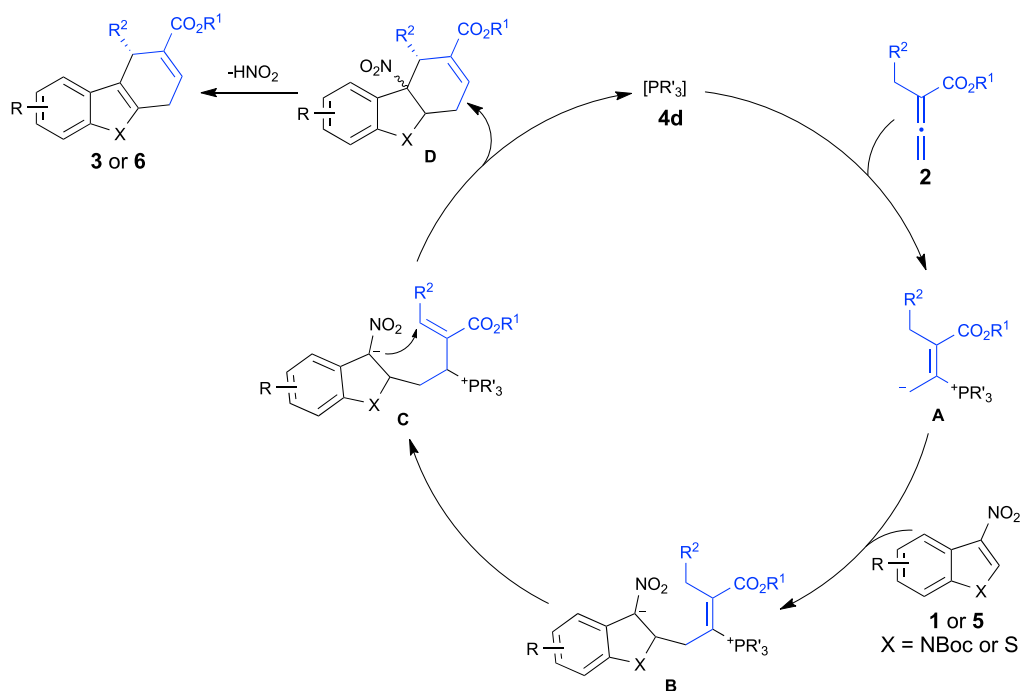


**Figure 1. Proposed Mechanism**

## SUPPLEMENTAL INFORMATION

Supplemental Information can be found online at <https://doi.org/10.1016/j.isci.2020.100840>.

## ACKNOWLEDGMENTS

The authors acknowledge financial support from the National Natural Science Foundation of China (grant no. 21702198), the Anhui Provincial Natural Science Foundation (grant no. 1808085MB30), "1000-Youth Talents Plan," and the Fundamental Research Funds for the Central Universities (WK2340000090).

## AUTHOR CONTRIBUTIONS

H.W. carried out the experimental and data analysis work. Q.H. and M.W. prepared some starting materials. C.G. designed the reaction and directed the project. The paper was written by C.G. with assistance of H.W., Q.H., and M.W.

## DECLARATION OF INTERESTS

The authors declare no conflict of interest.

Received: November 14, 2019

Revised: December 31, 2019

Accepted: January 9, 2020

Published: February 21, 2020

## REFERENCES

- Andrews, I.P., and Kwon, O. (2012). Enantioselective total synthesis of (+)-ibophyllidine via an asymmetric phosphine-catalyzed [3 + 2] annulation. *Chem. Sci.* 3, 2510–2514.
- Awata, A., and Arai, T. (2014). Pyridine/Copper catalyst: asymmetric exo'-selective [3+2] cycloaddition using imino ester and electrophilic indole. *Angew. Chem. Int. Ed.* 53, 10462–10465.
- Baskar, B., Dakas, P.-Y., and Kumar, K. (2011). Natural product biosynthesis inspired concise and stereoselective synthesis of benzopyrones and related scaffolds. *Org. Lett.* 13, 1988–1991.
- Cai, L., Zhang, K., and Kwon, O. (2016). Catalytic asymmetric total synthesis of (–)-actinophylllic acid. *J. Am. Chem. Soc.* 138, 3298–3301.
- Carmosin, R.J., Carson, J.R., and Pitis, P.M.. (2000). Octahydropyrrolo-[3,4-C]-carbazoles useful as analgesic agents. US Patent No. 6063803.

- Chen, J., Chen, J.-J., Yao, X., and Gao, K. (2011). Kopsihainanines A and B, two unusual alkaloids from kopsihainanensis. *Org. Biomol. Chem.* 9, 5334–5336.
- Chen, X.-M., Lei, C.-W., Yue, D.-F., Zhao, J.-Q., Wang, Z.-H., Zhang, X.-M., Xu, X.-Y., and Yuan, W.-C. (2019). Organocatalytic asymmetric dearomatization of 3-nitroindoles and 3-nitrobenzothiophenes via thiol-triggered diastereo- and enantioselective double Michael addition reaction. *Org. Lett.* 21, 5452–5456.
- Cheng, Q., Zhang, F., Cai, Y., Guo, Y.-L., and You, S.-L. (2018). Stereodivergent synthesis of tetrahydrofuroindoles through Pd-catalyzed asymmetric dearomatic formal [3+2] cycloaddition. *Angew. Chem. Int. Ed.* 57, 2134–2138.
- Cheng, Q., Zhang, H.-J., Yue, W.-J., and You, S.-L. (2000). One pot preparation of bicyclopentenones from propargylmalonates (and propargylsulfonamides) and allylic acetates by a tandem action of catalysts. *J. Am. Chem. Soc.* 122, 10220–10221.
- Cheng, Q., Zhang, H.-J., Yue, W.-J., and You, S.-L. (2017). Palladium-catalyzed highly stereoselective dearomatic [3 + 2] cycloaddition of nitrobenzofurans. *Chem.* 3, 428–436.
- Cowen, B.J., and Miller, S.J. (2009). Enantioselective catalysis and complexity generation from allenotes. *Chem. Soc. Rev.* 38, 3102–3116.
- Fan, Y.C., and Kwon, O. (2013). Advances in nucleophilic phosphine catalysis of alkenes, allenes, alkynes, and MBHADs. *Chem. Commun. (Camb.)* 49, 11588–11619.
- Gerten, A.L., and Stanley, L.M. (2016). Enantioselective dearomatic [3 + 2] cycloadditions of indoles with azomethineylides derived from alanine imino esters. *Org. Chem. Front.* 3, 339–343.
- Gu, B.-Q., Zhang, H., Su, R.-H., and Deng, W.-P. (2016). Organocatalytic asymmetric synthesis of dihydrocarbazoles via a formal [4+2] cycloaddition of in situ generated o-quinodimethanes with enals. *Tetrahedron* 72, 6595–6602.
- Guo, H., Fan, Y.C., Sun, Z., Wu, Y., and Kwon, O. (2018). Phosphine organocatalysis. *Chem. Rev.* 118, 10049–10293.
- Han, X., Zhong, F., Wang, Y., and Lu, Y. (2012). Versatile enantioselective [3+2] cyclization between imines and allenotes catalyzed by dipeptide-based phosphines. *Angew. Chem. Int. Ed.* 51, 767–770.
- Knölker, H.-J., and Reddy, K.R. (2002). Isolation and synthesis of biologically active carbazole alkaloids. *Chem. Rev.* 102, 4303–4427.
- Li, H., and Lu, Y. (2017). Enantioselective construction of all-carbon quaternary stereogenic centers by using phosphine catalysis. *Asian J. Org. Chem.* 6, 1130–1145.
- Li, K., Gonçalves, T.P., Huang, K.-W., and Lu, Y. (2019). Dearomatization of 3-nitroindoles by a phosphine-catalyzed enantioselective [3+2] annulation reaction. *Angew. Chem. Int. Ed.* 58, 5427–5431.
- Li, W., and Zhang, J. (2016a). Recent developments in the synthesis and utilization of chiral β-aminophosphine derivatives as catalysts or ligands. *Chem. Soc. Rev.* 45, 1657–1677.
- Li, Y., Tur, F., Nielsen, R.P., Jiang, H., Jensen, F., and Jørgensen, K.A. (2016b). Enantioselective formal [4+2] cycloadditions to 3-nitroindoles by trienamine catalysis: synthesis of chiral dihydrocarbazoles. *Angew. Chem. Int. Ed.* 55, 1020–1024.
- Liu, H., Liu, Y., Yuan, C., Wang, G.-P., Zhu, S.-F., Wu, Y., Wang, B., Sun, Z., Xiao, Y., Zhou, Q.-L., and Guo, H. (2016). Enantioselective synthesis of spirobarbiturate-cyclohexenes through phosphine-catalyzed asymmetric [4 + 2] annulation of barbiturate-derived alkenes with allenotes. *Org. Lett.* 18, 1302–1305.
- Long, L., Sun, W., Yang, D., Li, G., and Wang, R. (2016). Additive effects on asymmetric catalysis. *Chem. Rev.* 116, 4006–4123.
- López, F., and Mascareñas, J.L. (2014). [4+2] and [4+3] catalytic cycloadditions of allenes. *Chem. Soc. Rev.* 43, 2904–2915.
- Lu, L.-Q., Chen, J.-R., and Xiao, W.-J. (2012). Development of cascade reactions for the concise construction of diverse heterocyclic architectures. *Acc. Chem. Res.* 45, 1278–1293.
- Lu, X., Zhang, C., and Xu, Z. (2001). Reactions of electron-deficient alkynes and allenes under phosphine catalysis. *Acc. Chem. Res.* 34, 535–544.
- Madalengoitia, J.S., and Macdonald, T.L. (1993). Synthesis of tetrahydrofurocarbazolones via intramolecular Diels-Alder reactions. *Tetrahedron Lett.* 34, 6237–6240.
- Methot, J.L., and Roush, W.R. (2004). Nucleophilic phosphine organocatalysis. *Adv. Synth. Catal.* 346, 1035–1050.
- Ni, H., Chan, W.-L., and Lu, Y. (2018). Phosphine-catalyzed asymmetric organic reactions. *Chem. Rev.* 118, 9344–9411.
- Rivinoja, D.J., Gee, Y.S., Gardiner, M.G., Ryan, J.H., and Hyland, C.J.T. (2017). Thediastereoselective synthesis of pyrroloindolines by Pd-catalyzed dearomatic cycloaddition of 1-tosyl-2-vinylaziridine to 3-nitroindoles. *ACS Catal.* 7, 1053–1056.
- Roche, S.P., and Porco, J.A., Jr. (2011). Dearomatization strategies in the synthesis of complex natural products. *Angew. Chem. Int. Ed.* 50, 4068–4093.
- Saxton, J.E. (1996). Recent progress in the chemistry of the monoterpenoidindole alkaloids. Recent progress in the chemistry of the monoterpenoidindole alkaloids. *Nat. Prod. Rep.* 14, 559–590.
- Schmidt, A.W., Reddy, K.R., and Knölker, H.-J. (2012). Occurrence, biogenesis, and synthesis of biologically active carbazole alkaloids. *Chem. Rev.* 112, 3193–3328.
- Sings, H.L., Harris, G.H., and Dombrowski, A.W. (2001). Dihydrocarbazole alkaloids from aspergillustubingensis. *J. Nat. Prod.* 64, 836–838.
- So, S.S., and Mattson, A.E. (2012). Urea activation of α-nitrodiaoesters: an organocatalytic approach to N–H insertion reactions. *J. Am. Chem. Soc.* 134, 8798–8801.
- Sun, M., Zhu, Z.-Q., Gu, L., Wan, X., Mei, G.-J., and Shi, F. (2018). Catalytic asymmetric dearomatic [3 + 2] cycloaddition of electron-deficient indoles with all-carbon 1,3-dipoles. *J. Org. Chem.* 83, 2341–2348.
- Sun, W., Li, G., Hong, L., and Wang, R. (2016). Asymmetric dearomatization of phenols. *Org. Biomol. Chem.* 14, 2164–2176.
- Suo, J.-J., Liu, W., Du, J., Ding, C.-H., and Hou, X.-L. (2018). Diastereo- and enantioselective Palladium-catalyzed dearomatic [3+2] cycloaddition of 3-nitroindoles. *Chem. Asian J.* 13, 959–963.
- Takizawa, S., Arteaga, F.A., Yoshida, Y., Suzuki, M., and Sasai, H. (2014). Enantioselective organocatalyzed formal [4+2] cycloaddition of ketimines with allenotes: easy access to a tetrahydropyridine framework with a chiral tetrasubstituted stereogenic carbon center. *Asian J. Org. Chem.* 3, 412–415.
- Tan, F., and Cheng, H.-G. (2019). Catalytic asymmetric synthesis of tetrahydrocarbazoles. *Chem. Commun. (Camb.)* 55, 6151–6164.
- Tran, Y.S., and Kwon, O. (2005). An application of the phosphine-catalyzed [4 + 2] annulation in indole alkaloid synthesis: formal syntheses of (±)-alstonerine and (±)-macroline. *Org. Lett.* 7, 4289–4291.
- Tran, Y.S., and Kwon, O. (2007). Phosphine-catalyzed [4 + 2] annulation: synthesis of cyclohexenes. *J. Am. Chem. Soc.* 129, 12632–12633.
- Tran, Y.S., Martin, T.J., and Kwon, O. (2011). Phosphine-catalyzed [4+2] Annulations of 2-alkylallenotes and oefins: synthesis of multisubstituted cyclohexenes. *Chem. Asian J.* 6, 2101–2106.
- Trost, B.M., Ehmke, V., O’Keefe, B.M., and Bringley, D.A. (2014). Palladium-catalyzed dearomatic trimethylenemethane cycloaddition reactions. *J. Am. Chem. Soc.* 136, 8213–8216.
- Wang, H., and Guo, C. (2019a). Enantioselective γ-addition of pyrazole and imidazole heterocycles to allenotes catalyzed by chiral phosphine. *Angew. Chem. Int. Ed.* 58, 2854–2858.
- Wang, H., Zhang, J., Tu, Y., and Zhang, J. (2019b). Phosphine-catalyzed enantioselective dearomatic [3+2] cycloaddition of 3-nitroindoles and 2-nitrobenzofurans. *Angew. Chem. Int. Ed.* 58, 5422–5426.
- Wang, J.-C., and Krische, M.J. (2003). Intramolecular organocatalytic [3+2] dipolar cycloaddition: stereospecific cycloaddition and the total synthesis of (±)-hirsutene. *Angew. Chem. Int. Ed.* 42, 5855–5857.
- Wang, T., and Ye, S. (2010). Diastereoselective synthesis of 6-trifluoromethyl-5,6-dihydropyrans via phosphine-catalyzed [4 + 2] annulation of α-benzylallenotes with ketones. *Org. Lett.* 12, 4168–4171.

- Wang, T., Han, X., Zhong, F., Yao, W., and Lu, Y. (2016). Amino acid-derived bifunctional phosphines for enantioselective transformations. *Acc. Chem. Res.* 49, 1369–1378.
- Wang, Z., Xu, X., and Kwon, O. (2014). Phosphine catalysis of allenes with electrophiles. *Chem. Soc. Rev.* 43, 2927–2940.
- Wei, Y., and Shi, M. (2010). Multifunctional chiral phosphine organocatalysts in catalytic asymmetric Morita–Baylis–Hillman and related reactions. *Acc. Chem. Res.* 43, 1005–1018.
- Wei, Y., and Shi, M. (2017). Lu's [3 + 2] cycloaddition of allenes with electrophiles: discovery, development and synthetic application. *Org. Chem. Front.* 4, 1876–1890.
- Wu, W.-T., Zhang, L., and You, S.-L. (2016). Catalytic asymmetric dearomatization (CADA) reactions of phenol and aniline derivatives. *Chem. Soc. Rev.* 45, 1570–1580.
- Wurz, R.P., and Fu, G.C. (2005). Catalytic asymmetric synthesis of piperidine derivatives through the [4 + 2] annulation of imines with allenes. *J. Am. Chem. Soc.* 127, 12234–12235.
- Xiao, H., Chai, Z., Wang, H.-F., Wang, X.-W., Cao, D.-D., Liu, W., Lu, Y.-P., Yang, Y.-Q., and Zhao, G. (2011). Bifunctional N-acyl-aminophosphine-catalyzed asymmetric [4+2] cycloadditions of allenoates and imines. *Chem. Eur. J.* 17, 10562–10565.
- Xie, P., and Huang, Y. (2015). Morita–Baylis–Hillman adduct derivatives (MBHADs): versatile reactivity in Lewis base-promoted annulation. *Org. Biomol. Chem.* 13, 8578–8595.
- Yang, X.-H., Li, J.-P., Wang, D.-C., Xie, M.-S., Qu, G.-R., and Guo, H.-M. (2019). Enantioselectivedearomatic [3+2] cycloaddition of 2-nitrobenzofurans with aldehyde-derived Morita–Baylis–Hillman carbonates. *Chem. Commun. (Camb.)* 55, 9144–9147.
- Ye, L.-W., Zhou, J., and Tang, Y. (2008). Phosphine-triggered synthesis of functionalized cyclic compounds. *Chem. Soc. Rev.* 37, 1140–1152.
- You, S.-L. (2016). Asymmetric Dearomatization Reactions (WileyVCH).
- Yu, H., Zhang, L., Li, Z., Liu, H., Wang, B., Xiao, Y., and Guo, H. (2014). Phosphine-catalyzed [4+2] cycloaddition of sulfamate-derived cyclic imines with allenoates: synthesis of sulfamate-fused tetrahydropyridines. *Tetrahedron* 70, 340–348.
- Yu, S., and Ma, S. (2012). Allenes in catalytic asymmetric synthesis and natural product syntheses. *Angew. Chem. Int. Ed.* 51, 3074–3112.
- Yue, D.-F., Zhao, J.-Q., Chen, X.-Z., Zhou, Y., Zhang, X.-M., Xu, X.-Y., and Yuan, W.-C. (2017). Multiple hydrogen-bonding bifunctional thiourea-catalyzed asymmetric dearomatic [4 + 2] annulation of 3-nitroindoles: highly enantioselective access to hydrocarbazole skeletons. *Org. Lett.* 19, 4508–4511.
- Yue, D.-F., Zhao, J.-Q., Chen, Y.-Z., Zhang, X.-M., Xu, X.-Y., and Yuan, W.-C. (2018). Zinc-catalyzed enantioselectivedearomatic [3+2] cycloaddition reaction of 3-nitrobenzothiophenes and 3-nitrothieno[2,3-b]pyridine with 3-isothiocyanato oxindoles. *Adv. Synth. Catal.* 360, 1420–1425.
- Zhang, J.-Q., Tong, F., Sun, B.-B., Fan, W.-T., Chen, J.-B., Hu, D., and Wang, X.-W. (2018). Pd-Catalyzed Asymmetric dearomative cycloaddition for construction of optically active pyrroloindoline and cyclopentaindoline derivatives: access to 3-aminopyrroloindolines. *J. Org. Chem.* 83, 2882–2891.
- Zhao, J.-Q., Wu, Z.-J., Zhou, M.-Q., Xu, X.-Y., Zhang, X.-M., and Yuan, W.-C. (2015a). Zn-catalyzed diastereo- and enantioselective cascade reaction of 3-isothiocyanato oxindoles and 3-nitroindoles: stereocontrolled syntheses of polycyclic spirooxindoles. *Org. Lett.* 17, 5020–5023.
- Zhao, J.-Q., Zhou, M.-Q., Wu, Z.-J., Wang, Z.-H., Yue, D.-F., Xu, X.-Y., Zhang, X.-M., and Yuan, W.-C. (2015b). Asymmetric michael/cyclization cascade reaction of 3-isothiocyanato oxindoles and 3-nitroindoles with amino-thiocarbamate catalysts: enantioselective synthesis of polycyclic spirooxindoles. *Org. Lett.* 17, 2238–2241.
- Zhao, J.-Q., Zhou, X.-J., Zhou, Y., Xu, X.-Y., Zhang, X.-M., and Yuan, W.-C. (2018). Diastereo- and enantioselectivedearomatic [3 + 2] cycloaddition reaction of 2-nitrobenzofurans with 3-isothiocyanato oxindoles. *Org. Lett.* 20, 909–912.
- Zhao, J.-Q., Yang, L., You, Y., Wang, Z.-H., Xie, K.-X., Zhang, X.-M., Xu, X.-Y., and Yuan, W.-C. (2019). Phosphine-catalyzed dearomatic (3 + 2) annulation of 2-nitrobenzofurans and nitrobenzothiophenes with allenoates. *Org. Biomol. Chem.* 17, 5294–5304.
- Zheng, C., and You, S.-L. (2016). Catalytic asymmetric dearomatization by transition-metal catalysis: a method for transformations of aromatic compounds. *Chem* 1, 830–857.
- Zhong, F., Han, X., Wang, Y., and Lu, Y. (2012). Highlyenantioselective [4 + 2] annulations catalyzed by amino acid-based phosphines: synthesis of functionalized cyclohexenes and 3-spirocyclohexene-2-oxindoles. *Chem. Sci.* 3, 1231–1234.
- Zhou, L., Xu, B., and Zhang, J. (2015). Metal-Free dehydrogenative Diels–Alder reactions of 2-methyl-3-alkylindoles with dienophiles: rapid access to tetrahydrocarbazoles, carbazoles, and heteroacenes. *Angew. Chem. Int. Ed.* 54, 9092–9096.
- Zhu, X.-F., Lan, J., and Kwon, O. (2003). An expedient phosphine-catalyzed [4 + 2] annulation: synthesis of highly functionalized tetrahydropyridines. *J. Am. Chem. Soc.* 125, 4716–4717.
- Zhuo, C.-X., Zhang, W., and You, S.-L. (2012). Catalytic asymmetric dearomatization reactions. *Angew. Chem. Int. Ed.* 51, 12662–12686.
- Zhuo, C.-X., Zheng, C., and You, S.-L. (2014). Transition-metal-catalyzed asymmetric allylicdearomatization reactions. *Acc. Chem. Res.* 47, 2558–2573.

**Supplemental Information**

**Enantioselective [4+2] Annulation**

**to the Concise Synthesis**

**of Chiral Dihydrocarbazoles**

**Haiyang Wang, Qingdong Hu, Mingxu Wang, and Chang Guo**

## Supplemental Figures for NMR spectra:

**Figure S1.**  $^1\text{H}$  NMR spectrum of **3a**, related to **Scheme 2**.

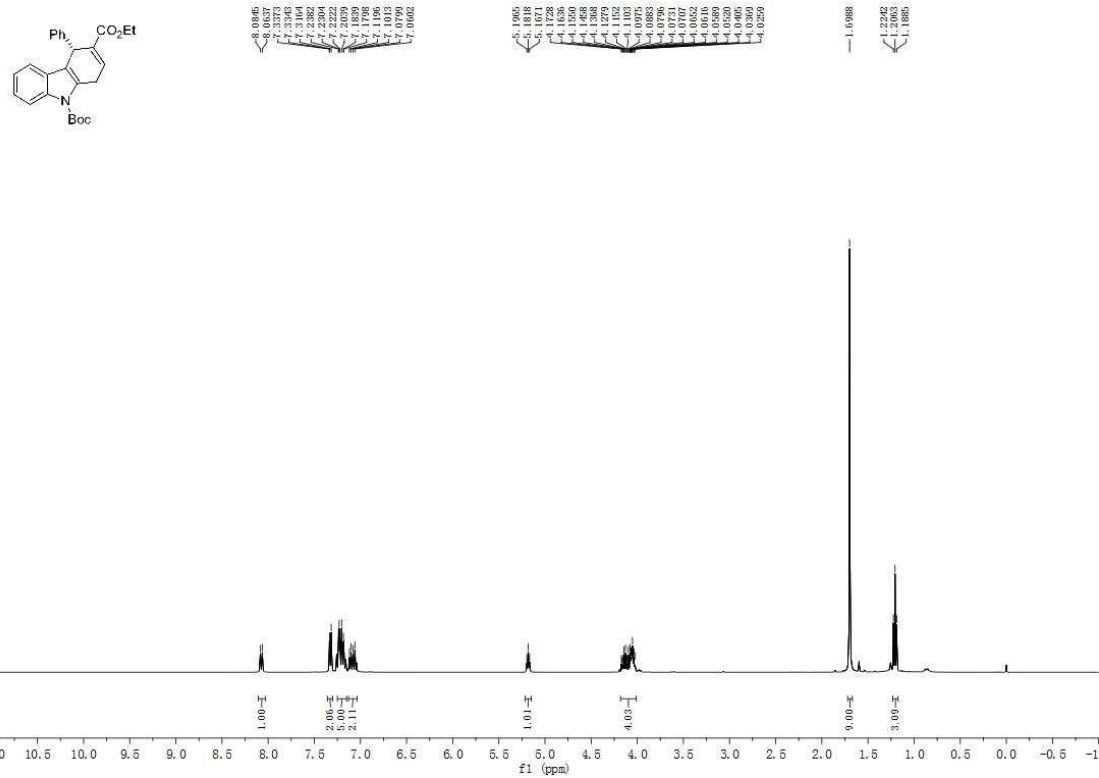


**Figure S2.**  $^{13}\text{C}$  NMR spectrum of **3a**, related to **Scheme 2**.

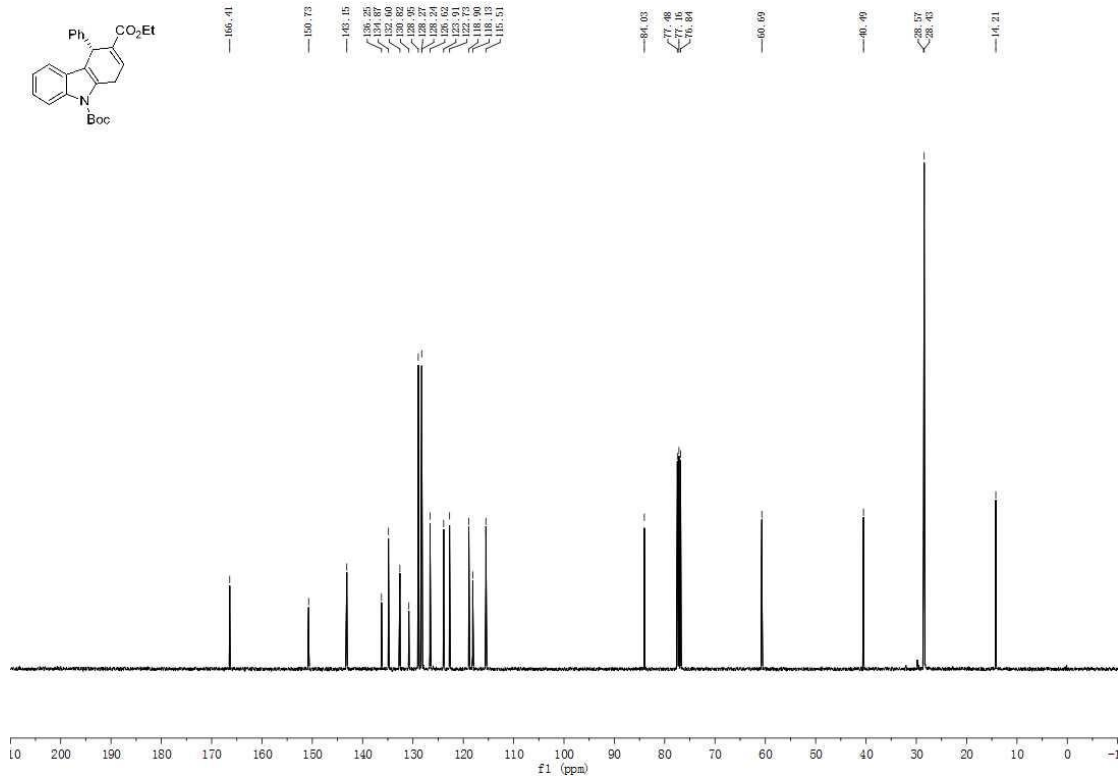


**Figure S3.**  $^1\text{H}$  NMR spectrum of **3b**, related to **Scheme 2**.

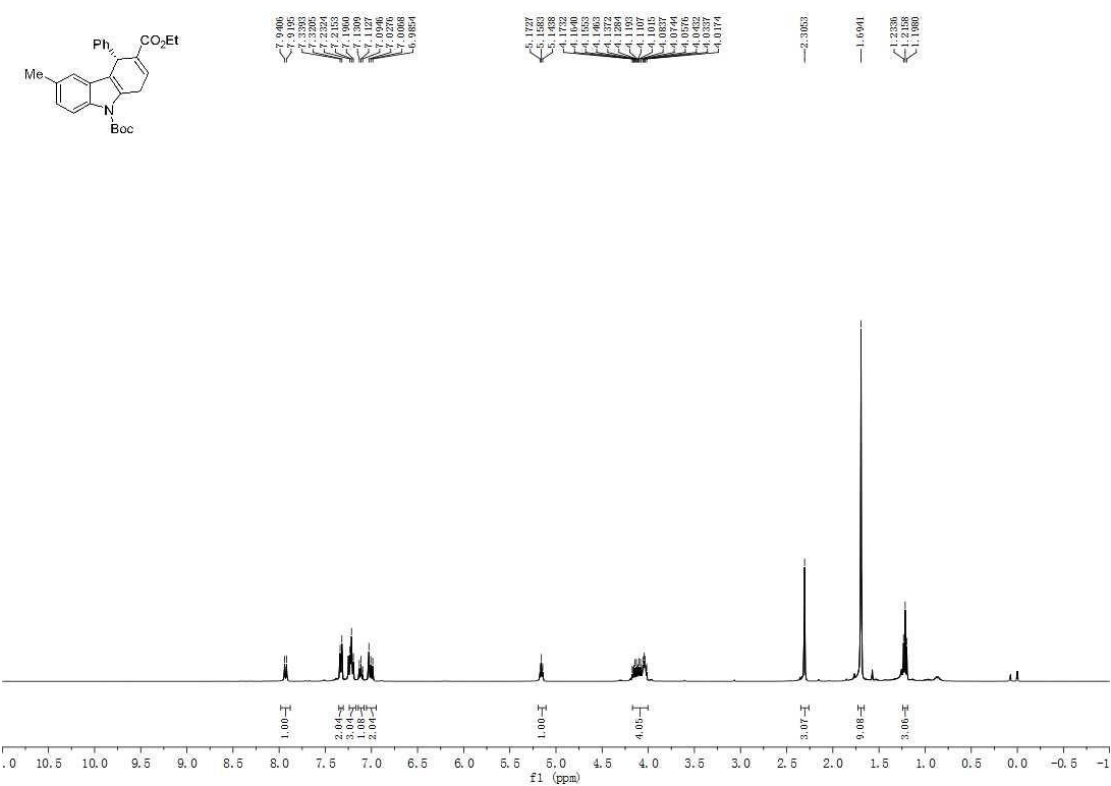


**Figure S4.**  $^{13}\text{C}$  NMR spectrum of **3b**, related to **Scheme 2**.

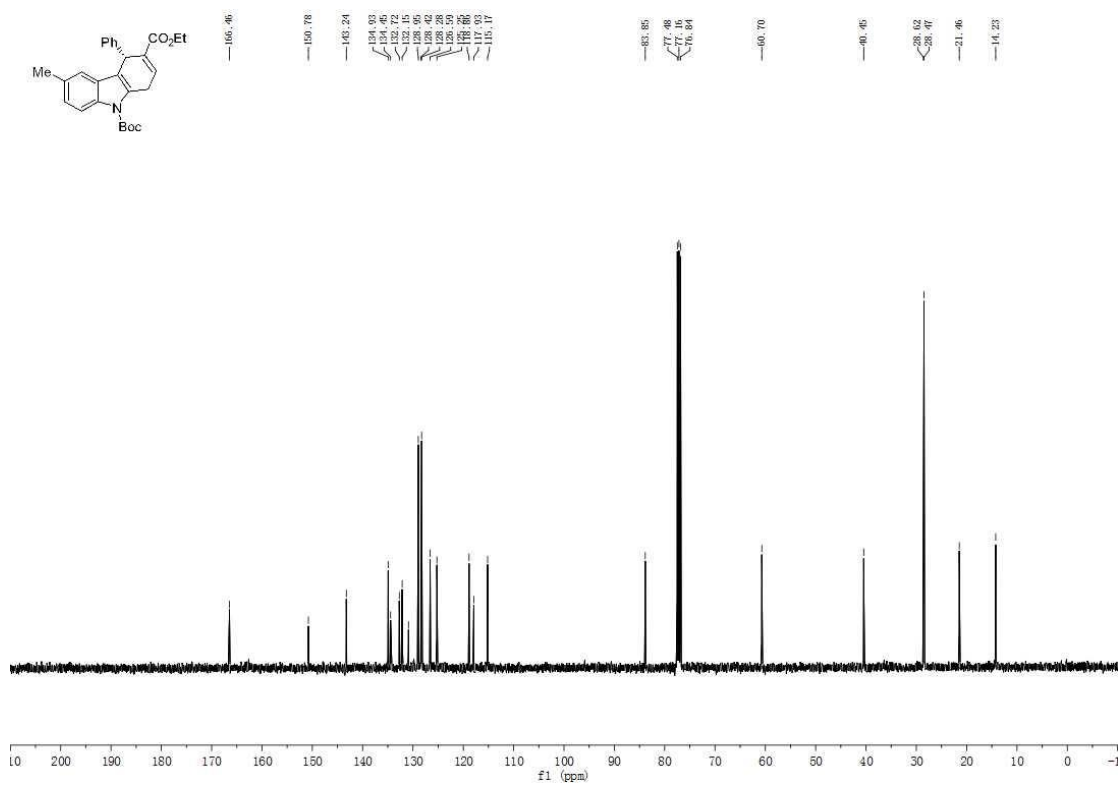


**Figure S5.**  $^1\text{H}$  NMR spectrum of **3c**, related to **Scheme 2**.

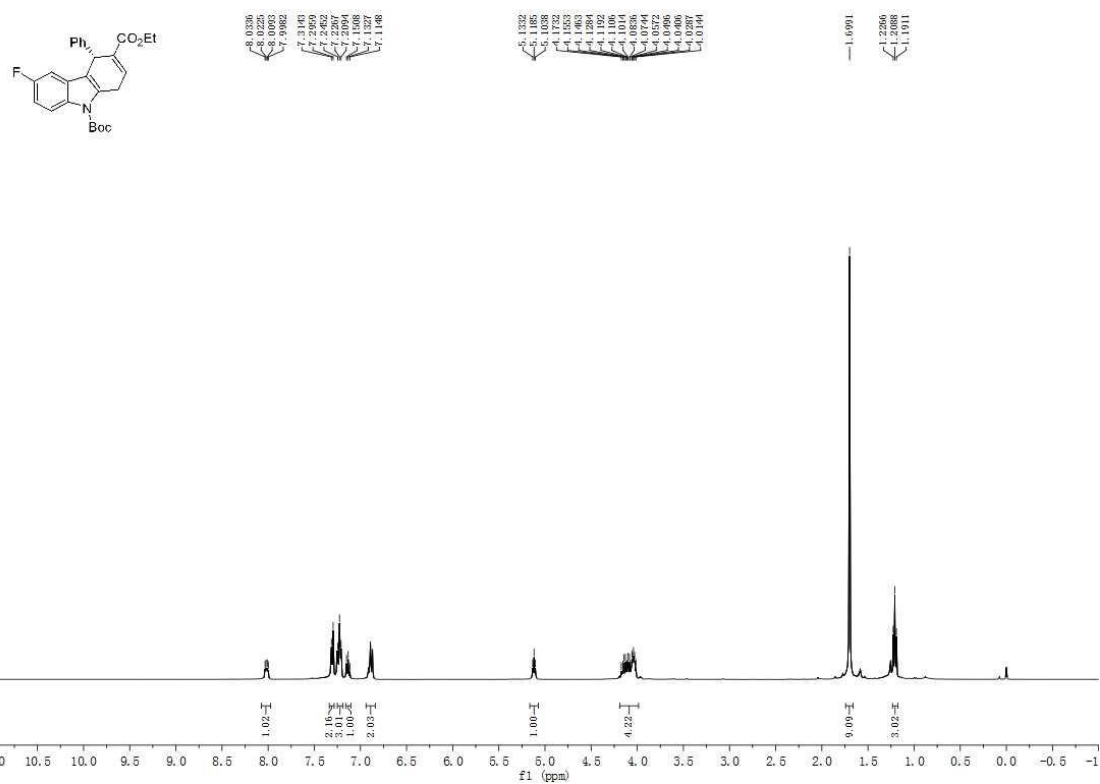


**Figure S6.**  $^{13}\text{C}$  NMR spectrum of **3c**, related to **Scheme 2**.

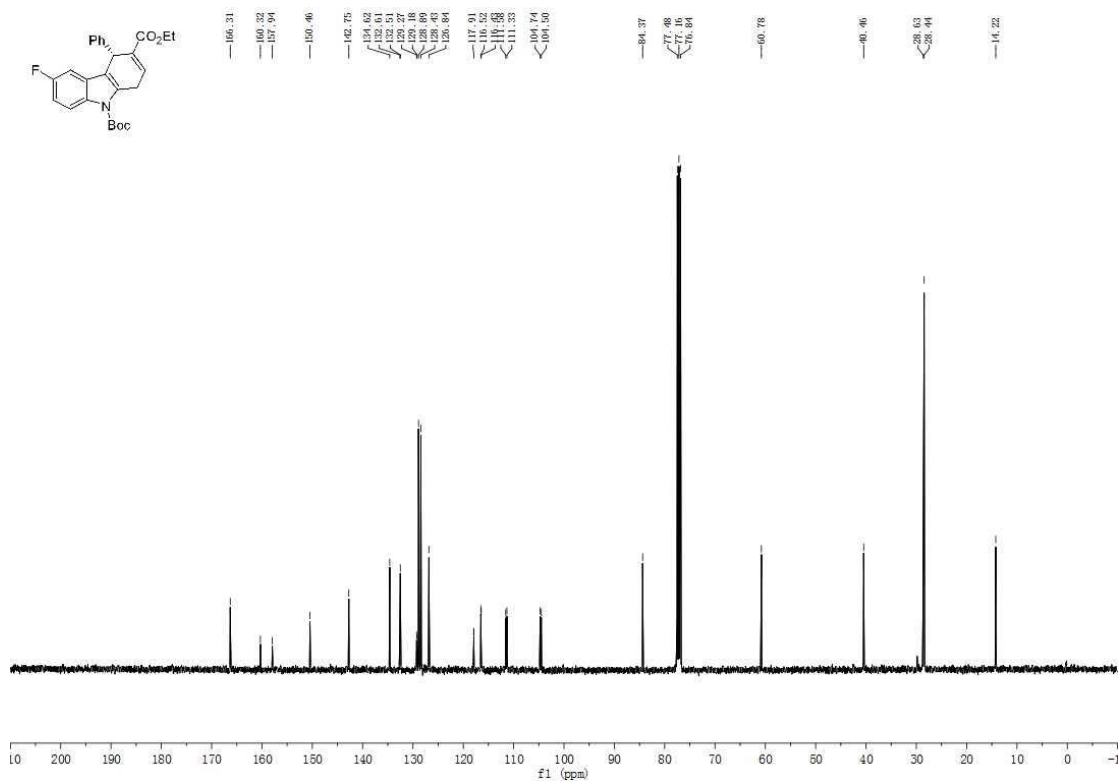


**Figure S7.**  $^{19}\text{F}$  NMR spectrum of **3c**, related to **Scheme 2**.

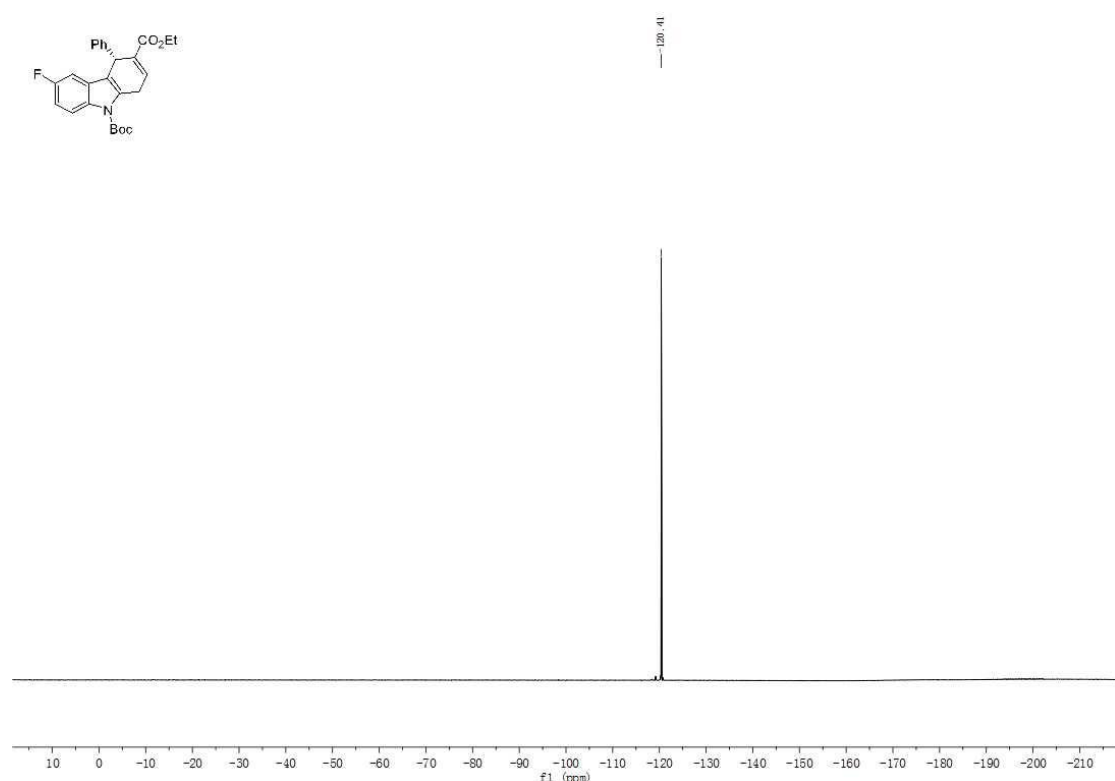


**Figure S8.**  $^1\text{H}$  NMR spectrum of **3d**, related to **Scheme 2**.

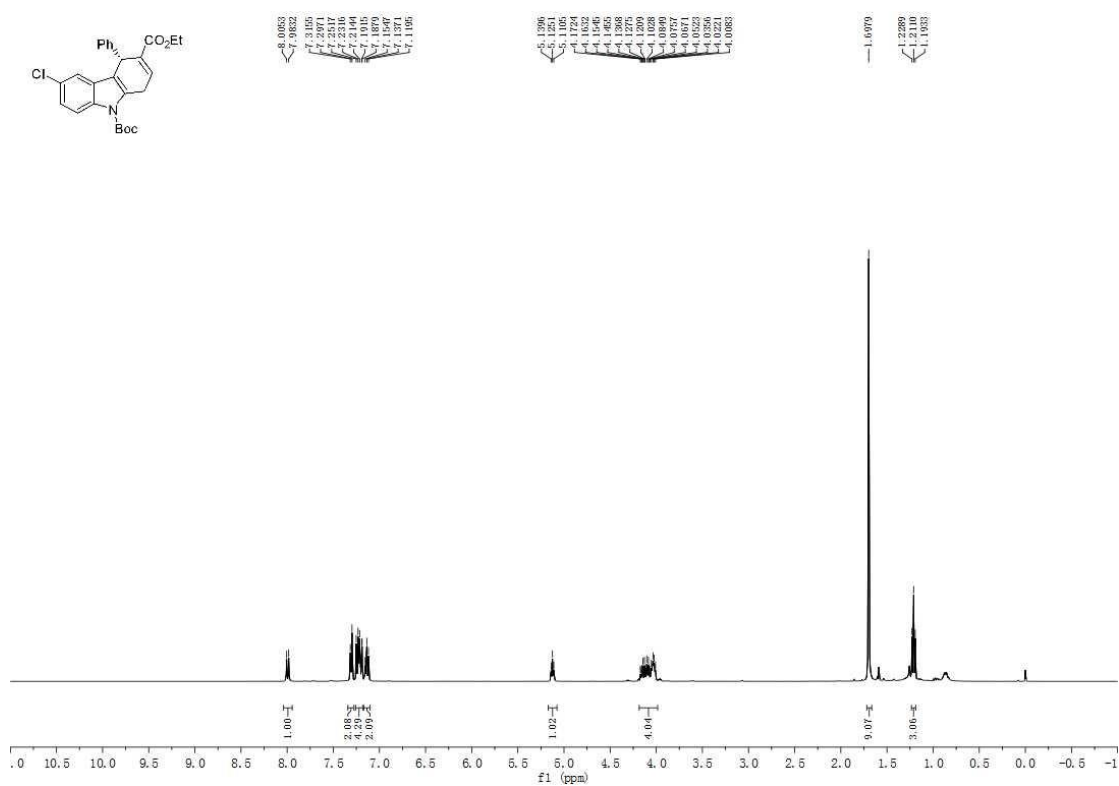


**Figure S9.**  $^{13}\text{C}$  NMR spectrum of **3d**, related to **Scheme 2**.

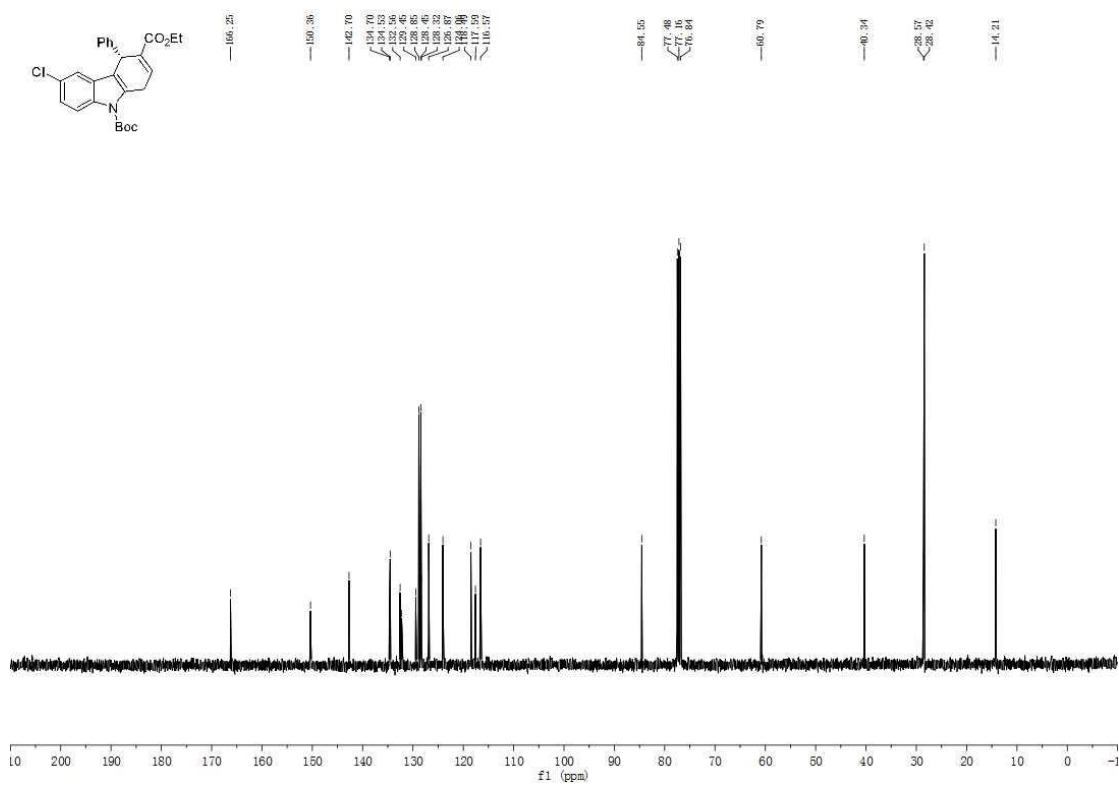


**Figure S10.**  $^1\text{H}$  NMR spectrum of **3e**, related to **Scheme 2**.

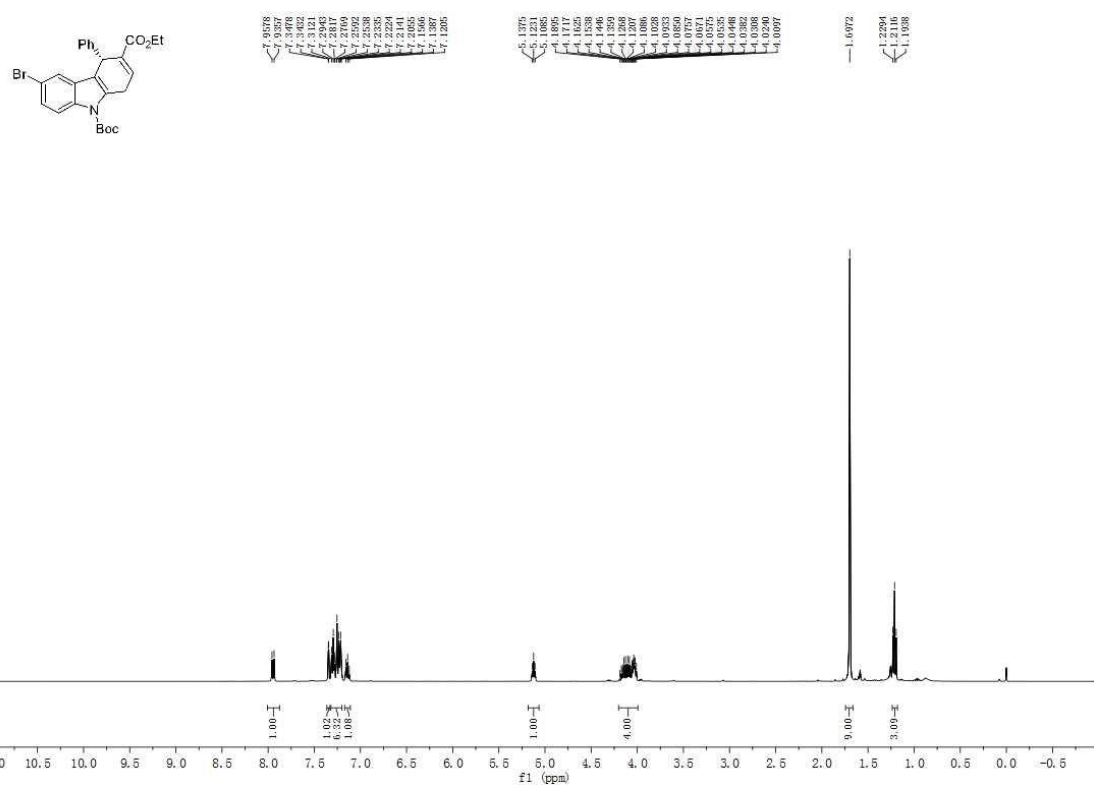


**Figure S11.**  $^{13}\text{C}$  NMR spectrum of **3e**, related to **Scheme 2**.

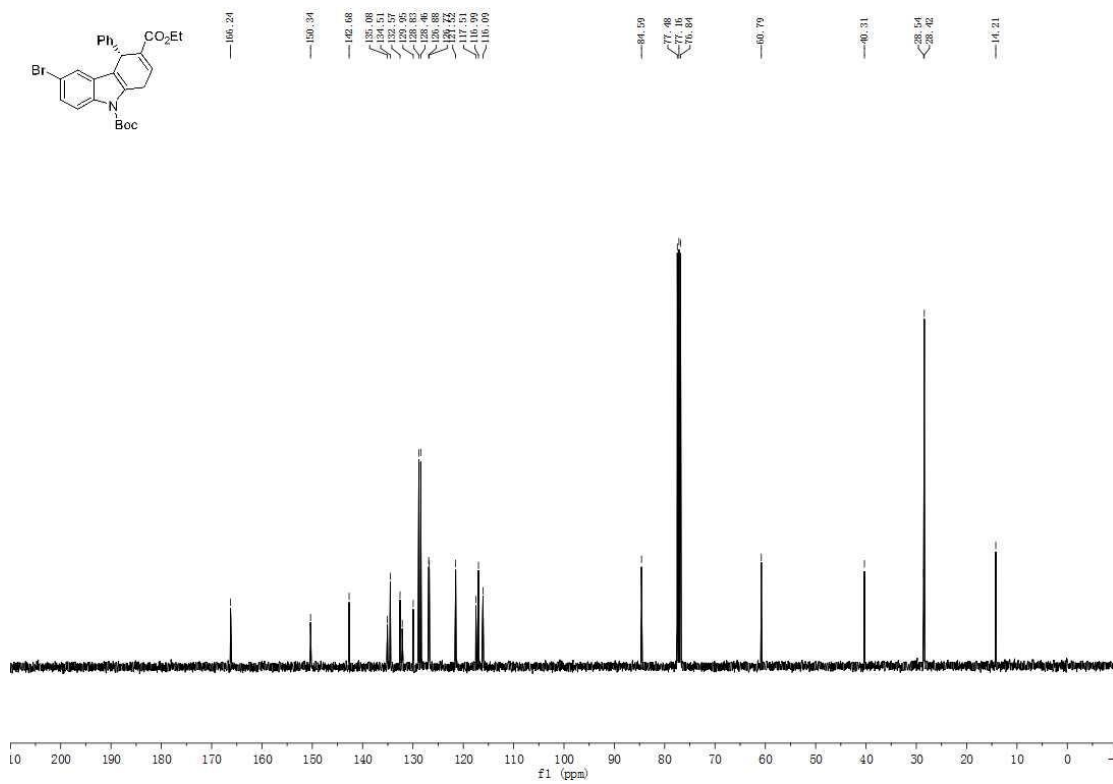


**Figure S12.**  $^1\text{H}$  NMR spectrum of **3f**, related to **Scheme 2**.

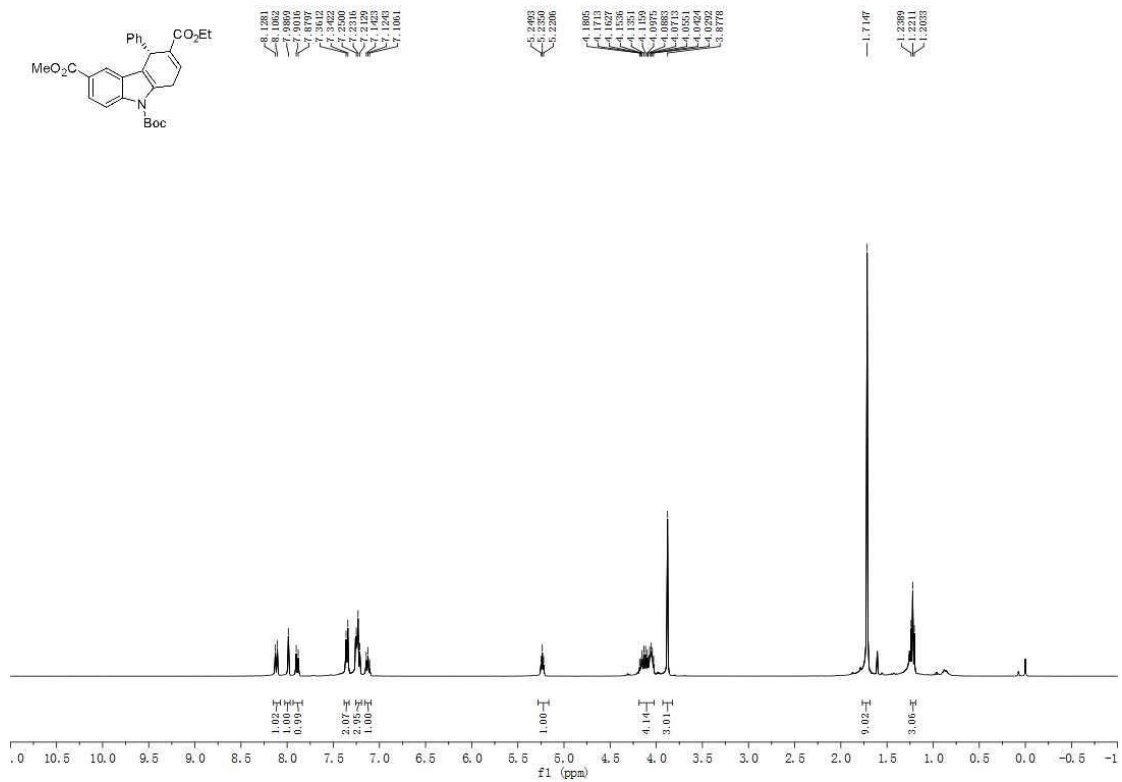


**Figure S13.**  $^{13}\text{C}$  NMR spectrum of **3f**, related to **Scheme 2**.

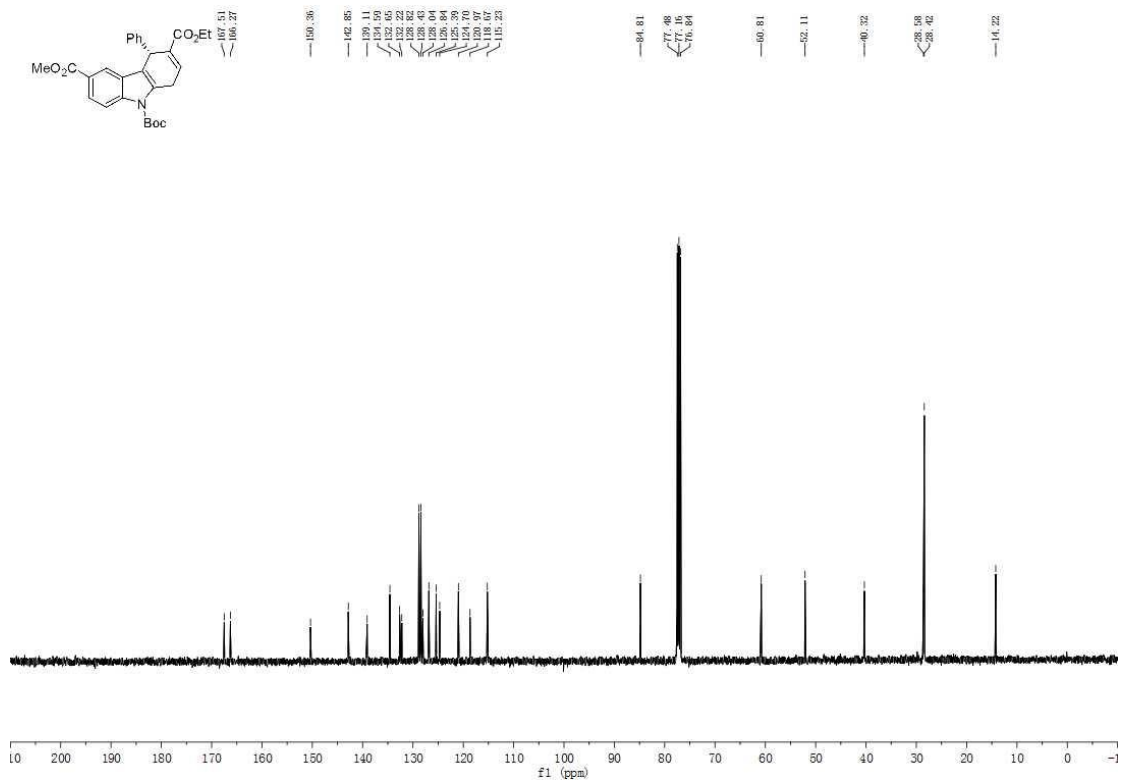


**Figure S14.**  $^1\text{H}$  NMR spectrum of **3g**, related to **Scheme 2**.

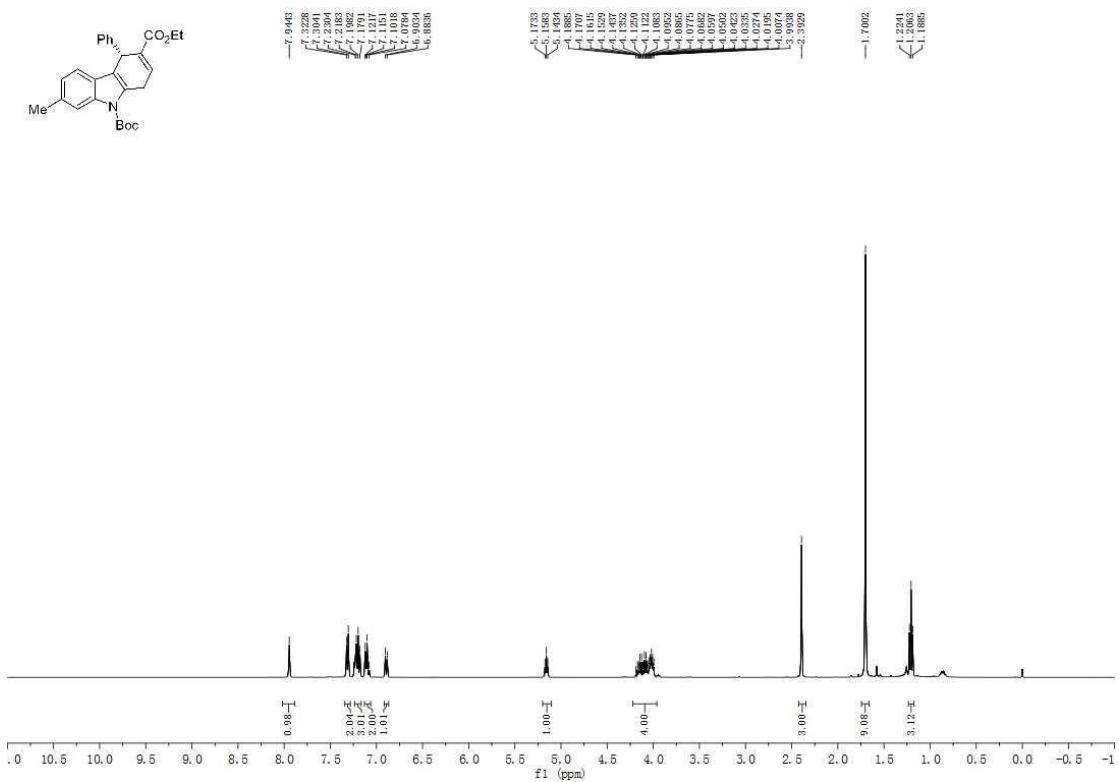


**Figure S15.**  $^{13}\text{C}$  NMR spectrum of **3g**, related to **Scheme 2**.

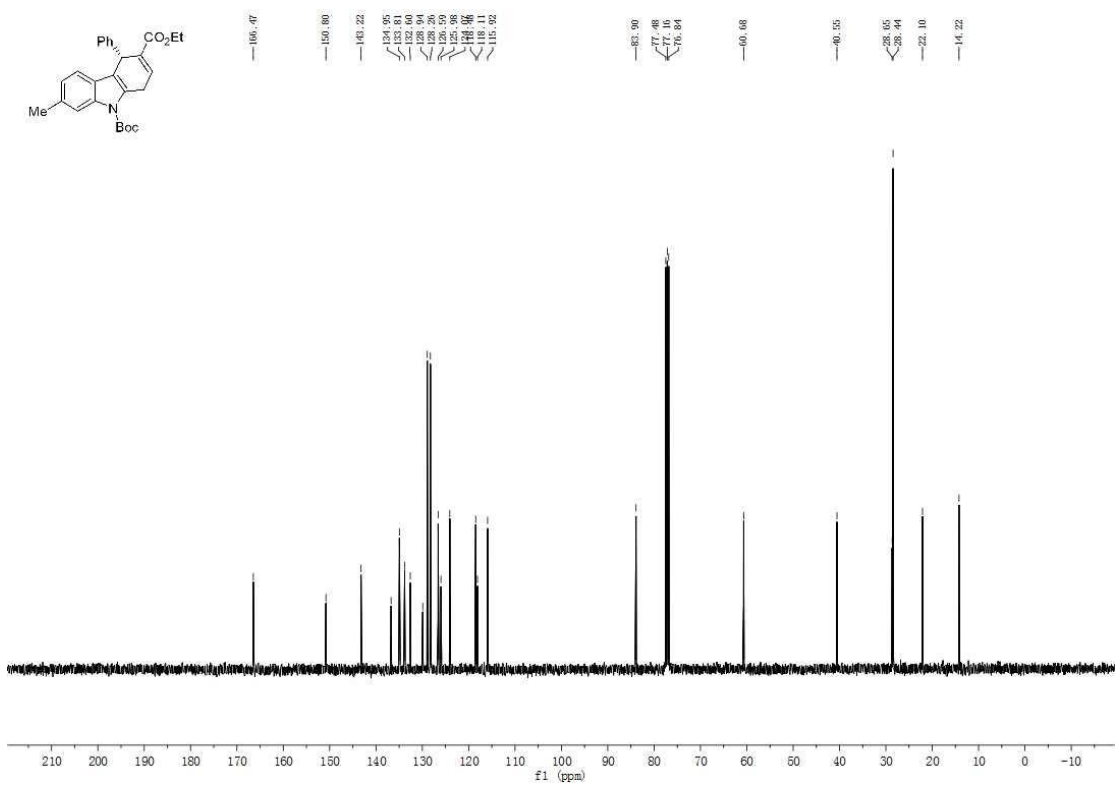


**Figure S16.**  $^1\text{H}$  NMR spectrum of **3h**, related to **Scheme 2**.

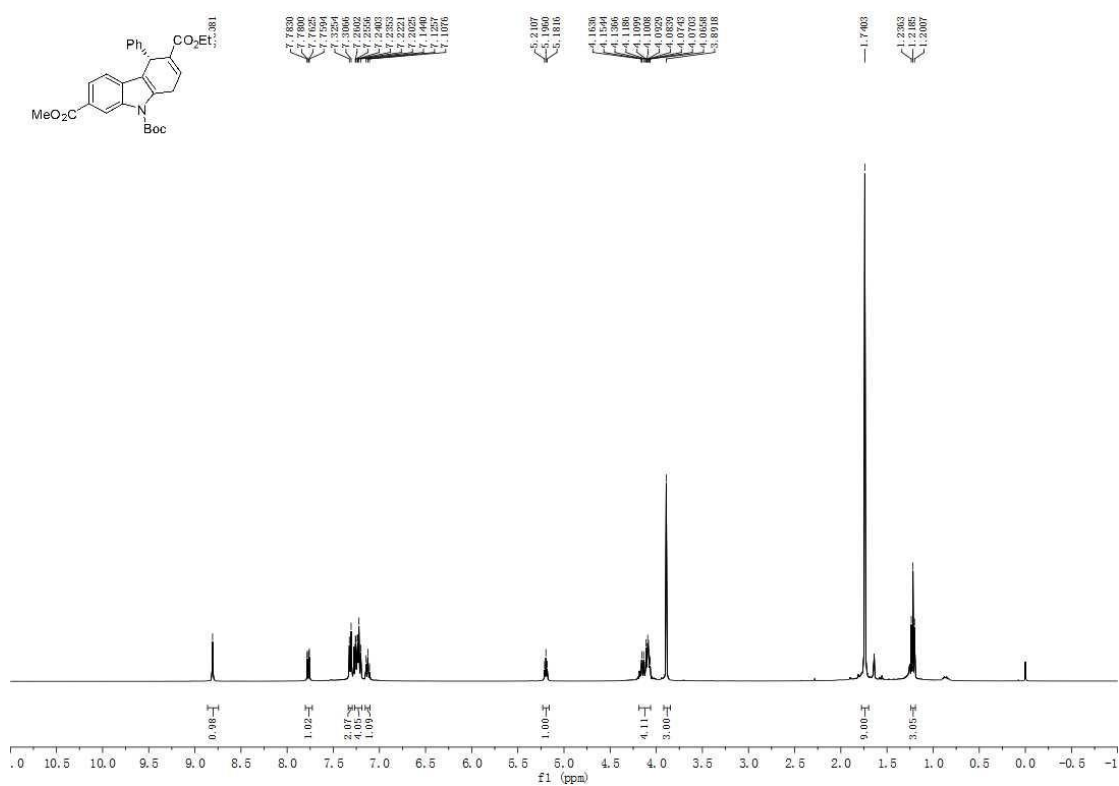


**Figure S17.**  $^{13}\text{C}$  NMR spectrum of **3h**, related to **Scheme 2**.

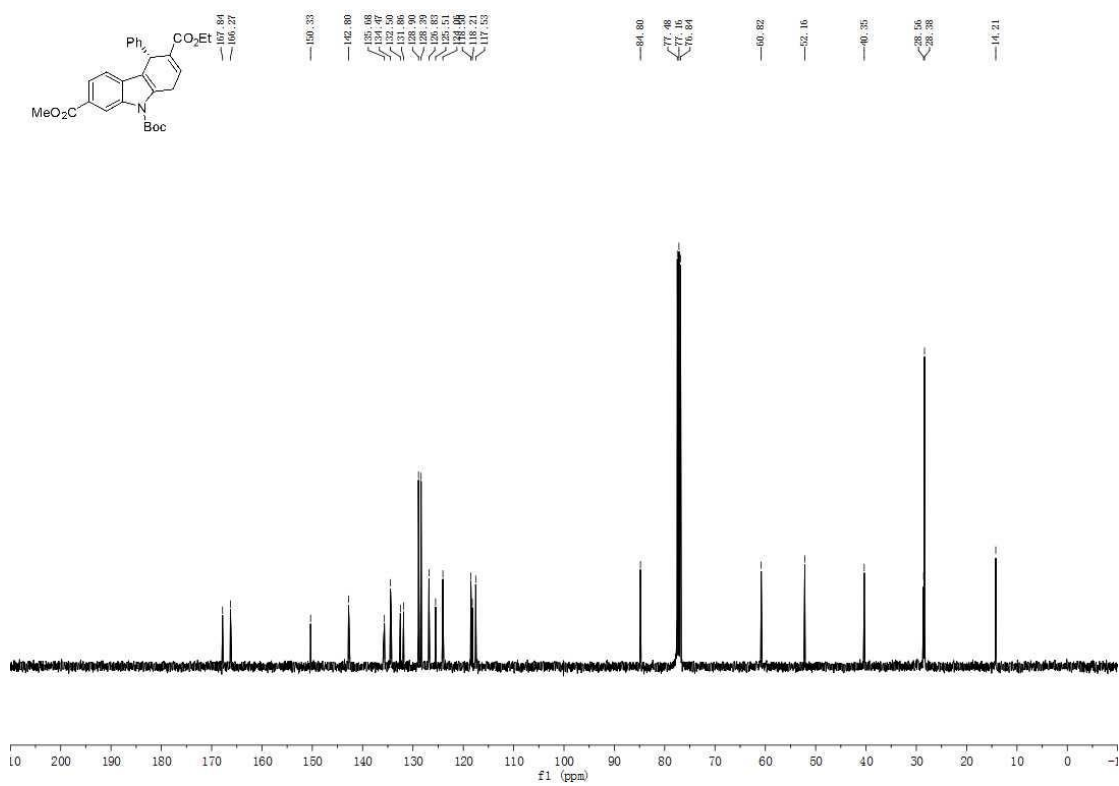


**Figure S18.**  $^1\text{H}$  NMR spectrum of **3i**, related to **Scheme 2**.

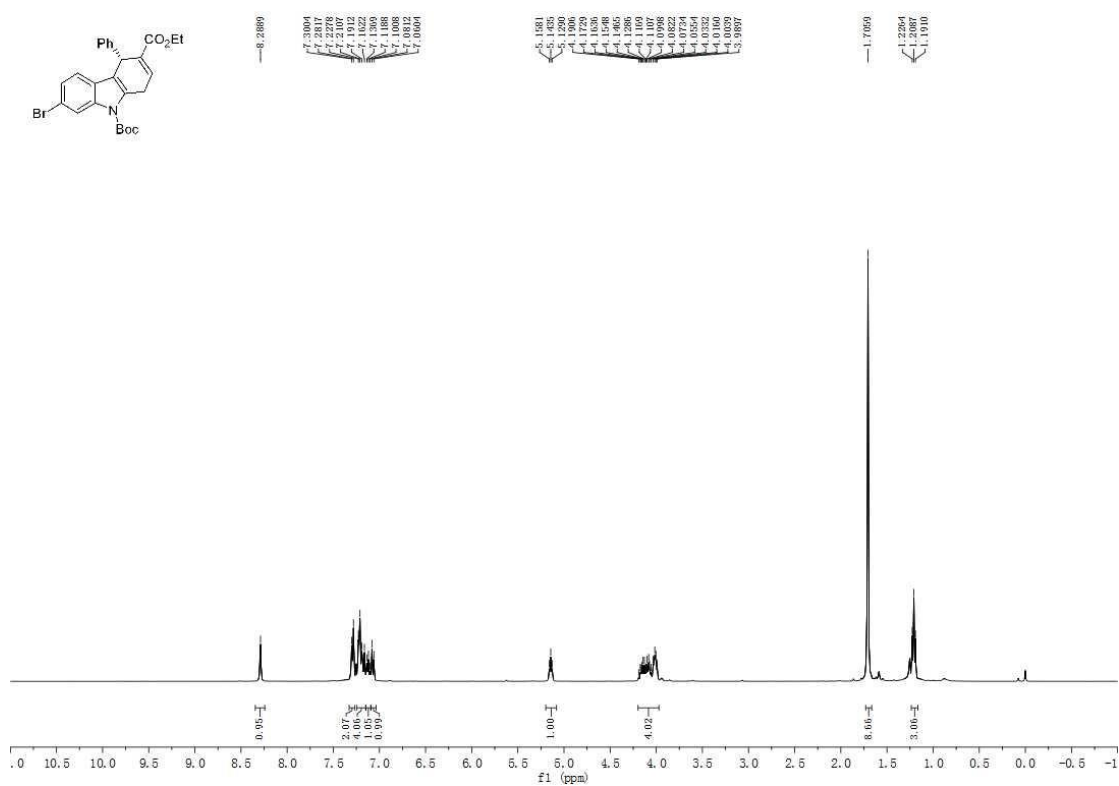


**Figure S19.**  $^{13}\text{C}$  NMR spectrum of **3i**, related to **Scheme 2**.

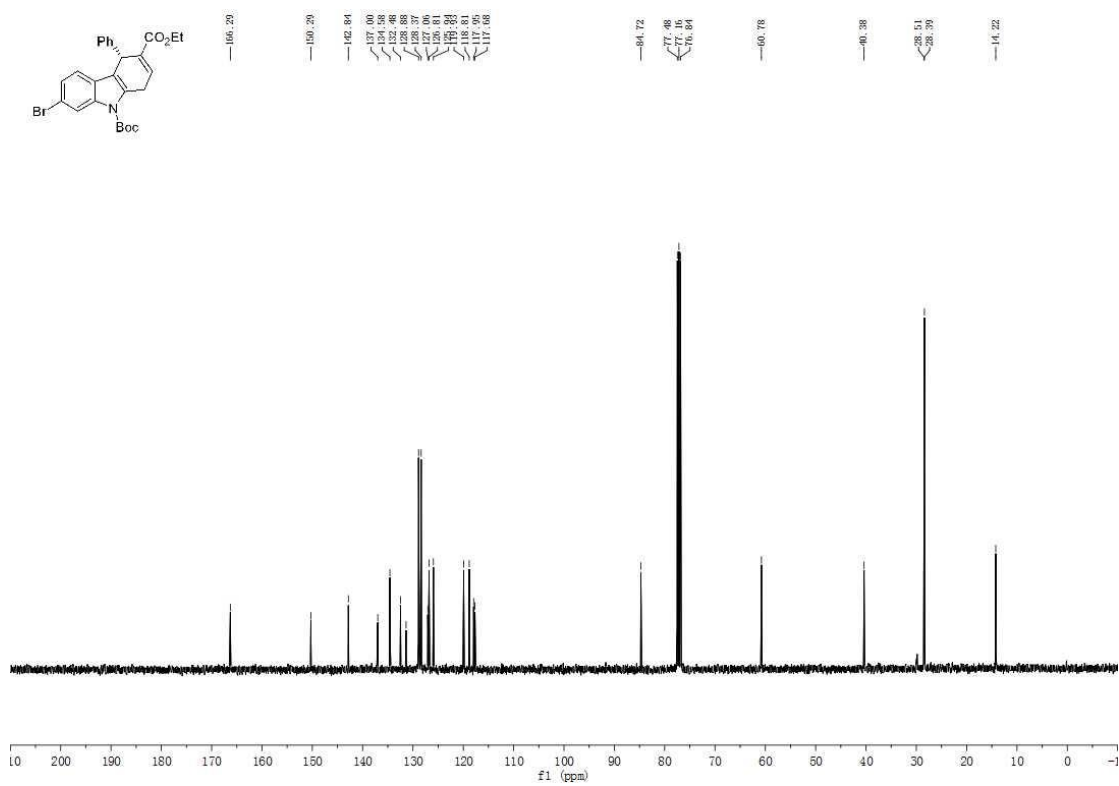


**Figure S20.**  $^1\text{H}$  NMR spectrum of **3j**, related to **Scheme 2**.

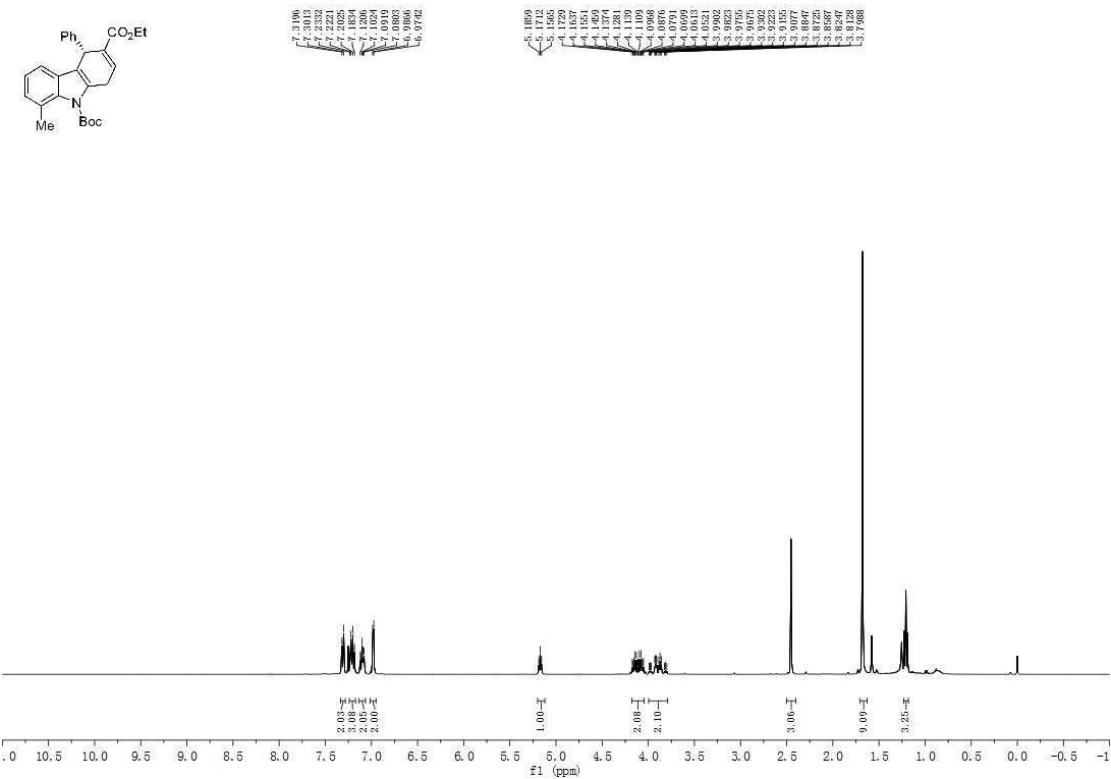


**Figure S21.**  $^{13}\text{C}$  NMR spectrum of **3j**, related to **Scheme 2**.

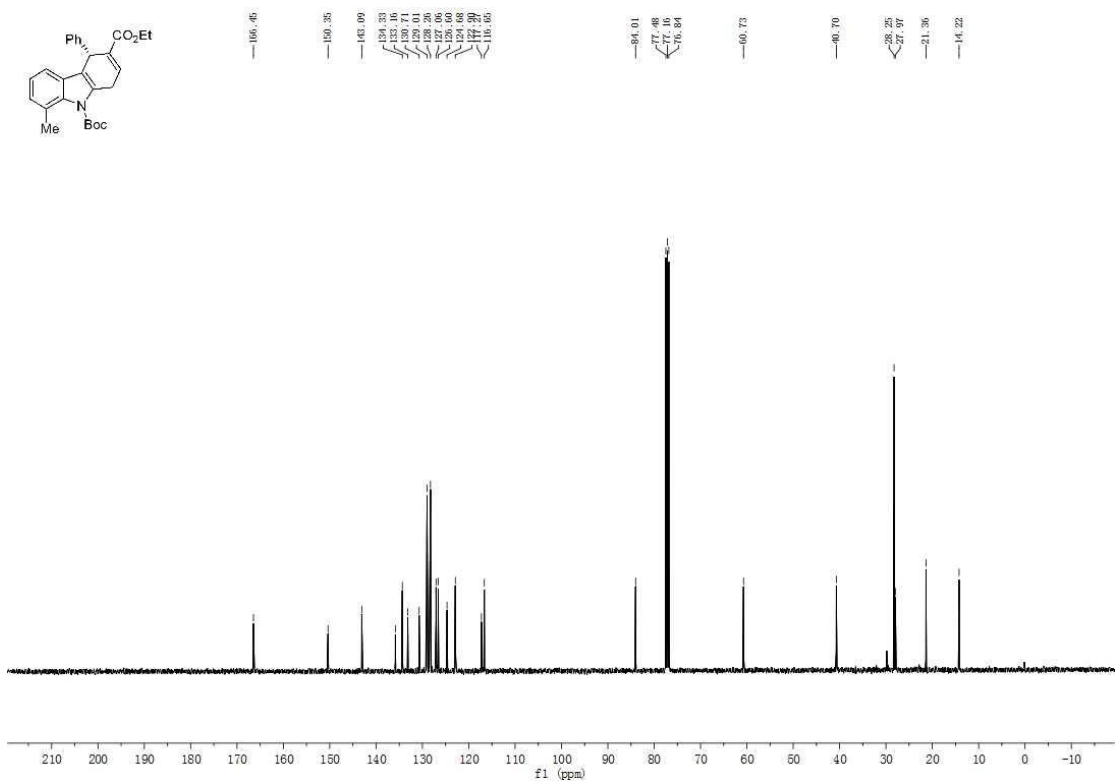


**Figure S22.**  $^1\text{H}$  NMR spectrum of **3k**, related to **Scheme 2**.

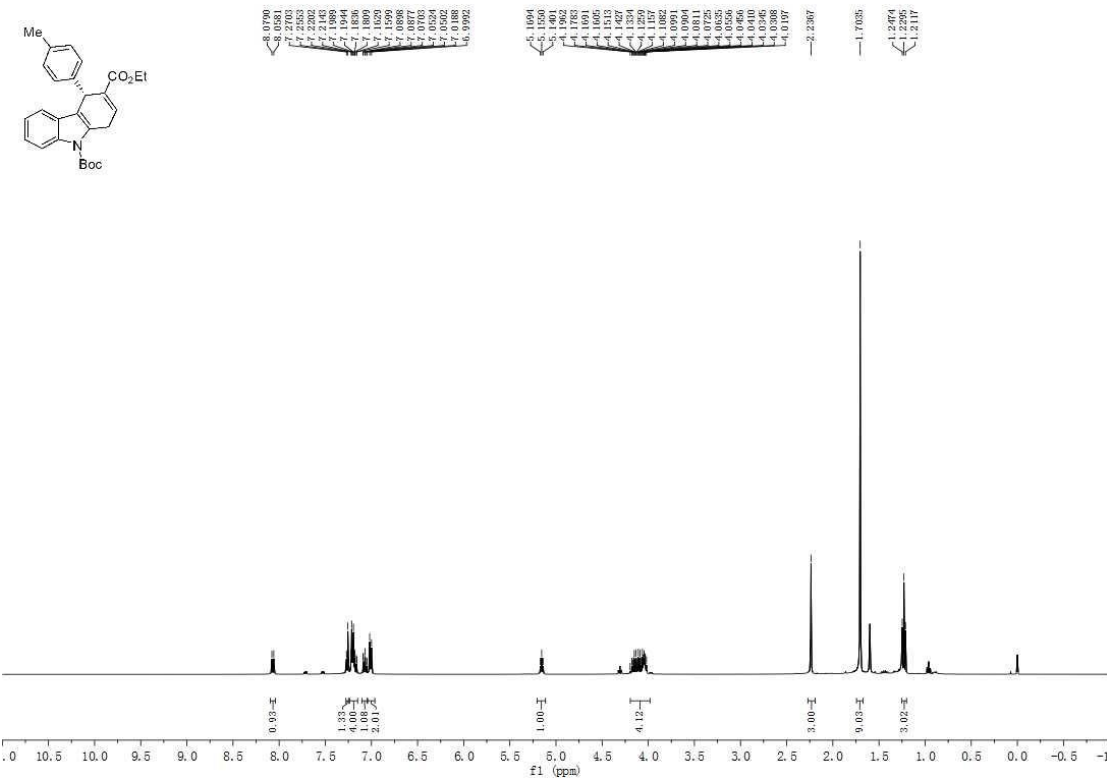


**Figure S23.**  $^{13}\text{C}$  NMR spectrum of **3k**, related to **Scheme 2**.

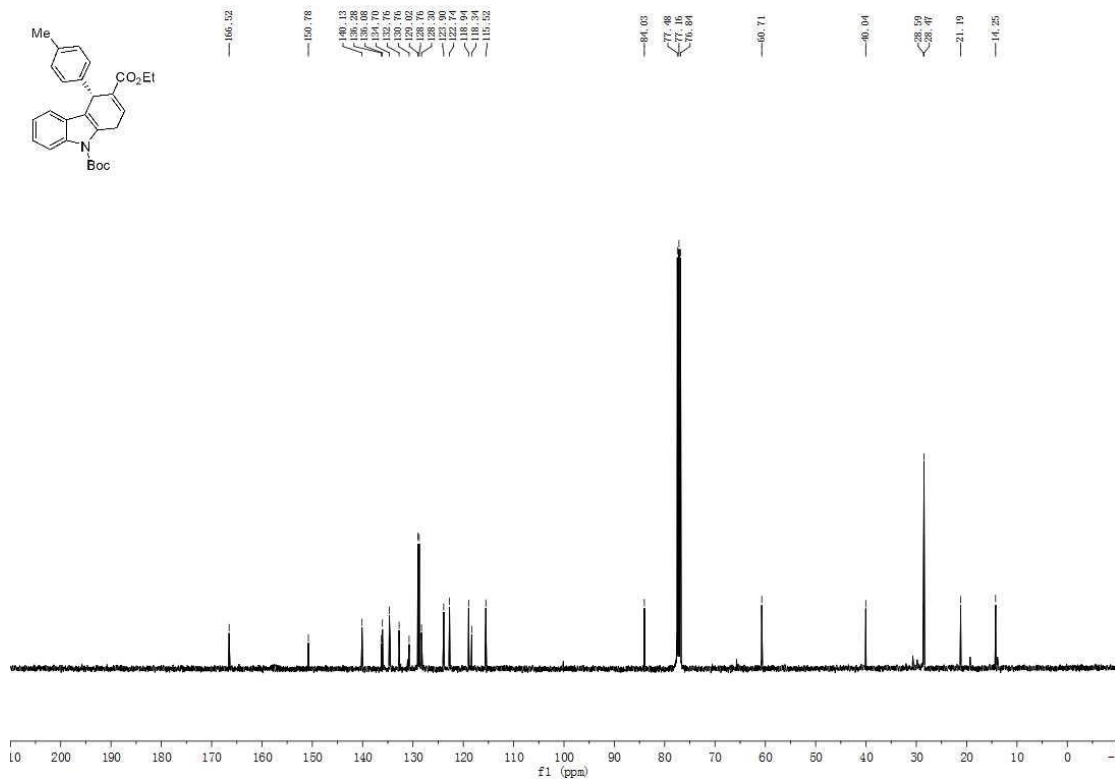


**Figure S24.**  $^1\text{H}$  NMR spectrum of **3I**, related to **Scheme 2**.

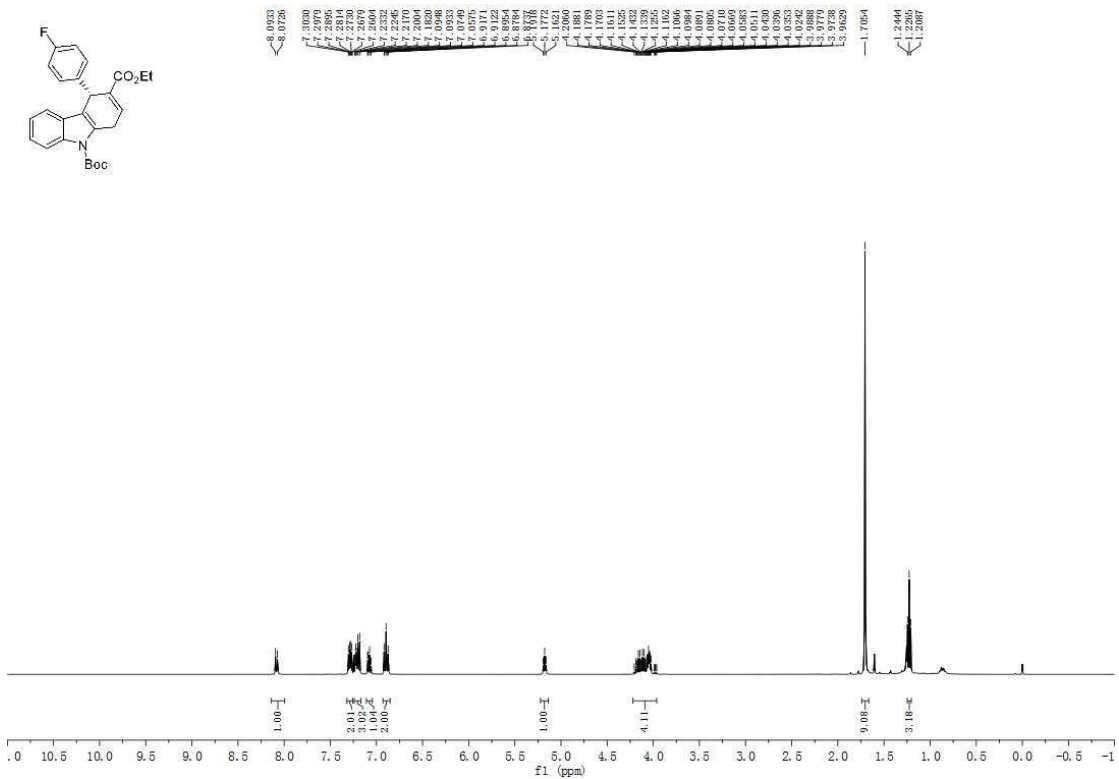


**Figure S25.**  $^{13}\text{C}$  NMR spectrum of **3I**, related to **Scheme 2**.

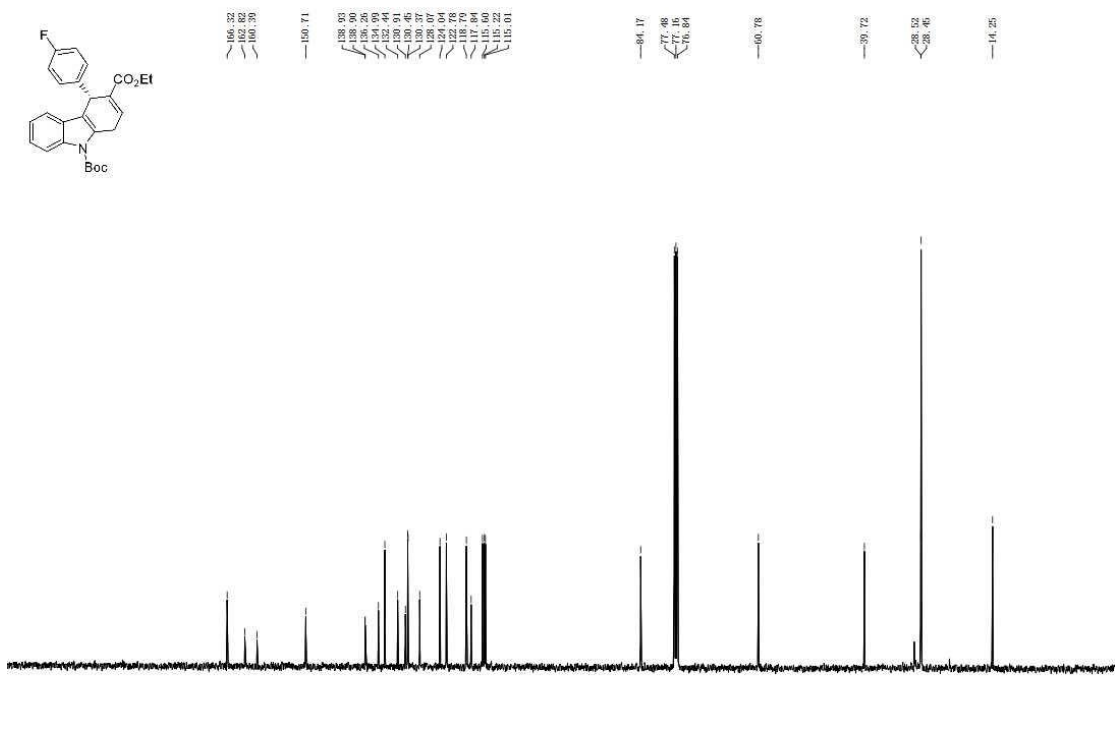


**Figure S26.**  $^{19}\text{F}$  NMR spectrum of **3l**, related to **Scheme 2**.

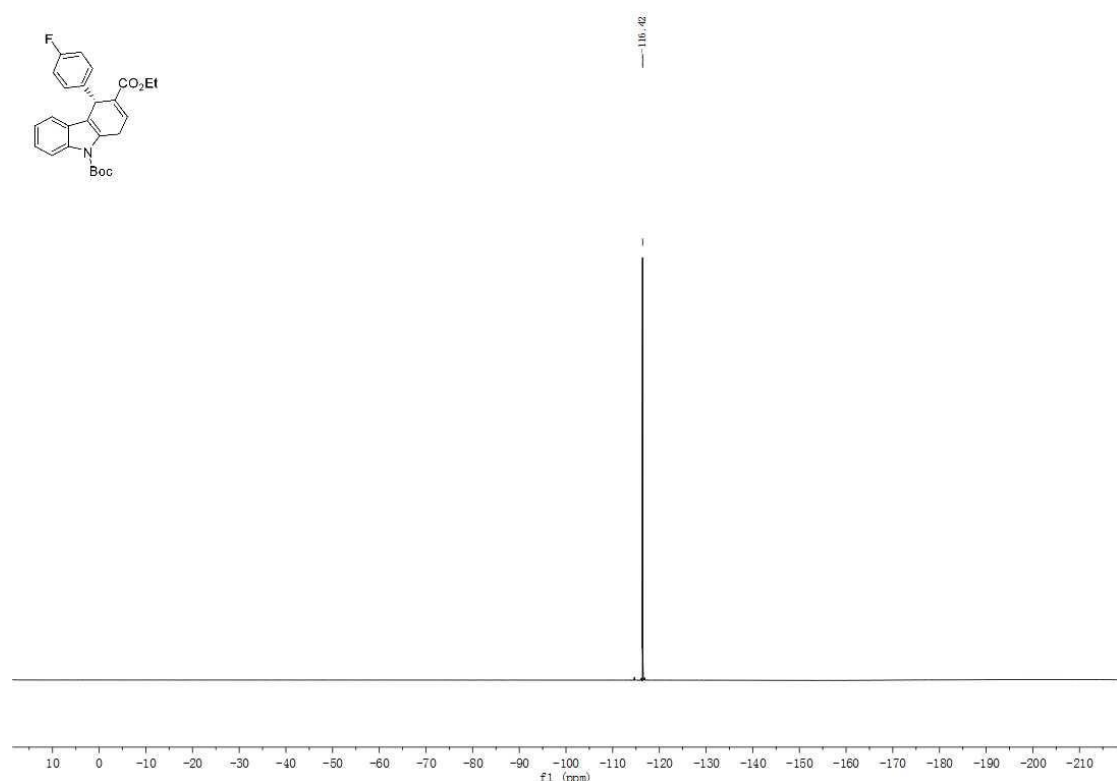


**Figure S27.**  $^1\text{H}$  NMR spectrum of **3m**, related to **Scheme 2**.

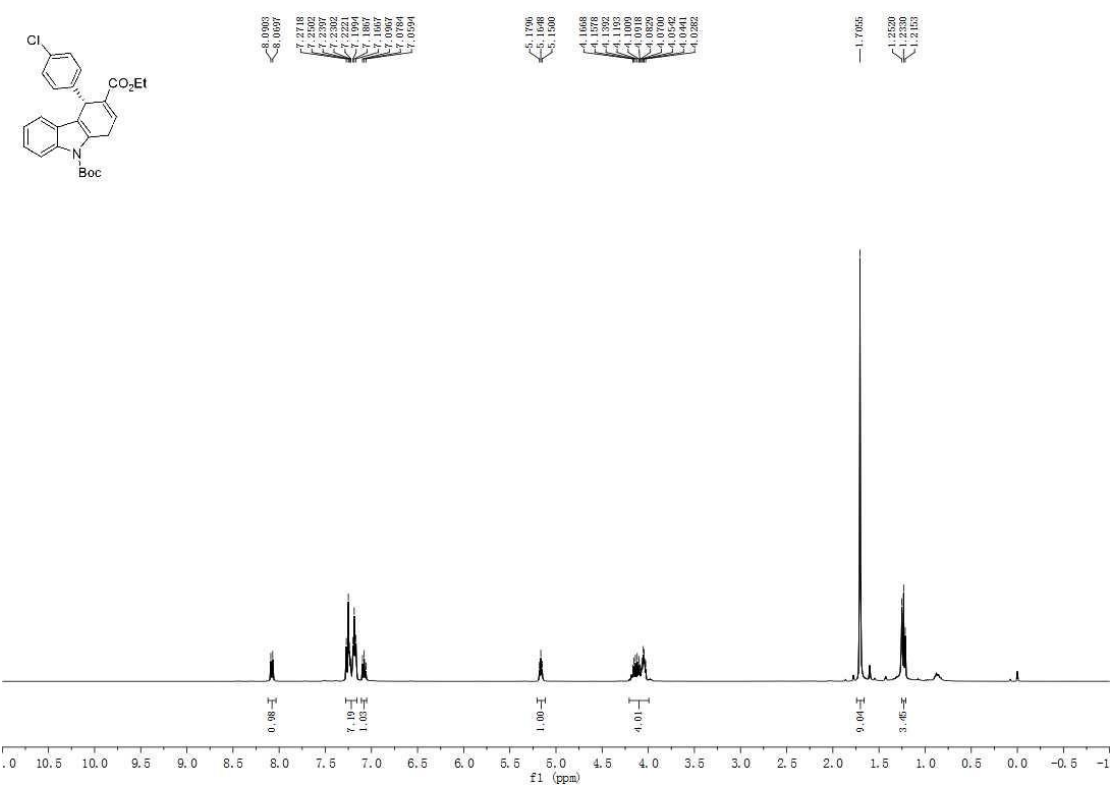


**Figure S28.**  $^{13}\text{C}$  NMR spectrum of **3m**, related to **Scheme 2**.

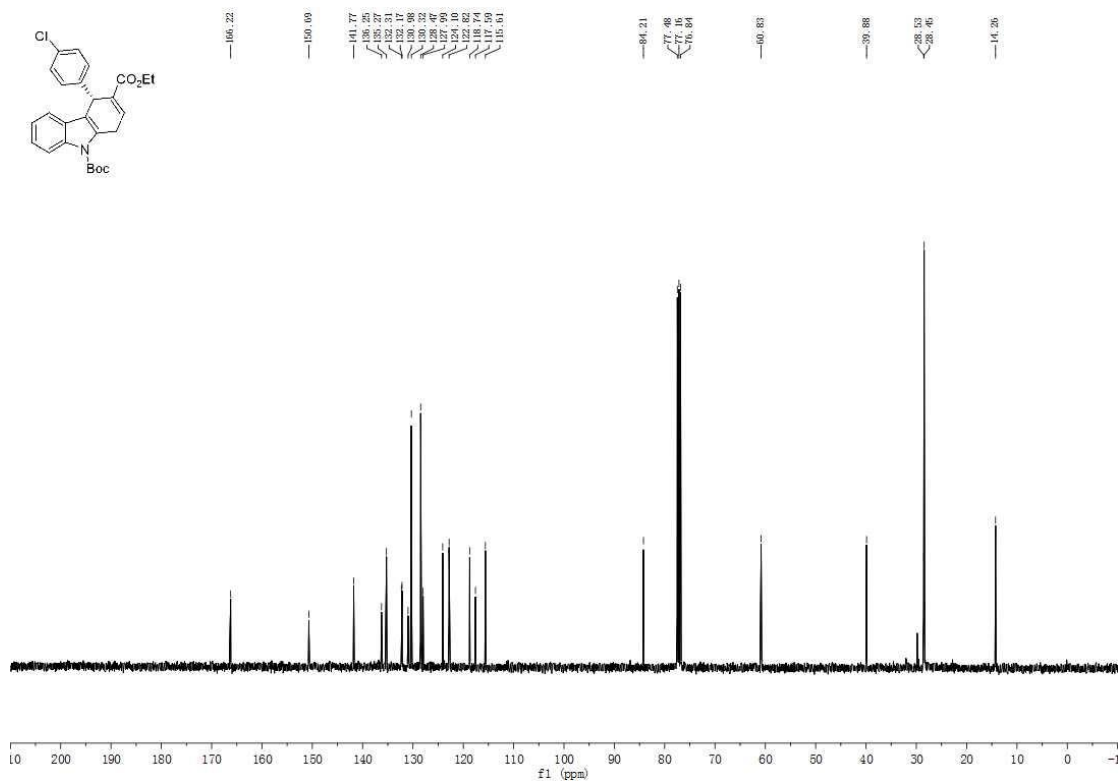


**Figure S29.**  $^1\text{H}$  NMR spectrum of **3n**, related to **Scheme 2**.

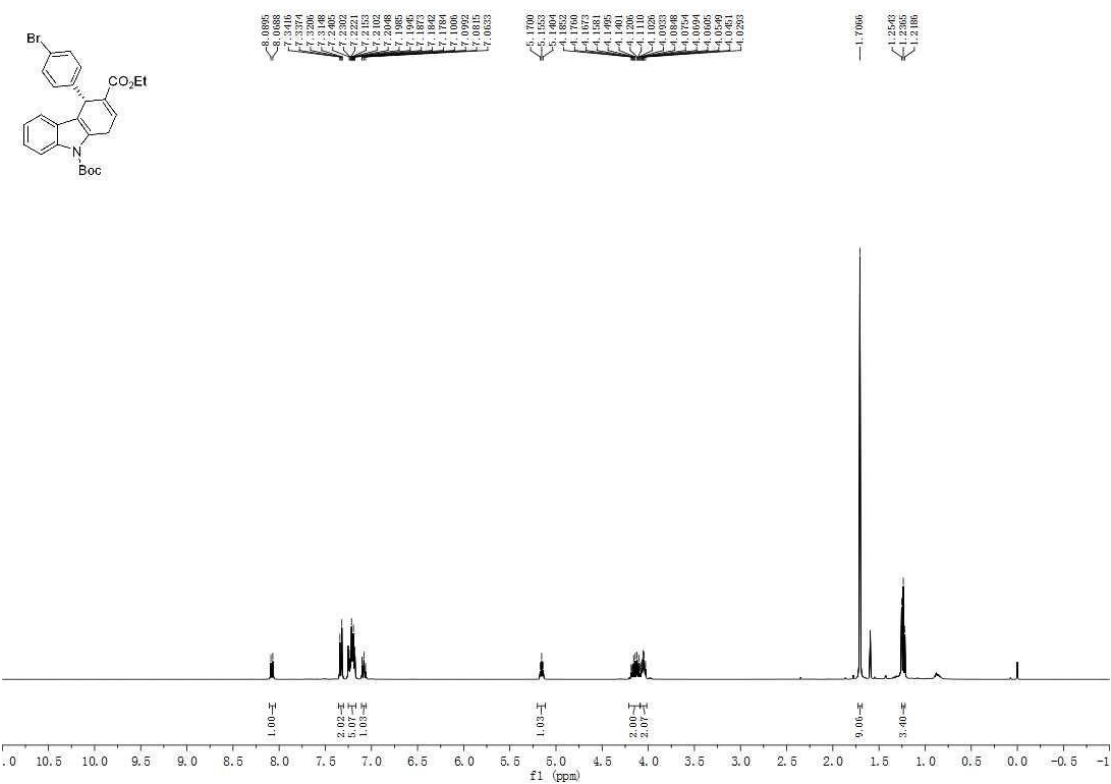


**Figure S30.**  $^{13}\text{C}$  NMR spectrum of **3n**, related to **Scheme 2**.

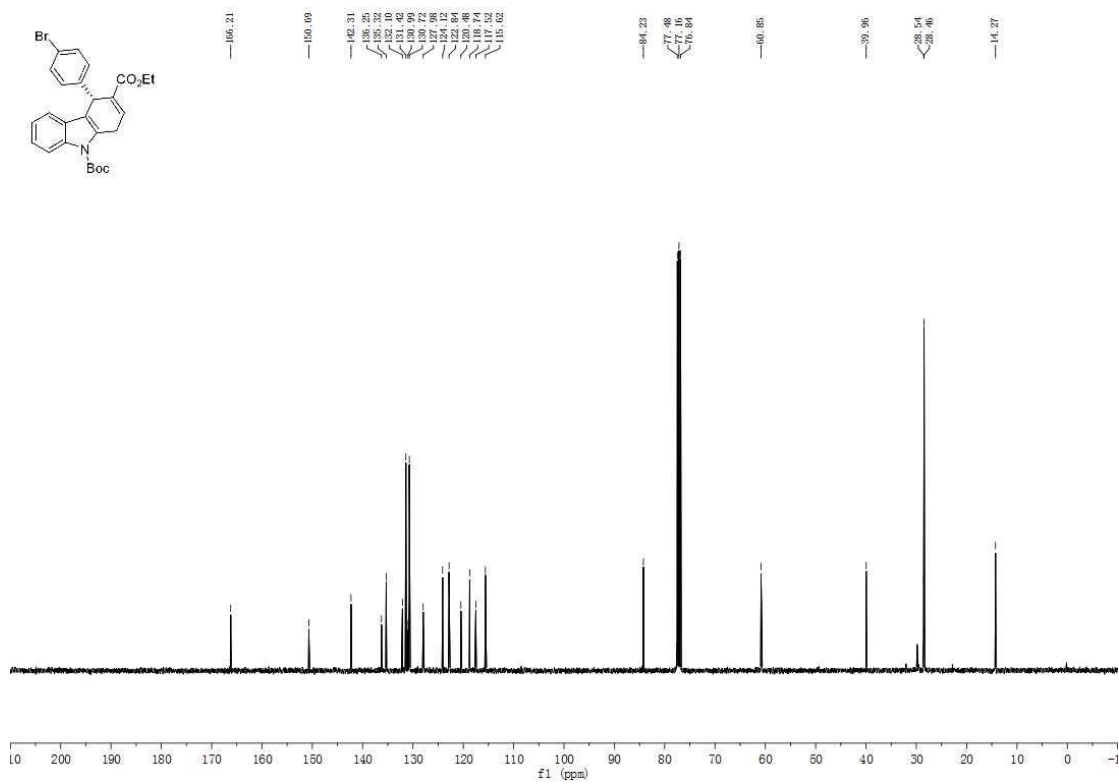


**Figure S31.**  $^1\text{H}$  NMR spectrum of **3o**, related to **Scheme 2**.

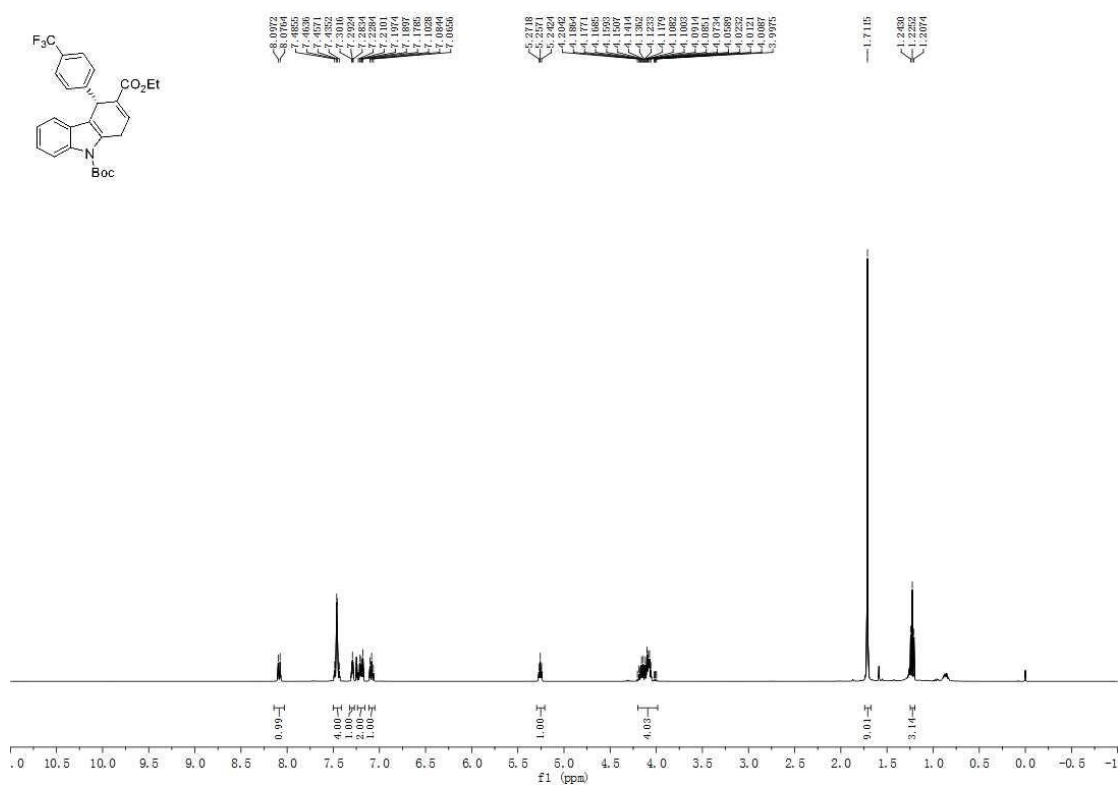


**Figure S32.**  $^{13}\text{C}$  NMR spectrum of **3o**, related to **Scheme 2**.

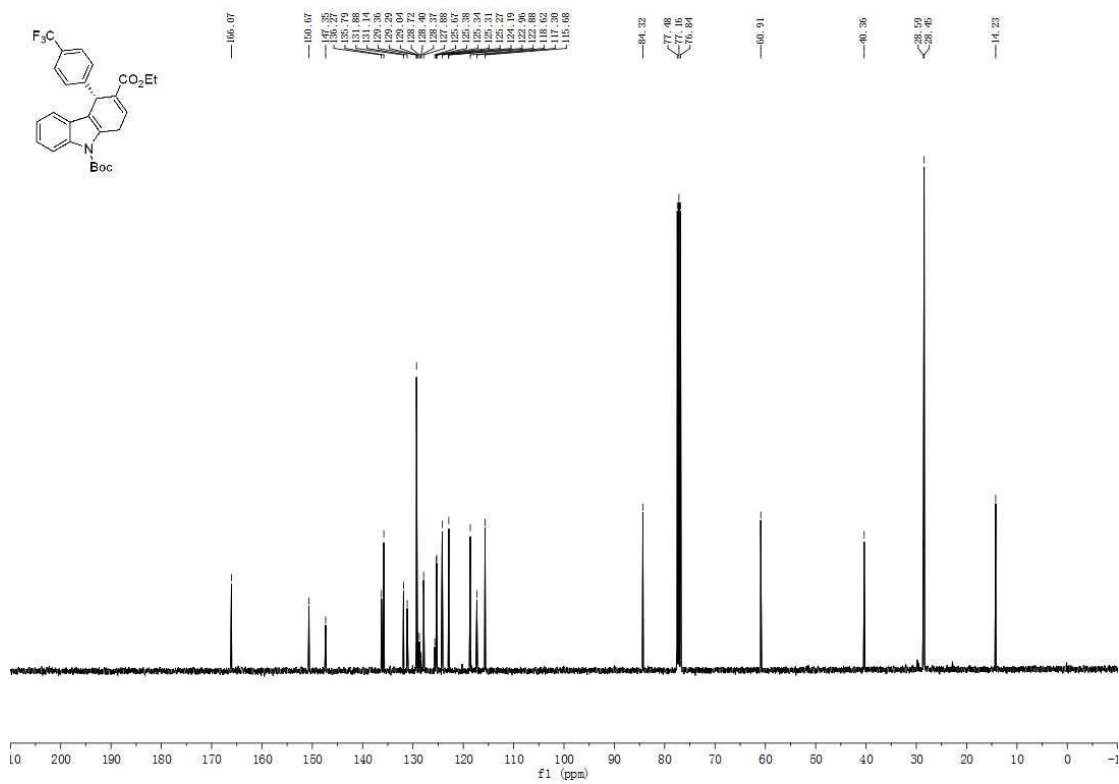


**Figure S33.**  $^{19}\text{F}$  NMR spectrum of **3o**, related to **Scheme 2**.

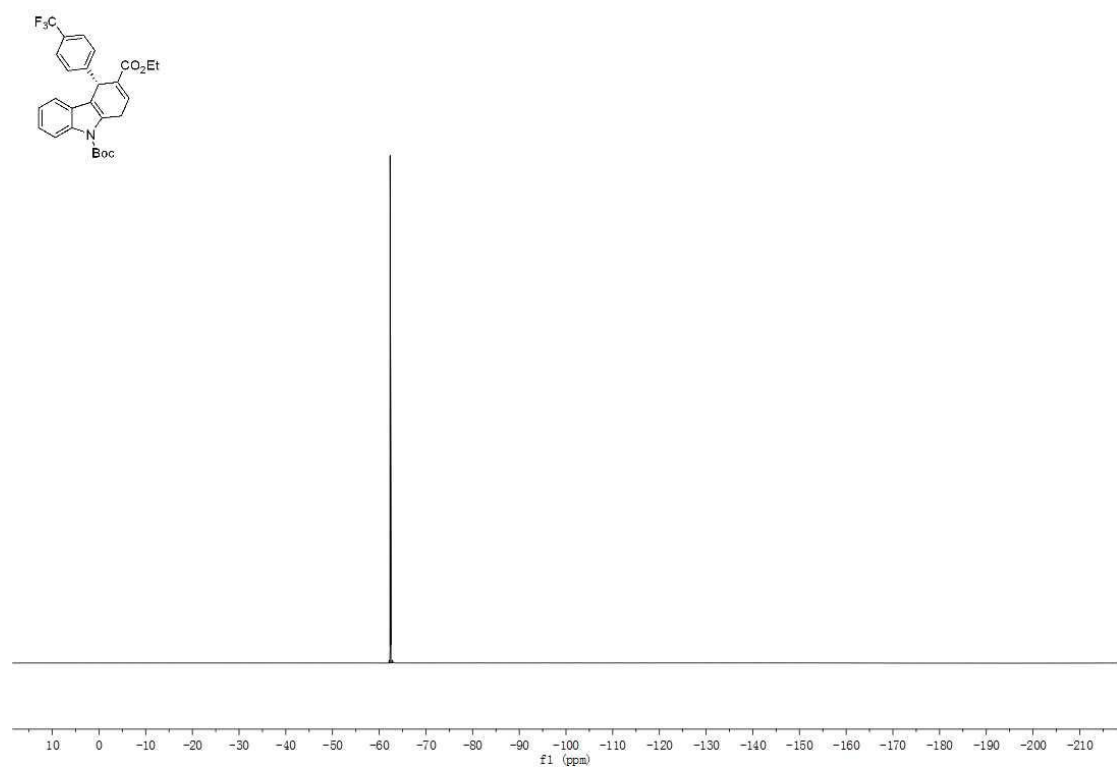


**Figure S34.**  $^1\text{H}$  NMR spectrum of **3p**, related to **Scheme 2**.

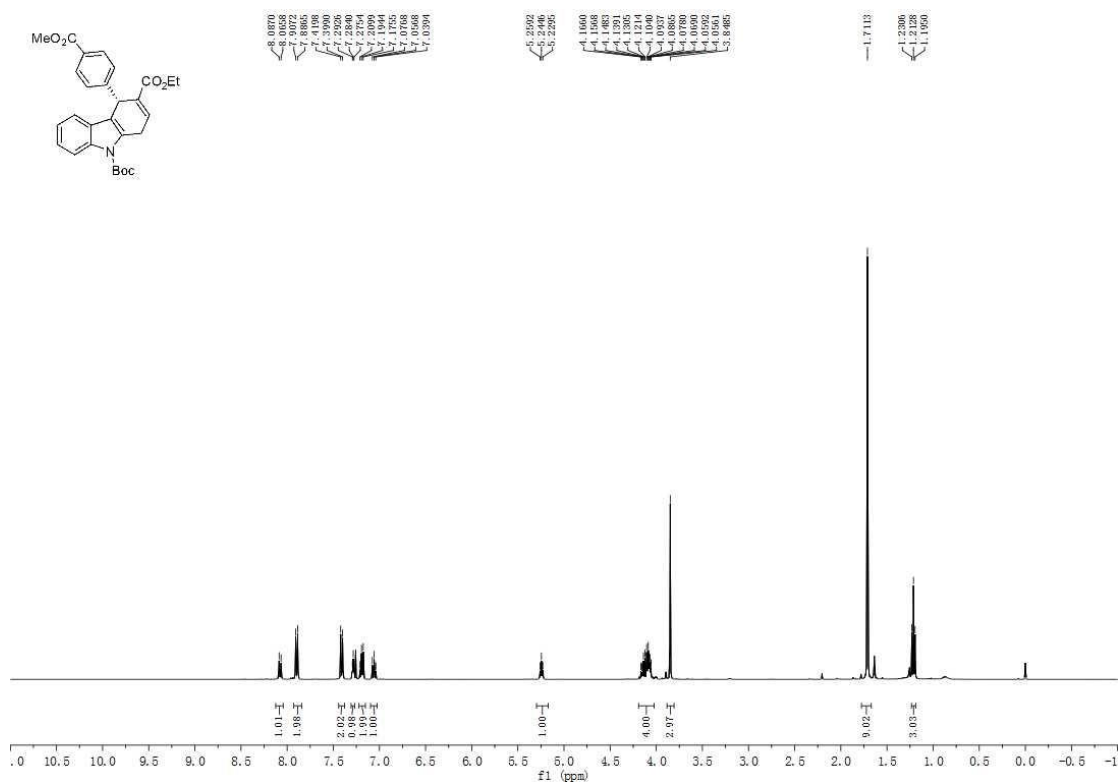


**Figure S35.**  $^{13}\text{C}$  NMR spectrum of **3p**, related to **Scheme 2**.

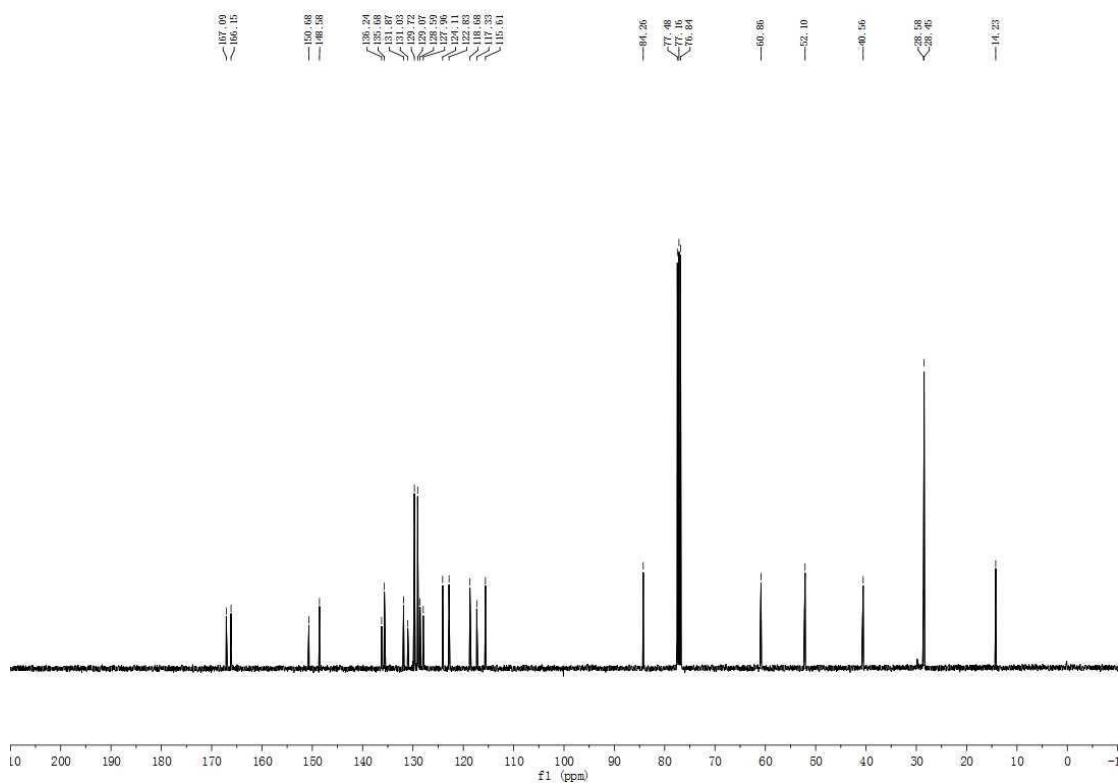


**Figure S36.**  $^1\text{H}$  NMR spectrum of **3q**, related to **Scheme 2**.

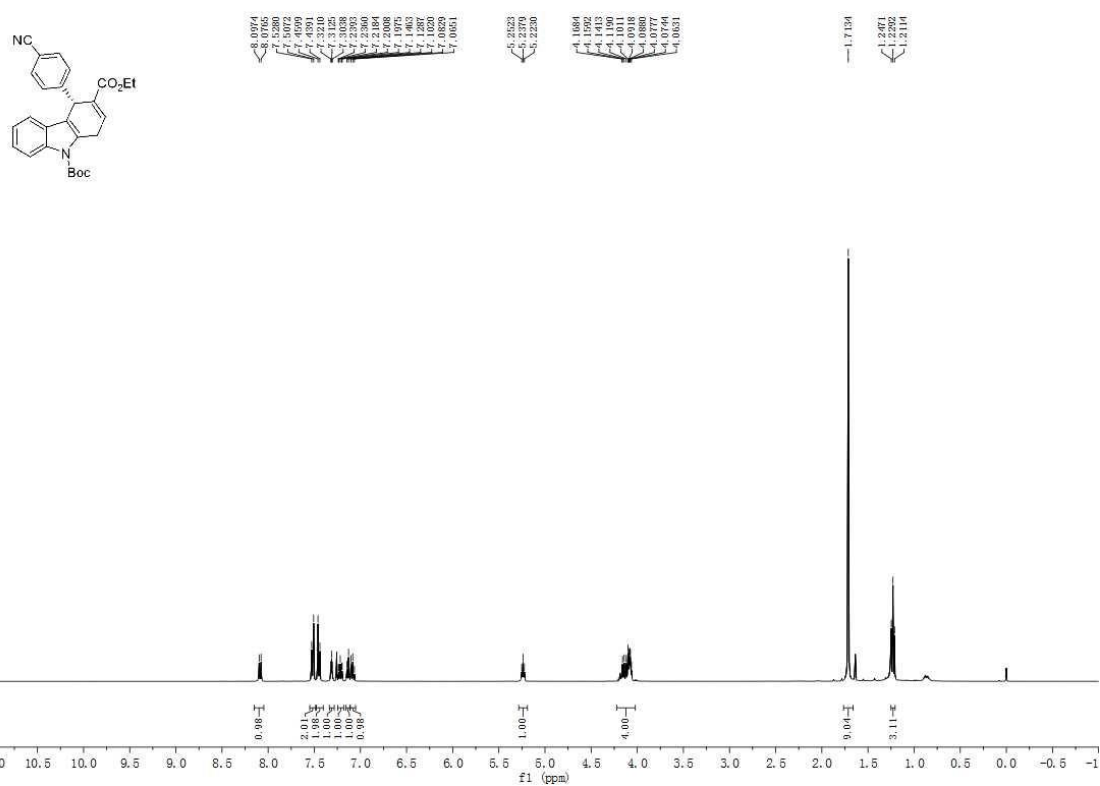


**Figure S37.**  $^{13}\text{C}$  NMR spectrum of **3q**, related to **Scheme 2**.

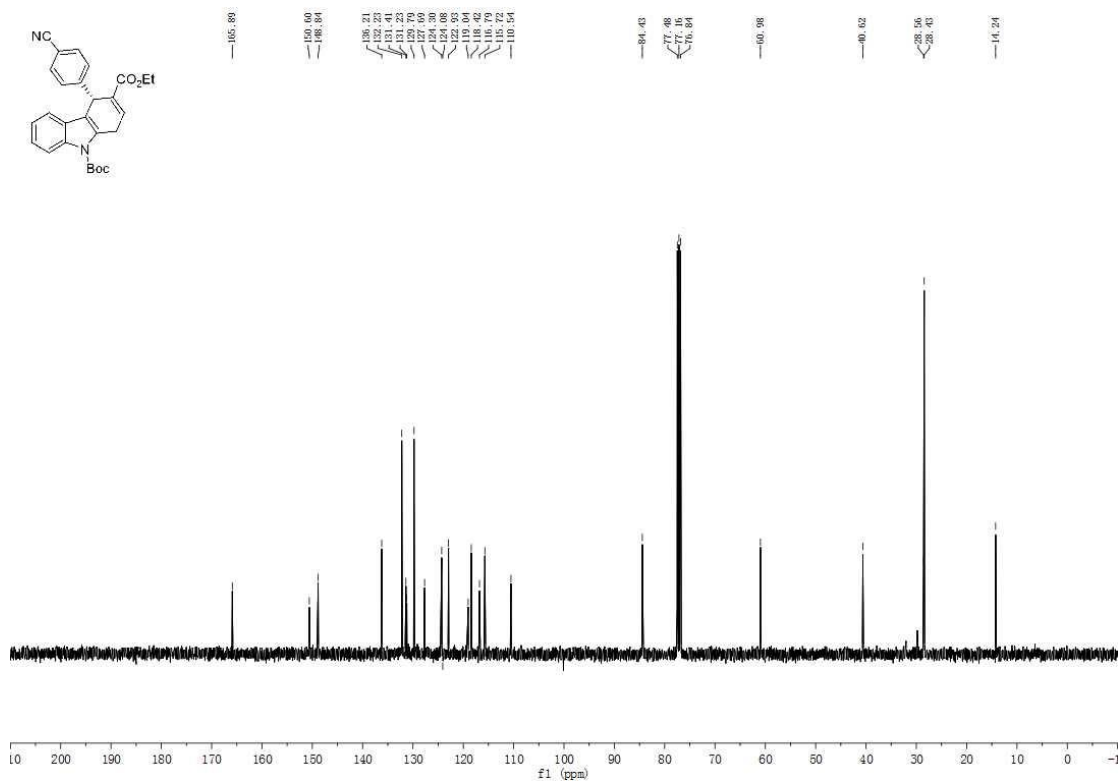


**Figure S38.**  $^1\text{H}$  NMR spectrum of **3r**, related to **Scheme 2**.

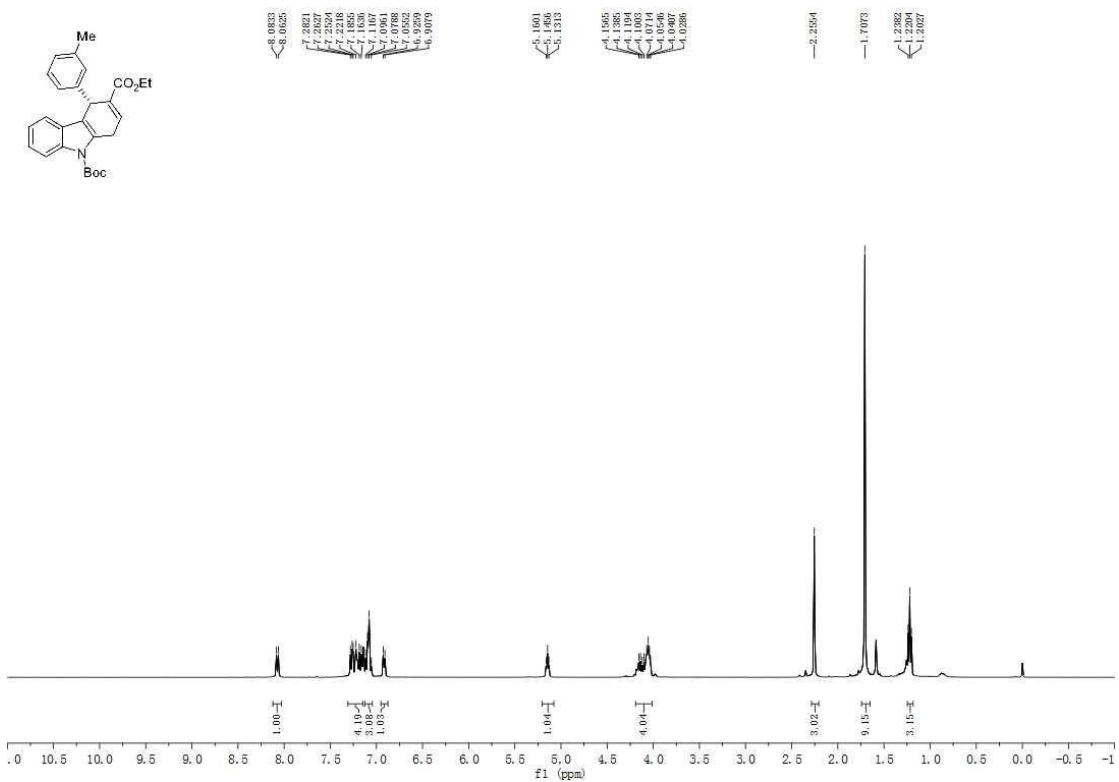


**Figure S39.**  $^{13}\text{C}$  NMR spectrum of **3r**, related to **Scheme 2**.

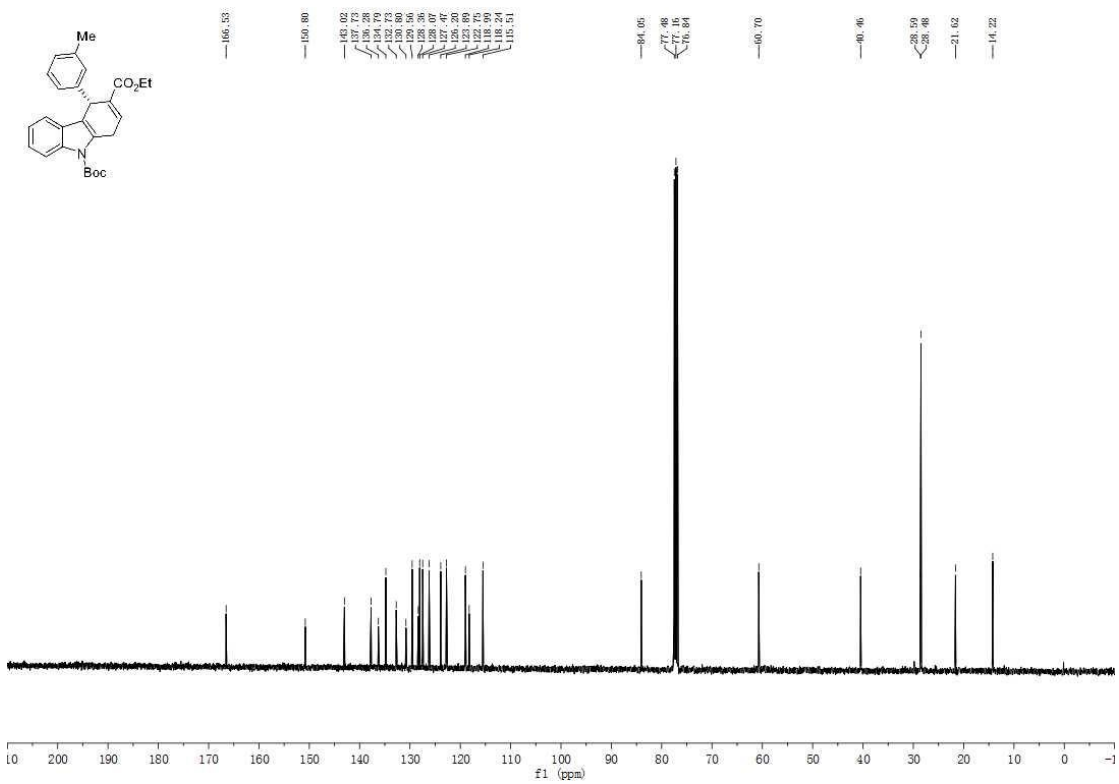


**Figure S40.**  $^1\text{H}$  NMR spectrum of **3s**, related to **Scheme 2**.

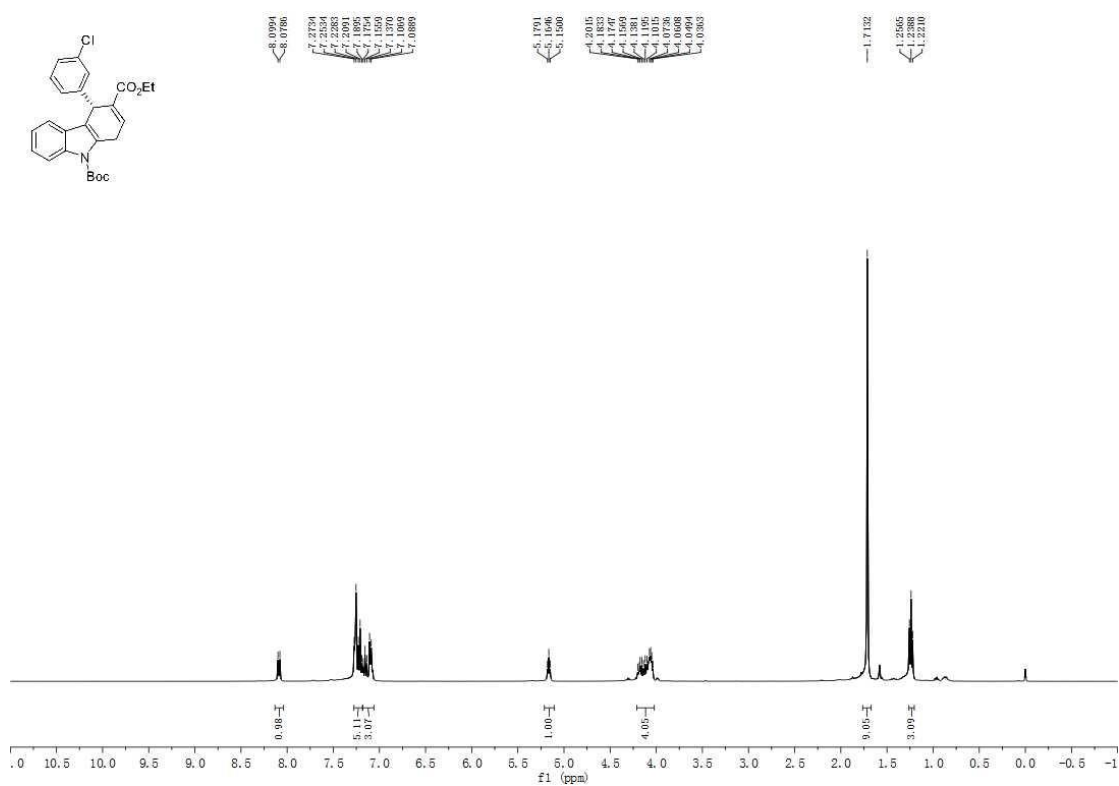


**Figure S42.**  $^1\text{H}$  NMR spectrum of **3t**, related to **Scheme 2**.

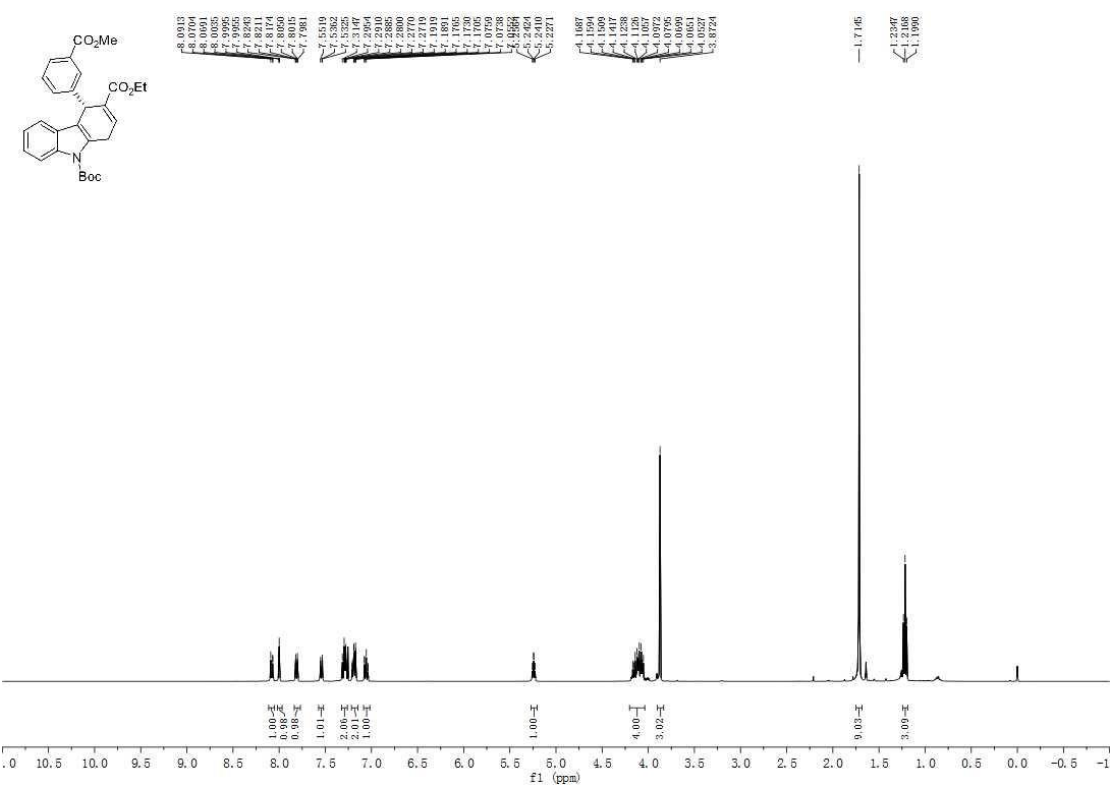


**Figure S43.**  $^{13}\text{C}$  NMR spectrum of **3t**, related to **Scheme 2**.

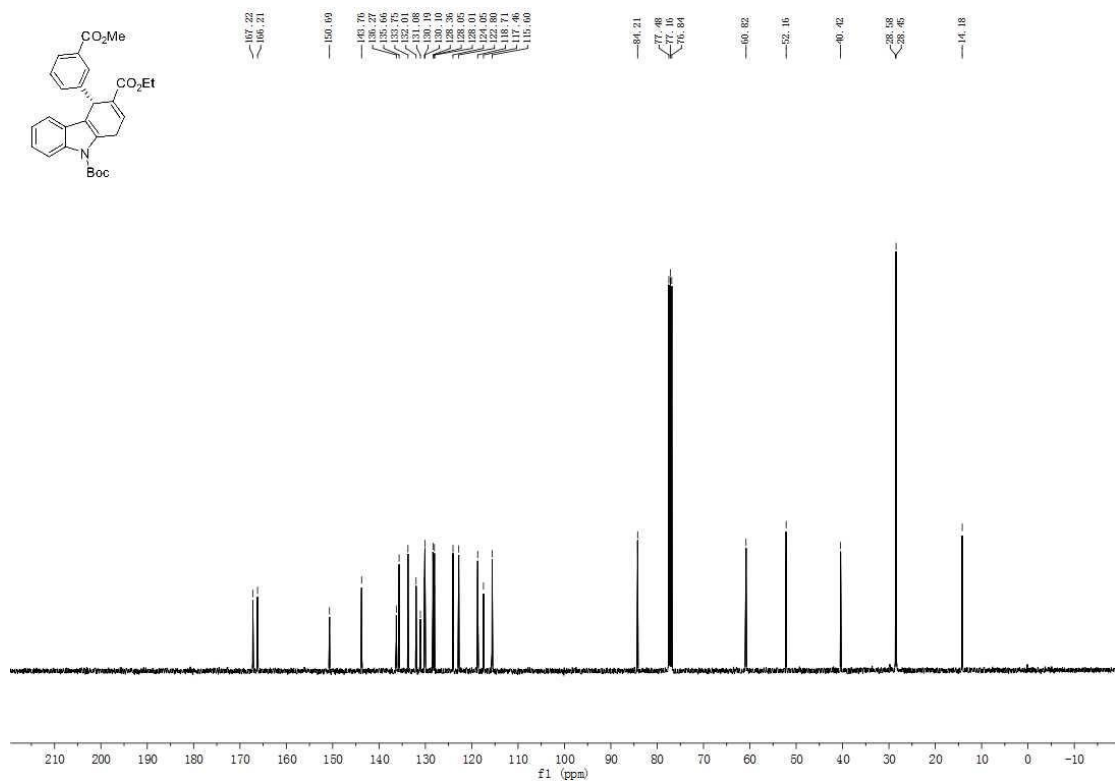


**Figure S44.**  $^1\text{H}$  NMR spectrum of **3u**, related to **Scheme 2**.

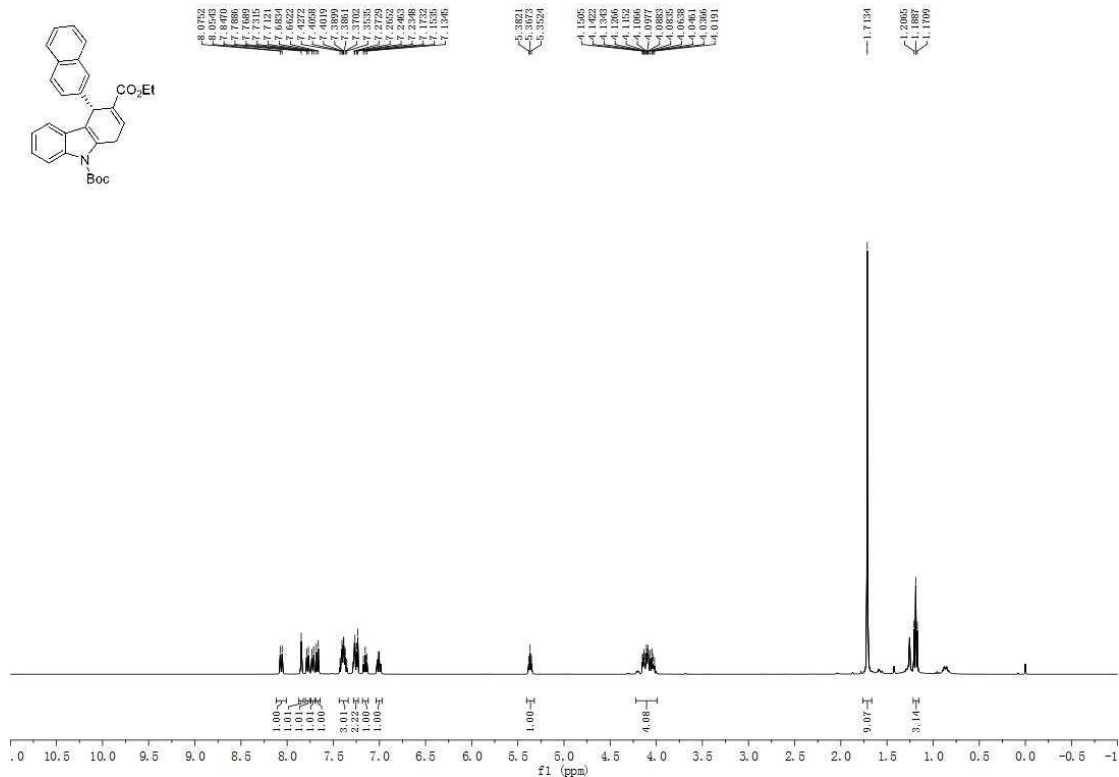


**Figure S45.**  $^{13}\text{C}$  NMR spectrum of **3u**, related to **Scheme 2**.

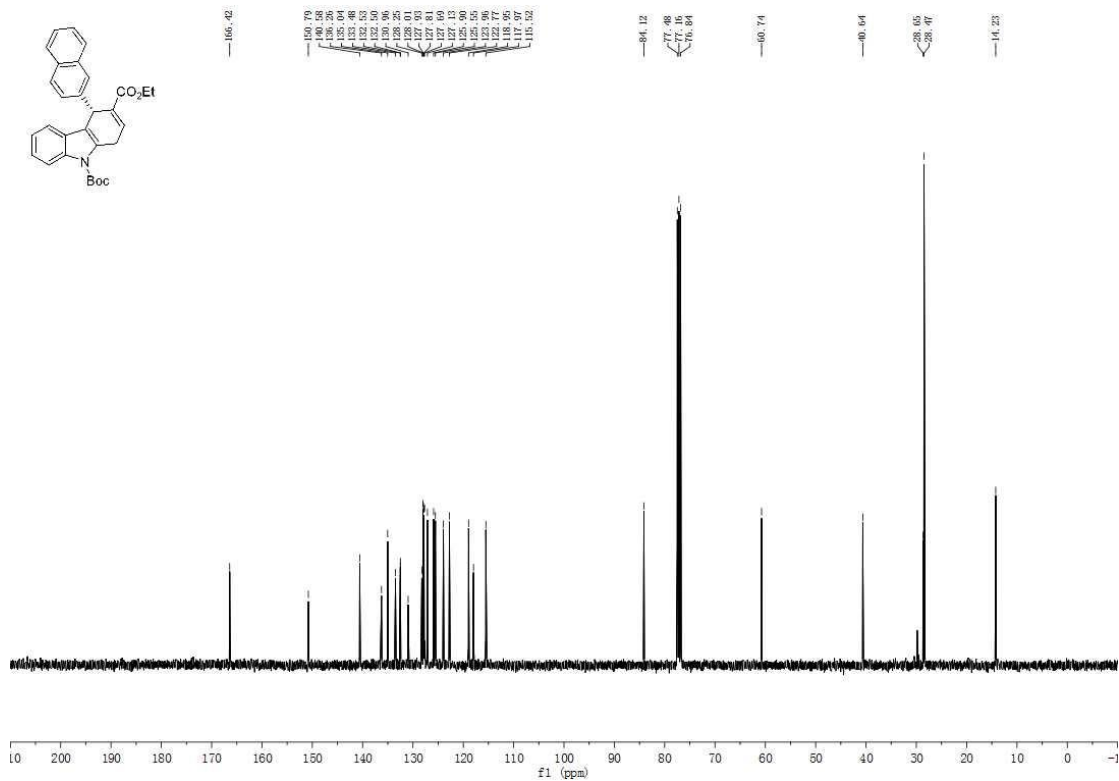


**Figure S46.**  $^1\text{H}$  NMR spectrum of **3v**, related to **Scheme 2**.

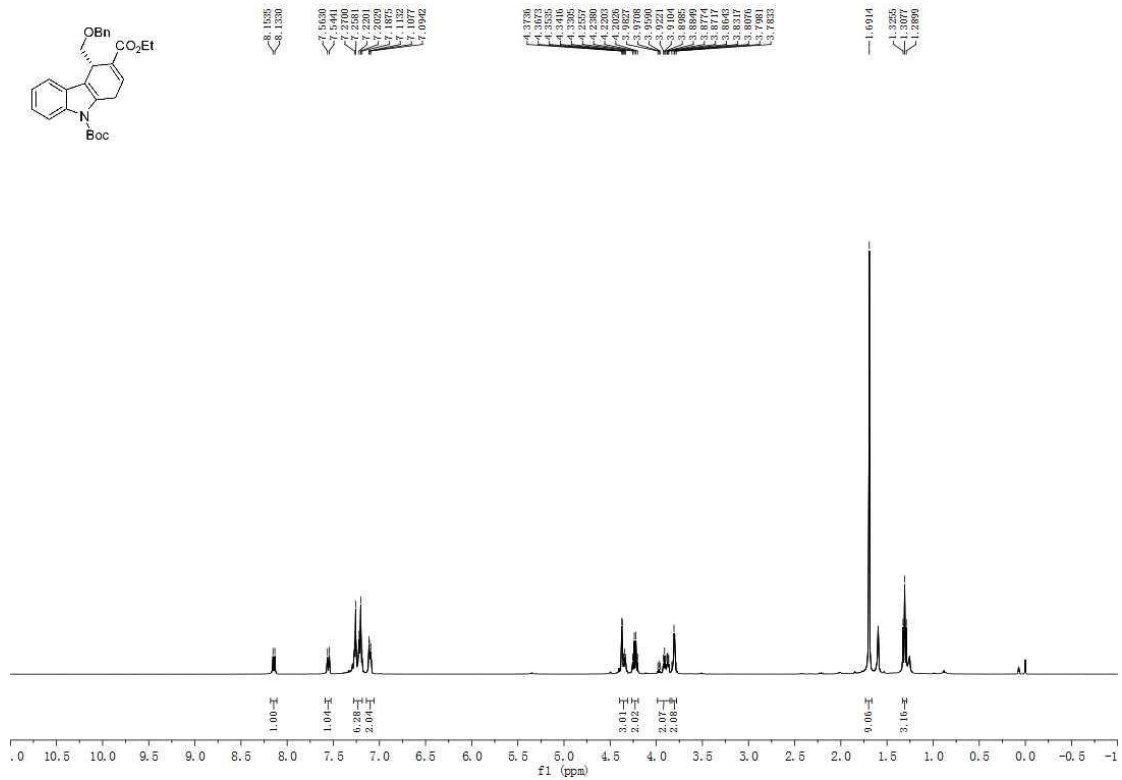


**Figure S47.**  $^{13}\text{C}$  NMR spectrum of **3v**, related to **Scheme 2**.

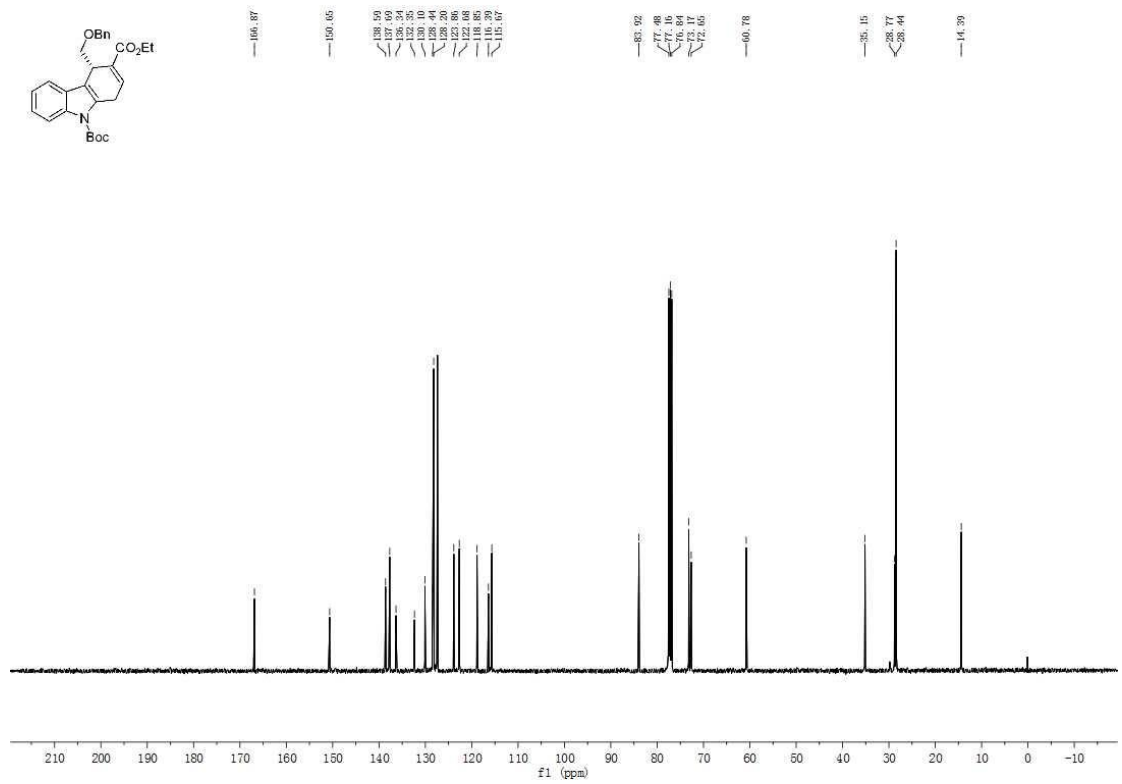


**Figure S48.**  $^1\text{H}$  NMR spectrum of **3w**, related to **Scheme 2**.

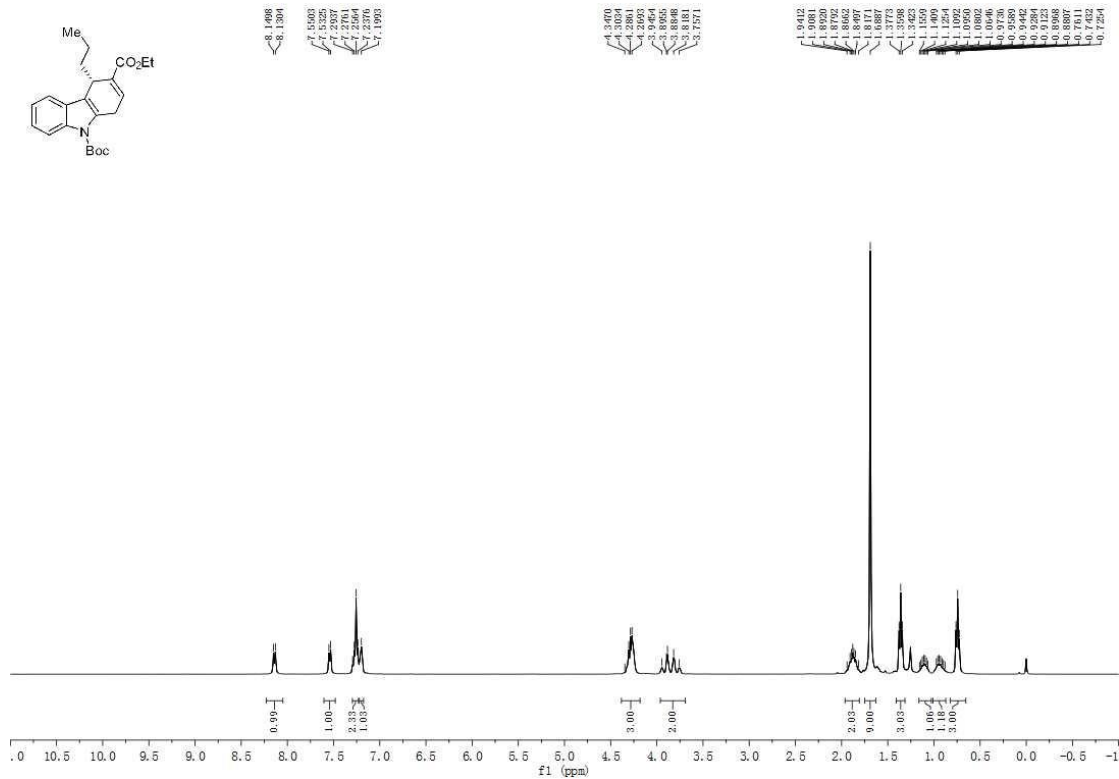


**Figure S49.**  $^{13}\text{C}$  NMR spectrum of **3w**, related to **Scheme 2**.

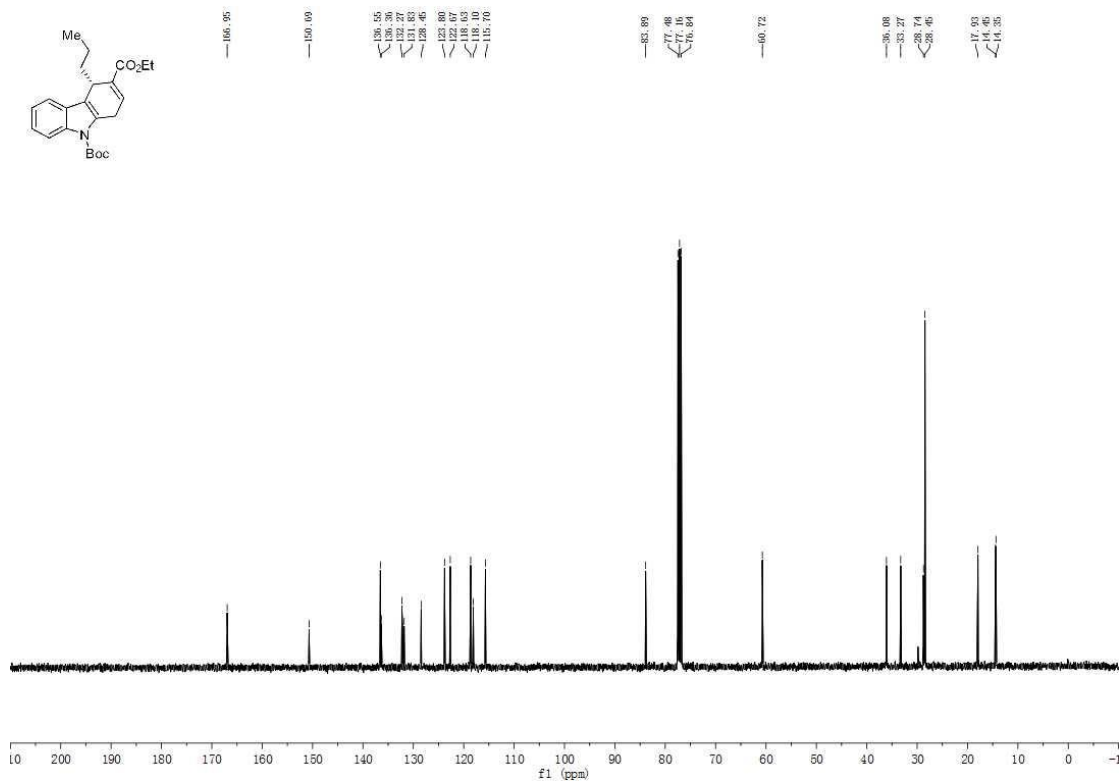


**Figure S50.**  $^1\text{H}$  NMR spectrum of **3x**, related to **Scheme 2**.

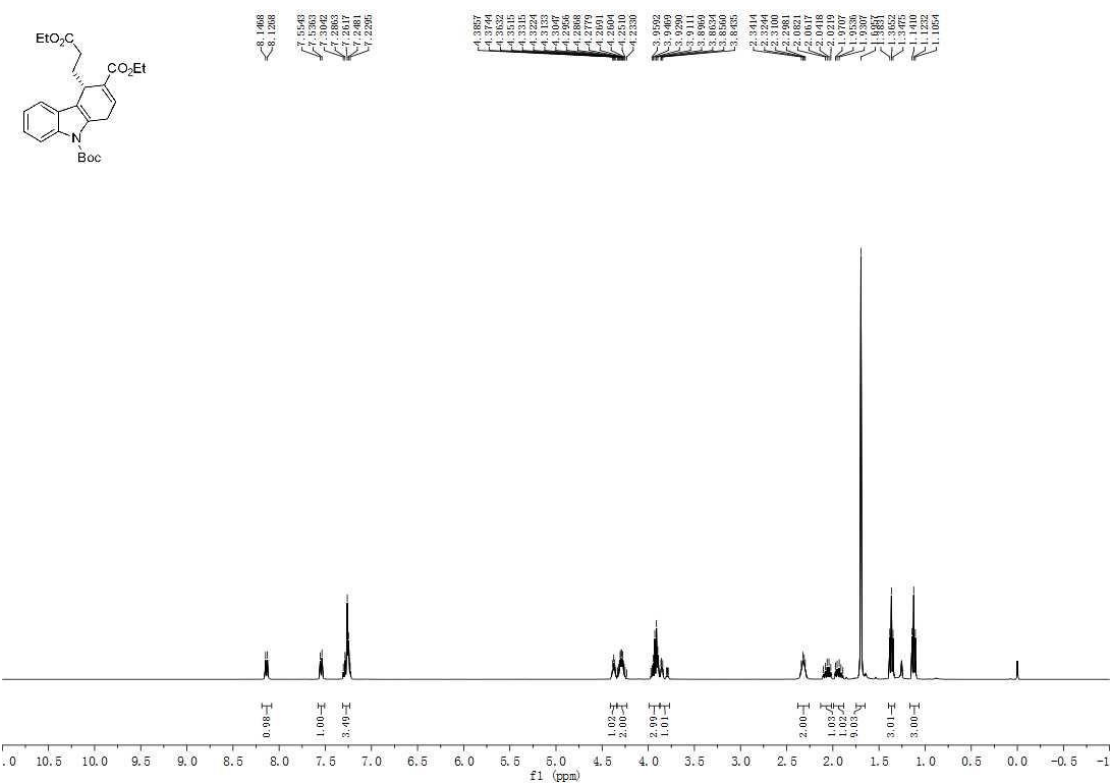


**Figure S51.**  $^{13}\text{C}$  NMR spectrum of **3x**, related to **Scheme 2**.

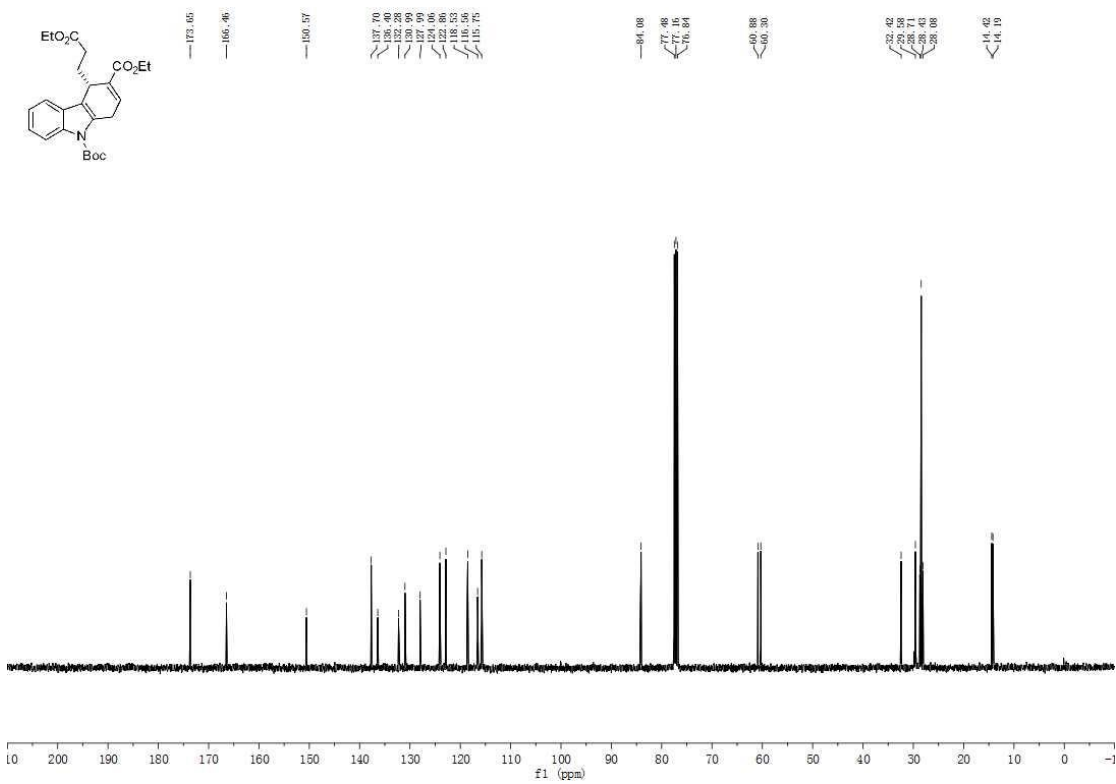


**Figure S52.**  $^1\text{H}$  NMR spectrum of **3y**, related to **Scheme 2**.

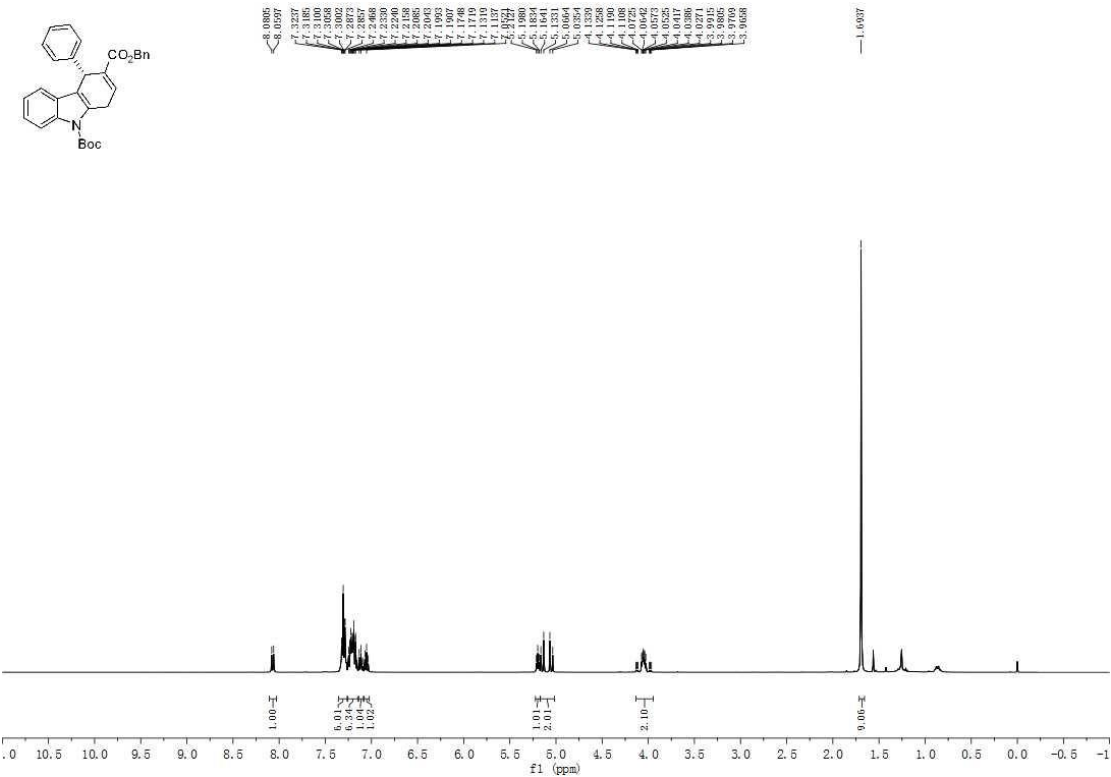


**Figure S53.**  $^{13}\text{C}$  NMR spectrum of **3y**, related to **Scheme 2**.

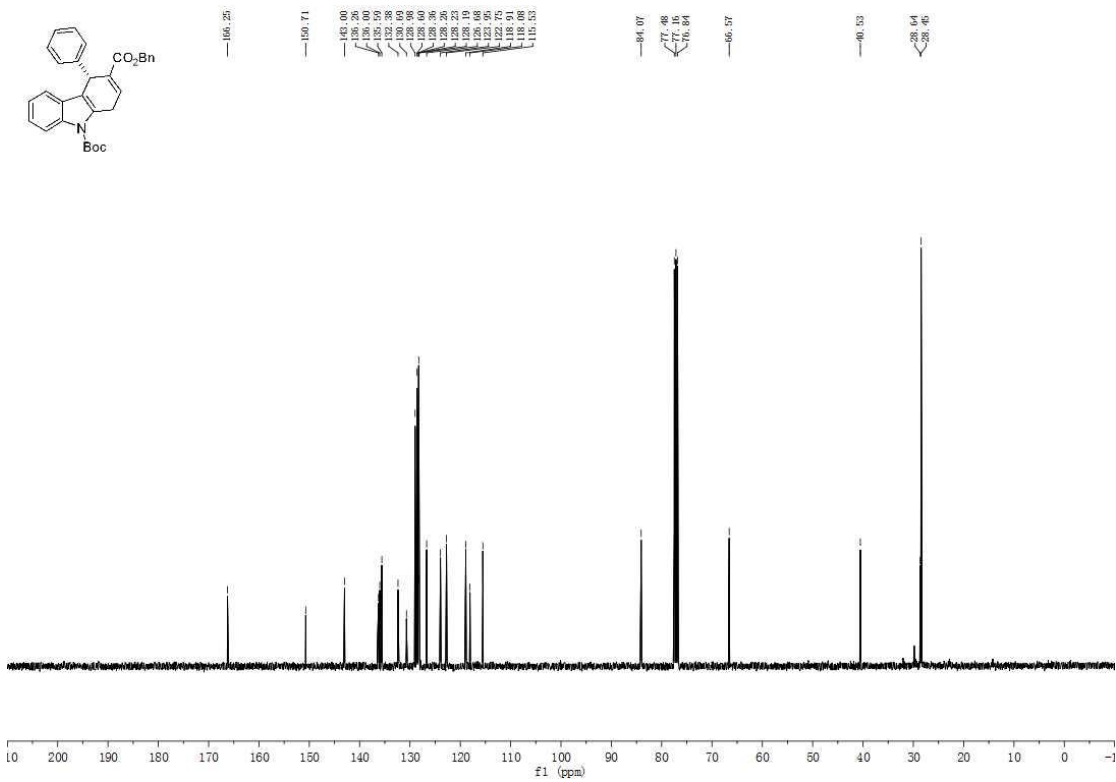


**Figure S54.**  $^1\text{H}$  NMR spectrum of **3z**, related to **Scheme 2**.

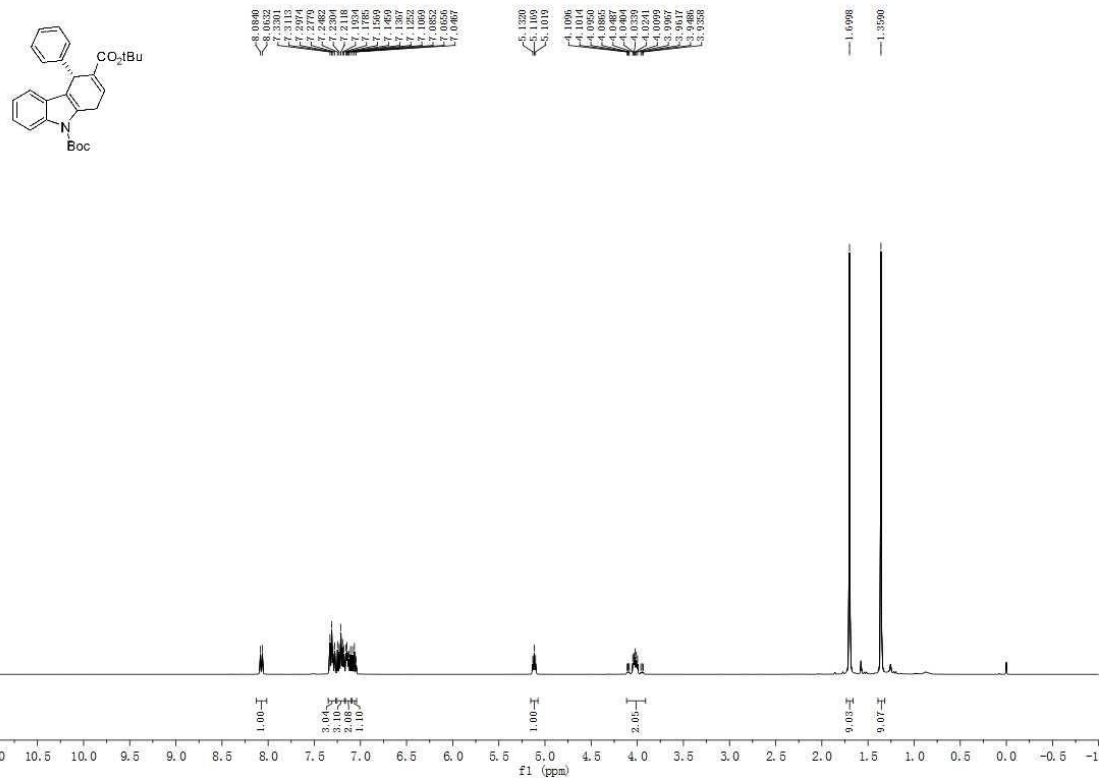


**Figure S55.**  $^{13}\text{C}$  NMR spectrum of **3z**, related to **Scheme 2**.

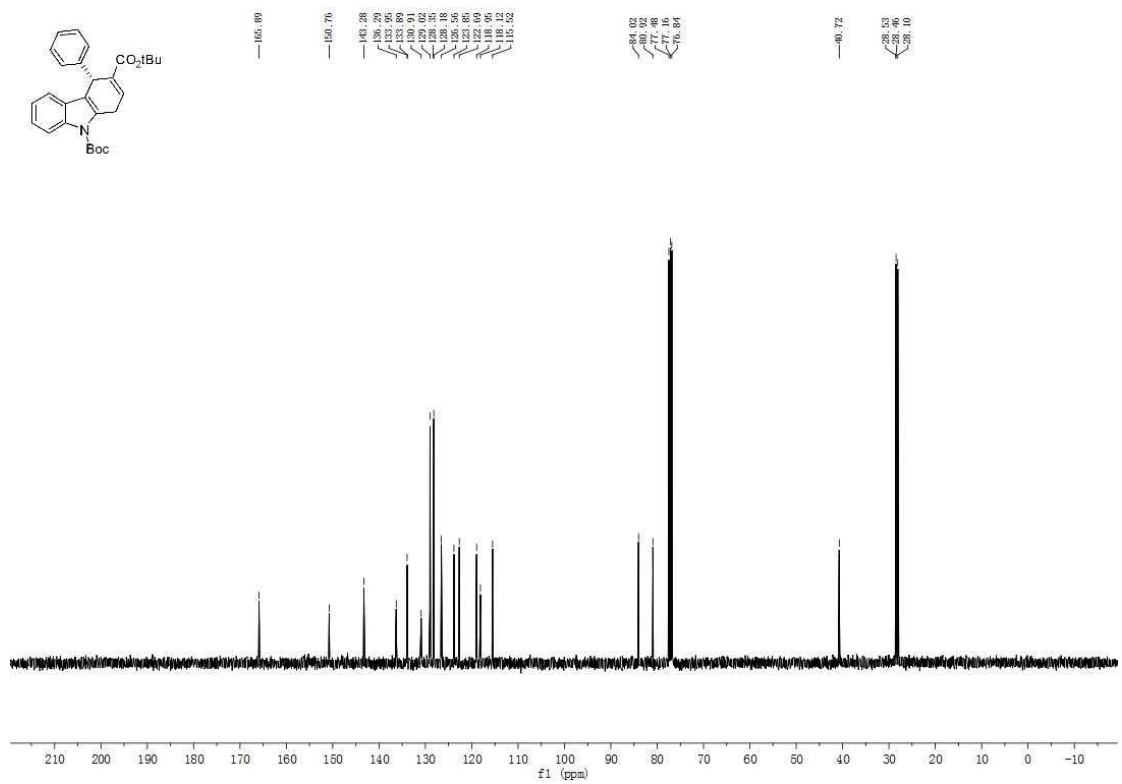


**Figure S56.**  $^1\text{H}$  NMR spectrum of **6a**, related to **Scheme 3**.

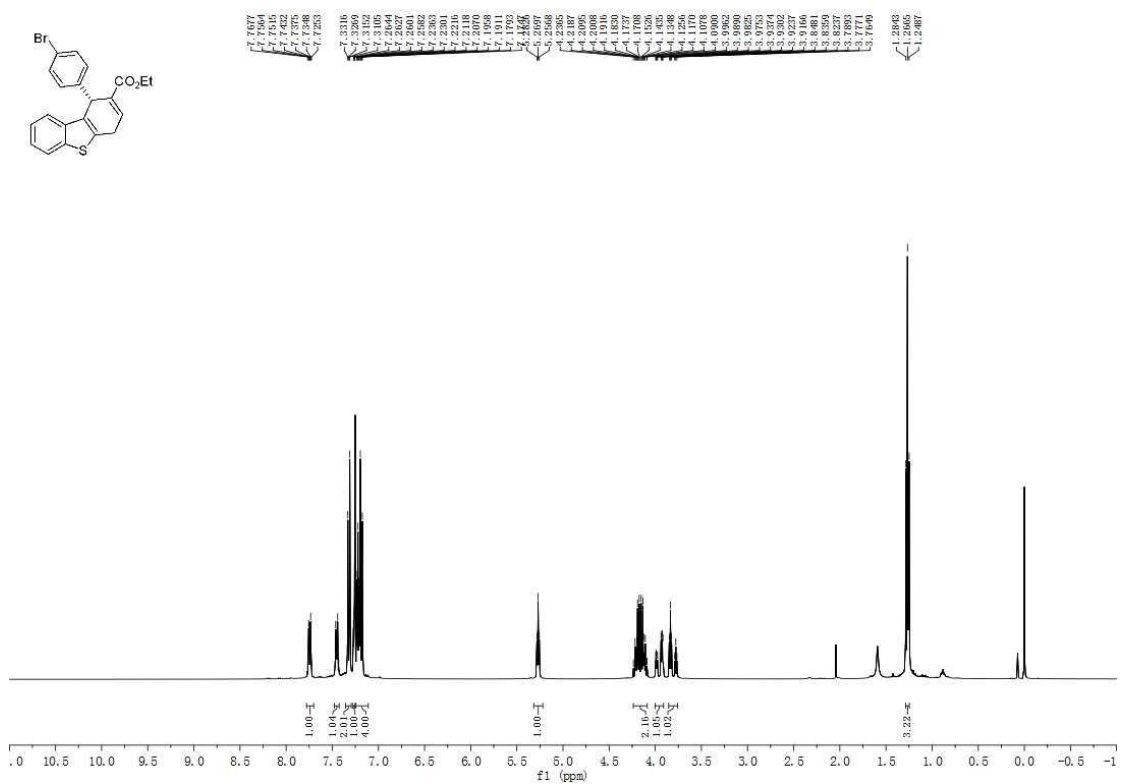


**Figure S57.**  $^{13}\text{C}$  NMR spectrum of **6a**, related to **Scheme 3**.

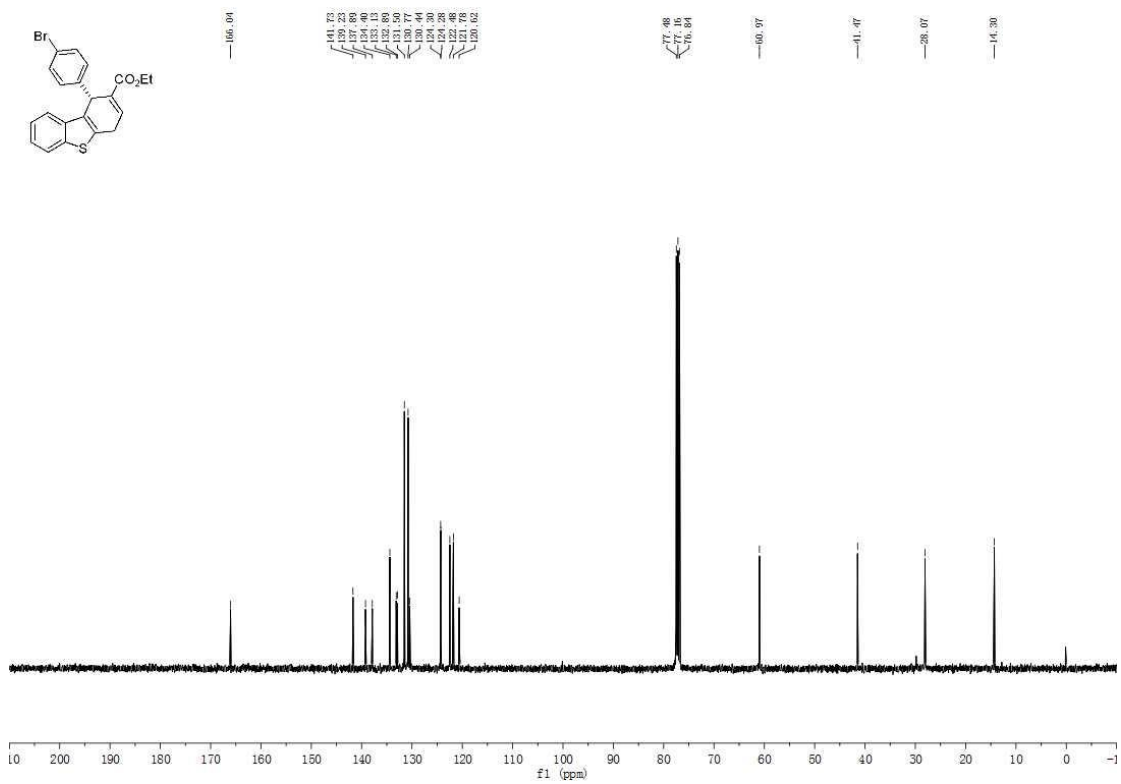


**Figure S58.**  $^1\text{H}$  NMR spectrum of **6b**, related to **Scheme 3**.

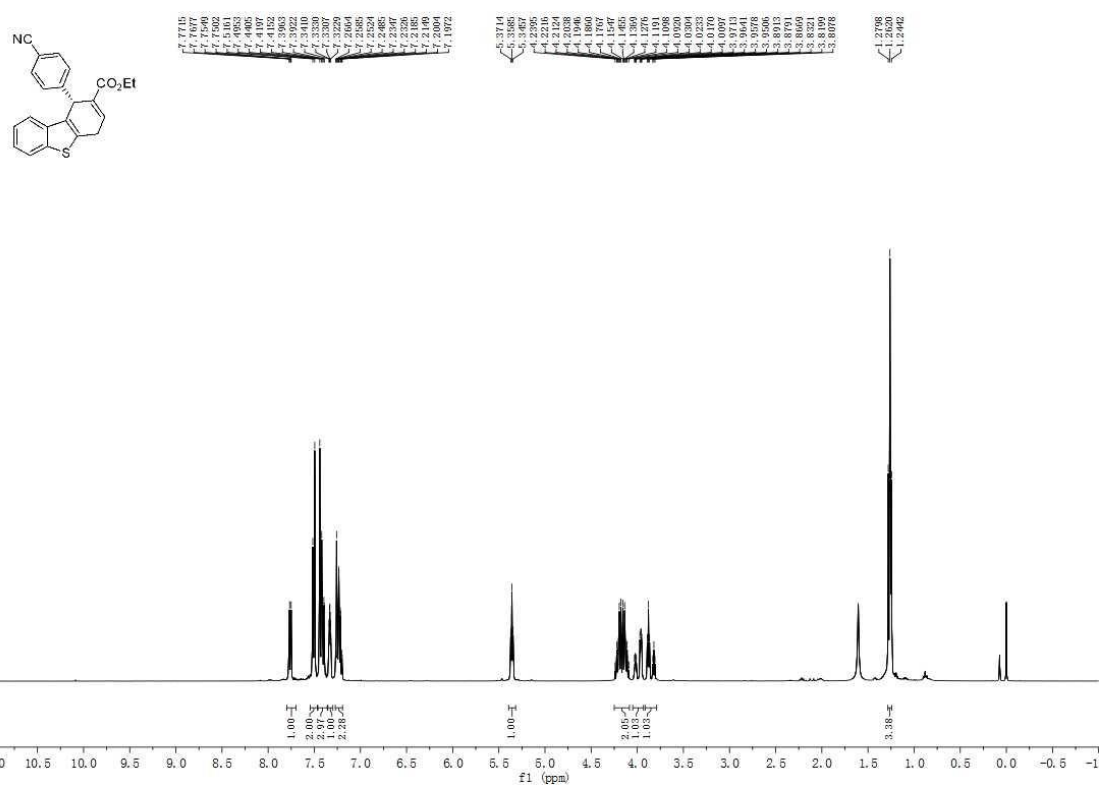


**Figure S59.**  $^{13}\text{C}$  NMR spectrum of **6b**, related to **Scheme 3**.

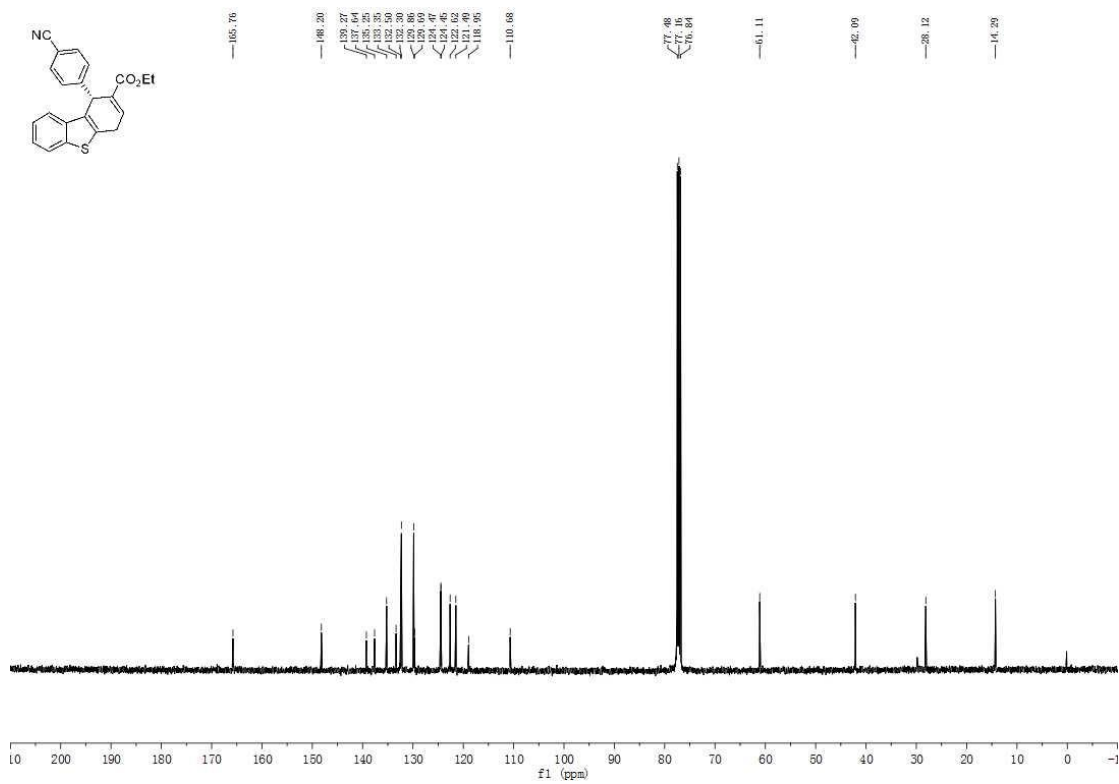


**Figure S60.**  $^1\text{H}$  NMR spectrum of **6c**, related to **Scheme 3**.

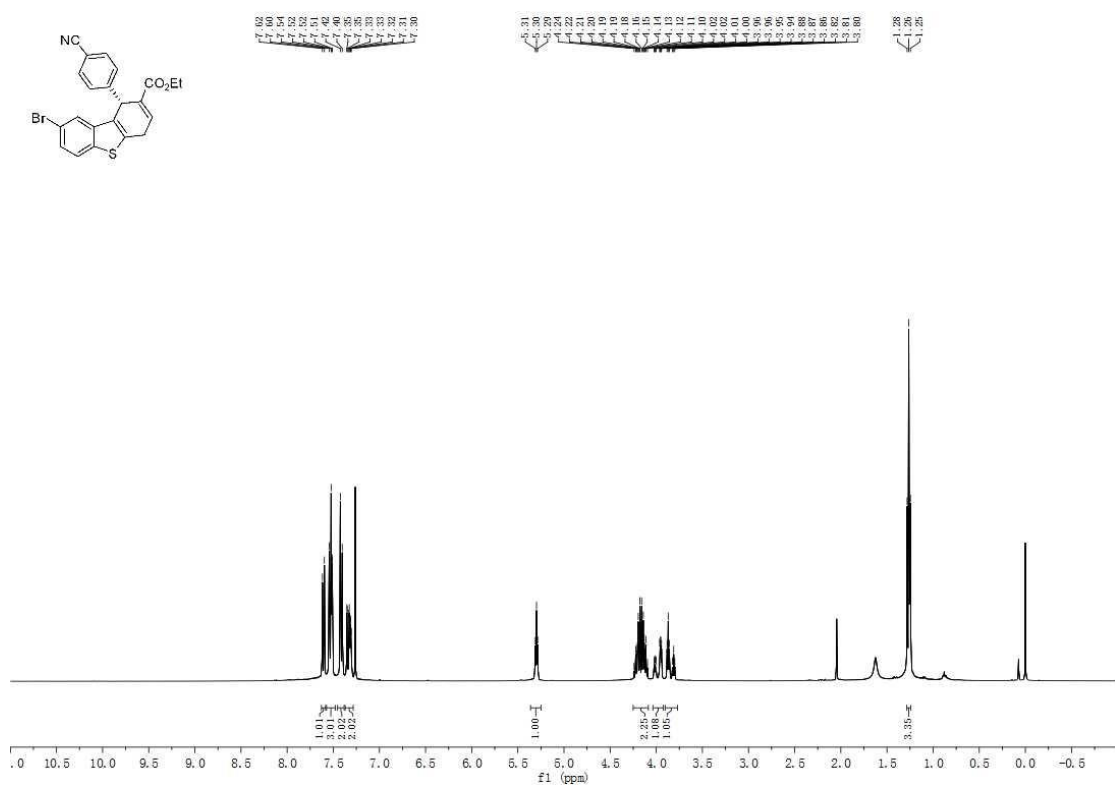


**Figure S61.**  $^{13}\text{C}$  NMR spectrum of **6c**, related to **Scheme 3**.

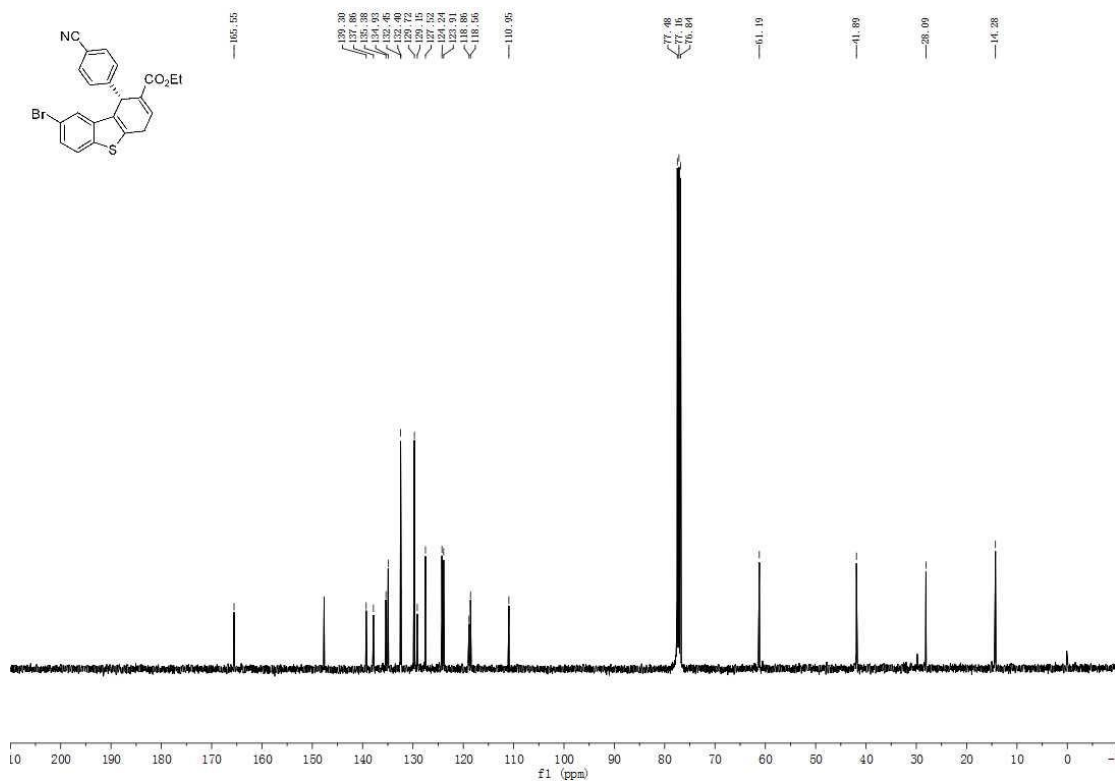


**Figure S62.**  $^1\text{H}$  NMR spectrum of **6d**, related to **Scheme 3**.

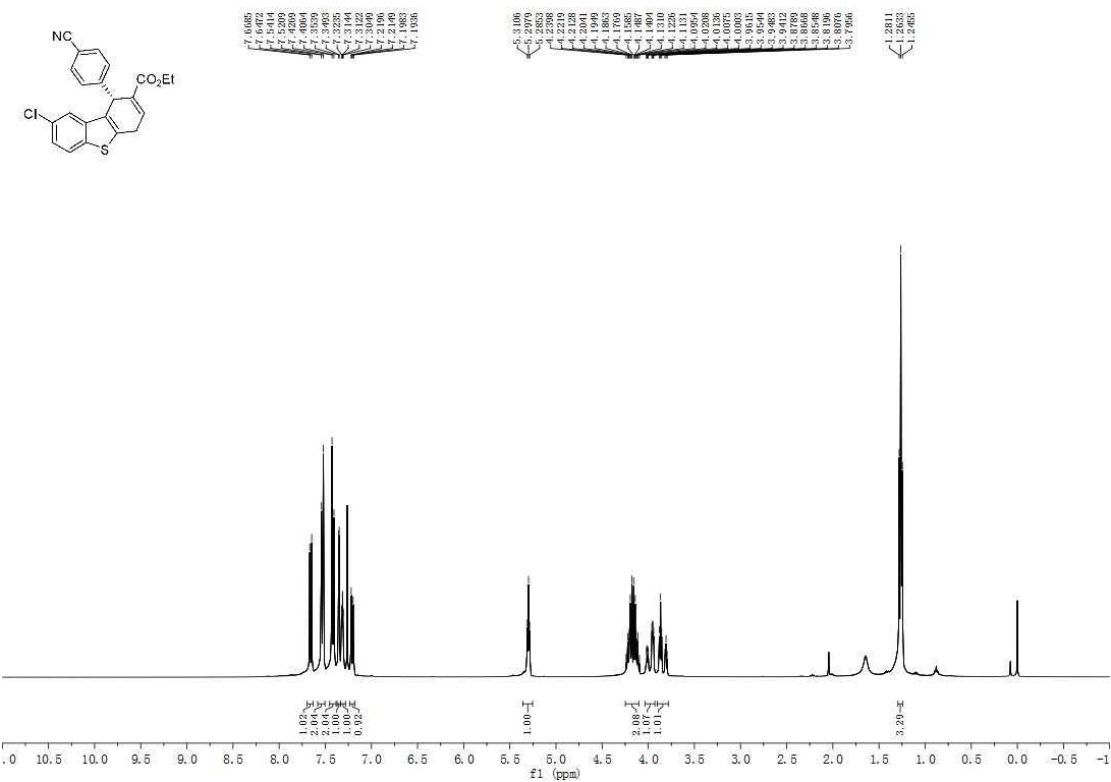


**Figure S63.**  $^{13}\text{C}$  NMR spectrum of **6d**, related to **Scheme 3**.

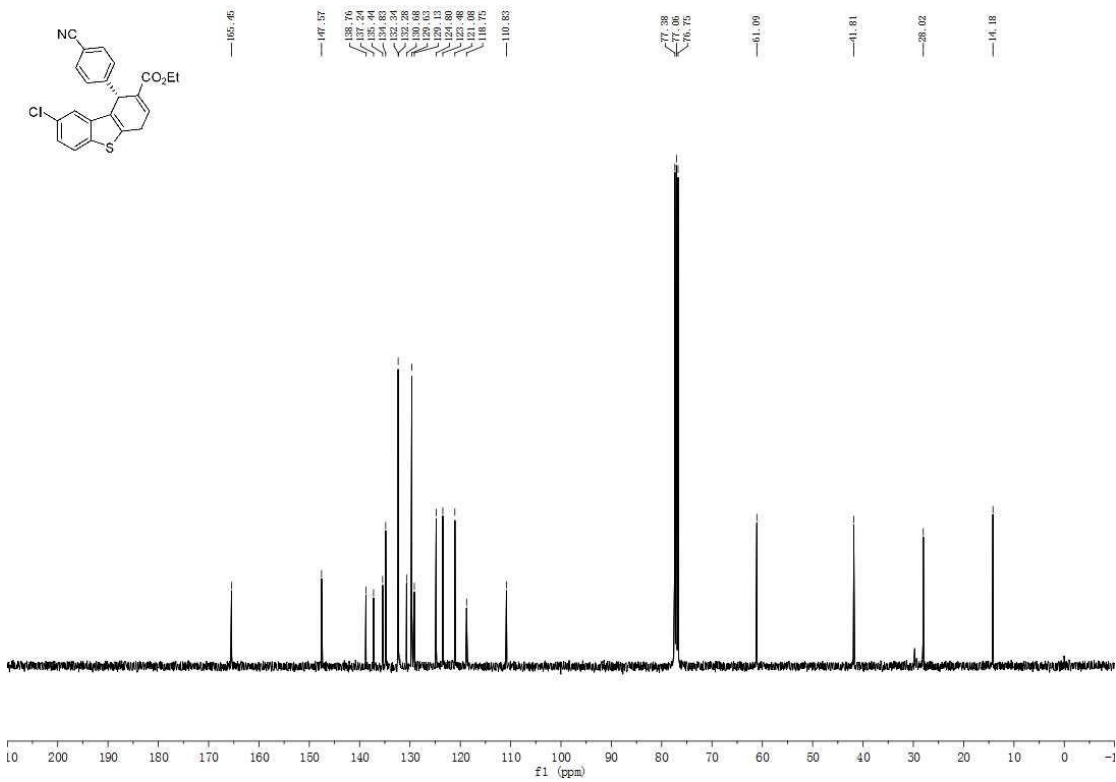


**Figure S64.**  $^1\text{H}$  NMR spectrum of **6e**, related to **Scheme 3**.

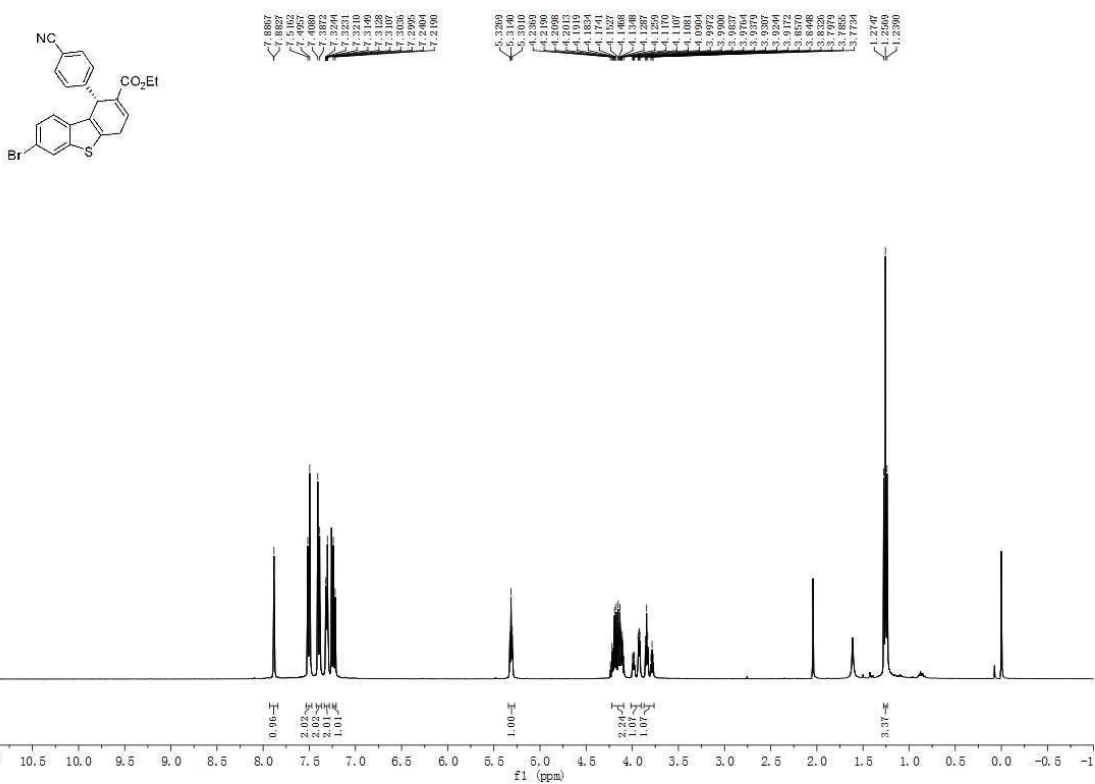


**Figure S65.**  $^{13}\text{C}$  NMR spectrum of **6e**, related to **Scheme 3**.

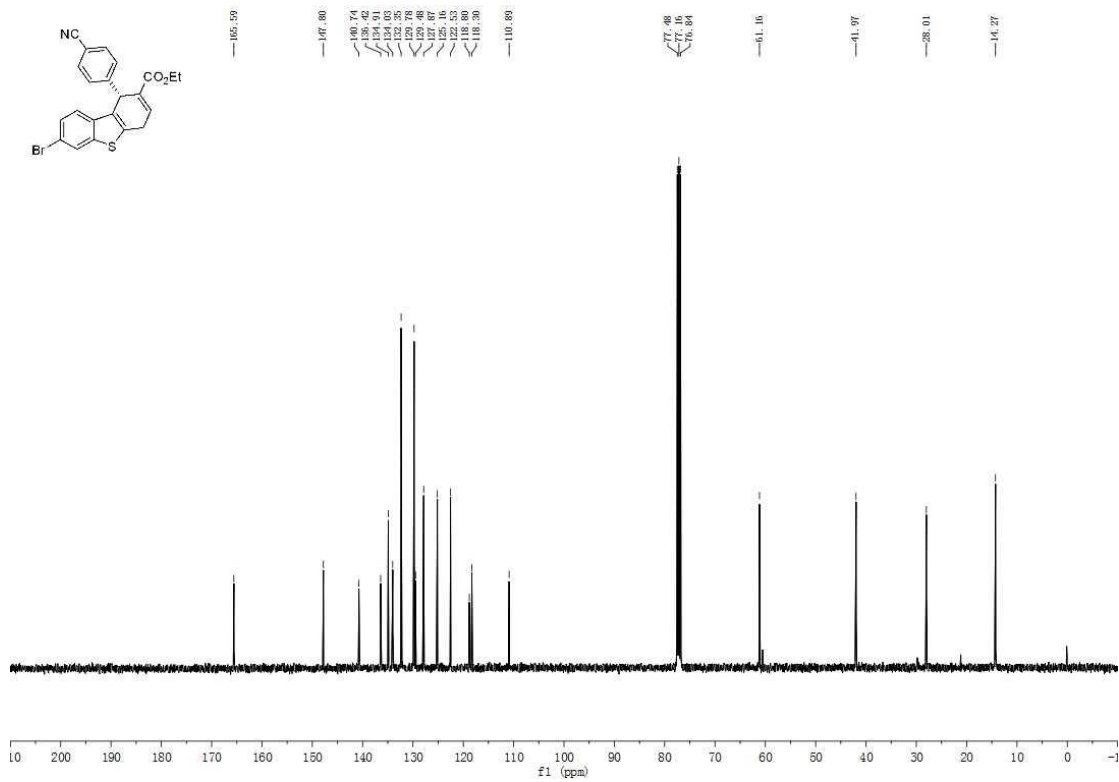


**Figure S66.**  $^1\text{H}$  NMR spectrum of **6f**, related to **Scheme 3**.

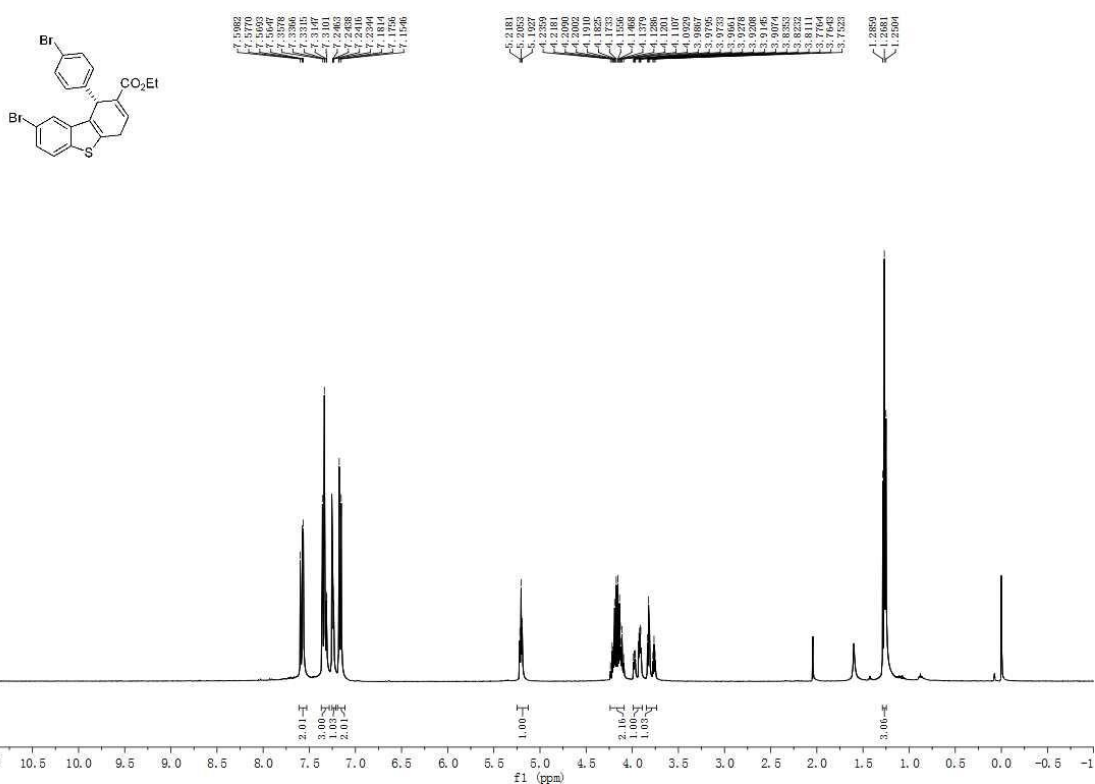


**Figure S67.**  $^{13}\text{C}$  NMR spectrum of **6f**, related to **Scheme 3**.

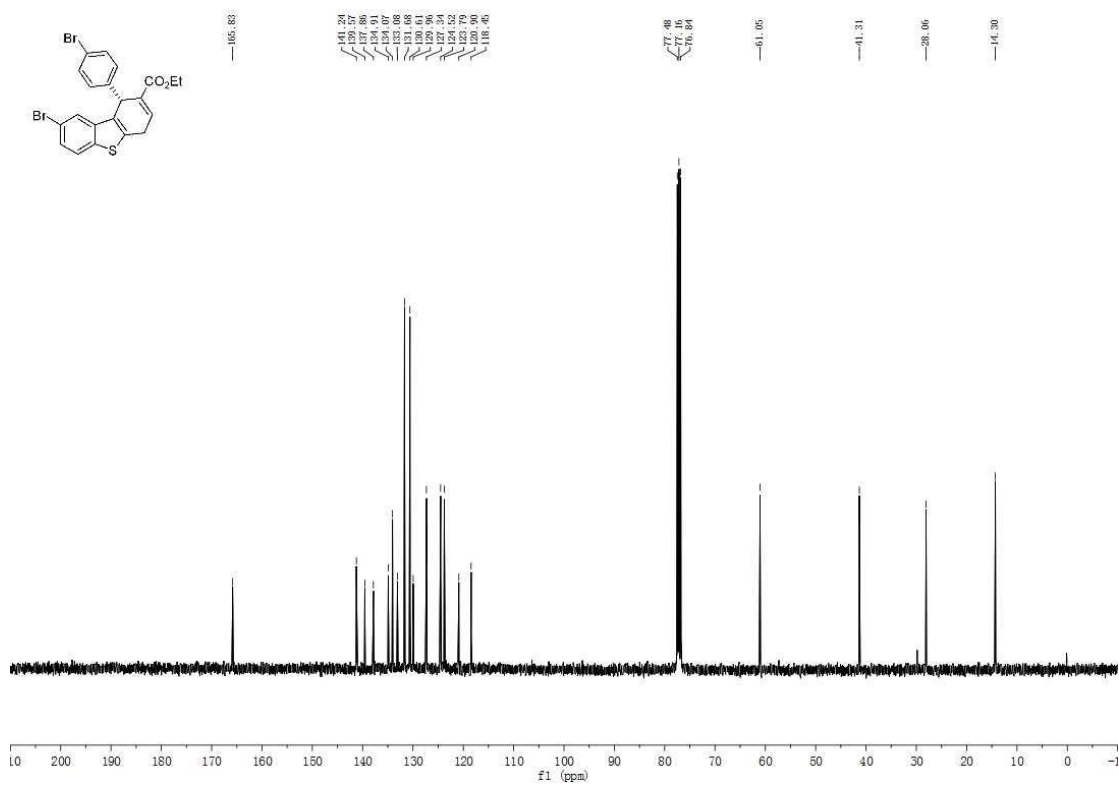


**Figure S68.**  $^1\text{H}$  NMR spectrum of **6g**, related to **Scheme 3**.

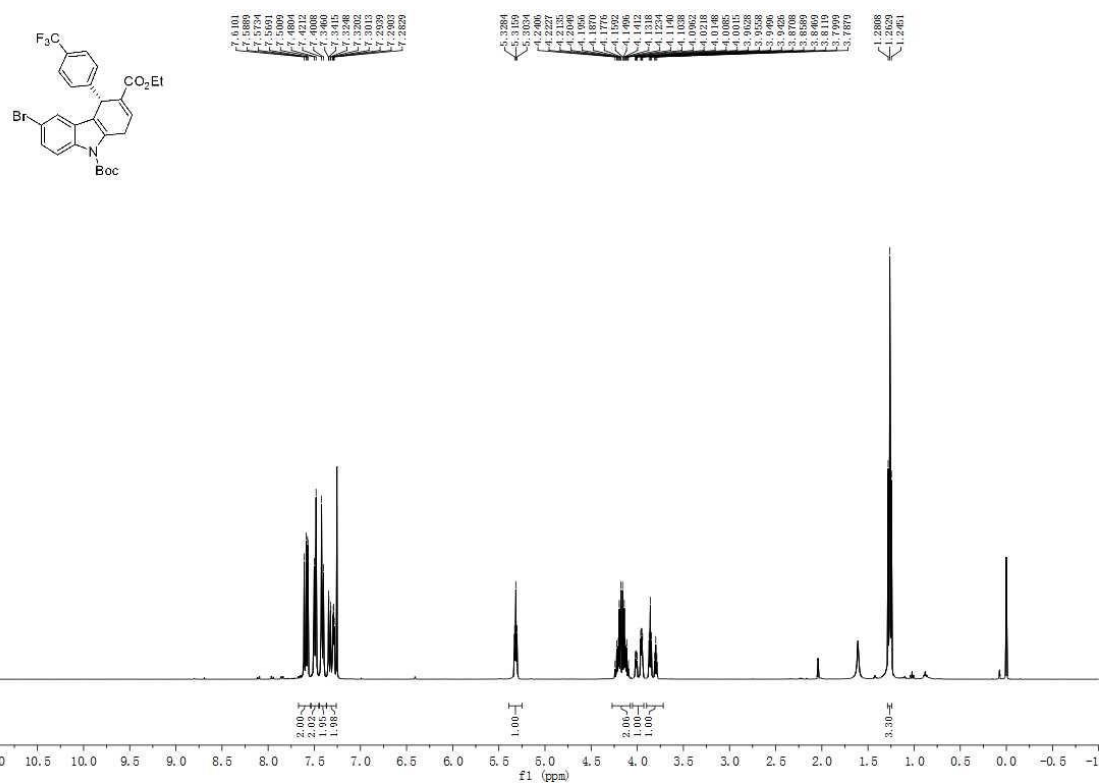


**Figure S69.**  $^{13}\text{C}$  NMR spectrum of **6g**, related to **Scheme 3**.

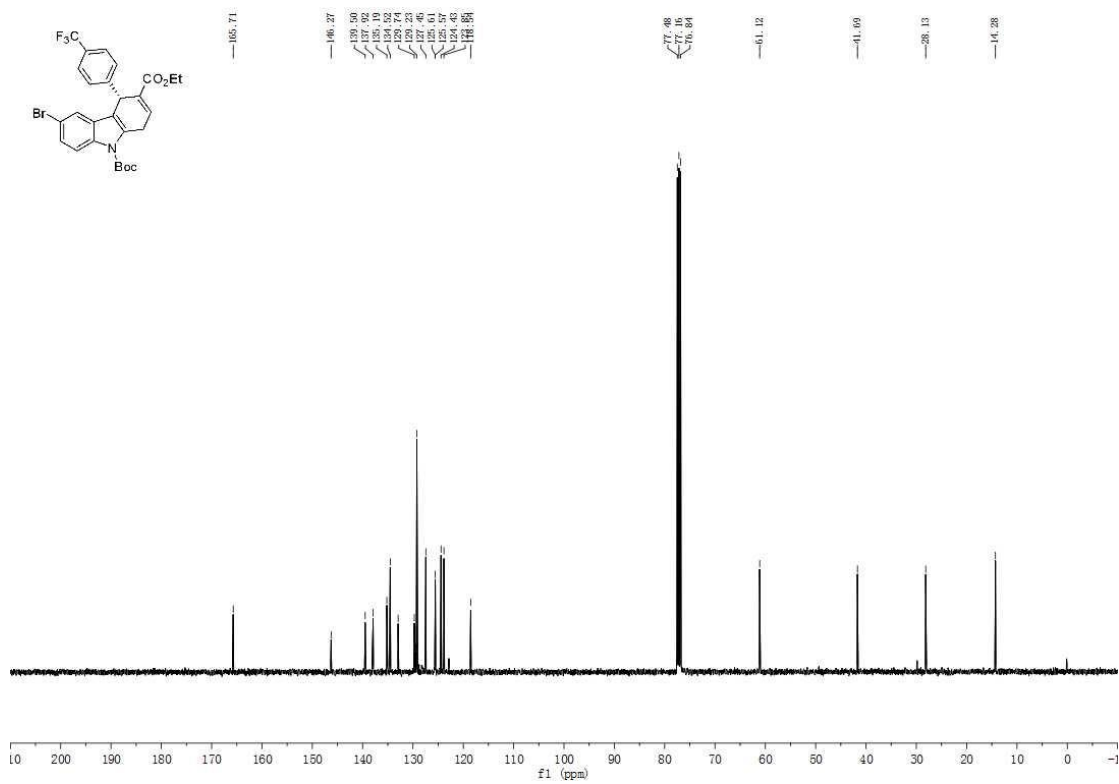


**Figure S70.**  $^{19}\text{F}$  NMR spectrum of **6g**, related to **Scheme 3**.

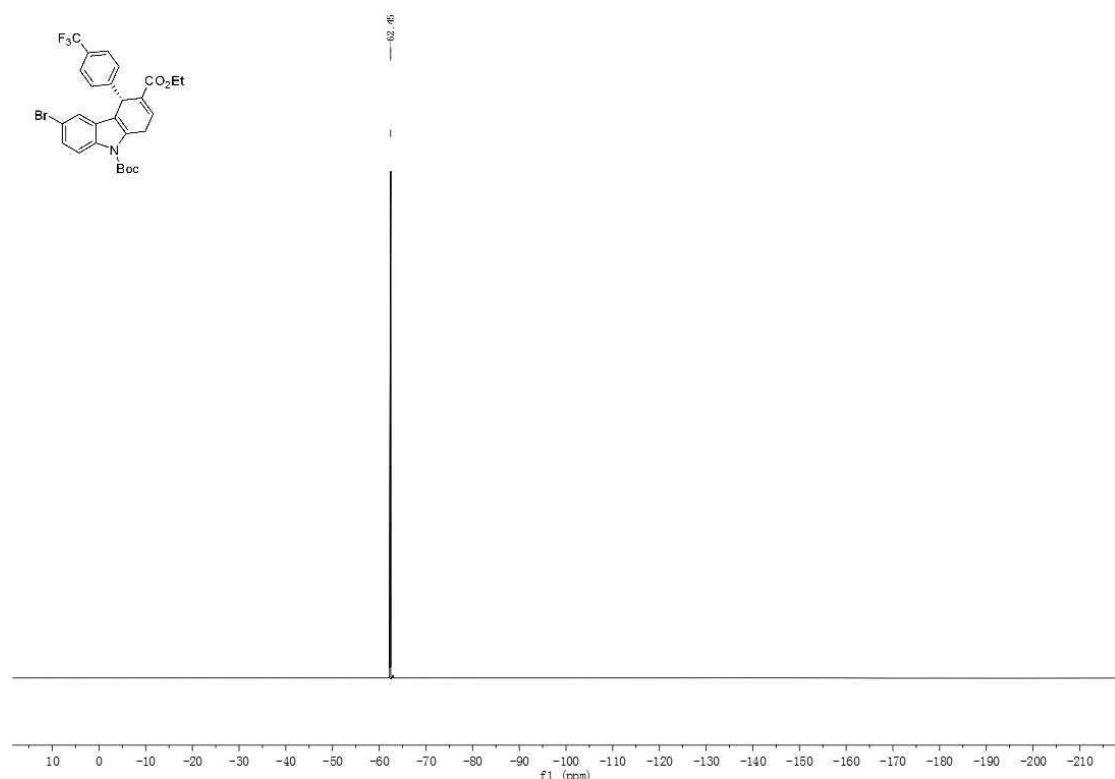


**Figure S71.**  $^1\text{H}$  NMR spectrum of **6h**, related to **Scheme 3**.

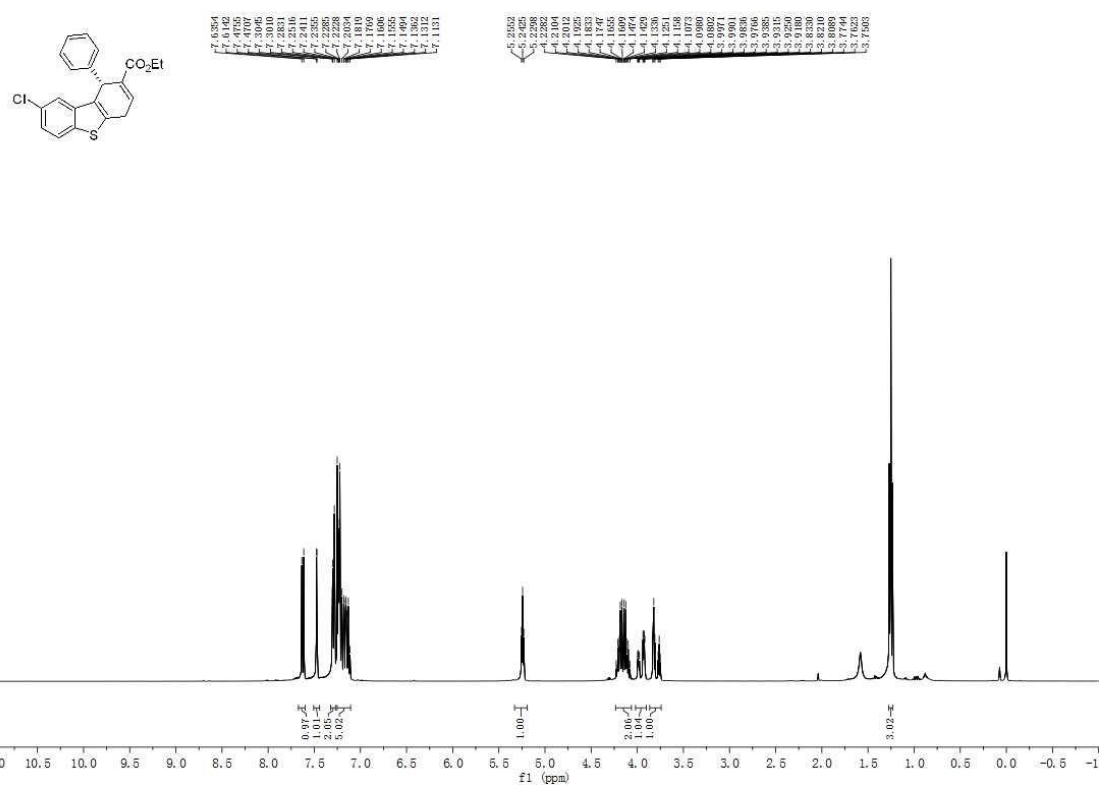


**Figure S72.**  $^{13}\text{C}$  NMR spectrum of **6h**, related to **Scheme 3**.

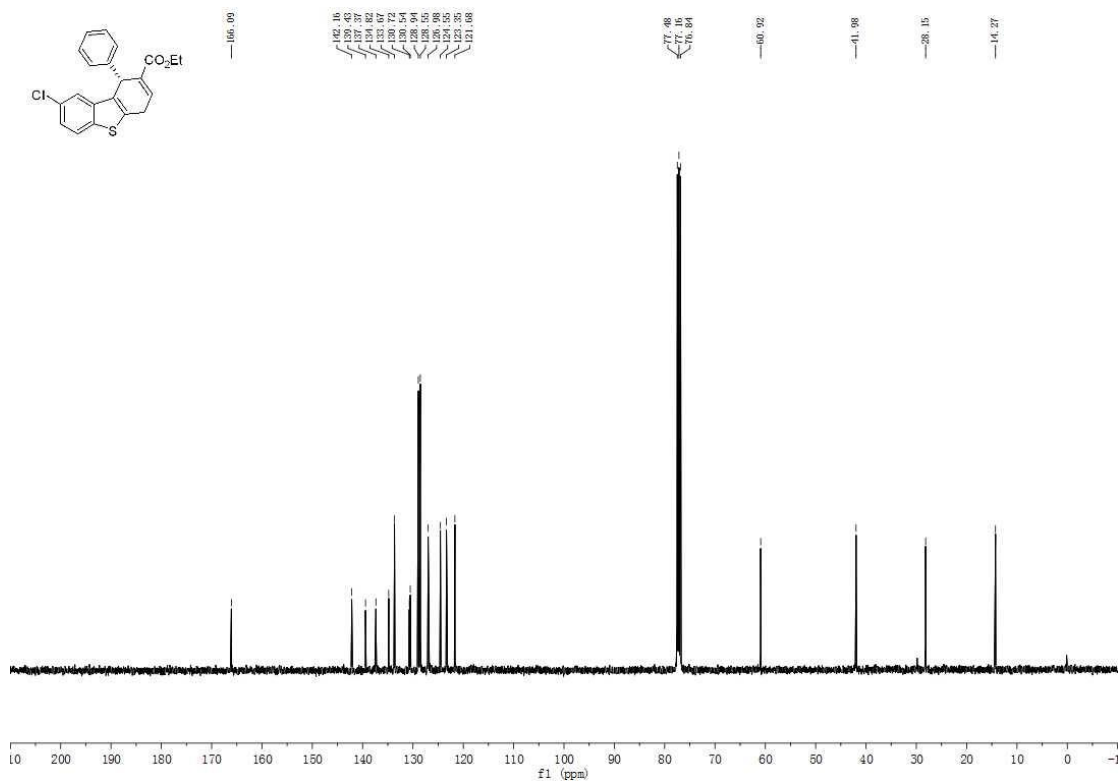


**Figure S73.**  $^1\text{H}$  NMR spectrum of **7**, related to **Scheme 4**.

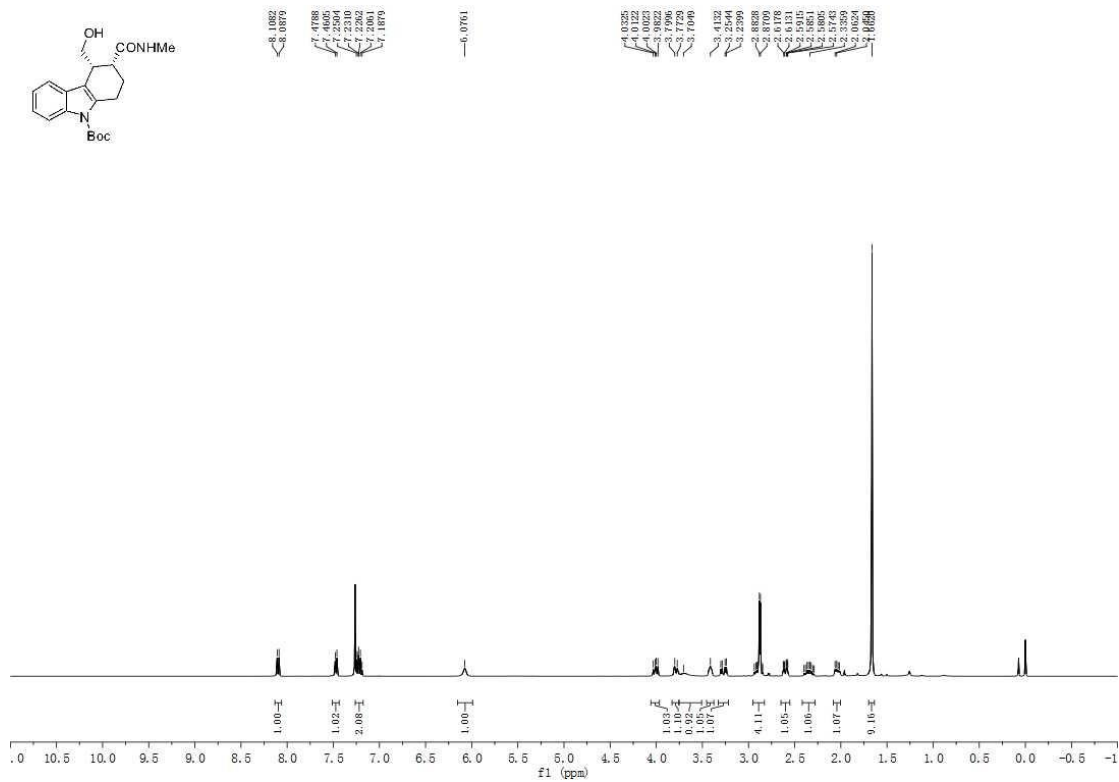


**Figure S74.**  $^{13}\text{C}$  NMR spectrum of **7**, related to **Scheme 4**.

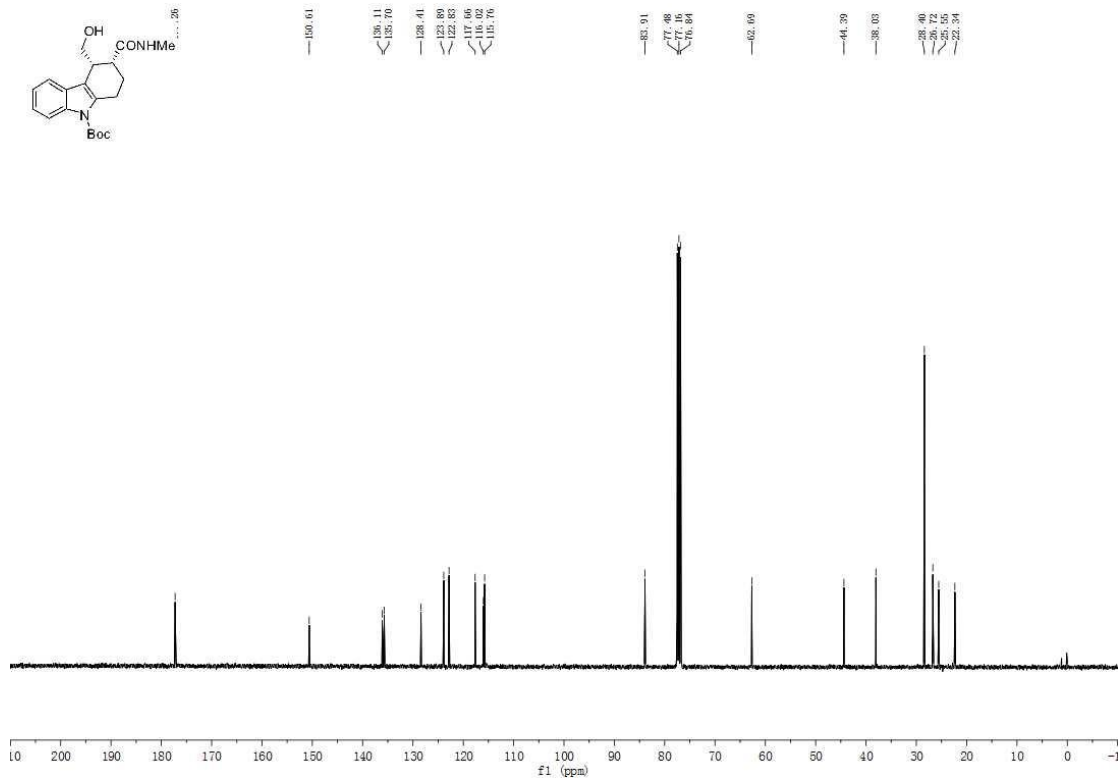


**Figure S75.**  $^1\text{H}$  NMR spectrum of **8**, related to **Scheme 4**.

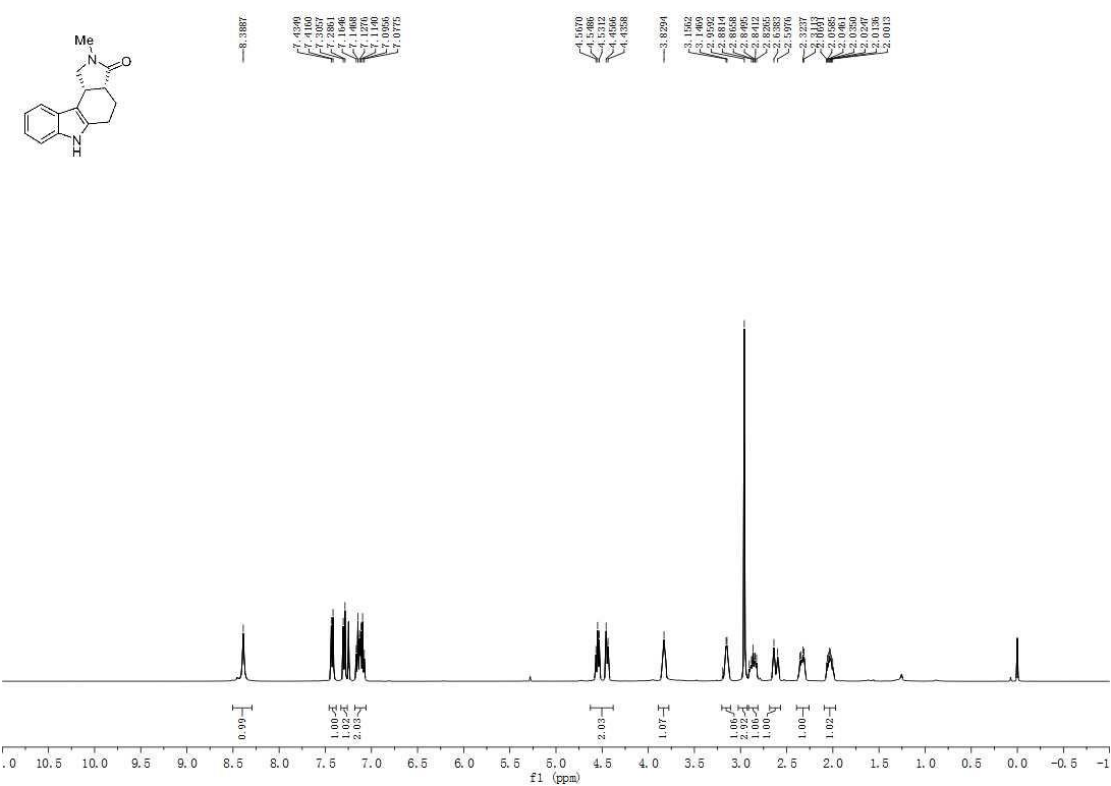


**Figure S76.**  $^{13}\text{C}$  NMR spectrum of **8**, related to **Scheme 4**.

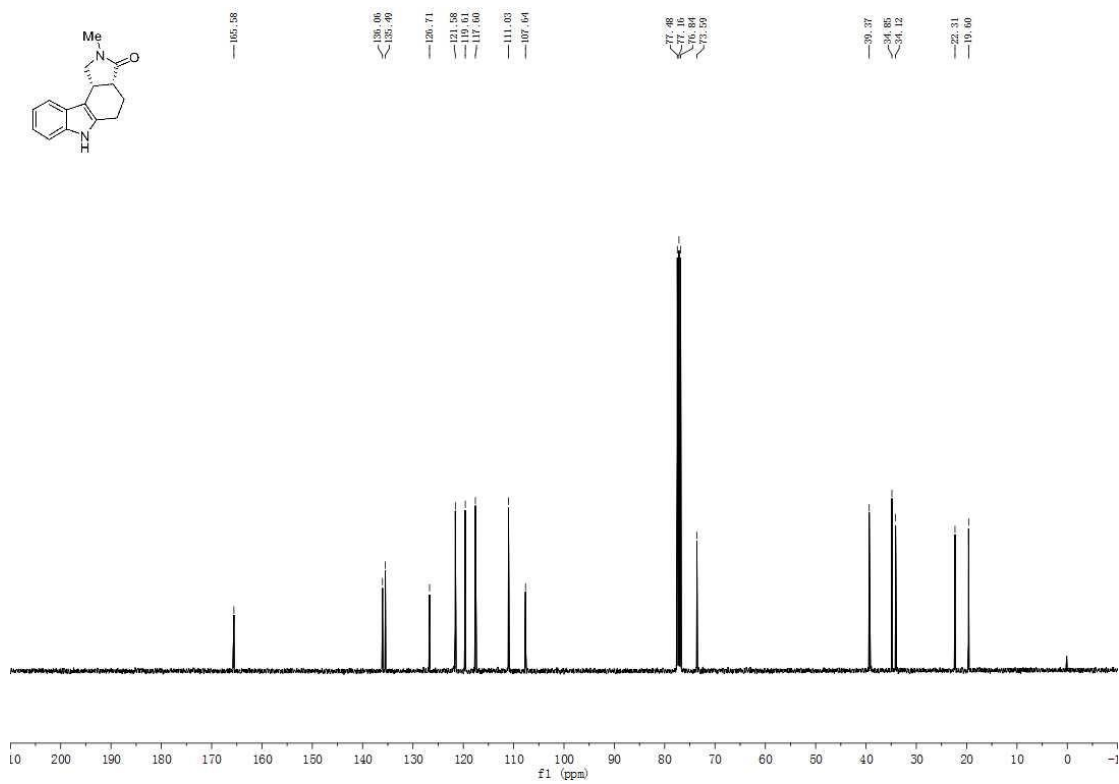


**Figure S77.**  $^1\text{H}$  NMR spectrum of **9**, related to **Scheme 4**.

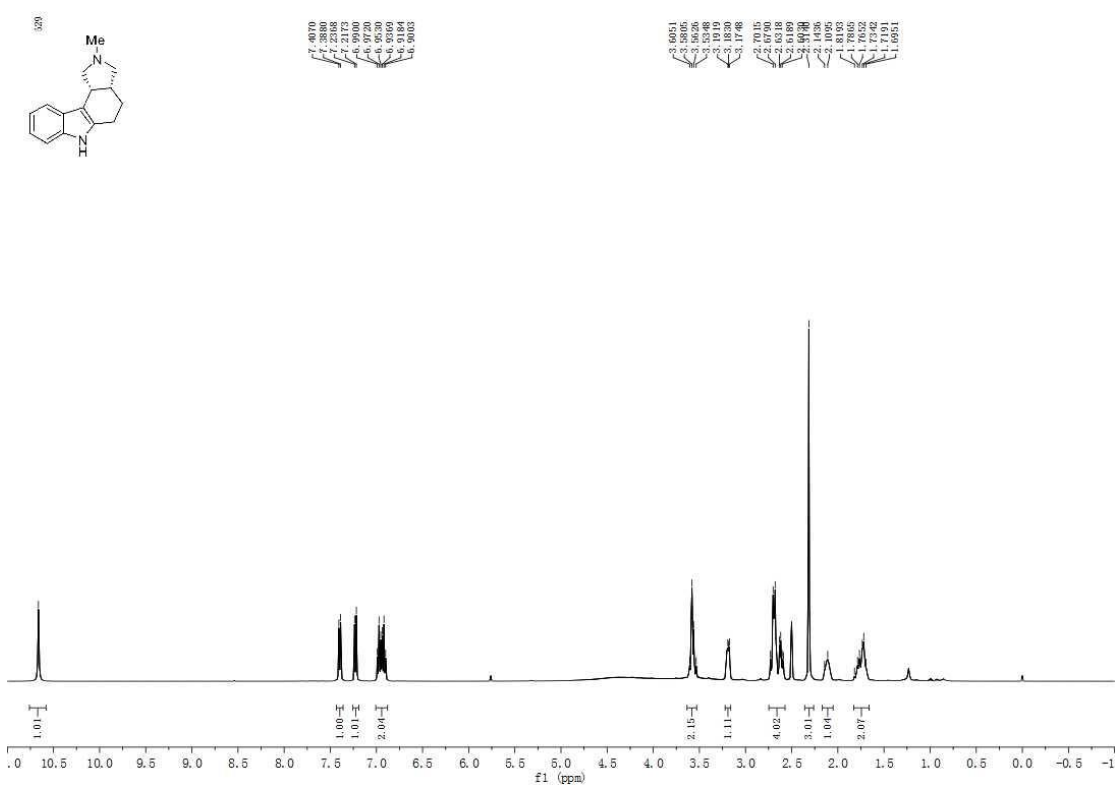


**Figure S78.**  $^{13}\text{C}$  NMR spectrum of **9**, related to **Scheme 4**.

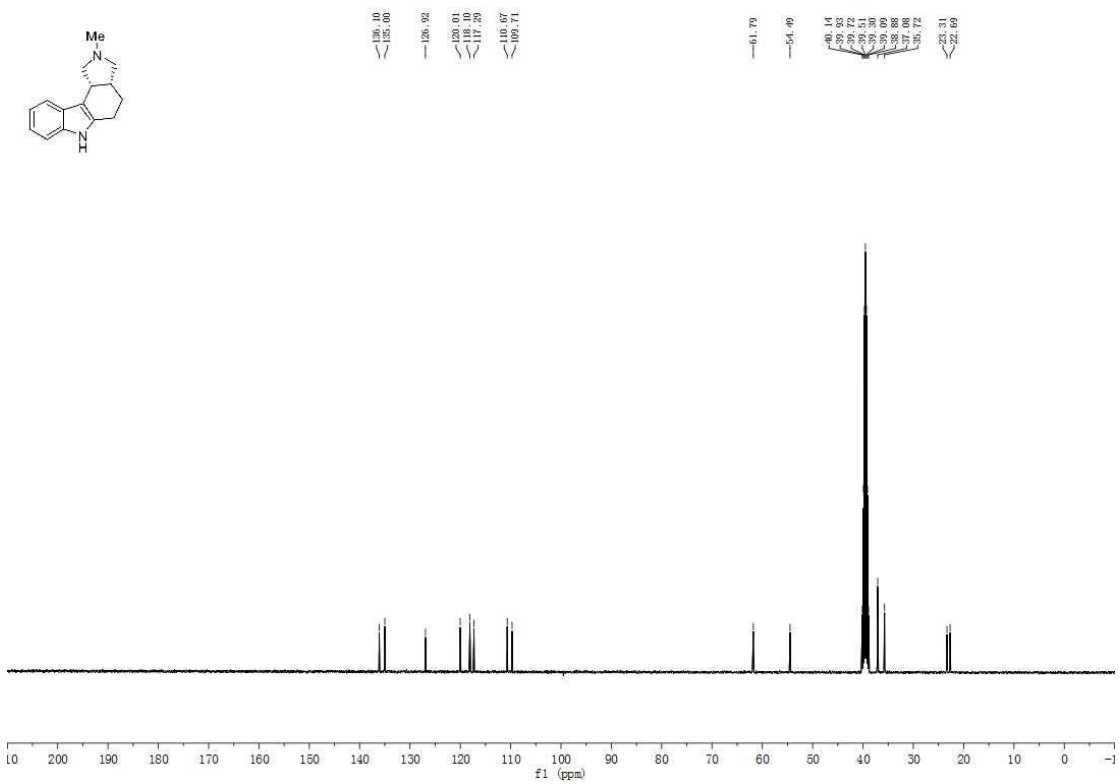


**Figure S79.**  $^1\text{H}$  NMR spectrum of **10**, related to **Table 1**.

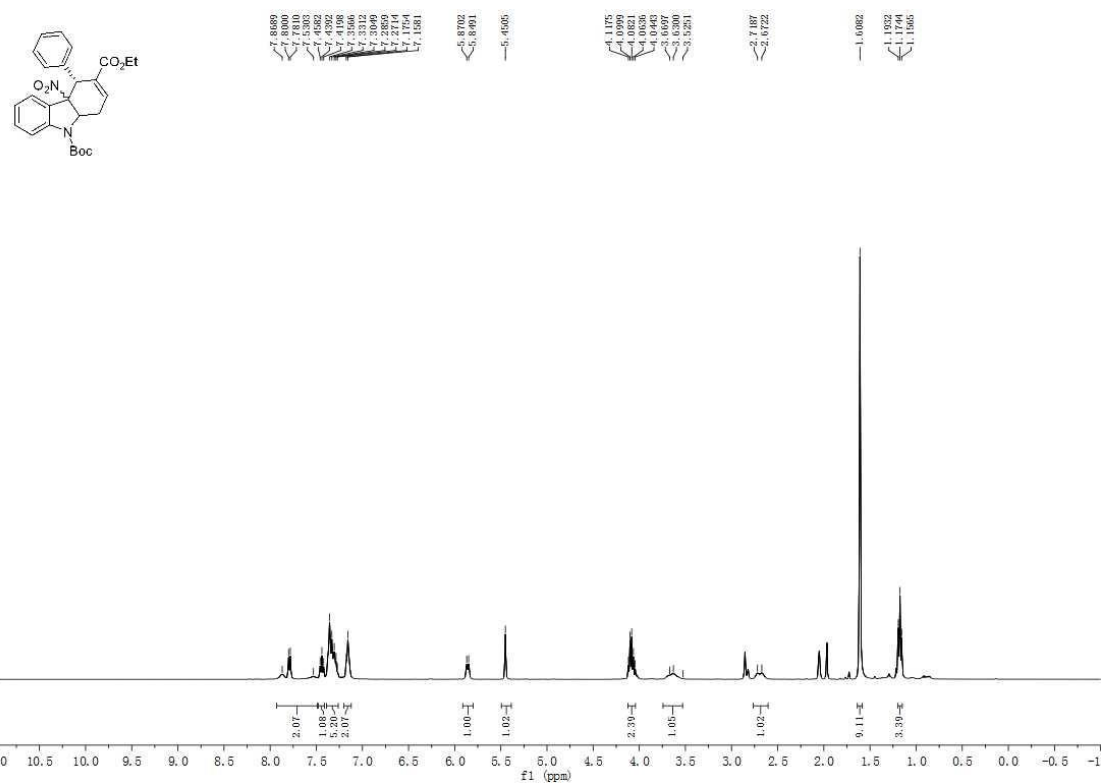
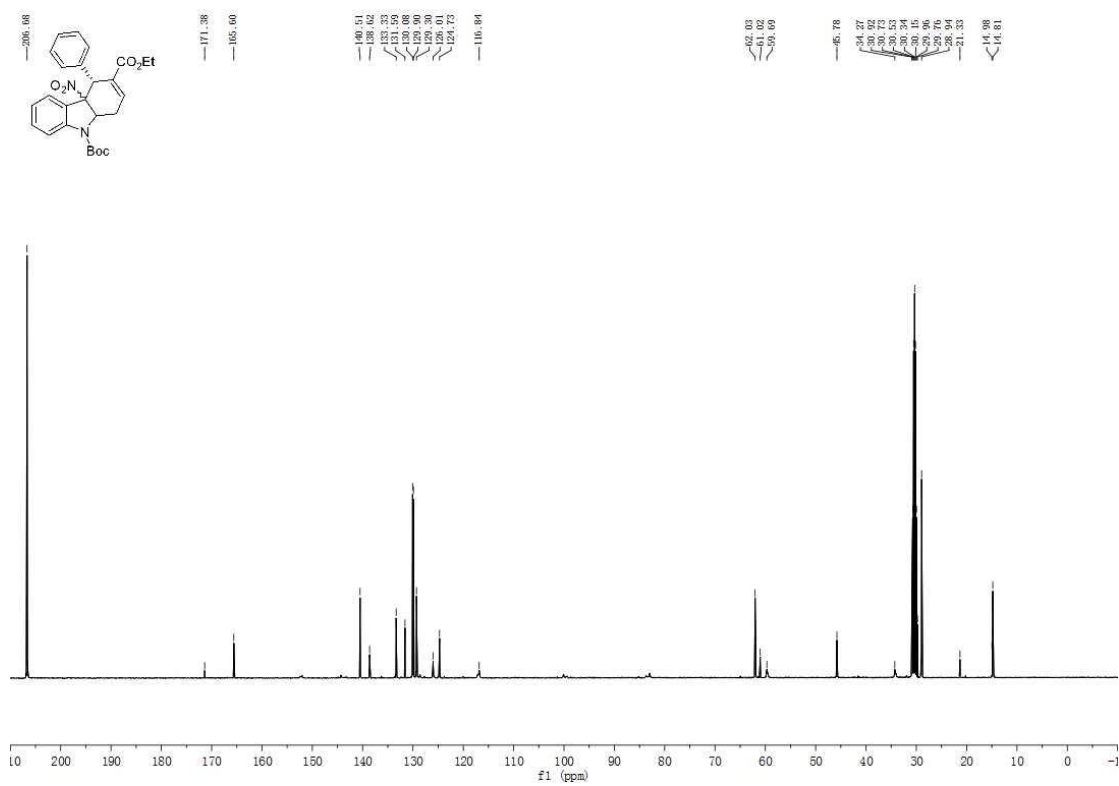


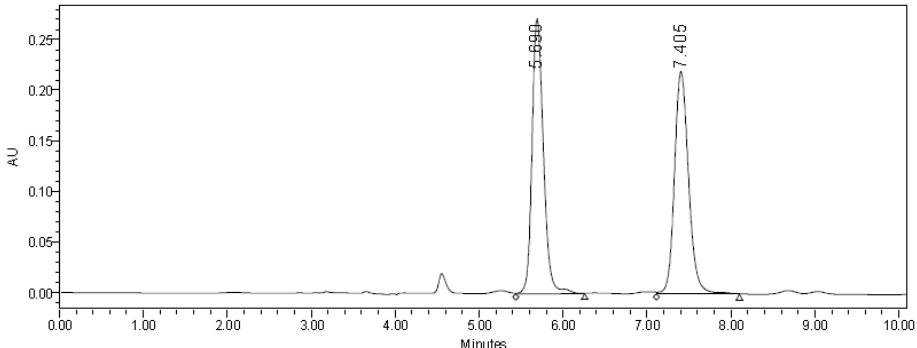
**Figure S80.**  $^{13}\text{C}$  NMR spectrum of **10**, related to **Table 1**.



## Supplemental Figures for HPLC spectra

**Figure S81.** HPLC spectra of *rac*-3a, related to **Scheme 2**.

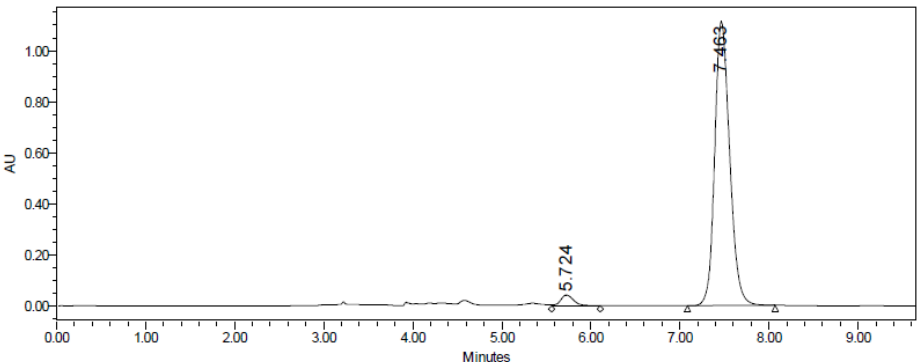
SAMPLE INFORMATION	
Sample Name:	why-g05-72-5-rac-IA-3%
Sample Type:	Unknown
Vial:	61
Injection #:	2
Injection Volume:	10.00 ul
Run Time:	100.0 Minutes
Acquired By:	System
Sample Set Name	
Acq. Method Set:	3%
Processing Method	5 72 5 RAC
Channel Name:	2998 Ch1 254nm@1.2nm
Proc. Chnl. Descr.:	2998 Ch1 254nm@1.2nm
Date Acquired:	9/24/2019 2:39:18 PM CST
Date Processed:	9/24/2019 2:53:07 PM CST



	RT	Area	% Area	Height
1	5.690	2560919	50.07	271284
2	7.405	2554055	49.93	219595

**Figure S82.** HPLC spectra of 3a, related to **Scheme 2**.

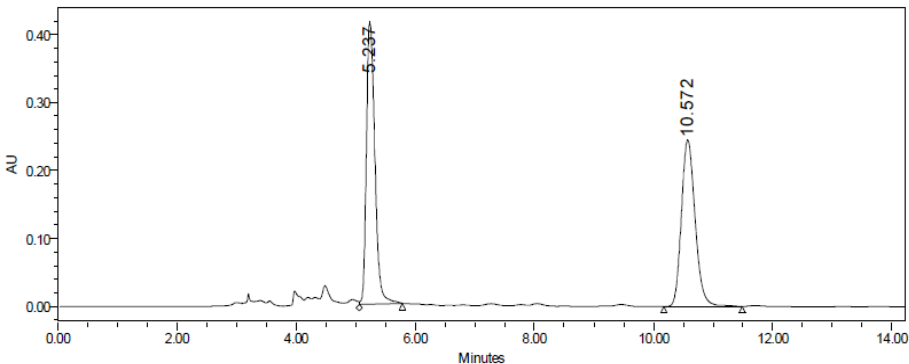
SAMPLE INFORMATION	
Sample Name:	why-g05-72-5-IA-3%
Sample Type:	Unknown
Vial:	37
Injection #:	1
Injection Volume:	10.00 ul
Run Time:	100.0 Minutes
Acquired By:	System
Sample Set Name	
Acq. Method Set:	3%
Processing Method	5 72 5
Channel Name:	2998 Ch1 254nm@1.2nm
Proc. Chnl. Descr.:	2998 Ch1 254nm@1.2nm
Date Acquired:	4/13/2019 4:32:02 PM CST
Date Processed:	7/19/2019 4:19:16 PM CST



	RT	Area	% Area	Height
1	5.724	434402	3.24	42393
2	7.463	12978962	96.76	1111415

**Figure S83.** HPLC spectra of **rac-3b**, related to **Scheme 2**.

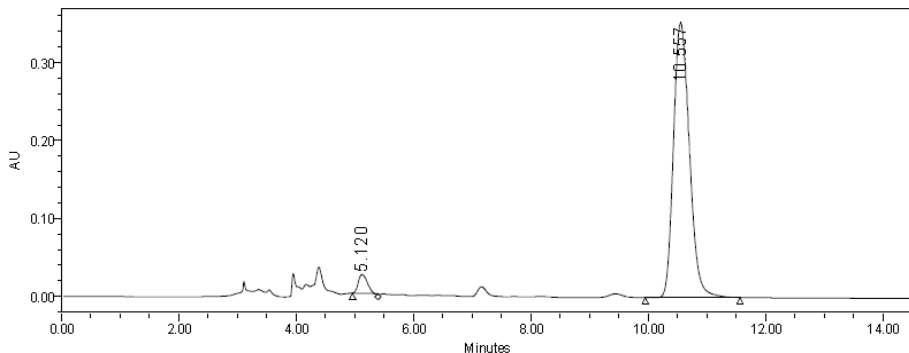
SAMPLE INFORMATION				
Sample Name:	why-g05-102-1-IA-3%	Acquired By:	System	
Sample Type:	Unknown	Sample Set Name		
Vial:	45	Acq. Method Set:	3%	
Injection #:	1	Processing Method	5 102 1	
Injection Volume:	10.00 ul	Channel Name:	2998 Ch1 254nm@1.2nm	
Run Time:	100.0 Minutes	Proc. Chnl. Descr.:	2998 Ch1 254nm@1.2nm	
Date Acquired:	5/5/2019 4:48:39 PM CST			
Date Processed:	7/19/2019 4:24:54 PM CST			



	RT	Area	% Area	Height
1	5.237	4069692	50.92	415006
2	10.572	3922670	49.08	245275

**Figure S84.** HPLC spectra of **3b**, related to **Scheme 2**.

SAMPLE INFORMATION				
Sample Name:	why-g05-102-2-IA-3%	Acquired By:	System	
Sample Type:	Unknown	Sample Set Name		
Vial:	80	Acq. Method Set:	3%	
Injection #:	1	Processing Method	5 102 2	
Injection Volume:	10.00 ul	Channel Name:	2998 Ch1 254nm@1.2nm	
Run Time:	100.0 Minutes	Proc. Chnl. Descr.:	2998 Ch1 254nm@1.2nm	
Date Acquired:	5/7/2019 3:50:53 PM CST			
Date Processed:	9/23/2019 8:46:36 PM CST			



	RT	Area	% Area	Height
1	5.120	260126	3.78	24045
2	10.557	6618616	96.22	352534

**Figure S85.** HPLC spectra of **rac-3c**, related to **Scheme 2**.

SAMPLE INFORMATION				
Sample Name:	why-g05-118-1-IA-1.5%	Acquired By:	System	
Sample Type:	Unknown	Sample Set Name		
Vial:	7	Acq. Method Set:	1.5%	
Injection #:	1	Processing Method	5 118 1	
Injection Volume:	10.00 $\mu$ l	Channel Name:	2998 Ch1 254nm@1.2nm	
Run Time:	100.0 Minutes	Proc. Chnl. Descr.:	2998 Ch1 254nm@1.2nm	
Date Acquired:	5/23/2019 10:26:54 AM CST			
Date Processed:	7/19/2019 4:27:37 PM CST			

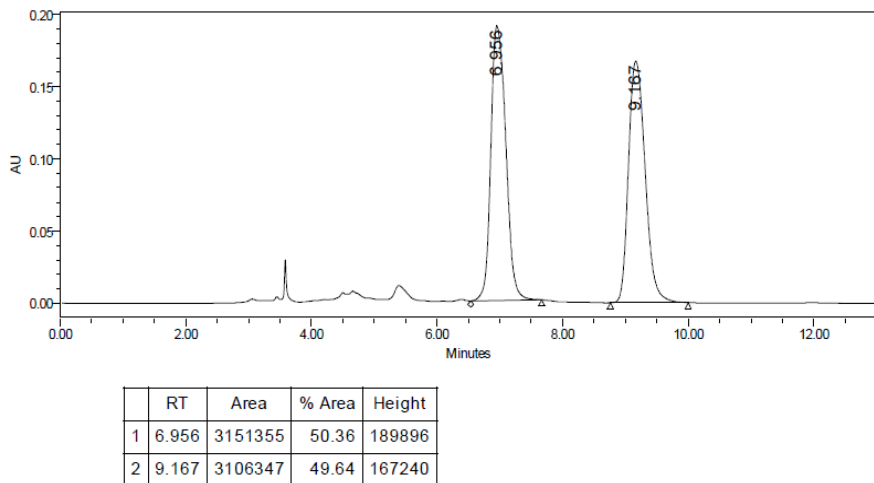


**Figure S86.** HPLC spectra of **3c**, related to **Scheme 2**.

SAMPLE INFORMATION				
Sample Name:	why-g05-118-2-IA-1.5%	Acquired By:	System	
Sample Type:	Unknown	Sample Set Name		
Vial:	43	Acq. Method Set:	1.5%	
Injection #:	1	Processing Method	5 118 2	
Injection Volume:	10.00 $\mu$ l	Channel Name:	2998 Ch1 254nm@1.2nm	
Run Time:	100.0 Minutes	Proc. Chnl. Descr.:	2998 Ch1 254nm@1.2nm	
Date Acquired:	5/23/2019 10:41:01 AM CST			
Date Processed:	7/19/2019 4:28:16 PM CST			

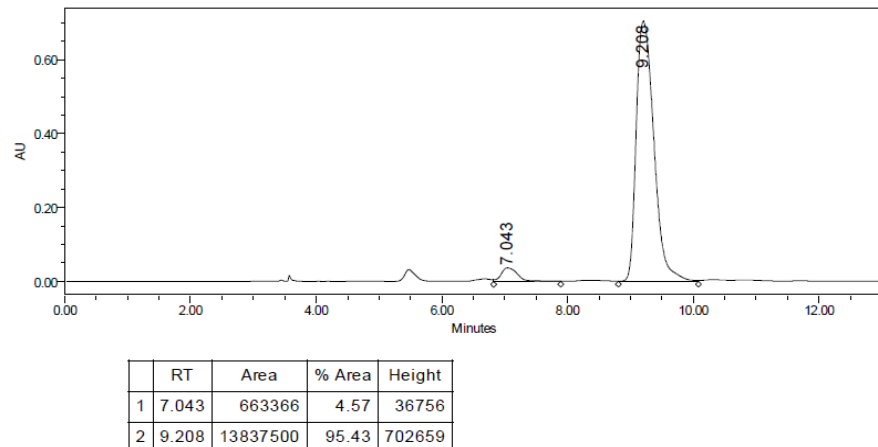


**Figure S87.** HPLC spectra of *rac*-3d, related to **Scheme 2**.

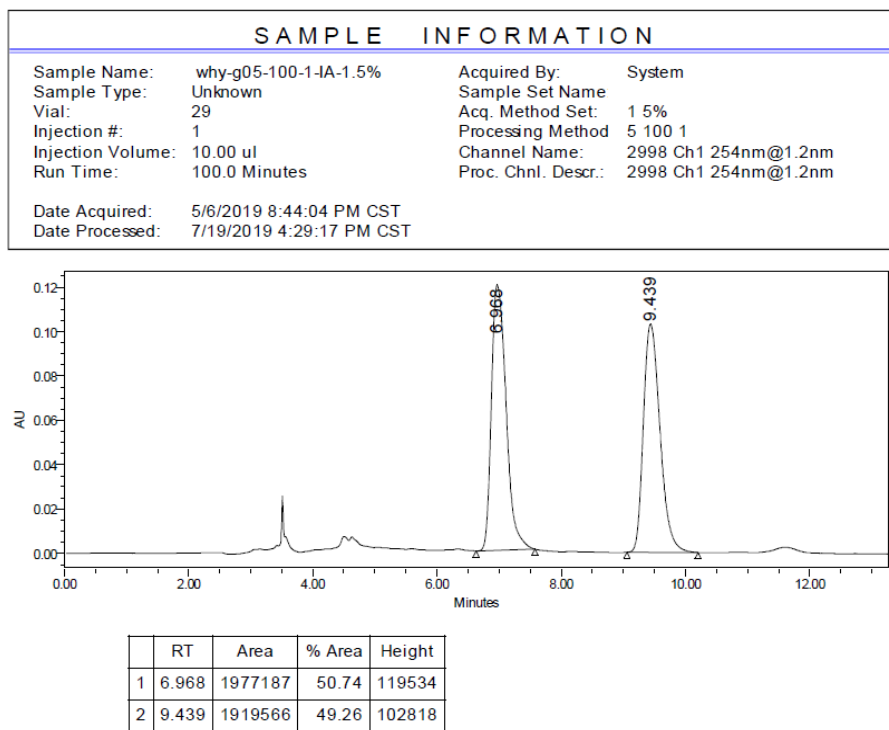


**Figure S88.** HPLC spectra of 3d, related to **Scheme 2**.

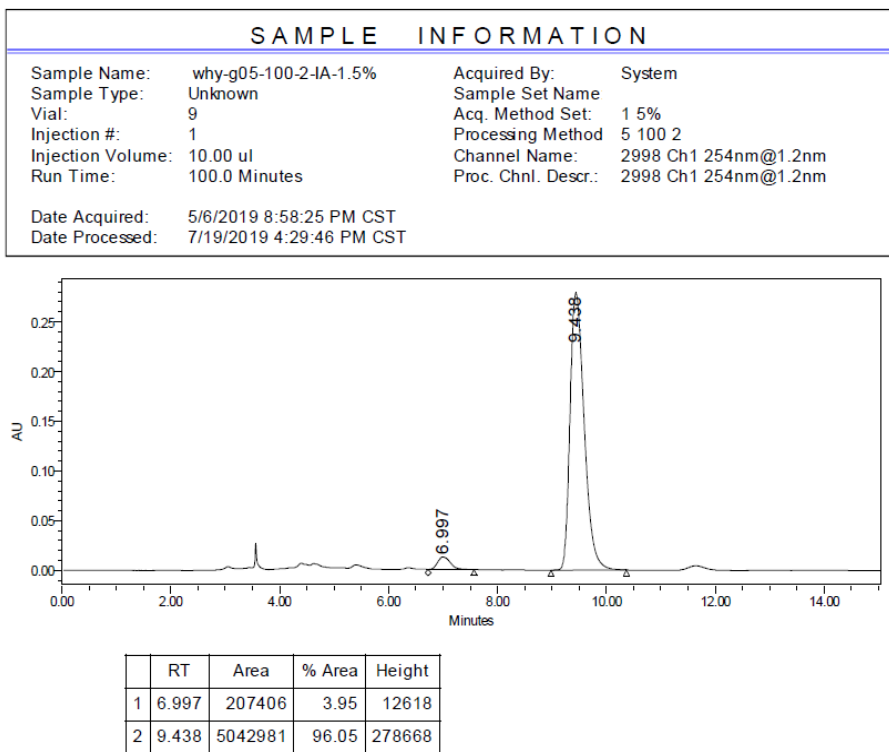
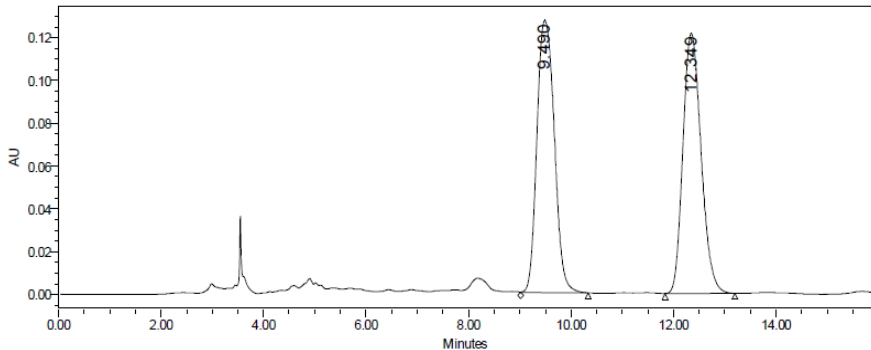
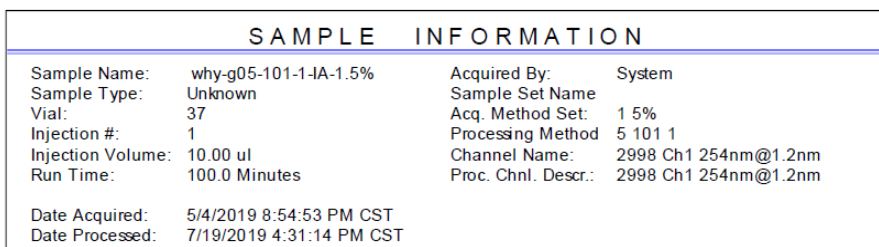
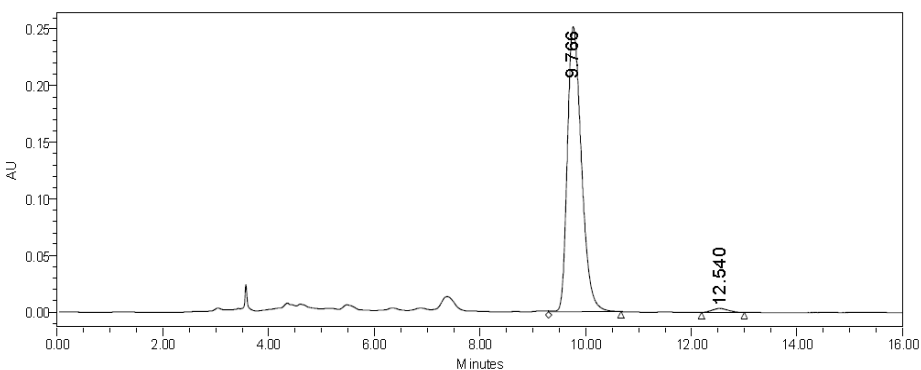
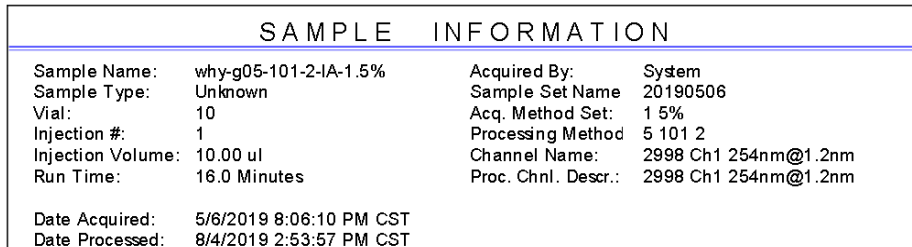


**Figure S89.** HPLC spectra of *rac*-**3e**, related to **Scheme 2**.



	RT	Area	% Area	Height
1	9.490	3002746	50.01	127223
2	12.349	3001033	49.99	121658

**Figure S90.** HPLC spectra of **3e**, related to **Scheme 2**.



	RT	Area	% Area	Height
1	9.766	4614701	98.50	251558
2	12.540	70049	1.50	3342

**Figure S91.** HPLC spectra of *rac*-3f, related to **Scheme 2**.

SAMPLE INFORMATION				
Sample Name:	why-g05-103-1-IA-10%	Acquired By:	System	
Sample Type:	Unknown	Sample Set Name		
Vial:	46	Acq. Method Set:	10%	
Injection #:	1	Processing Method	5 103 1	
Injection Volume:	10.00 $\mu$ l	Channel Name:	2998 Ch1 254nm@1.2nm	
Run Time:	100.0 Minutes	Proc. Chnl. Descr.:	2998 Ch1 254nm@1.2nm	
Date Acquired:	5/5/2019 5:09:33 PM CST			
Date Processed:	7/19/2019 4:32:50 PM CST			

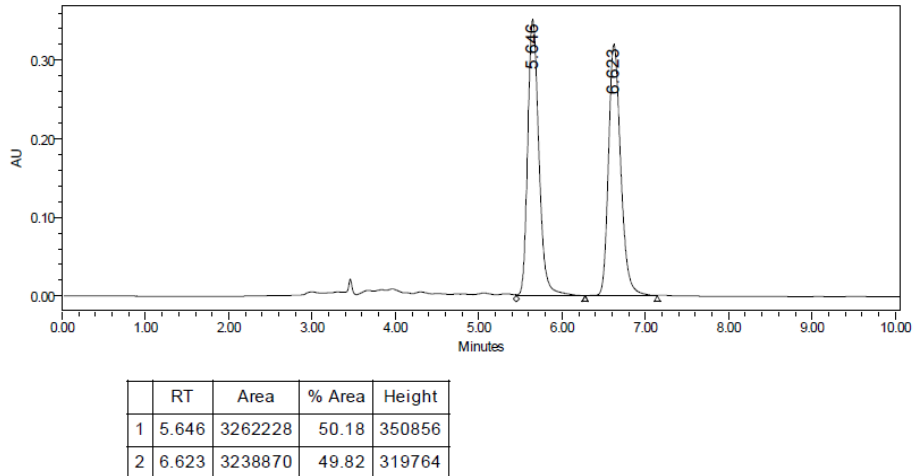


**Figure S92.** HPLC spectra of 3f, related to **Scheme 2**.

SAMPLE INFORMATION				
Sample Name:	why-g05-103-2-IA-10%	Acquired By:	System	
Sample Type:	Unknown	Sample Set Name		
Vial:	105	Acq. Method Set:	10%	
Injection #:	1	Processing Method	5 103 2	
Injection Volume:	10.00 $\mu$ l	Channel Name:	2998 Ch1 254nm@1.2nm	
Run Time:	100.0 Minutes	Proc. Chnl. Descr.:	2998 Ch1 254nm@1.2nm	
Date Acquired:	5/8/2019 8:52:48 PM CST			
Date Processed:	7/19/2019 4:33:25 PM CST			

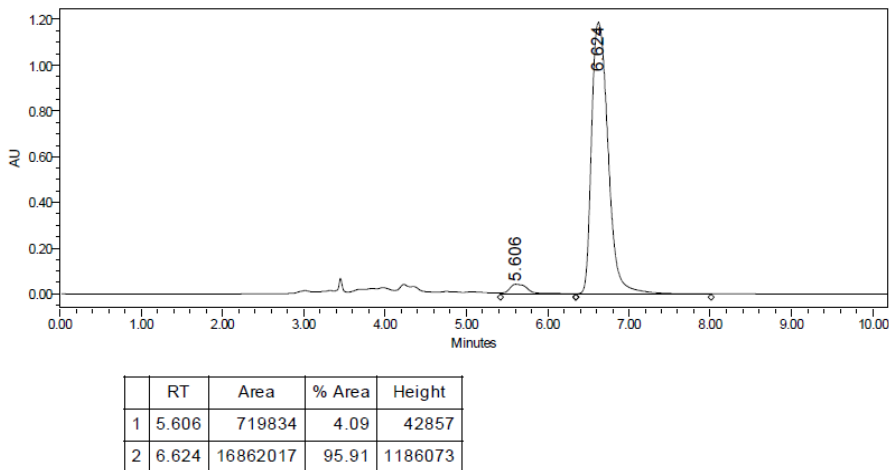


**Figure S93.** HPLC spectra of *rac*-3g, related to **Scheme 2**.

SAMPLE INFORMATION				
Sample Name:	why-g05-104-1-IA-3%	Acquired By:	System	
Sample Type:	Unknown	Sample Set Name		
Vial:	117	Acq. Method Set:	3%	
Injection #:	2	Processing Method	5 104 1	
Injection Volume:	10.00 $\mu$ l	Channel Name:	2998 Ch1 254nm@1.2nm	
Run Time:	100.0 Minutes	Proc. Chnl. Descr.:	2998 Ch1 254nm@1.2nm	
Date Acquired:	5/8/2019 8:09:13 PM CST			
Date Processed:	7/19/2019 4:34:27 PM CST			

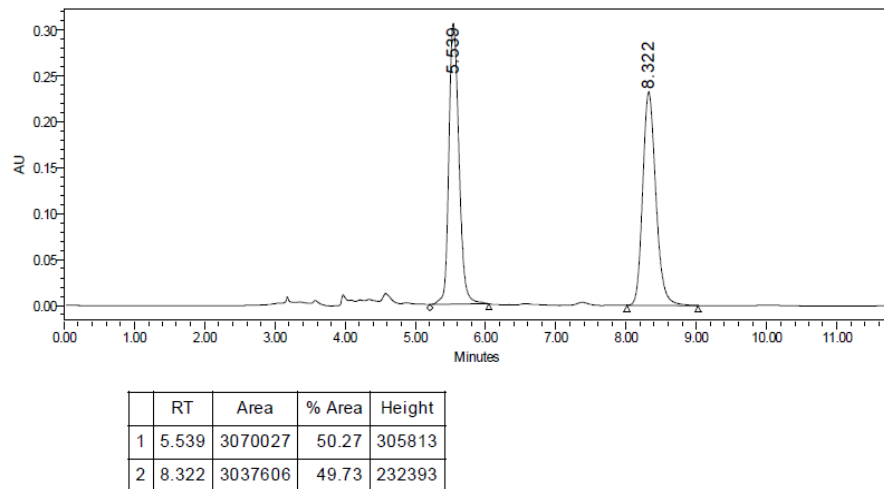


**Figure S94.** HPLC spectra of 3g, related to **Scheme 2**.

SAMPLE INFORMATION				
Sample Name:	why-g05-104-2-IA-3%	Acquired By:	System	
Sample Type:	Unknown	Sample Set Name		
Vial:	3	Acq. Method Set:	3%	
Injection #:	1	Processing Method	5 104 2	
Injection Volume:	10.00 $\mu$ l	Channel Name:	2998 Ch1 254nm@1.2nm	
Run Time:	100.0 Minutes	Proc. Chnl. Descr.:	2998 Ch1 254nm@1.2nm	
Date Acquired:	5/10/2019 2:32:38 PM CST			
Date Processed:	7/19/2019 4:35:27 PM CST			

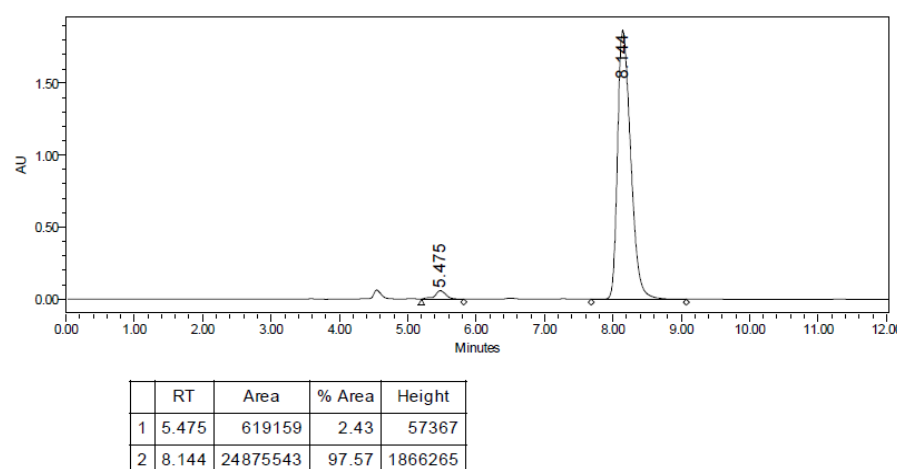


**Figure S95.** HPLC spectra of *rac*-**3h**, related to **Scheme 2**.

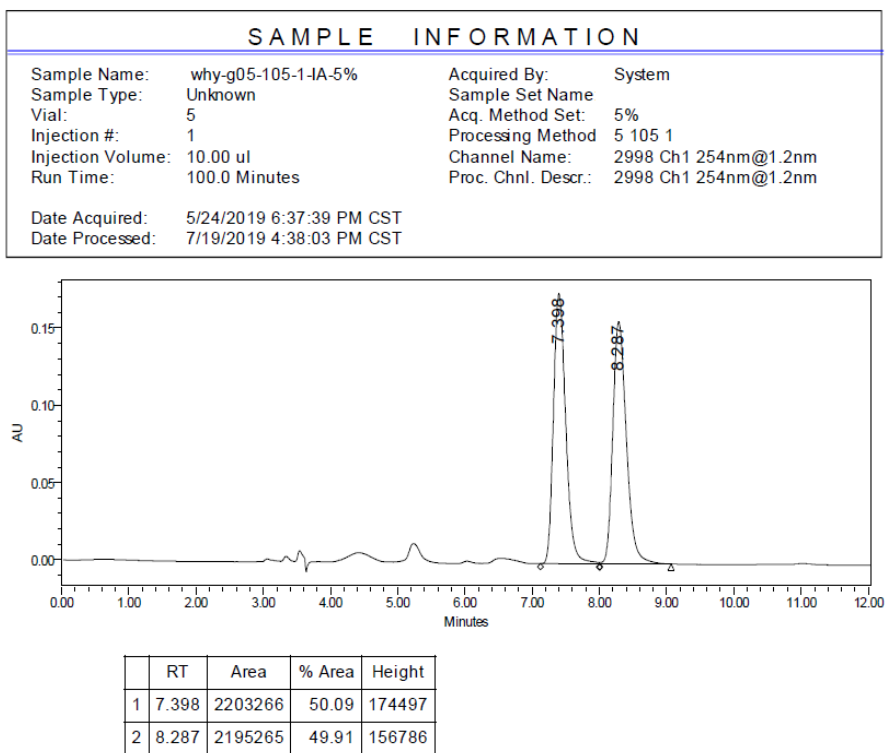


**Figure S96.** HPLC spectra of **3h**, related to **Scheme 2**.

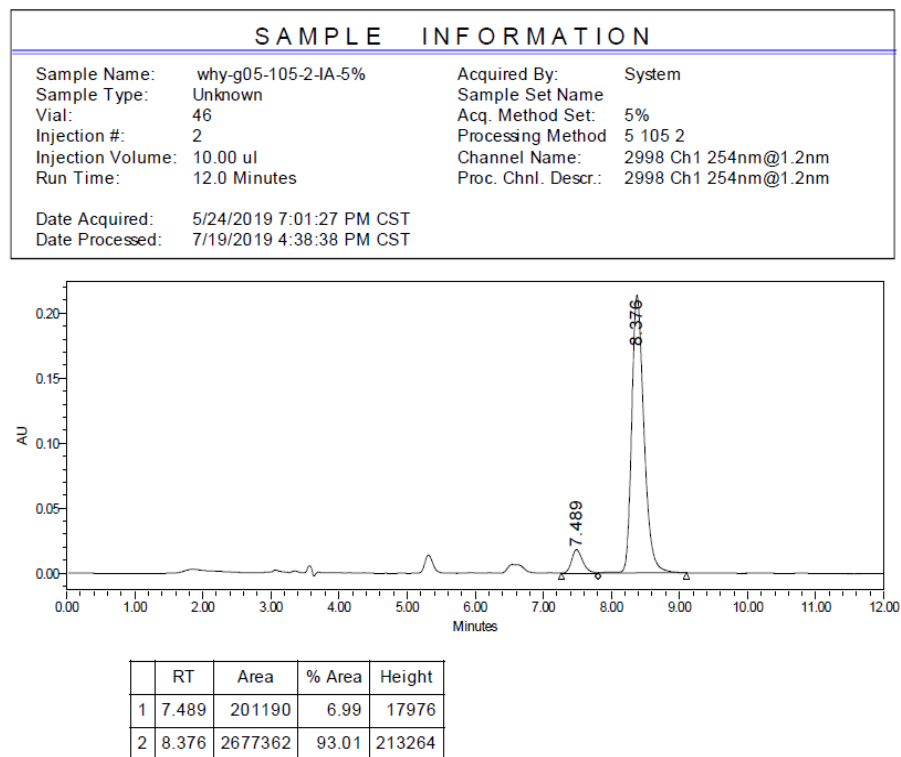


**Figure S97.** HPLC spectra of *rac*-**3i**, related to **Scheme 2**.

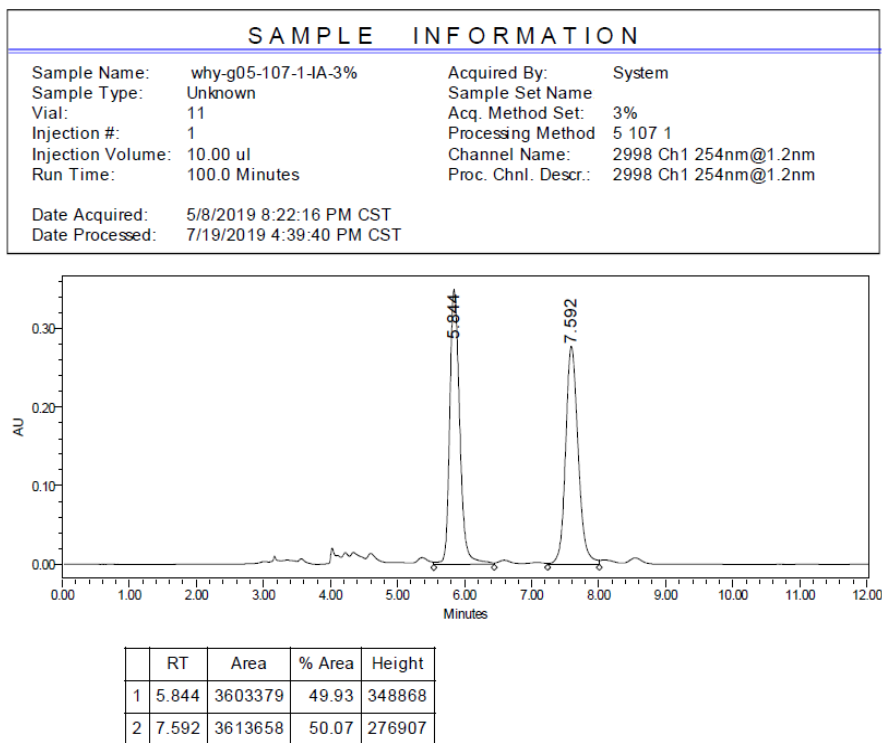


**Figure S98.** HPLC spectra of **3i**, related to **Scheme 2**.

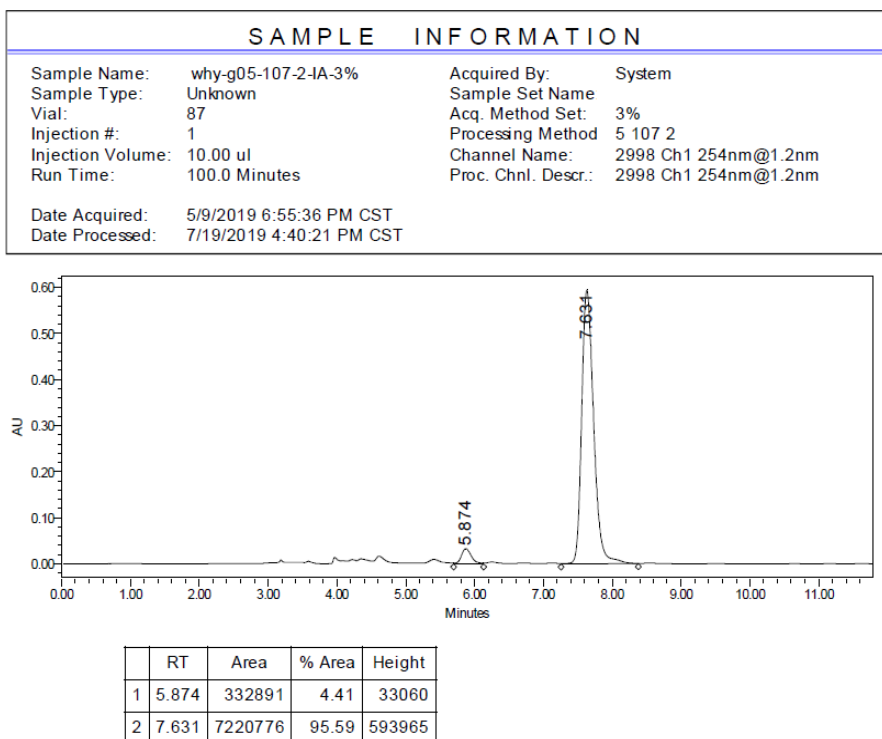


**Figure S99.** HPLC spectra of **rac-3j**, related to **Scheme 2**.

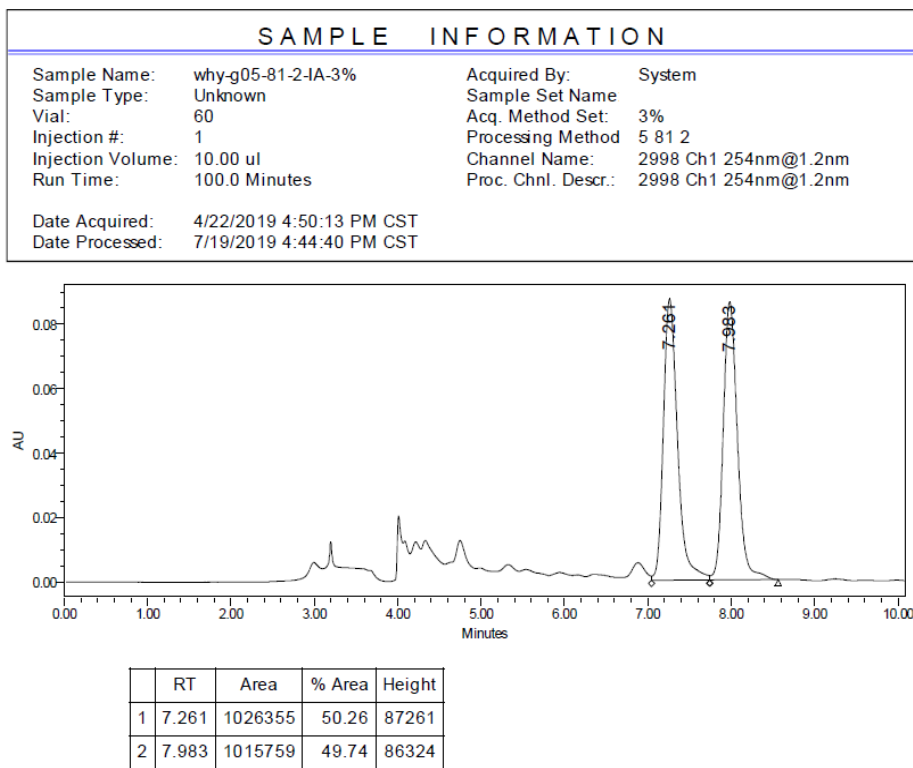


**Figure S100.** HPLC spectra of **3j**, related to **Scheme 2**.

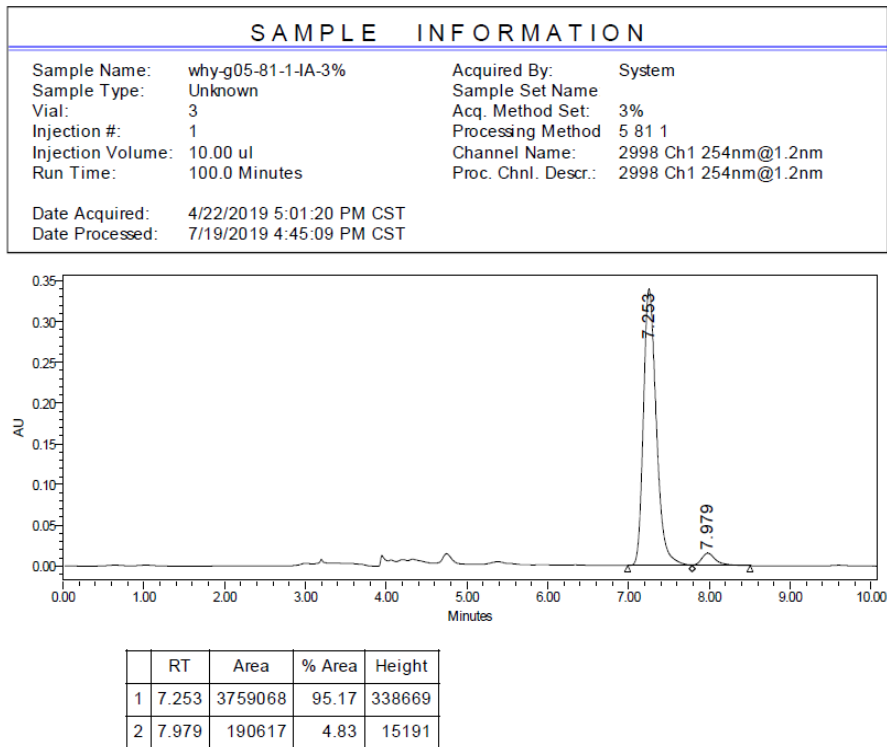
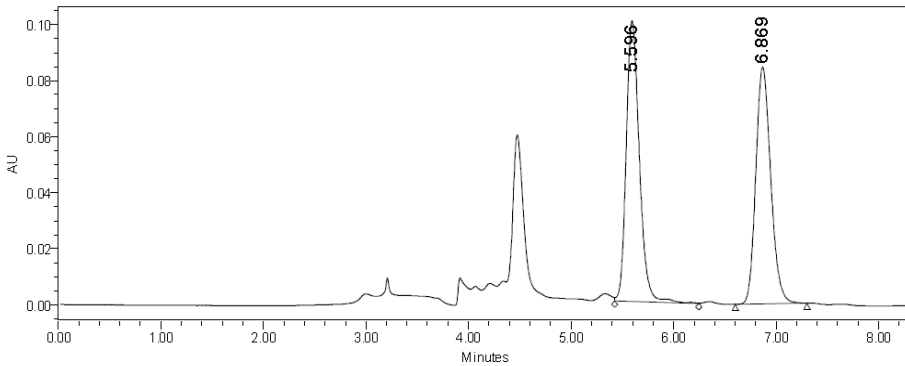
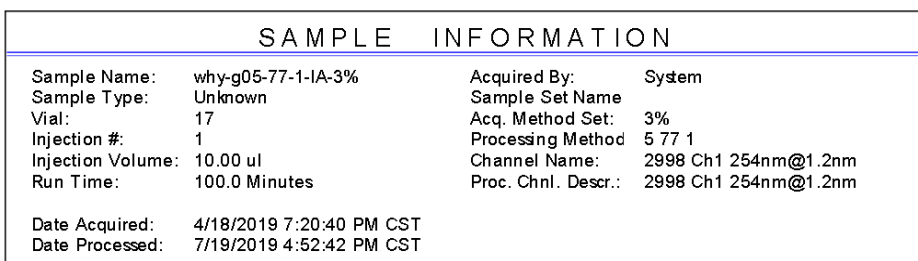
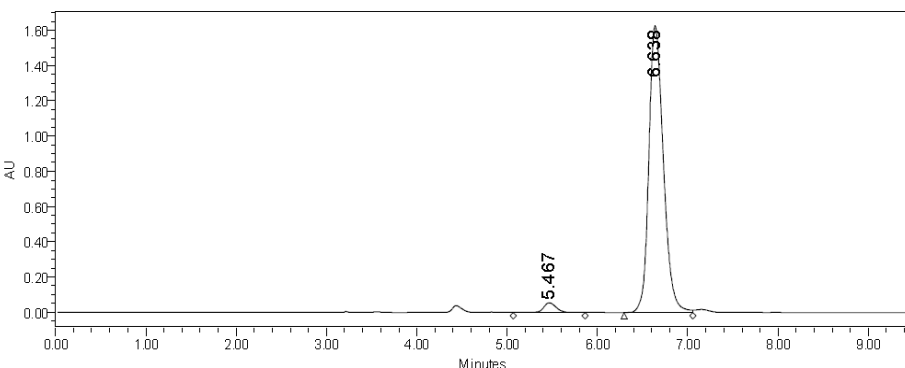
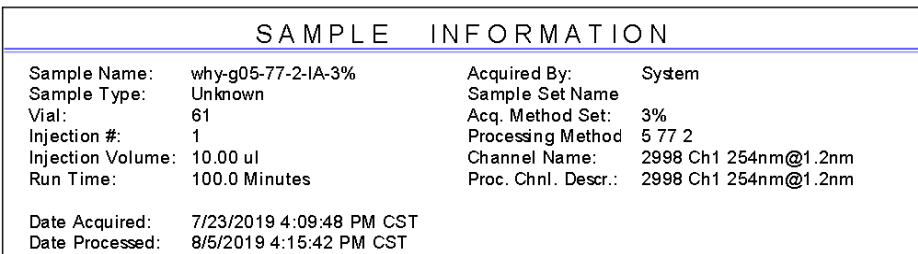


**Figure S101.** HPLC spectra of *rac*-**3k**, related to **Scheme 2**.



	RT	Area	% Area	Height
1	5.596	897583	51.14	100114
2	6.869	857680	48.86	84508

**Figure S102.** HPLC spectra of **3k**, related to **Scheme 2**.



	RT	Area	% Area	Height
1	5.467	548142	2.91	54996
2	6.638	18266140	97.09	1626763

**Figure S103.** HPLC spectra of *rac*-3I, related to **Scheme 2**.

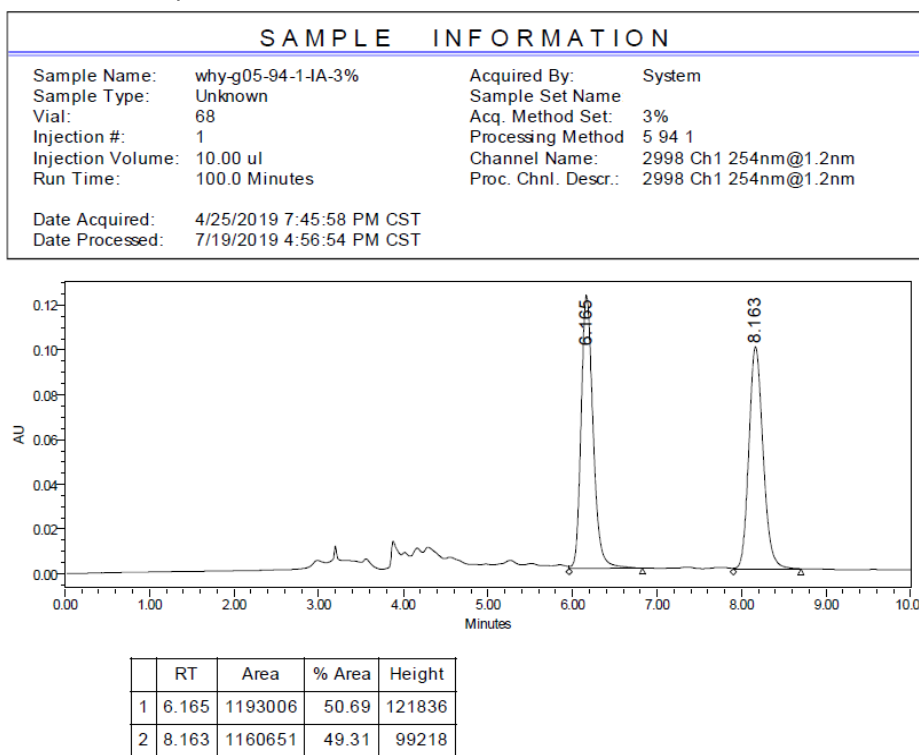


**Figure S104.** HPLC spectra of 3I, related to **Scheme 2**.

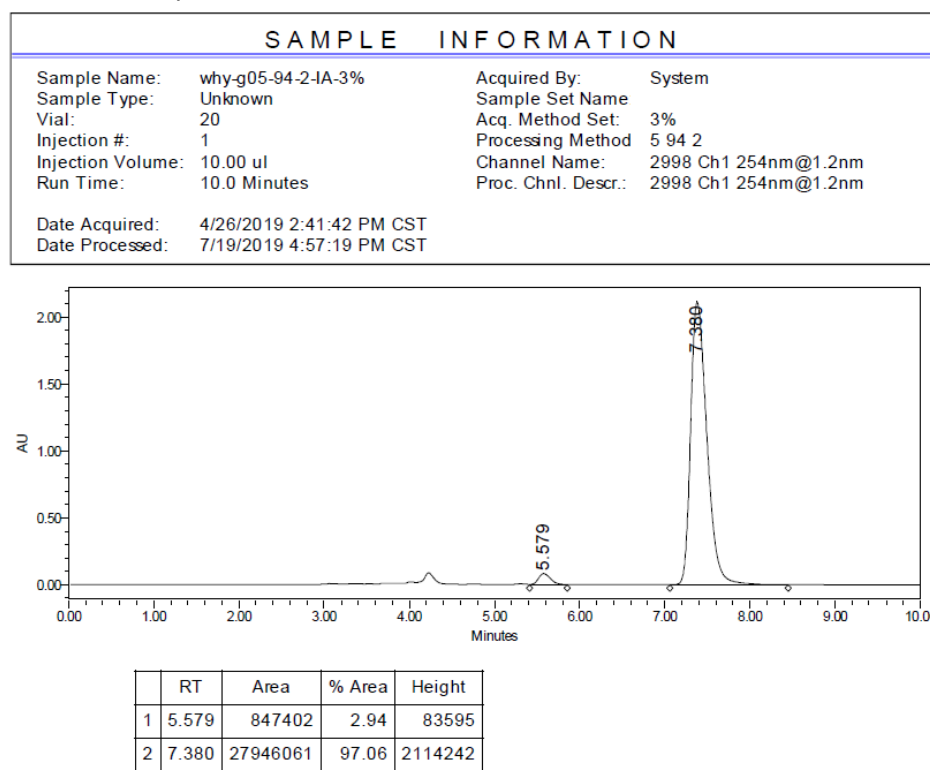


**Figure S105.** HPLC spectra of *rac*-**3m**, related to **Scheme 2**.

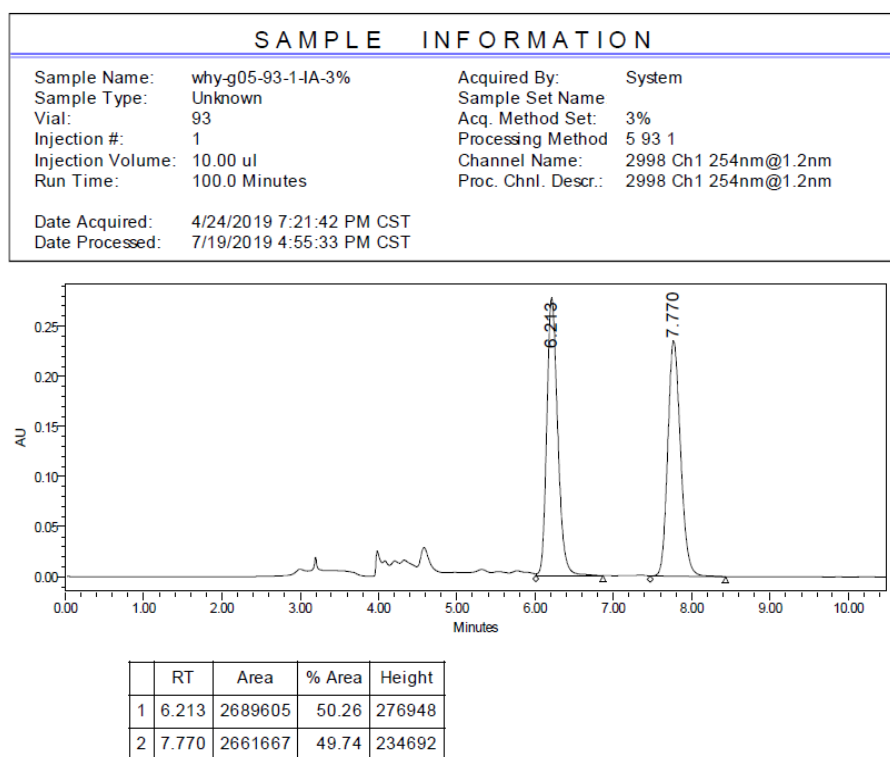


**Figure S106.** HPLC spectra of **3m**, related to **Scheme 2**.

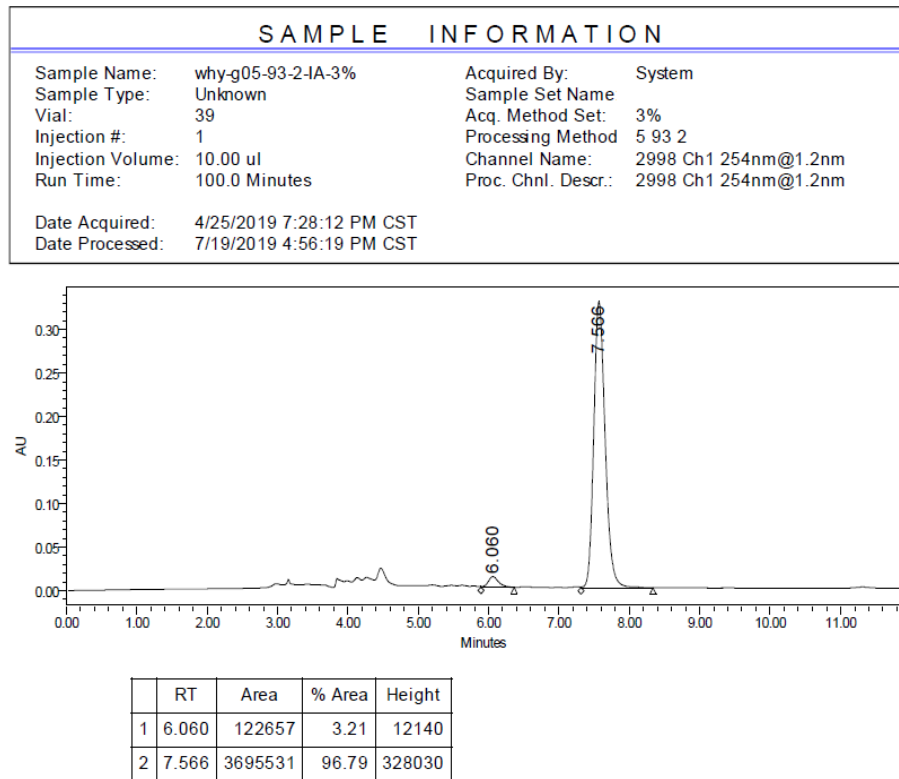
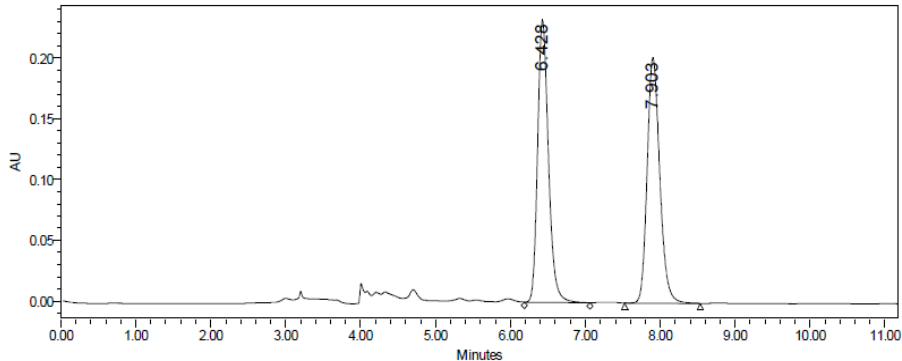
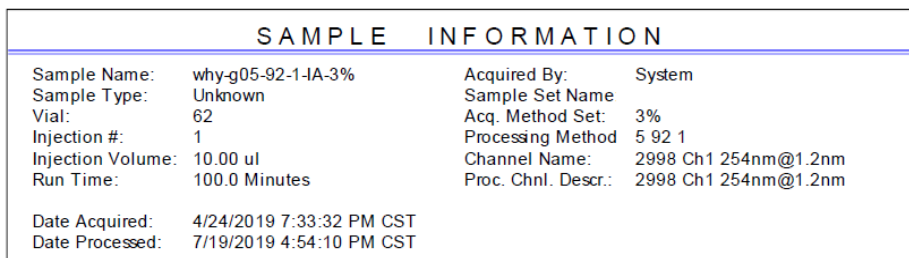
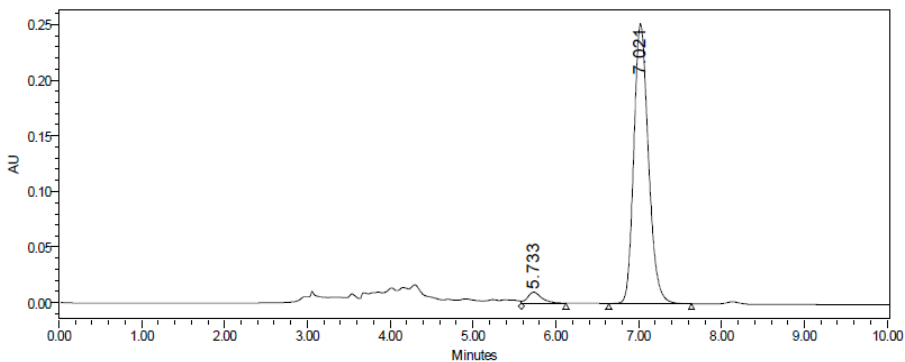
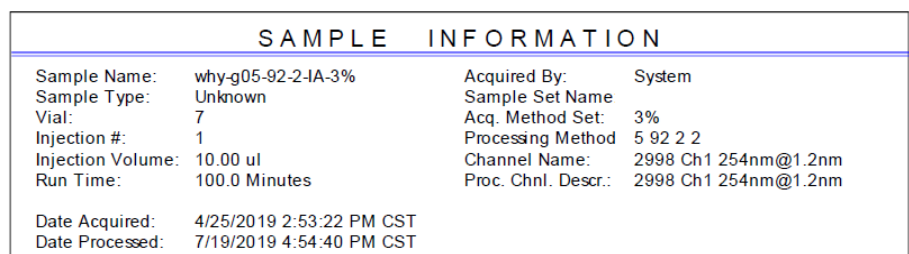


**Figure S107.** HPLC spectra of *rac*-**3n**, related to **Scheme 2**.



	RT	Area	% Area	Height
1	6.428	2345053	49.77	232209
2	7.903	2367186	50.23	202032

**Figure S108.** HPLC spectra of **3n**, related to **Scheme 2**.



	RT	Area	% Area	Height
1	5.733	112010	3.49	9656
2	7.021	3096909	96.51	251145

**Figure S109.** HPLC spectra of *rac*-**3o**, related to **Scheme 2**.

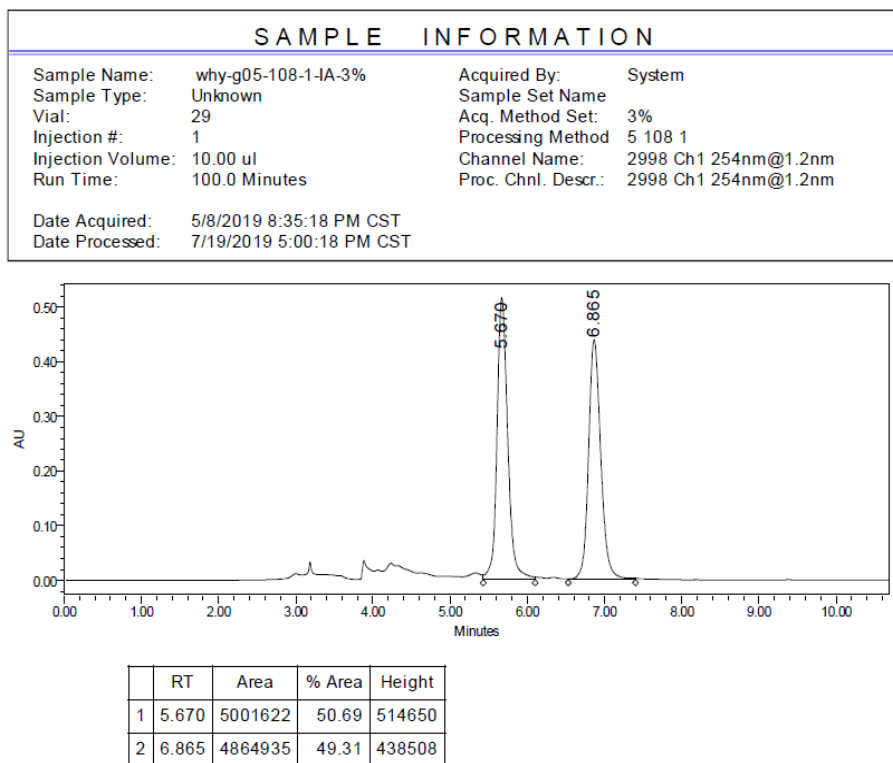


**Figure S110.** HPLC spectra of **3o**, related to **Scheme 2**.

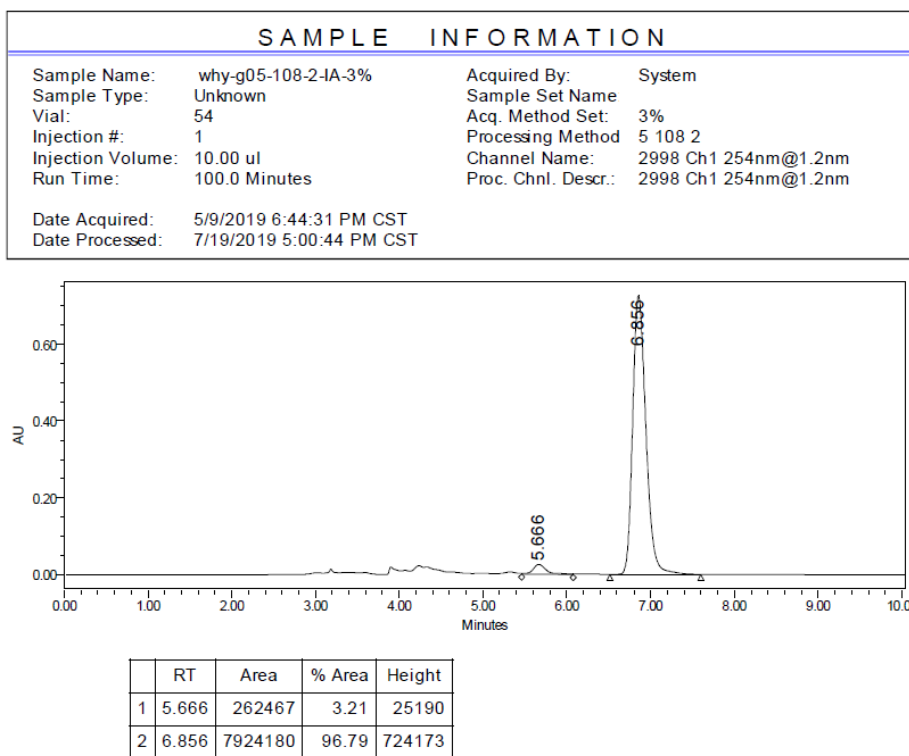


**Figure S111.** HPLC spectra of *rac*-**3p**, related to **Scheme 2**.

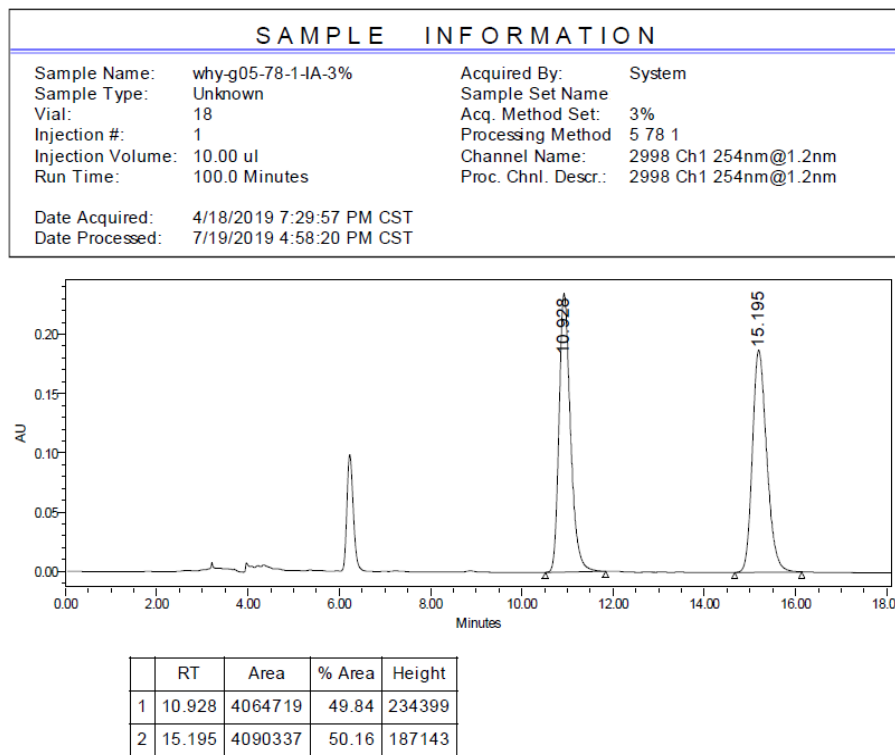


**Figure S112.** HPLC spectra of **3p**, related to **Scheme 2**.

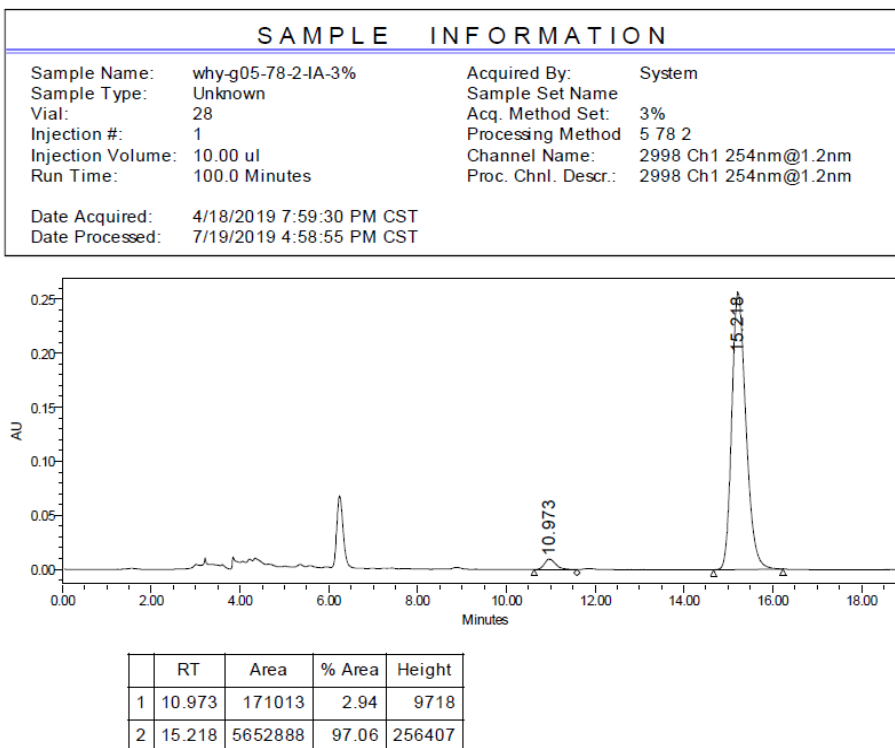


**Figure S113.** HPLC spectra of *rac*-**3q**, related to **Scheme 2**.

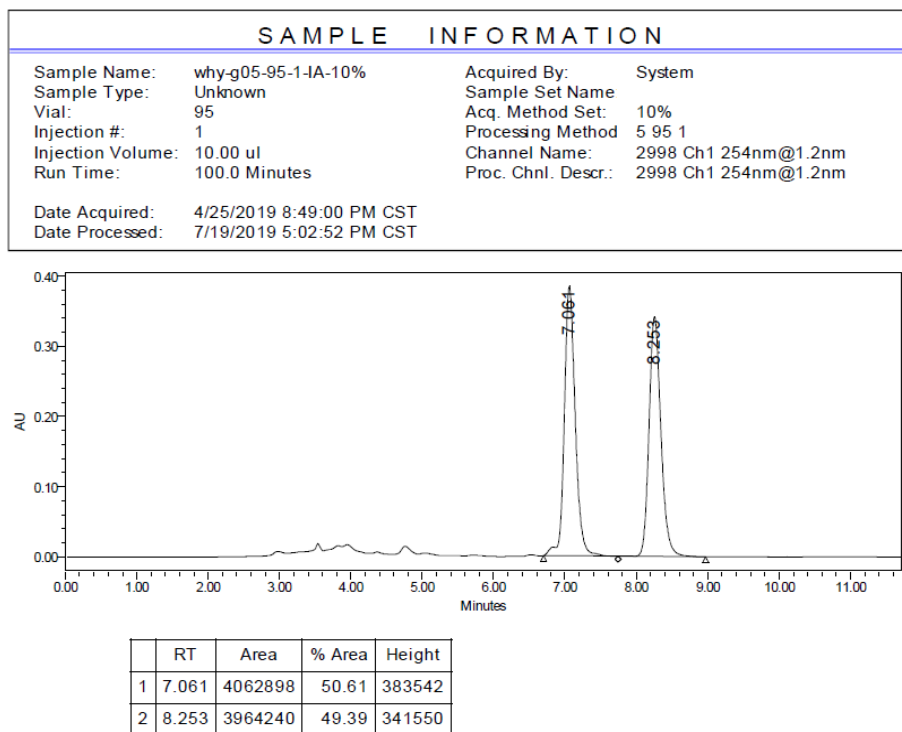


**Figure S114.** HPLC spectra of **3q**, related to **Scheme 2**.

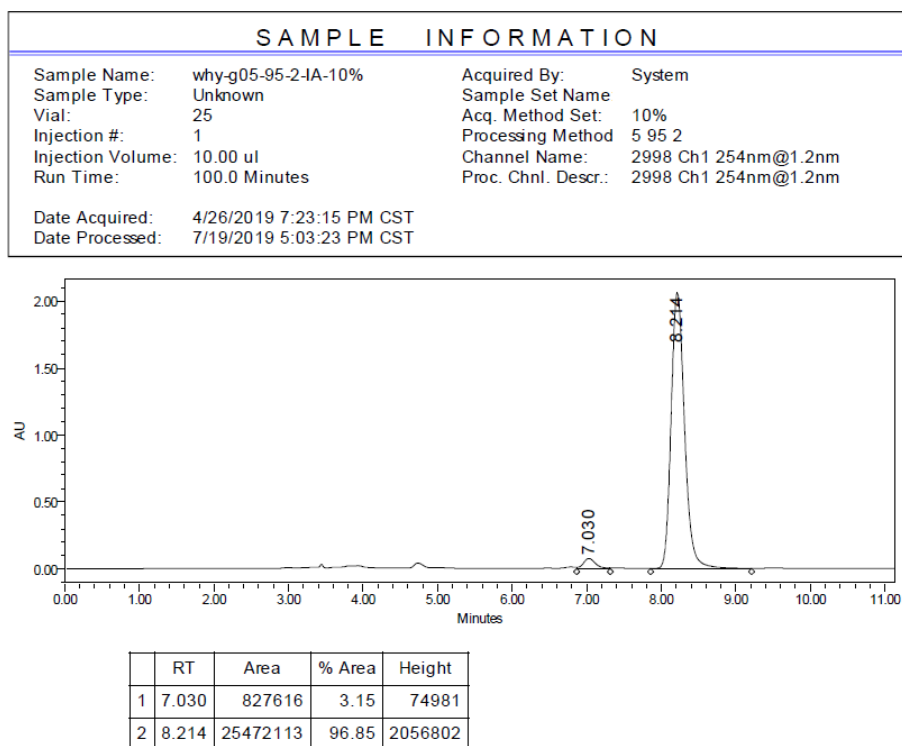
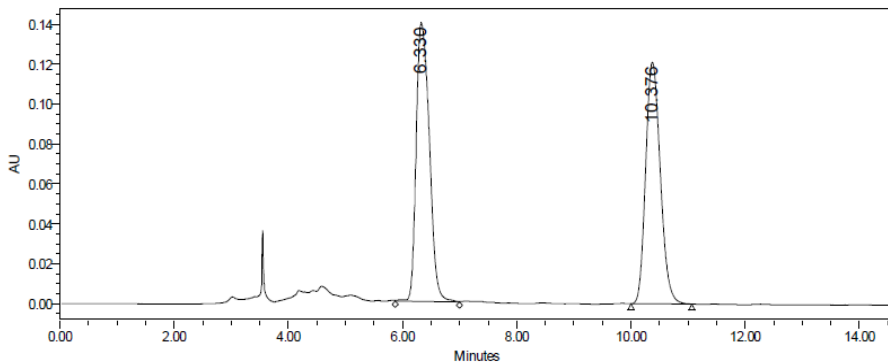


**Figure S115.** HPLC spectra of *rac*-**3r**, related to **Scheme 2**.

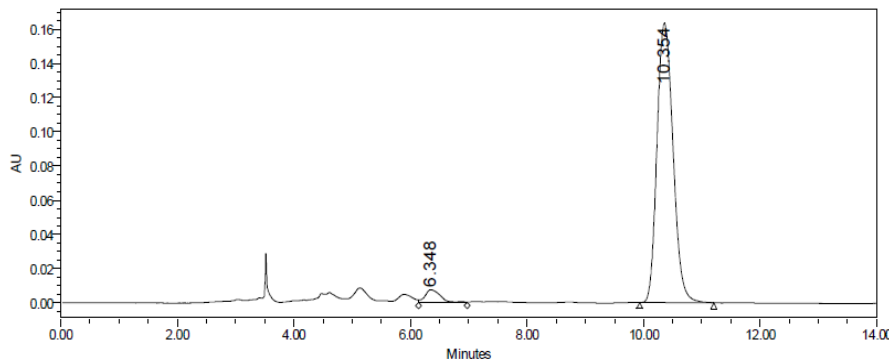
SAMPLE INFORMATION				
Sample Name:	why-g05-97-1-IA-1.5%	Acquired By:	System	
Sample Type:	Unknown	Sample Set Name		
Vial:	5	Acq. Method Set:	1.5%	
Injection #:	1	Processing Method	5.97.1	
Injection Volume:	10.00 $\mu$ l	Channel Name:	2998 Ch1 254nm@1.2nm	
Run Time:	100.0 Minutes	Proc. Chnl. Descr.:	2998 Ch1 254nm@1.2nm	
Date Acquired:	4/27/2019 8:11:01 PM CST			
Date Processed:	7/19/2019 5:03:57 PM CST			



	RT	Area	% Area	Height
1	6.330	2216005	50.51	139512
2	10.376	2171620	49.49	121179

**Figure S116.** HPLC spectra of **3r**, related to **Scheme 2**.

SAMPLE INFORMATION				
Sample Name:	why-g05-97-2-IA-1.5%	Acquired By:	System	
Sample Type:	Unknown	Sample Set Name		
Vial:	4	Acq. Method Set:	1.5%	
Injection #:	1	Processing Method	5.97.2	
Injection Volume:	10.00 $\mu$ l	Channel Name:	2998 Ch1 254nm@1.2nm	
Run Time:	14.0 Minutes	Proc. Chnl. Descr.:	2998 Ch1 254nm@1.2nm	
Date Acquired:	4/27/2019 8:26:29 PM CST			
Date Processed:	7/19/2019 5:04:21 PM CST			



	RT	Area	% Area	Height
1	6.348	132661	4.09	7406
2	10.354	3111023	95.91	163191

**Figure S117.** HPLC spectra of *rac*-**3s**, related to **Scheme 2**.

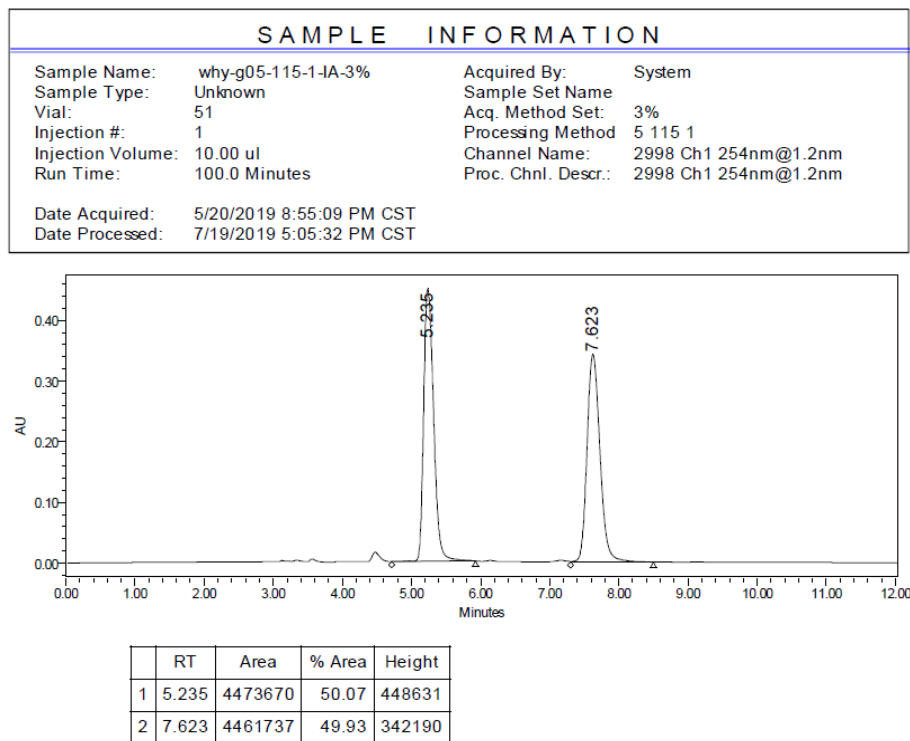


**Figure S118.** HPLC spectra of **3s**, related to **Scheme 2**.

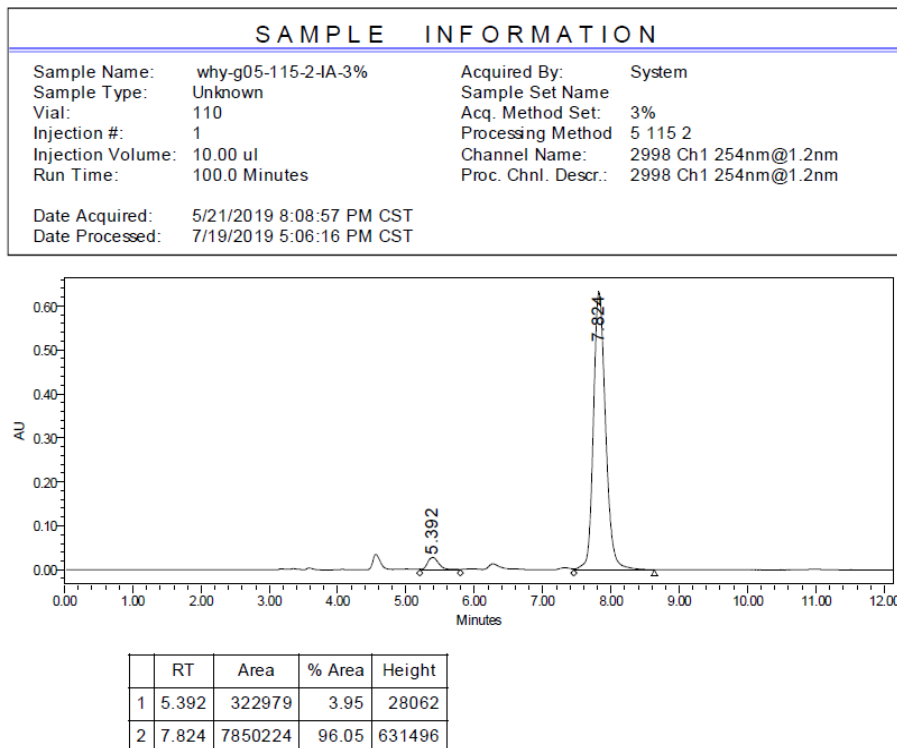


**Figure S119.** HPLC spectra of *rac*-3t, related to **Scheme 2**.

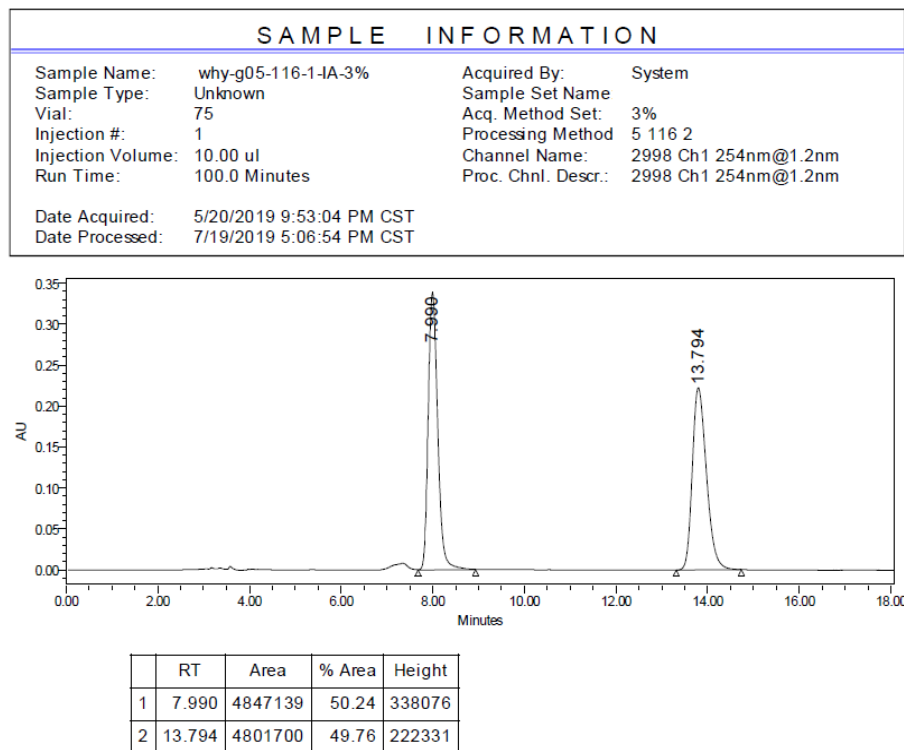


**Figure S120.** HPLC spectra of 3t, related to **Scheme 2**.

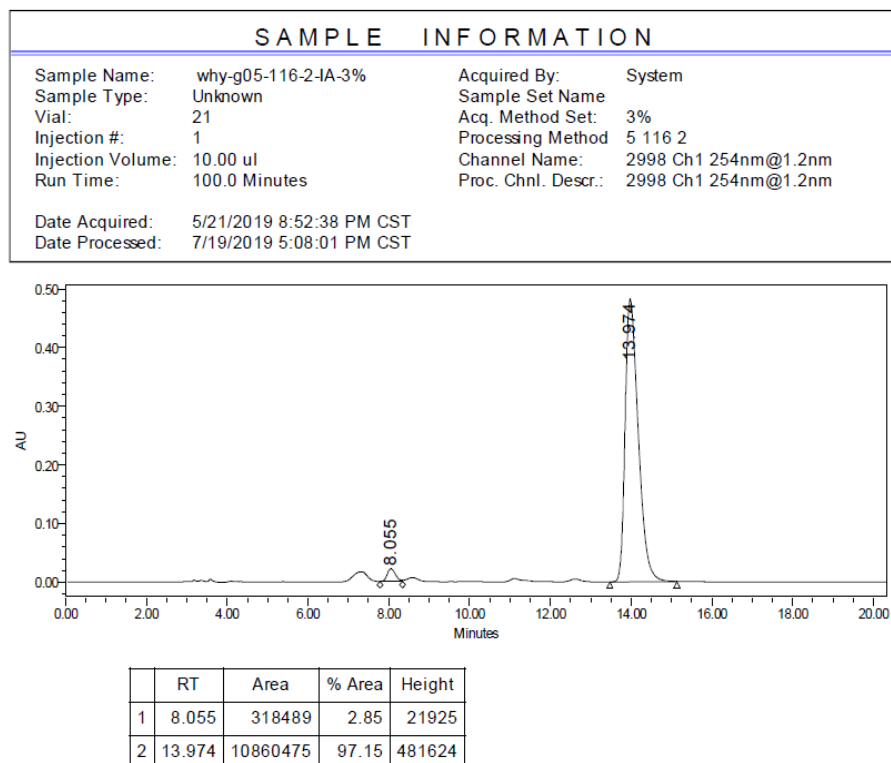


**Figure S121.** HPLC spectra of *rac*-**3u**, related to **Scheme 2**.

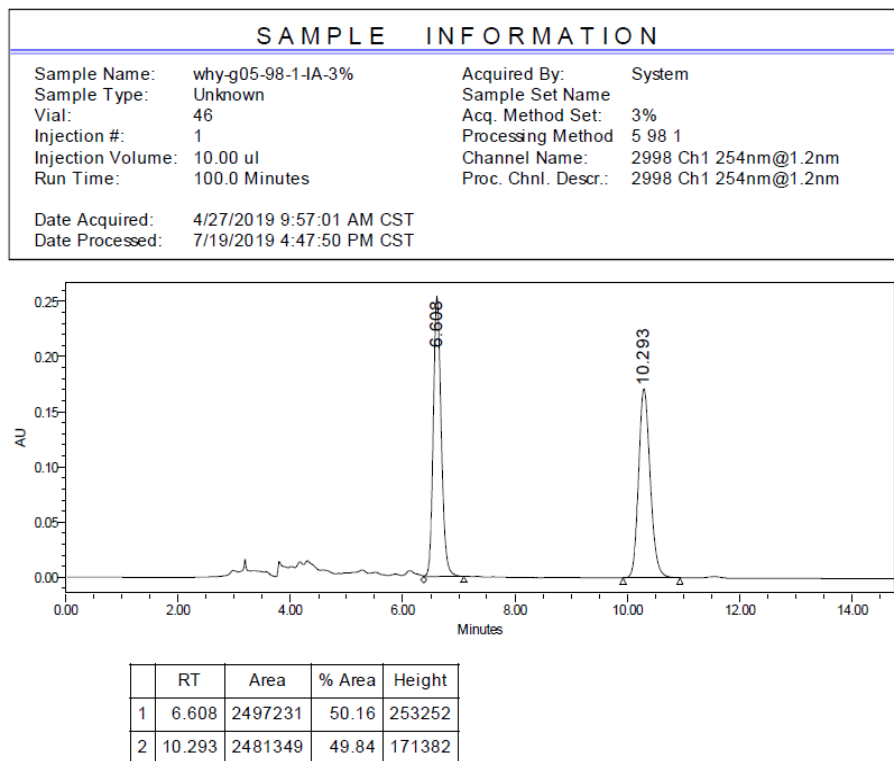


**Figure S122.** HPLC spectra of **3u**, related to **Scheme 2**.

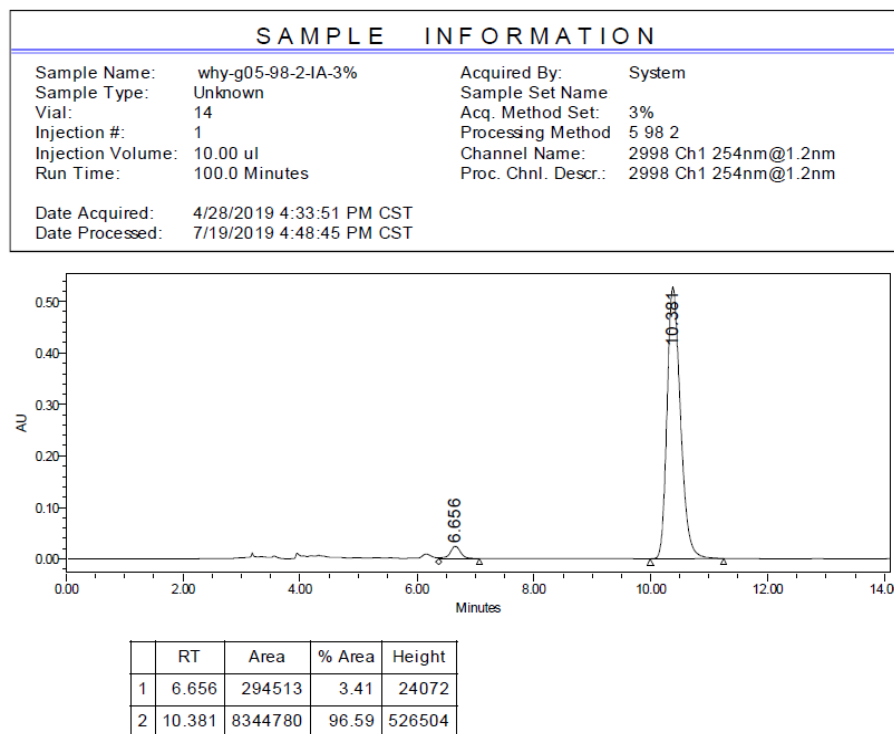


**Figure S123.** HPLC spectra of *rac*-**3v**, related to **Scheme 2**.

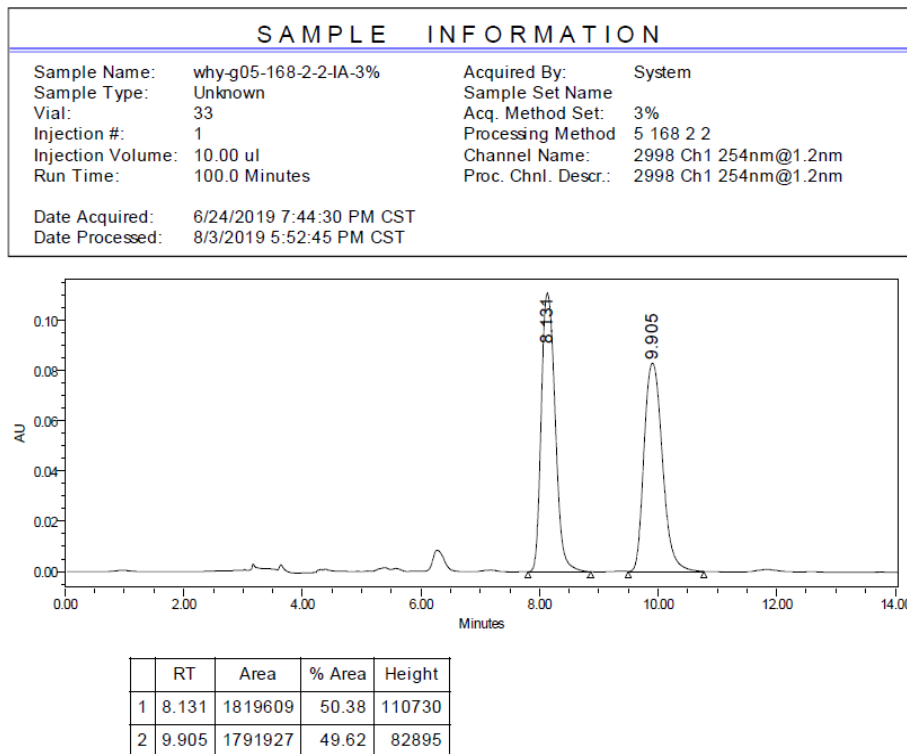


**Figure S124.** HPLC spectra of **3v**, related to **Scheme 2**.

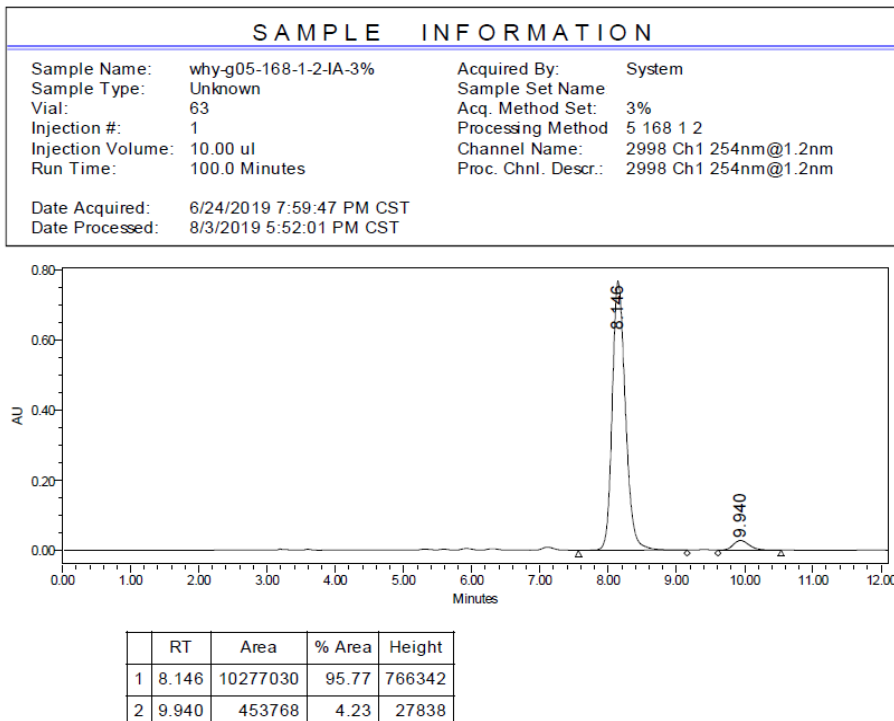


**Figure S125.** HPLC spectra of *rac*-3w, related to **Scheme 2**.

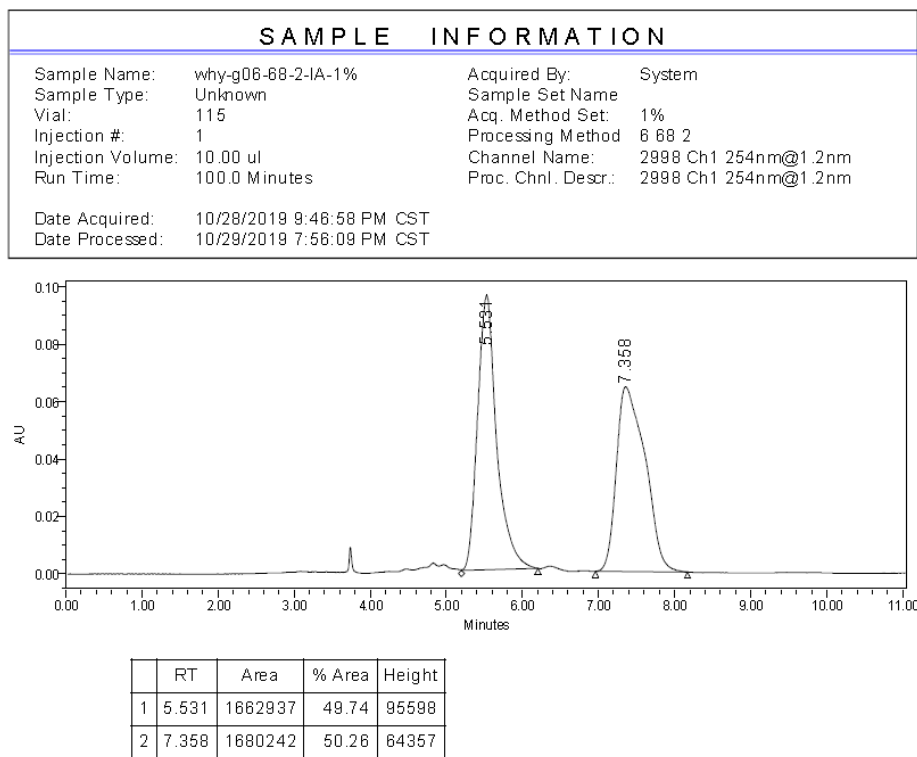


**Figure S126.** HPLC spectra of 3w, related to **Scheme 2**.

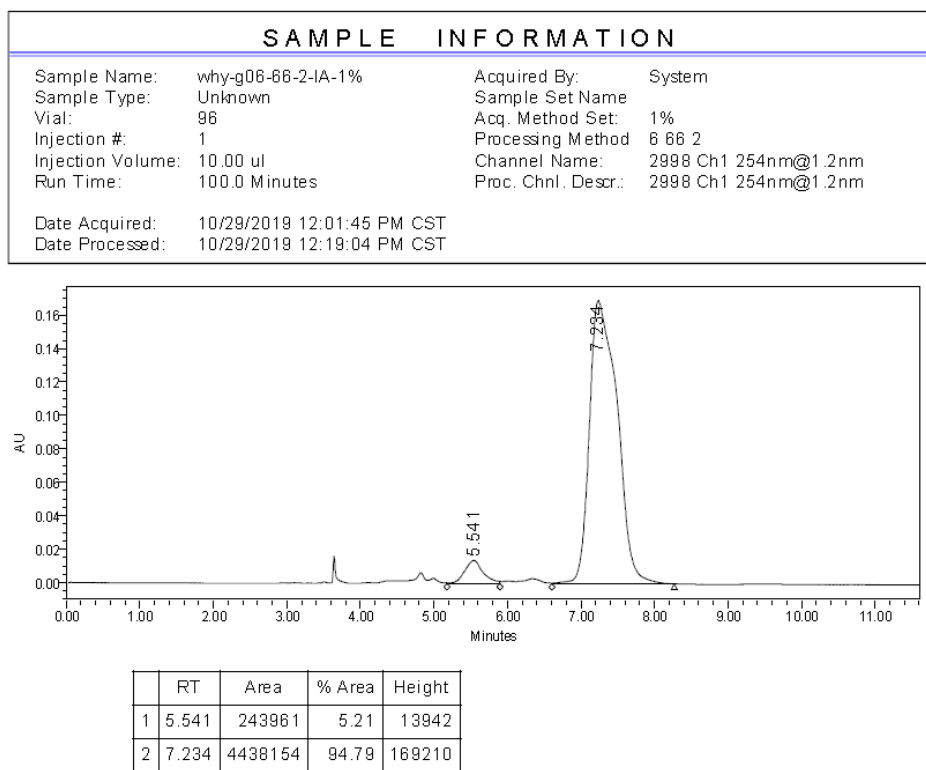


**Figure S127.** HPLC spectra of *rac*-**3x**, related to **Scheme 2**.

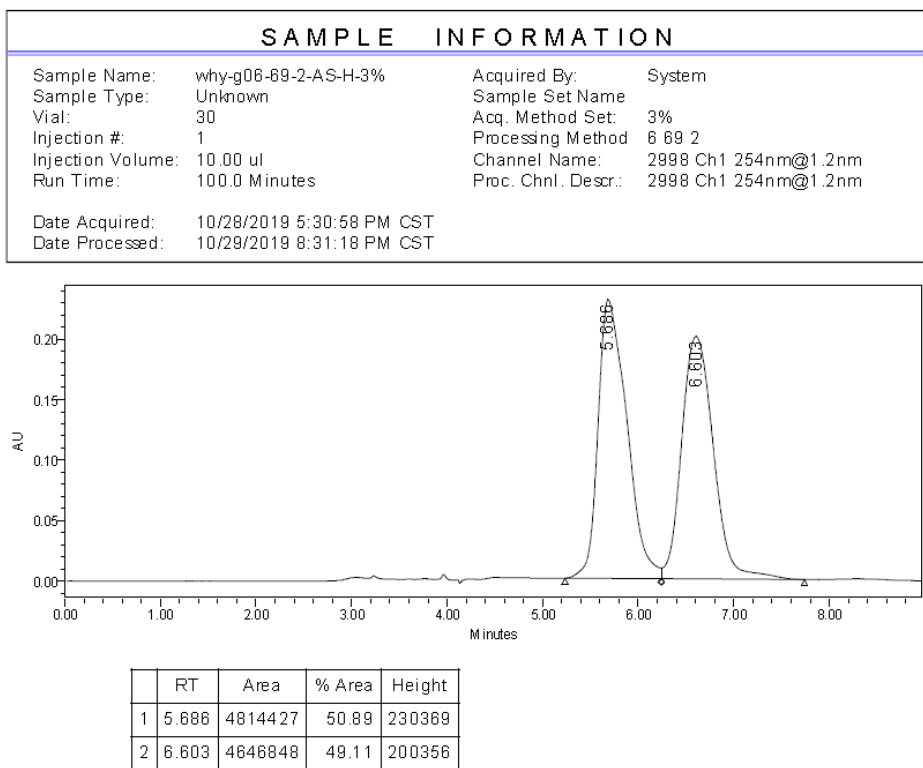


**Figure S128.** HPLC spectra of **3x**, related to **Scheme 2**.

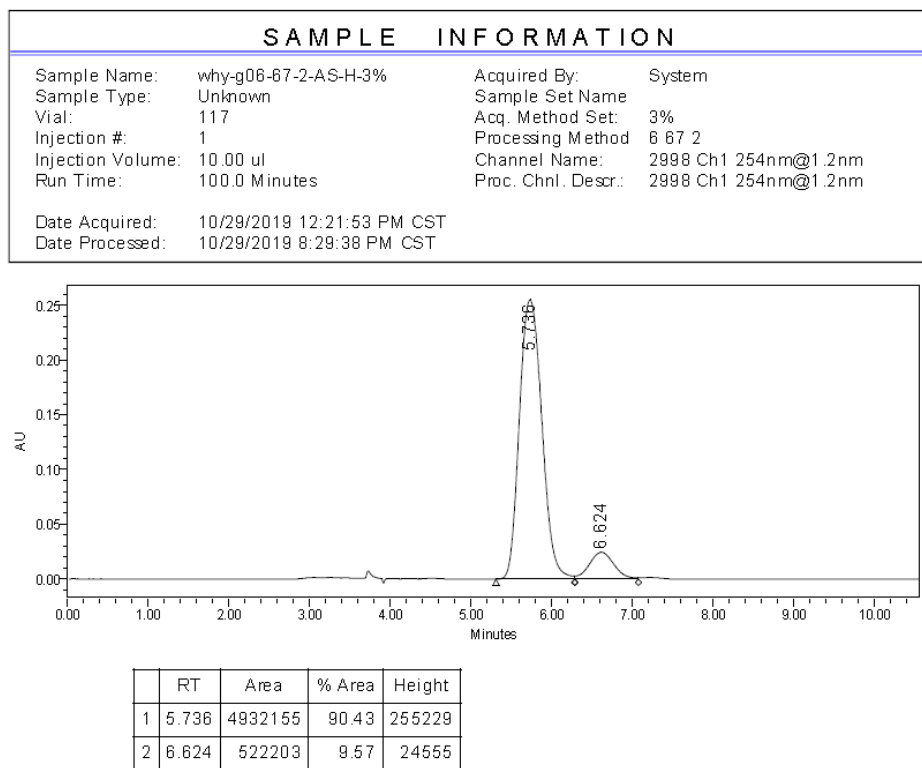


**Figure S129.** HPLC spectra of *rac*-3y, related to **Scheme 2**.

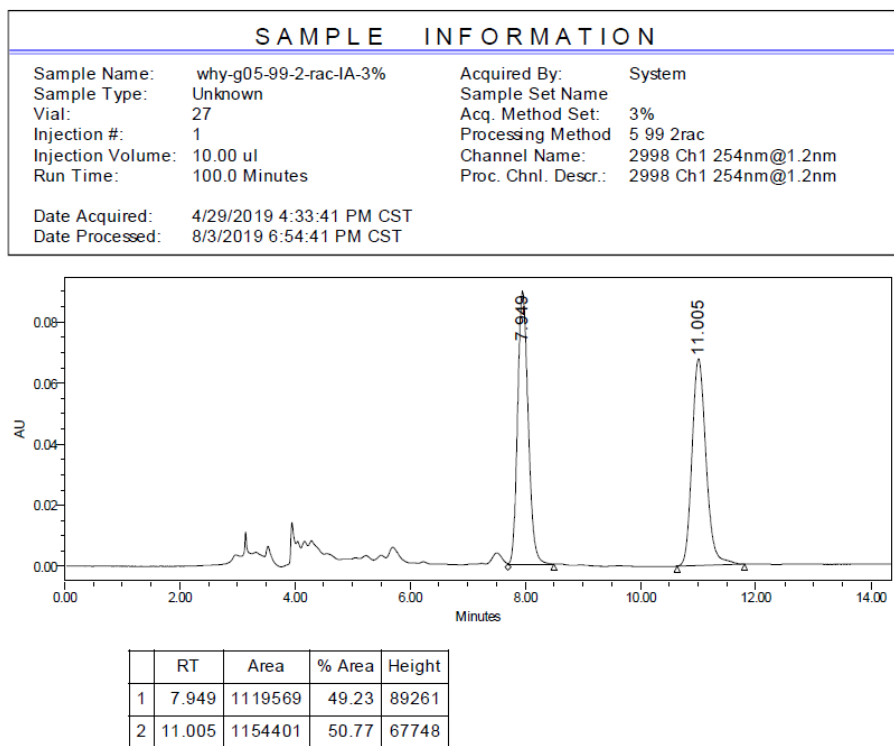


**Figure S130.** HPLC spectra of **3y**, related to **Scheme 2**.

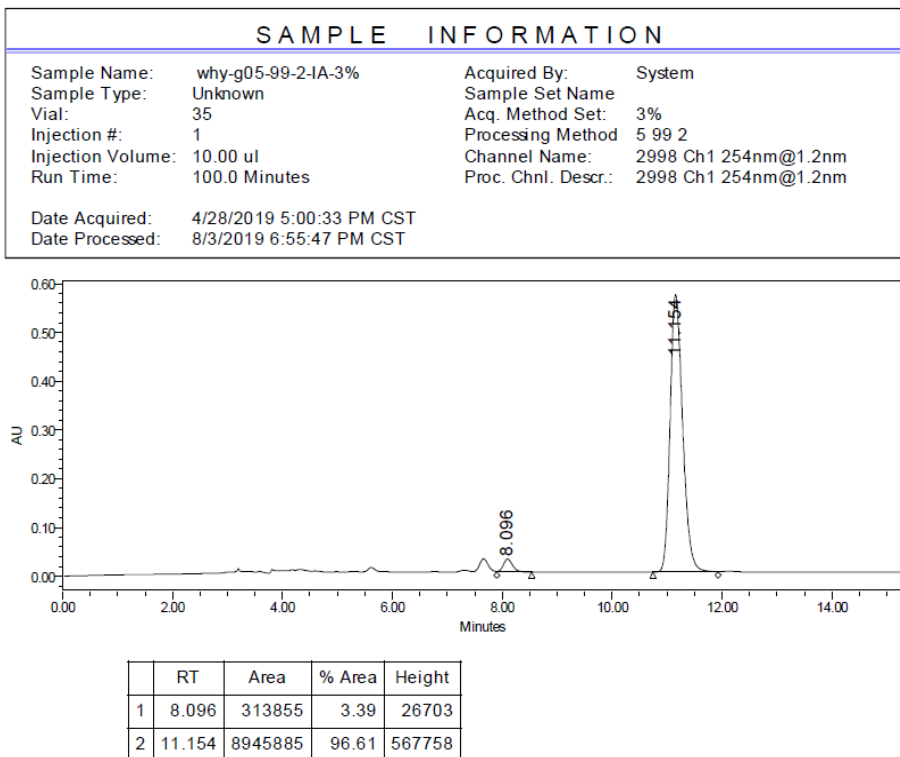
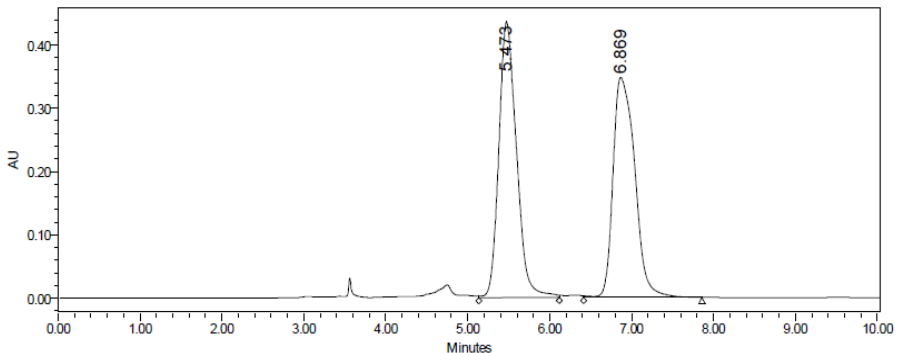


**Figure S131.** HPLC spectra of *rac*-3z, related to **Scheme 2**.

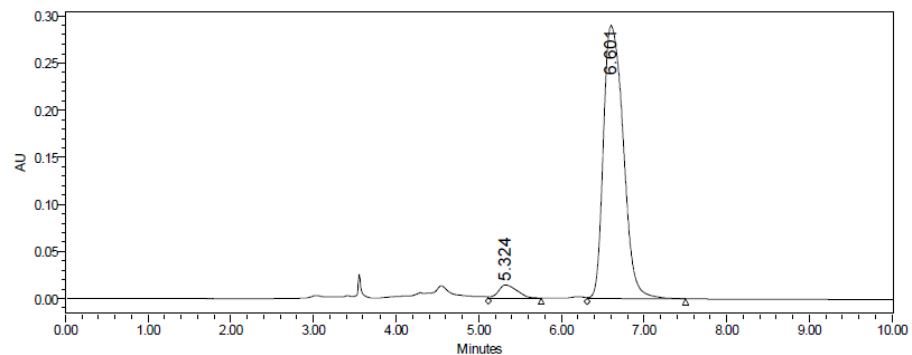
SAMPLE INFORMATION				
Sample Name:	why-g05-99-1-rac-IA-1.5%	Acquired By:	System	
Sample Type:	Unknown	Sample Set Name		
Vial:	44	Acq. Method Set:	1.5%	
Injection #:	1	Processing Method	5 99 1 rac	
Injection Volume:	10.00 $\mu$ l	Channel Name:	2998 Ch1 254nm@1.2nm	
Run Time:	100.0 Minutes	Proc. Chnl. Descr.:	2998 Ch1 254nm@1.2nm	
Date Acquired:	5/5/2019 5:25:59 PM CST			
Date Processed:	7/19/2019 4:50:47 PM CST			



	RT	Area	% Area	Height
1	5.473	6503943	50.32	435332
2	6.869	6420979	49.68	347760

**Figure S132.** HPLC spectra of **3z**, related to **Scheme 2**.

SAMPLE INFORMATION				
Sample Name:	why-g05-99-1-IA-1.5%	Acquired By:	System	
Sample Type:	Unknown	Sample Set Name		
Vial:	99	Acq. Method Set:	1.5%	
Injection #:	1	Processing Method	5 99 1 asy	
Injection Volume:	10.00 $\mu$ l	Channel Name:	2998 Ch1 254nm@1.2nm	
Run Time:	100.0 Minutes	Proc. Chnl. Descr.:	2998 Ch1 254nm@1.2nm	
Date Acquired:	5/6/2019 7:38:31 PM CST			
Date Processed:	7/19/2019 4:51:16 PM CST			



	RT	Area	% Area	Height
1	5.324	209937	4.16	13908
2	6.601	4839867	95.84	289449

**Figure S133.** HPLC spectra of *rac*-**6a**, related to **Scheme 3**.

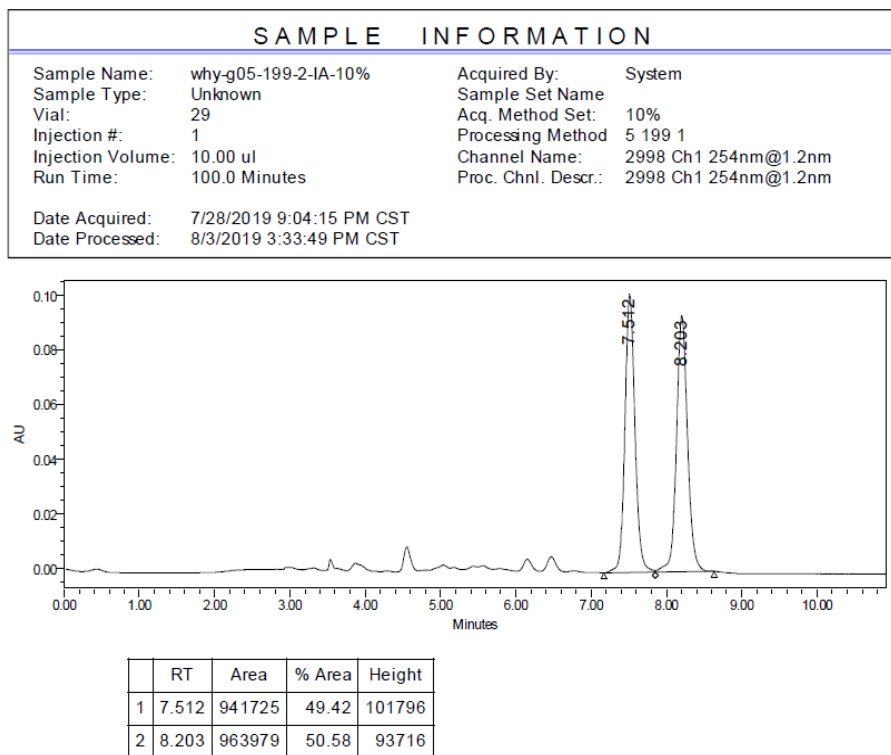


**Figure S134.** HPLC spectra of **6a**, related to **Scheme 3**.

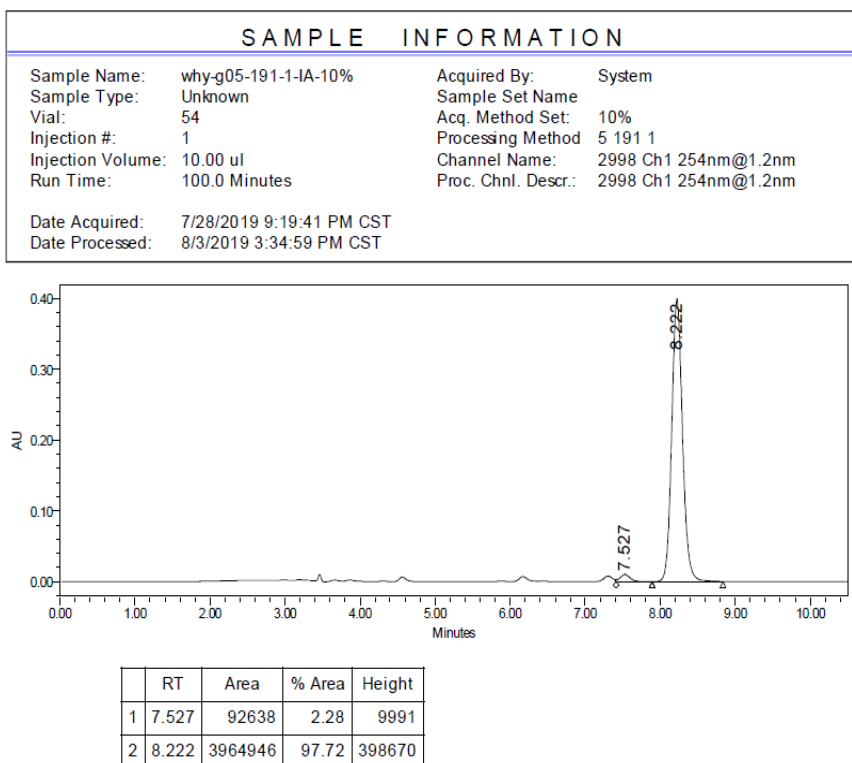
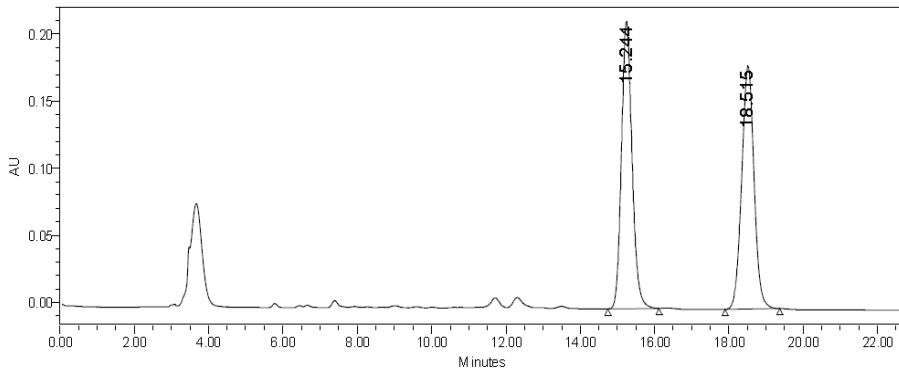


**Figure S135.** HPLC spectra of **rac-6b**, related to **Scheme 3**.

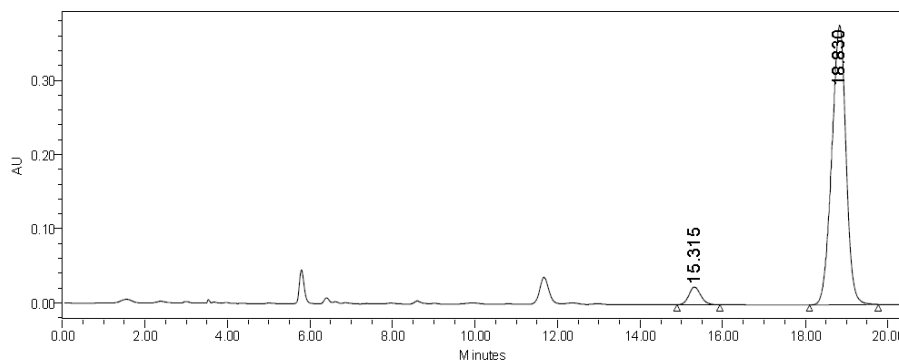
SAMPLE INFORMATION				
Sample Name:	why-g05-159-2-IA-10%	Acquired By:	System	
Sample Type:	Unknown	Sample Set Name		
Vial:	56	Acq. Method Set:	10%	
Injection #:	1	Processing Method	5 159 2	
Injection Volume:	10.00 $\mu$ l	Channel Name:	2998 Ch1 254nm@1.2nm	
Run Time:	100.0 Minutes	Proc. Chnl. Descr.:	2998 Ch1 254nm@1.2nm	
Date Acquired:	6/18/2019 6:54:46 PM CST			
Date Processed:	8/3/2019 3:26:09 PM CST			



	RT	Area	% Area	Height
1	15.244	4234718	50.08	213977
2	18.515	4220834	49.92	181236

**Figure S136.** HPLC spectra of **6b**, related to **Scheme 3**.

SAMPLE INFORMATION				
Sample Name:	why-g05-169-2-IA-10%	Acquired By:	System	
Sample Type:	Unknown	Sample Set Name		
Vial:	106	Acq. Method Set:	10%	
Injection #:	1	Processing Method	5 169 2	
Injection Volume:	10.00 $\mu$ l	Channel Name:	2998 Ch1 254nm@1.2nm	
Run Time:	100.0 Minutes	Proc. Chnl. Descr.:	2998 Ch1 254nm@1.2nm	
Date Acquired:	6/24/2019 6:55:34 PM CST			
Date Processed:	8/3/2019 3:28:10 PM CST			



	RT	Area	% Area	Height
1	15.315	467017	4.94	23666
2	18.830	8989230	95.06	376102

**Figure S137.** HPLC spectra of *rac*-**6c**, related to **Scheme 3**.

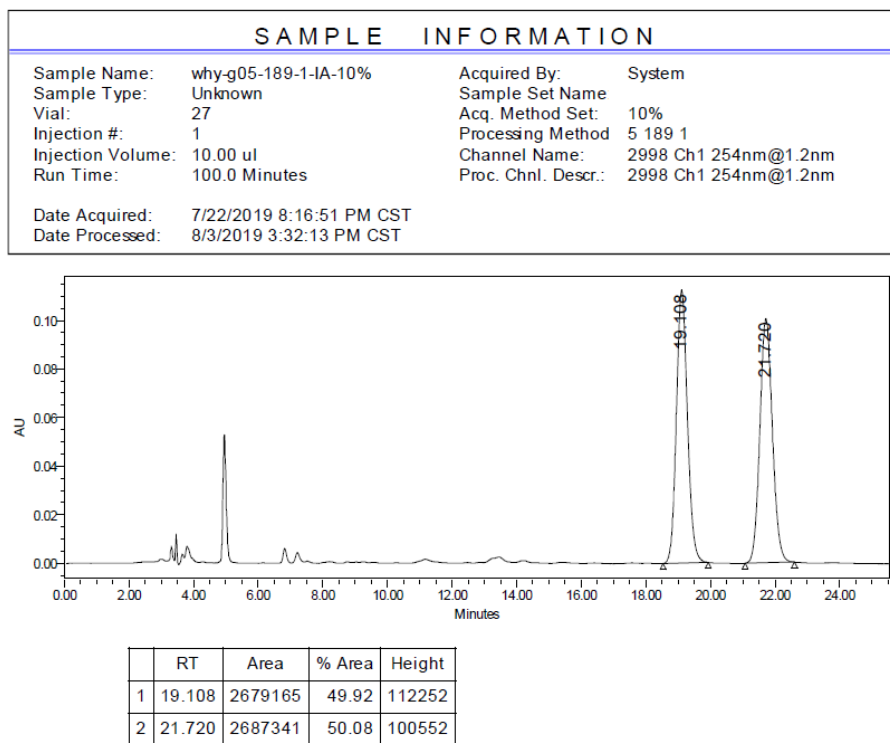


**Figure S138.** HPLC spectra of **6c**, related to **Scheme 3**.

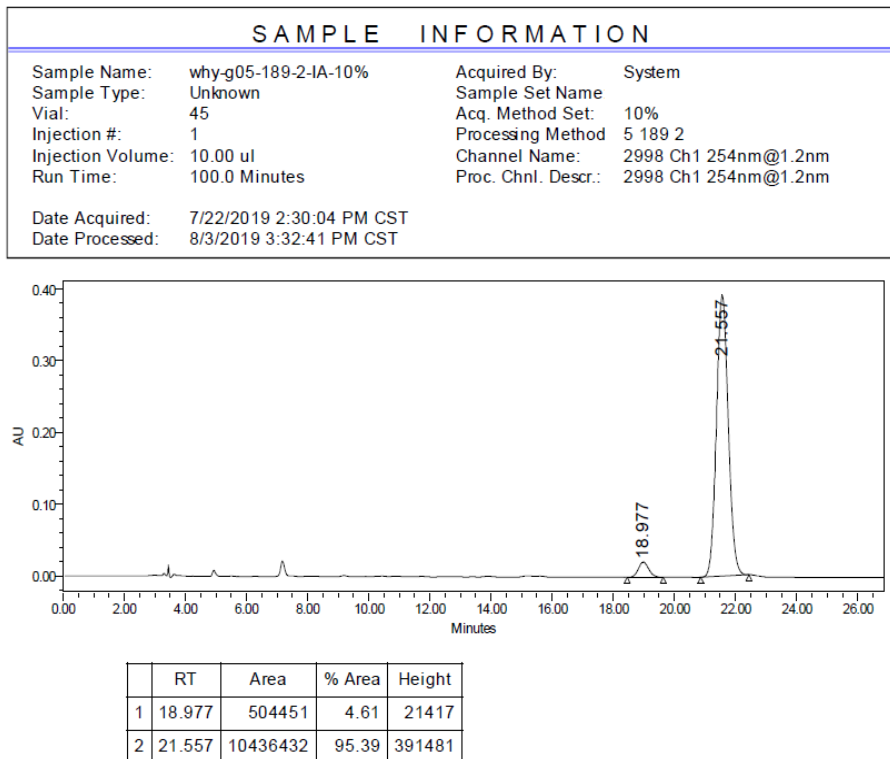


**Figure S139.** HPLC spectra of *rac*-**6d**, related to **Scheme 3**.

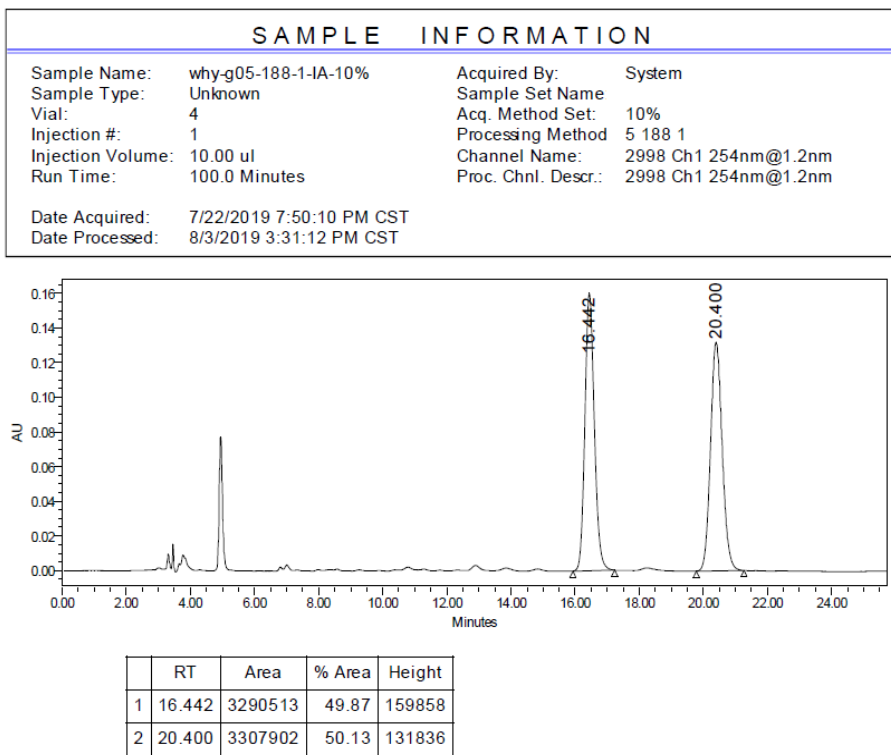


**Figure S140.** HPLC spectra of **6d**, related to **Scheme 3**.

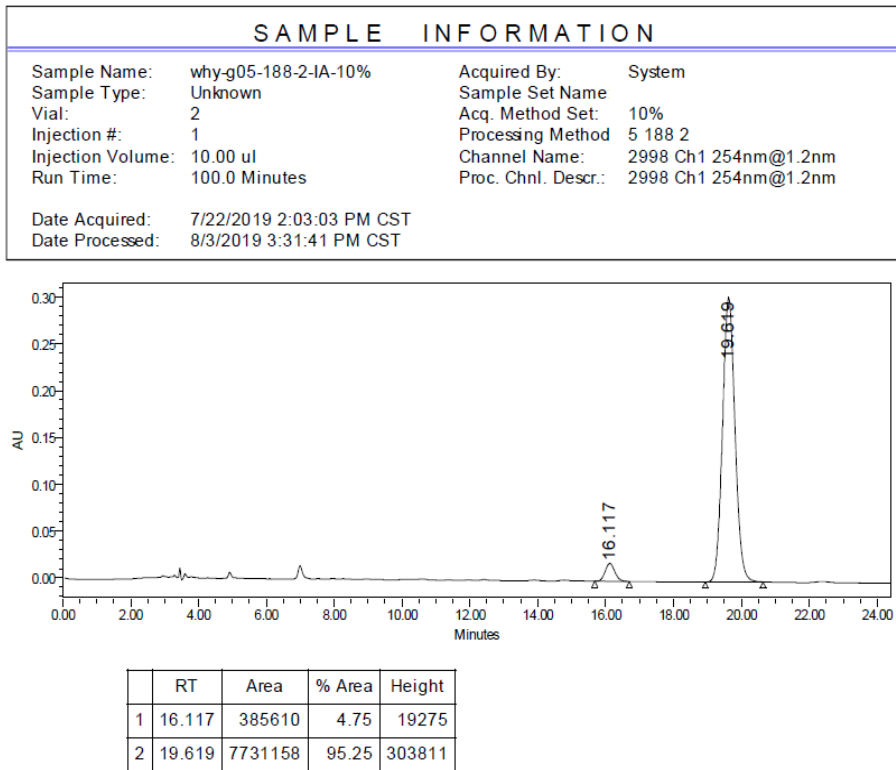


**Figure S141.** HPLC spectra of *rac*-**6e**, related to **Scheme 3**.

SAMPLE INFORMATION				
Sample Name:	why-g05-197-2-IA-10%	Acquired By:	System	
Sample Type:	Unknown	Sample Set Name		
Vial:	21	Acq. Method Set:	10%	
Injection #:	1	Processing Method	5 197 2	
Injection Volume:	10.00 $\mu$ l	Channel Name:	2998 Ch1 254nm@1.2nm	
Run Time:	100.0 Minutes	Proc. Chnl. Descr.:	2998 Ch1 254nm@1.2nm	
Date Acquired:	7/27/2019 6:48:52 PM CST			
Date Processed:	8/3/2019 3:38:05 PM CST			

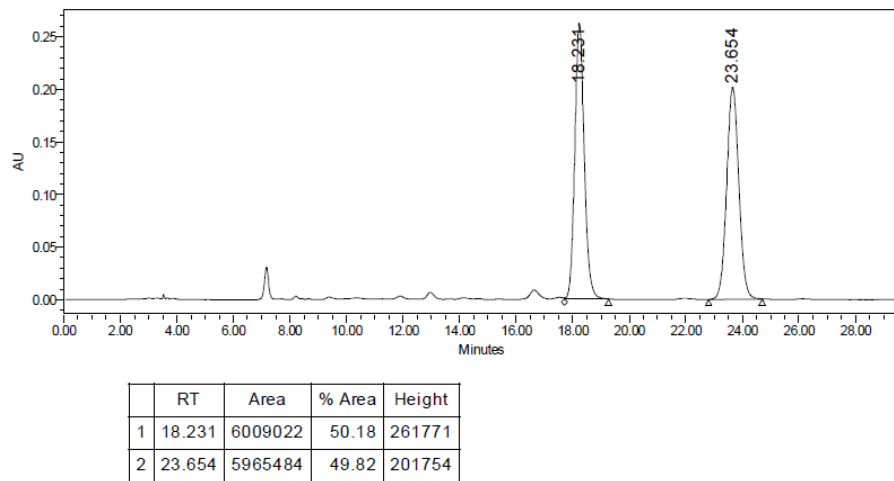


**Figure S142.** HPLC spectra of **6e**, related to **Scheme 3**.

SAMPLE INFORMATION				
Sample Name:	why-g05-194-2-IA-10%	Acquired By:	System	
Sample Type:	Unknown	Sample Set Name		
Vial:	16	Acq. Method Set:	10%	
Injection #:	1	Processing Method	5 194 2	
Injection Volume:	10.00 $\mu$ l	Channel Name:	2998 Ch1 254nm@1.2nm	
Run Time:	100.0 Minutes	Proc. Chnl. Descr.:	2998 Ch1 254nm@1.2nm	
Date Acquired:	7/28/2019 9:52:27 AM CST			
Date Processed:	8/3/2019 3:38:37 PM CST			

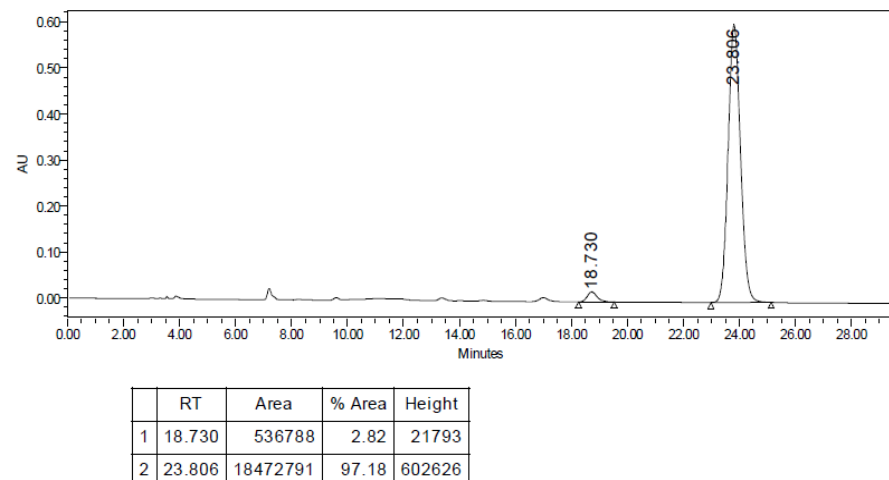


**Figure S143.** HPLC spectra of *rac*-**6f**, related to **Scheme 3**.

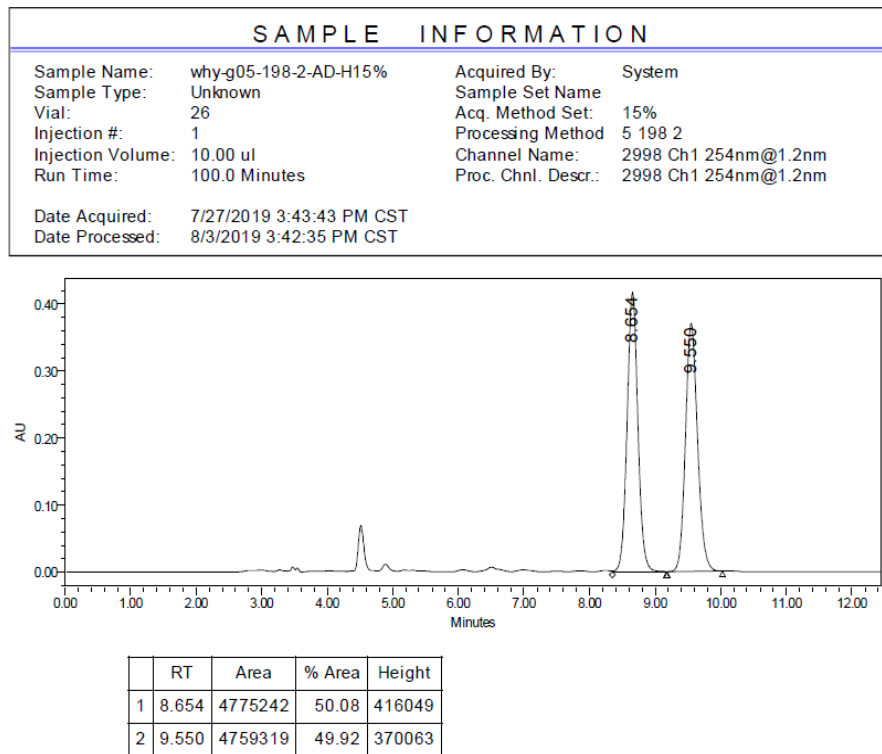


**Figure S144.** HPLC spectra of **6f**, related to **Scheme 3**.

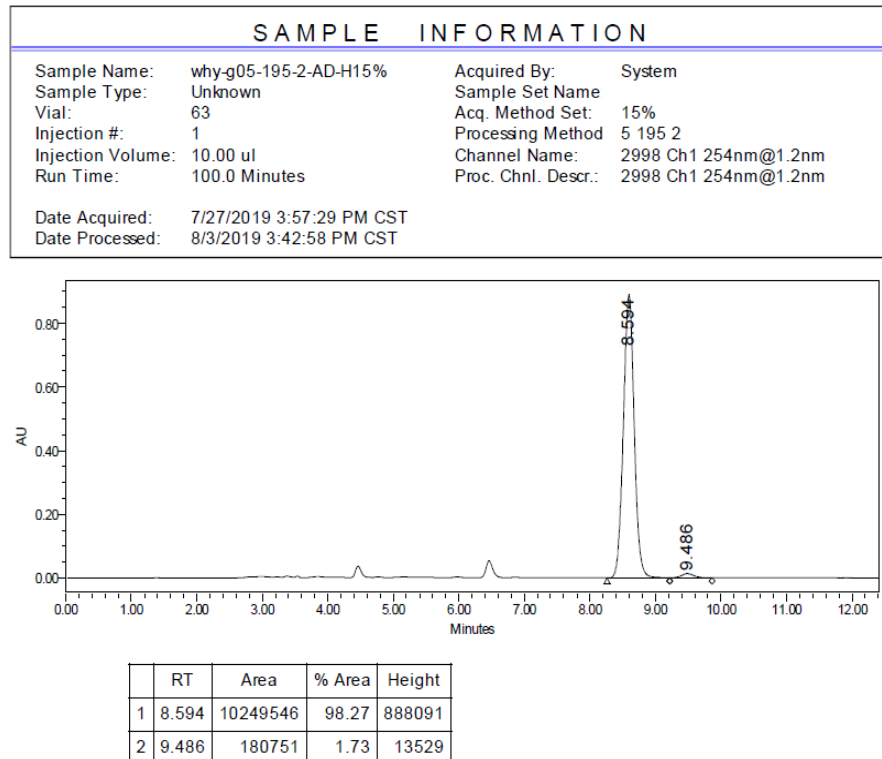
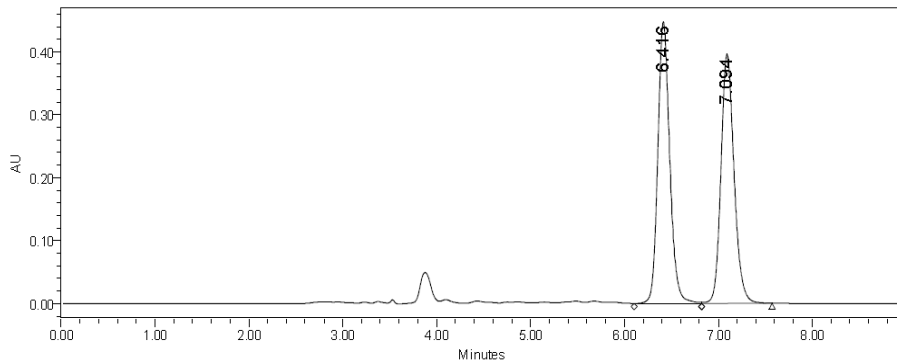


**Figure S145.** HPLC spectra of *rac*-**6g**, related to **Scheme 3**.

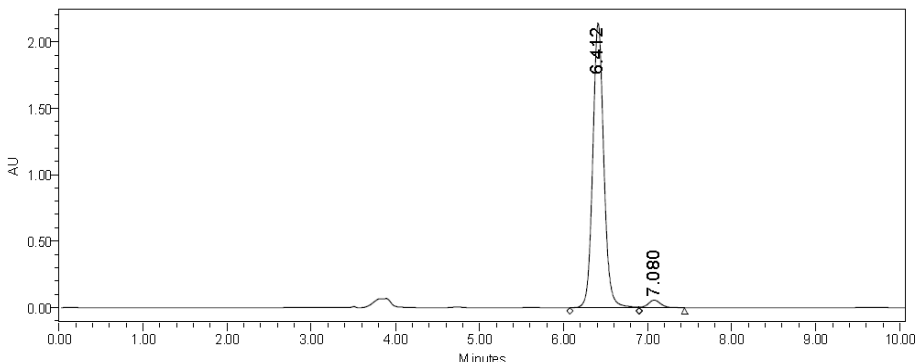
SAMPLE INFORMATION				
Sample Name:	why-g05-198-1-AD-H15%	Acquired By:	System	
Sample Type:	Unknown	Sample Set Name		
Vial:	104	Acq. Method Set:	15%	
Injection #:	1	Processing Method	5 198 1	
Injection Volume:	10.00 $\mu$ l	Channel Name:	2998 Ch1 254nm@1.2nm	
Run Time:	100.0 Minutes	Proc. Chnl. Descr.:	2998 Ch1 254nm@1.2nm	
Date Acquired:	7/27/2019 2:50:56 PM CST			
Date Processed:	8/3/2019 3:41:13 PM CST			



	RT	Area	% Area	Height
1	6.416	3934302	50.62	447162
2	7.094	3838527	49.38	395811

**Figure S146.** HPLC spectra of **6g**, related to **Scheme 3**.

SAMPLE INFORMATION				
Sample Name:	why-g05-195-1-AD-H15%	Acquired By:	System	
Sample Type:	Unknown	Sample Set Name		
Vial:	20	Acq. Method Set:	15%	
Injection #:	1	Processing Method	5 195 1	
Injection Volume:	10.00 $\mu$ l	Channel Name:	2998 Ch1 254nm@1.2nm	
Run Time:	100.0 Minutes	Proc. Chnl. Descr.:	2998 Ch1 254nm@1.2nm	
Date Acquired:	7/27/2019 3:01:35 PM CST			
Date Processed:	8/3/2019 3:41:58 PM CST			



	RT	Area	% Area	Height
1	6.412	19561736	97.09	2137082
2	7.080	585287	2.91	57468

**Figure S147.** HPLC spectra of *rac*-**6h**, related to **Scheme 3**.

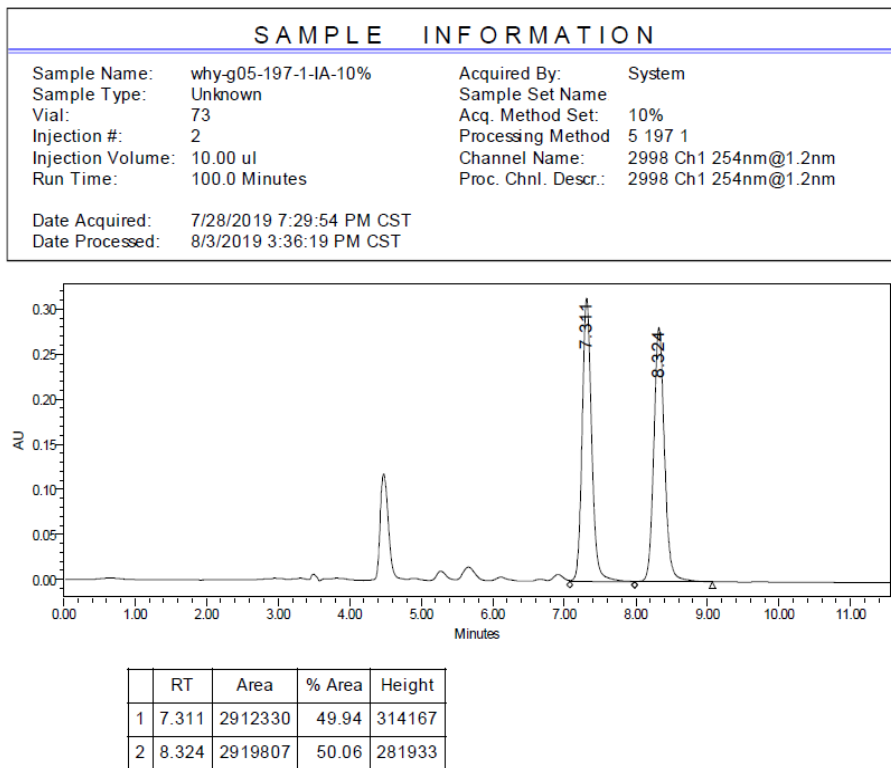


**Figure S148.** HPLC spectra of **6h**, related to **Scheme 3**.

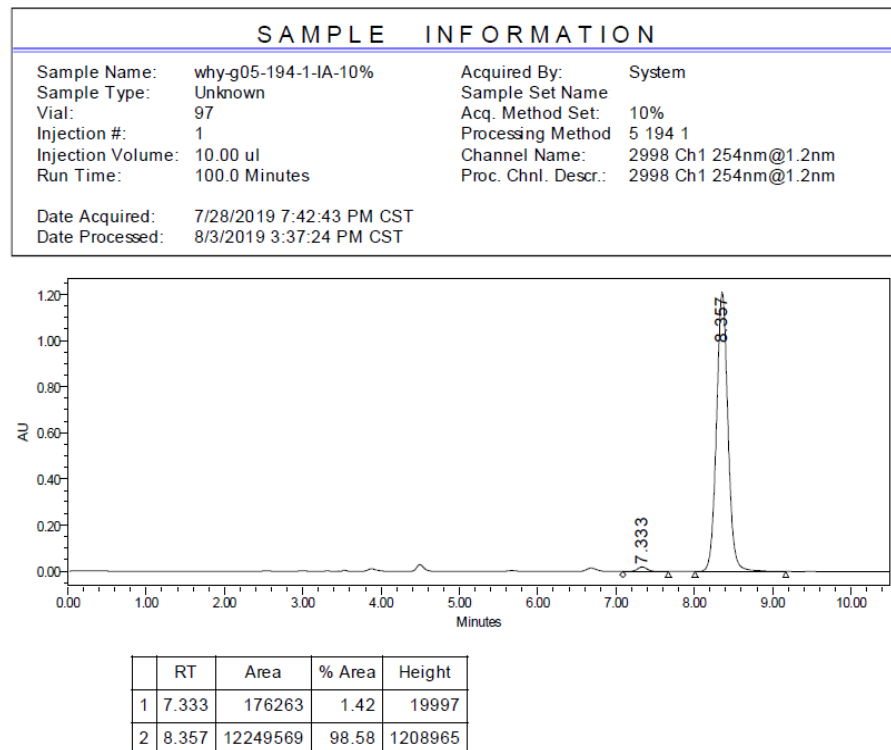
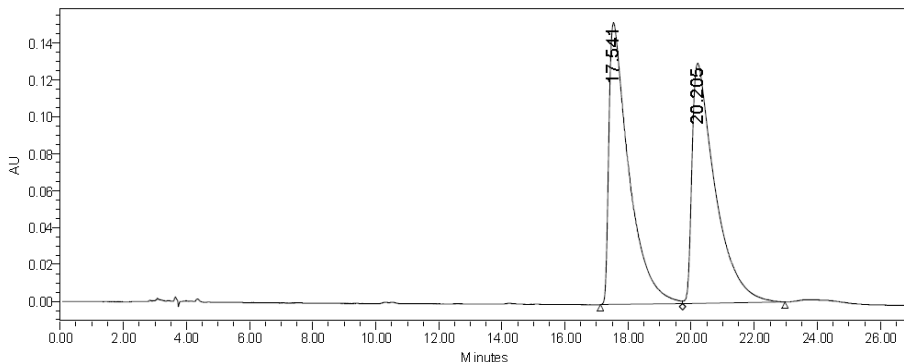


**Figure S149.** HPLC spectra of *rac*-7, related to **Scheme 4**.

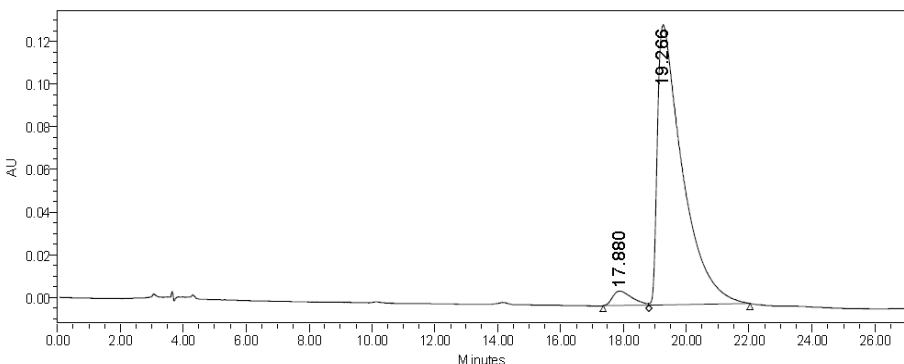
SAMPLE INFORMATION				
Sample Name:	why-g06-37-1-IA-5%	Acquired By:	System	
Sample Type:	Unknown	Sample Set Name		
Vial:	2	Acq. Method Set:	5%	
Injection #:	1	Processing Method	6 37 1 rac	
Injection Volume:	10.00 $\mu$ l	Channel Name:	2998 Ch1 254nm@1.2nm	
Run Time:	100.0 Minutes	Proc. Chnl. Descr.:	2998 Ch1 254nm@1.2nm	
Date Acquired:	8/26/2019 8:45:50 PM CST			
Date Processed:	9/24/2019 2:55:43 PM CST			



	RT	Area	% Area	Height
1	17.541	6673637	50.20	152291
2	20.205	6620390	49.80	129656

**Figure S150.** HPLC spectra of 7, related to **Scheme 4**.

SAMPLE INFORMATION				
Sample Name:	why-g06-37-1-asy-IA-5%	Acquired By:	System	
Sample Type:	Unknown	Sample Set Name		
Vial:	12	Acq. Method Set:	5%	
Injection #:	1	Processing Method	6 37 1 asy	
Injection Volume:	10.00 $\mu$ l	Channel Name:	2998 Ch1 254nm@1.2nm	
Run Time:	100.0 Minutes	Proc. Chnl. Descr.:	2998 Ch1 254nm@1.2nm	
Date Acquired:	9/21/2019 10:09:33 AM CST			
Date Processed:	9/24/2019 3:03:36 PM CST			



	RT	Area	% Area	Height
1	17.880	289188	3.85	6737
2	19.266	7230632	96.15	131152

**Figure S151.** HPLC spectra of *rac*-8, related to **Scheme 4**.

SAMPLE INFORMATION	
Sample Name:	why-g06-38-1-AD-H-10%
Sample Type:	Unknown
Vial:	72
Injection #:	1
Injection Volume:	10.00 $\mu$ l
Run Time:	100.0 Minutes
Acquired By:	System
Sample Set Name	
Acq. Method Set:	10%
Processing Method	6 38 1 rac
Channel Name:	2998 Ch1 254nm@1.2nm
Proc. Chnl. Descr.:	2998 Ch1 254nm@1.2nm
Date Acquired:	8/28/2019 3:59:26 PM CST
Date Processed:	9/24/2019 2:57:11 PM CST

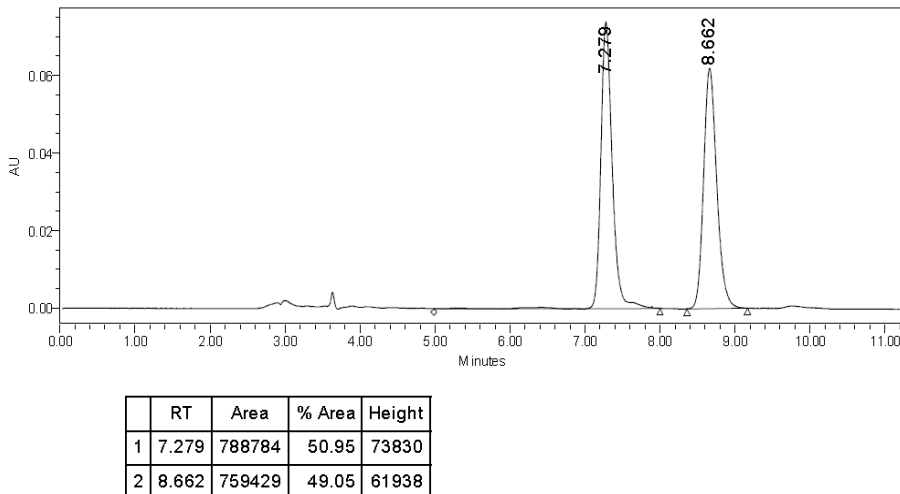
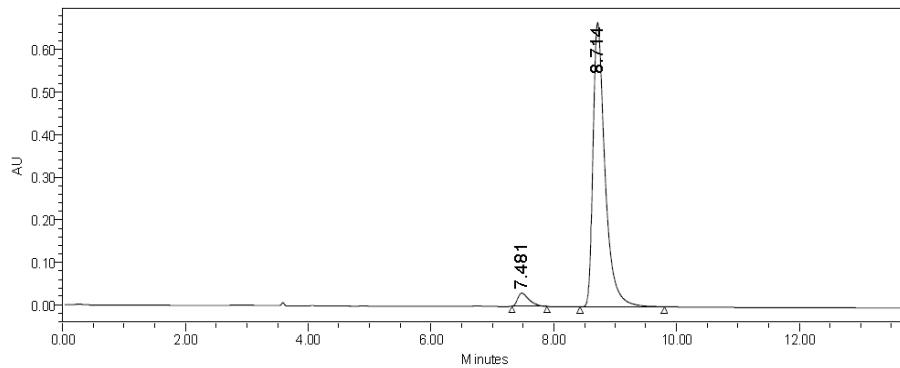


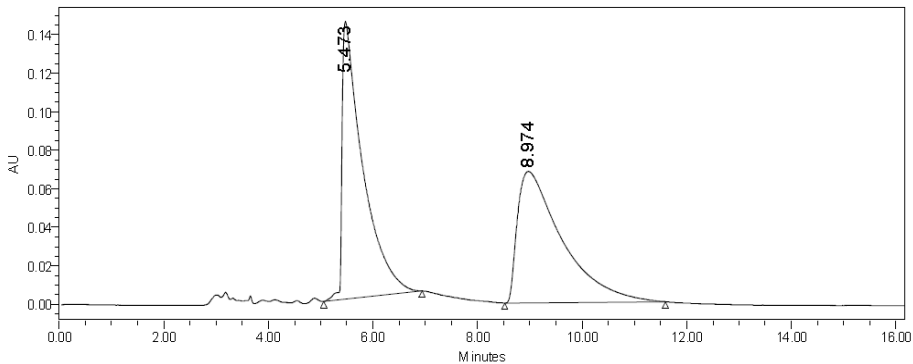
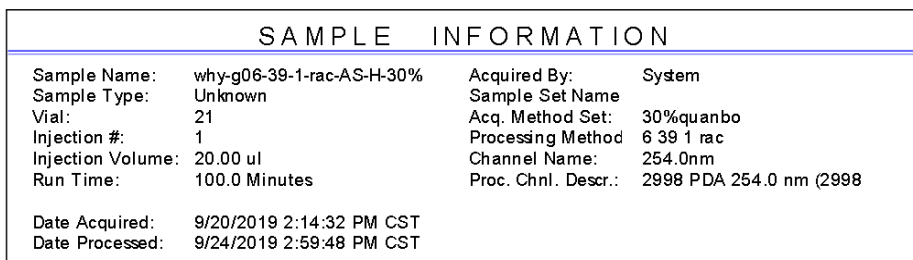
**Figure S152.** HPLC spectra of 8, related to **Scheme 4**.

SAMPLE INFORMATION	
Sample Name:	why-g06-38-1-asy-AD-H-10%
Sample Type:	Unknown
Vial:	2
Injection #:	1
Injection Volume:	10.00 $\mu$ l
Run Time:	100.0 Minutes
Acquired By:	System
Sample Set Name	
Acq. Method Set:	10%
Processing Method	6 38 1 ASY
Channel Name:	2998 Ch1 254nm@1.2nm
Proc. Chnl. Descr.:	2998 Ch1 254nm@1.2nm
Date Acquired:	9/23/2019 11:27:03 AM CST
Date Processed:	9/23/2019 2:37:07 PM CST



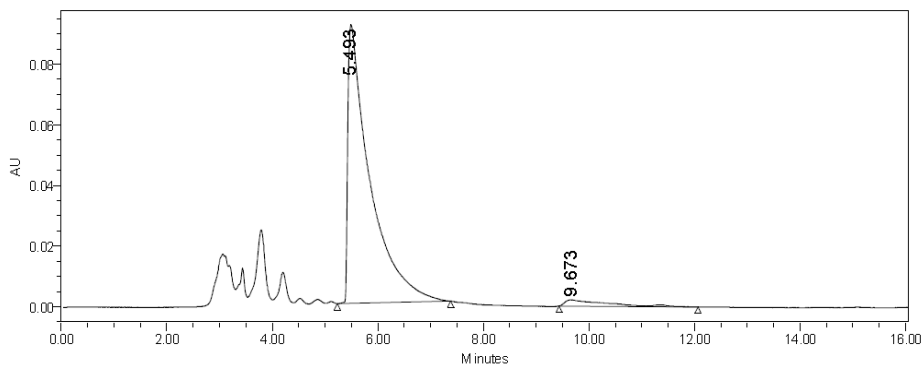
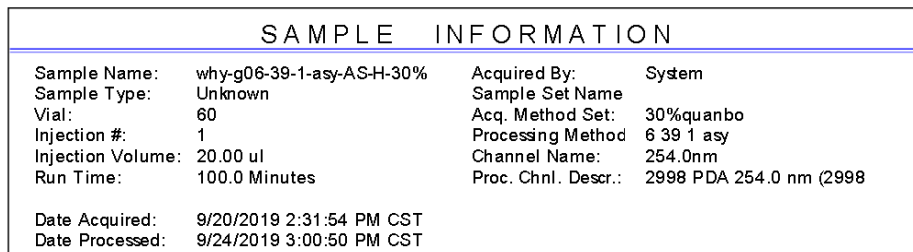
	RT	Area	% Area	Height
1	7.481	402073	4.23	30981
2	8.714	9113769	95.77	667895

**Figure S153.** HPLC spectra of *rac*-9, related to **Scheme 4**.



	RT	Area	% Area	Height
1	5.473	3973711	49.57	144135
2	8.974	4042019	50.43	68201

**Figure S154.** HPLC spectra of 9, related to **Scheme 4**.



	RT	Area	% Area	Height
1	5.493	2669826	95.84	91846
2	9.673	115750	4.16	2036

**Figure S155.** HPLC spectra of *rac*-**10**, related to **Table 1**.

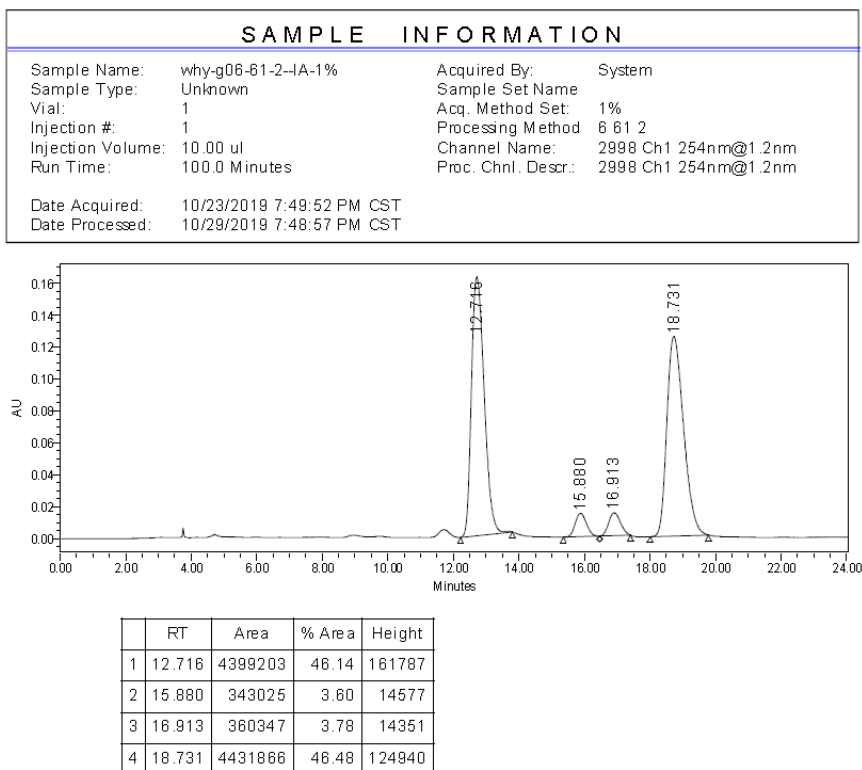
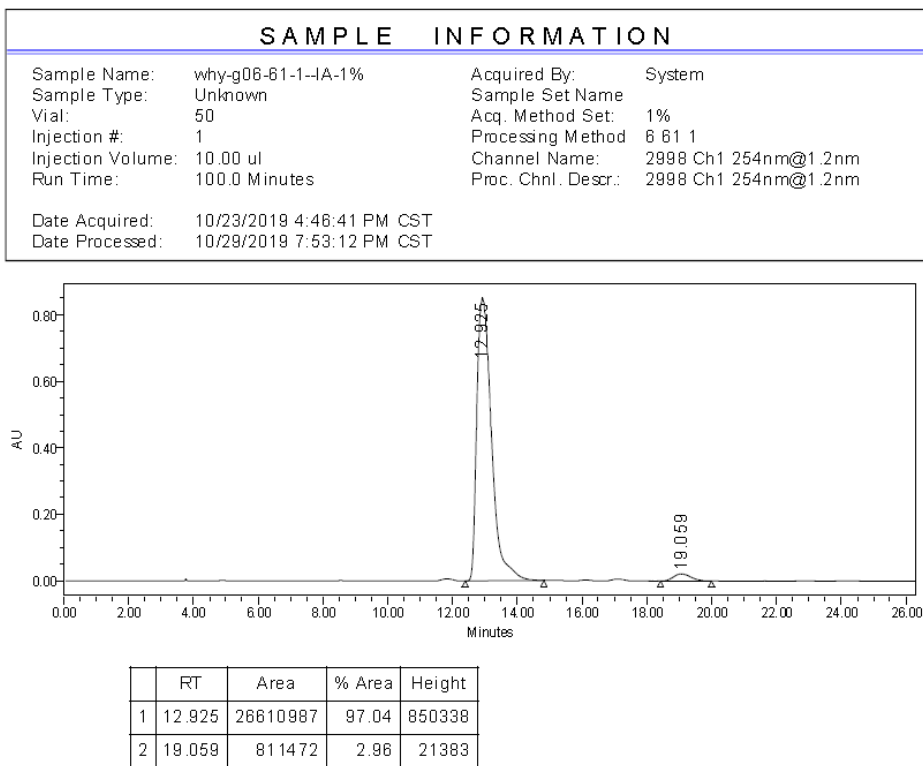
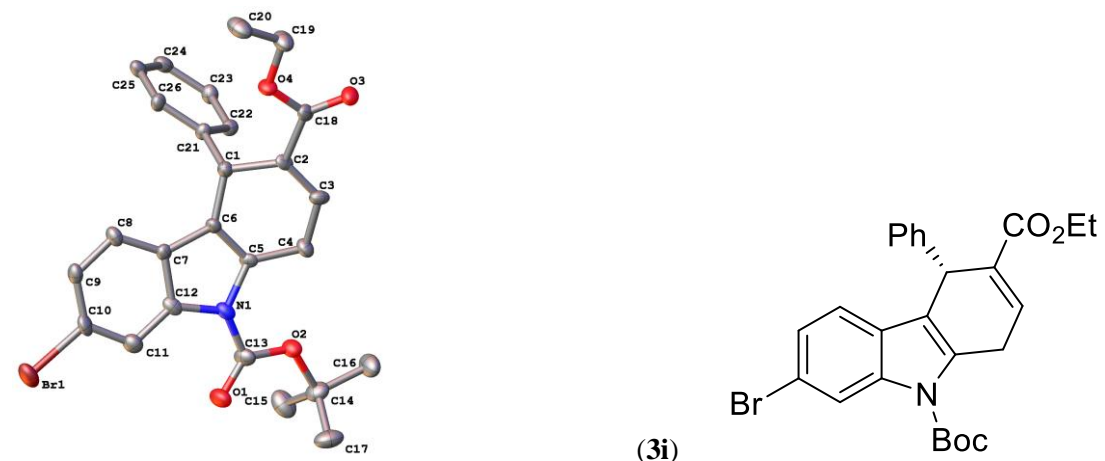


**Figure S156.** HPLC spectra of **10**, related to **Table 1**.



**Supplemental figures and tables for X-Ray structures**

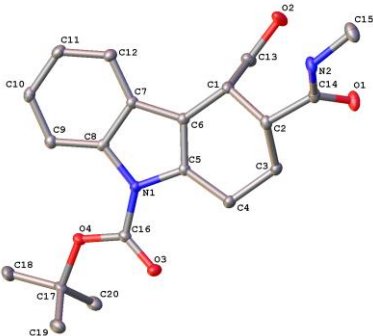
**Figure S157.** X-Ray crystal data of **3i**, related to **Scheme 2**.



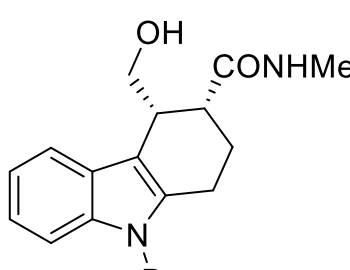
Chemical formula	C <sub>26</sub> H <sub>26</sub> BrNO <sub>4</sub>
Formula weight	496.39
Space group	P1
Z	4
$\alpha$ , Å	9.1215(5)
$b$ , Å	13.5175(7)
$c$ , Å	19.4869(10)
$\alpha$ , °	99.498(3)
$\beta$ , °	93.402(3)
$\gamma$ , °	96.017(3)
V, Å <sup>3</sup>	2349.5(2)
$\rho$ , g/cm <sup>3</sup>	1.403

**Figure S158..** X-Ray crystal data of **7**, related to **Scheme 4.**

---



(7)



C<sub>20</sub>H<sub>26</sub>N<sub>2</sub>O<sub>4</sub>

---

Chemical formula	C <sub>20</sub> H <sub>26</sub> N <sub>2</sub> O <sub>4</sub>
Formula weight	358.43
Space group	P2 <sub>1</sub> 2 <sub>1</sub> 2 <sub>1</sub>
Z	4
a, Å	7.87500(10)
b, Å	10.1406(2)
c, Å	23.0161(4)
α, °	90
β, °	90
γ, °	90
V, Å <sup>3</sup>	1838.00(5)
ρ,g/cm <sup>3</sup>	1.295

---

## Transparent Methods

### General Information

Unless otherwise noted, all reagents were purchased from commercial suppliers and used without further purification. NMR spectra were recorded on a Brucker-400 MHz spectrometer. Chemical shifts ( $\delta$ ) are given in ppm relative to TMS. The residual solvent signals were used as references and the chemical shifts converted to the TMS scale ( $\text{CHCl}_3$ :  $\delta$  7.26 for proton and  $\delta$  77.16 for carbon; DMSO:  $\delta$  2.49 for proton and  $\delta$  39.51 for carbon; Acetone:  $\delta$  2.05 for proton and  $\delta$  206.68 for carbon). Multiplicities were given as: s (singlet); d (doublet); t (triplet); q (quartet); dd (doublet of doublets); dt (doublet of triplets); m (multiplets); brs (broad signal). Coupling constants are reported as a  $J$  value in Hz. High resolution mass spectral analysis (HRMS) was performed on Waters XEVO G2 Q-TOF. The measurement of enantiomeric excesses was performed on Waters-Alliance (2998. Photodiode Array Detector, UV detection monitored at 254 nm). Chiralpak IA, AD-H and AS-H columns were purchased from Daicel Chemical Industries, LTD. The absolute configuration of 3i and 7 were assigned by the X-ray analysis. Optical rotations were determined at 589 nm (sodium D line) by using a Perkin-Elmer-343 polarimeter.

### Preparation of Substrates

#### Preparation of 3-Nitroindoles 1 and 3-Nitrobenzothiophenes 5

The 3-nitroindoles **1**(You et al, 2018), 3-nitrobenzothiophenes **5**(You et al, 2017) and Allenoates **2**(Kwon et al, 2007) were synthesized according to the literature.

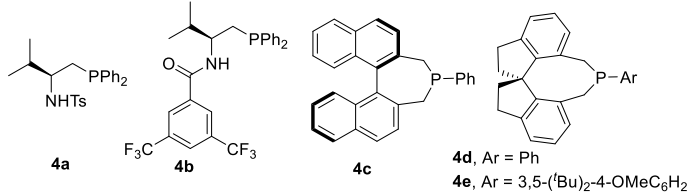
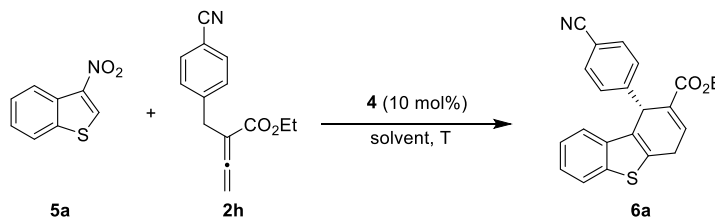
### Optimize reaction conditions

**Table S1:** Additives effect the reaction of 3-nitroindoles **1a** and allenotes **2a**, related to Table 1<sup>[a]</sup>.

Entry	Additive	T (°C)	t (h)	10 [%] <sup>[b]</sup>	ee [%] <sup>[c]</sup>	3a [%] <sup>[b]</sup>	ee [%] <sup>[c]</sup>	11 [%] <sup>[b]</sup>
				10 [%] <sup>[b]</sup>	ee [%] <sup>[c]</sup>	3a [%] <sup>[b]</sup>	ee [%] <sup>[c]</sup>	11 [%] <sup>[b]</sup>
1	-	rt	-	74	94	21	94	-
2	Silica gel (200 mg)	rt	3	8	94	92	94	-
3	Sc(OTf) <sub>3</sub> (20 mol%)	50	6	-	-	10	90	59
4	SnCl <sub>2</sub> (20 mol%)	50	6	24	94	44	94	
5	PhCOOH (20 mol%)	50	3	67	94	15	94	
6	Et <sub>3</sub> N (1.0 eqive)	50	3	66	94	16	94	
7	DABCO (1.0 eqive)	50	3	52	94	14	94	

[a] Reactions were conducted with **1a** (0.1 mmol), **2a** (0.15 mmol) and catalyst **4d** (0.01 mmol) in toluene(1.0 mL) at room temperature. [b] Yield of the isolated product after purification by chromatography on silica gel. [c] Enantiomeric excess determined by HPLC

**Table S2:** Optimization of the reaction of 3-nitrobenzothiophenes **5a** and allenote **2h**, related to Scheme 3<sup>[a]</sup>.



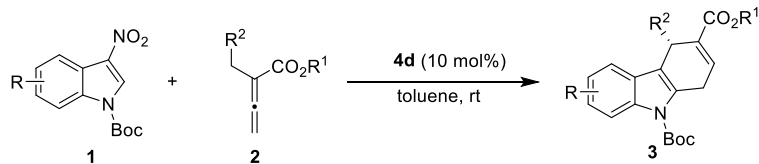
Entry	4	T (°C)	solvent	6a [%] <sup>[b]</sup>	ee [%] <sup>[d]</sup>
1	4a	rt	toluene	-	-
2	4b	rt	toluene	-	-
3	4c	rt	toluene	trace	-
4	4d	rt	toluene	50	82
5	4e	rt	toluene	24	12
6	4d	rt	THF	49	87
7	4d	rt	DCM	36	86
8	4d	rt	dioxane	trace	-
9	4d	0	THF	65	90
10	4d	0	toluene	72	90
11	4d	-20	toluene	trace	-

[a] Reactions were conducted with **5a** (0.1 mmol), **2h** (0.15 mmol) and catalyst **4** (0.01 mmol) in toluene(1.0 mL). [b] Yield of the isolated product after purification by chromatography on silica gel. [c] Enantiomeric excess determined by HPLC analysis.

### General procedure

All the racemic products were obtained by use of Cy<sub>3</sub>P as catalyst.

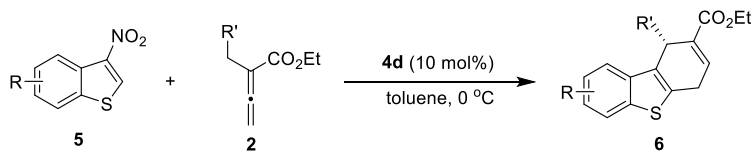
### Scheme S1. General procedure for phosphine-catalyzed enantioselective [4+2] annulation reaction of 3-nitroindoles **1** and allenotes **2**, related to Scheme 2.



A dried tube with a magnetic stir bar was charged with 3-nitroindole derivative **1** (0.10 mmol), allenote derivative **2** (0.15 mmol, 1.5 equiv.), catalyst **4d** (10 mol%), followed by the addition of toluene (1.0 mL), and the reaction mixture was stirred at room temperature. When the reaction was finished (determined by TLC). The mixture were added silica gel and toluene (1.0 mL) continued stir at room temperature when the aromatization process was finished (determined by TLC). Then solvent was evaporated and the residue was purified by column chromatography on silica gel using hexane/ethyl acetate as the eluent to afford the products **3**.

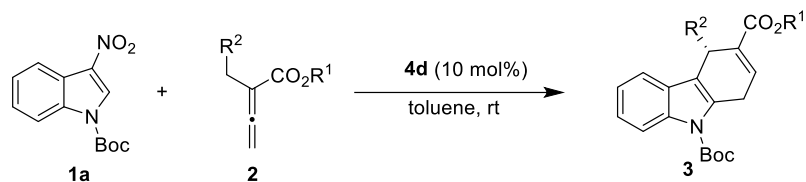
### Scheme S2. General procedure for phosphine-catalyzed enantioselective [4+2]

**annulation reaction of 3-nitrobenzothiophene 5 and allenolate 2, related to Scheme 3.**



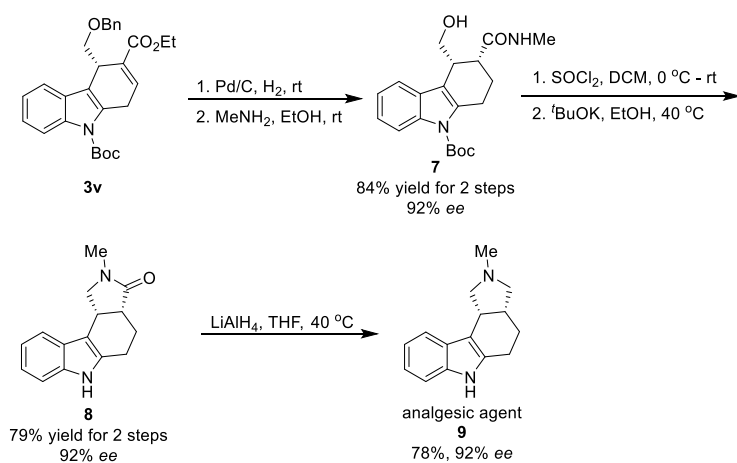
A dried tube with a magnetic stir bar was charged with 3-nitrobenzothiophenes derivative **5** (0.10 mmol), allenolate derivative **2** (0.15 mmol, 1.5 equiv.), catalyst **4d** (10 mol%), followed by the addition of toluene (1.0 mL), and the reaction mixture was stirred at 0 °C. When the reaction was finished (determined by TLC). The mixture were added silica gel and toluene (1.0 mL) continued stir at room temperature when the aromatization process was finished (determined by TLC). Then solvent was evaporated and the residue was purified by column chromatography on silica gel using hexane/ethyl acetate as the eluent to afford the products **6**.

**Scheme S3. 1-mol scale reaction, related to Scheme 2.**



A dried tube with a magnetic stir bar was charged with 3-nitroindole derivative **1a** (1.0 mmol), allenolate derivative **2o** (1.5 mmol, 1.5 equiv.), catalyst **4d** (10 mol%), followed by the addition of toluene (10.0 mL), and the reaction mixture was stirred at room temperature. When the reaction was finished (determined by TLC). The mixture were added silica gel (2.0 g) and toluene (10.0 mL) continued stir at room temperature when the aromatization was finished (determined by TLC). Then solvent was evaporated and the residue was purified by column chromatography on silica gel using hexane/ethyl acetate as the eluent to afford the products **3x** (251.4 mg, 56%, 92% ee).

**Scheme S3. Synthesis procedure of derivatization reaction, related to Scheme 4.**



A dried tube with a magnetic stir bar was charged with 3-nitroindole derivative **1a** (1.00 mmol), allenolate derivative **2m** (1.50 mmol, 1.5 equiv.), catalyst **4d** (10 mol%), followed by the addition

of toluene (10.0 mL), and the reaction mixture was stirred at room temperature. When the reaction was finished (determined by TLC). The mixture were added silica gel (2.0 g) and toluene (10.0 mL) continued stir at room temperature when the aromatization process was finished (determined by TLC). Then solvent was evaporated and the residue was purified by column chromatography on silica gel using hexane/ethyl acetate as the eluent to afford the products **3v** (261.6 mg, 57%, 92% ee).

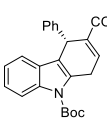
A suspension of **3v** (261.6 mg, 0.57 mmol) and 10% palladium on carbon (130.0 mg) in MeOH (10.0 mL) was maintained under an atmosphere of hydrogen gas for 8 h at rt. The insoluble solids were removed by filtration and the filtrate was concentrated. The residue was dissolved in MeNH<sub>2</sub> (30 wt. % in absolute EtOH 4.0 mL), and the resulting mixture was stirred 1 h. Then solvent was evaporated and the residue was purified by column chromatography on silica gel using hexane/ethyl acetate as the eluent to afford the product **7** (179.2 mg, 84%, 92% ee).

To a solution of **7** (179.2 mg, 0.48 mmol) in anhydrous DCM (5 mL) was slowly added SOCl<sub>2</sub> (1 mol/L in DCM, 2.0 mL) at 0 °C. The suspension was allowed to warm to room temperature and continues to stir 2 h. After that, the reaction mixture was reduced in vacuo. The residue was dissolved in EtOH (5.0 mL) and potassium tert-butoxide (336.0 mg, 3.0 mmol) was added and the reaction stirred at 40 °C for 36 h. The solvent was removed and the residue was purified by column chromatography using MeOH/DCM as the eluent to give **8** (91.2 mg, 79%, 92% ee).

To a solution of **7** (28.8 mg, 0.12 mmol) in anhydrous THF (5 mL) was added LiAlH<sub>4</sub> (45.6 mg, 1.2 mmol) at 0 °C. The suspension was allowed to warm to room temperature and continues to stir at 40 °C for 36 h. After that, saturated aqueous Na<sub>2</sub>SO<sub>4</sub> (4 mL) was added. The solid formed was filtered and washed with DCM. The organic layers were combined and dried with MgSO<sub>4</sub>. The solvent was removed and the residue was purified by column chromatography (DCM/MeOH/Et<sub>3</sub>N = 100/5/1) to give **8** (21.2 mg, 78%, 92% ee).

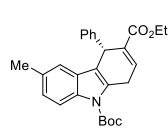
### Characterization of products

#### **9-(Tert-butyl) 3-ethyl (*S*)-4-phenyl-1,4-dihydro-9H-carbazole-3,9-dicarboxylate (3a)**

 Step 1: 18 h; Step 2: 3 h (Silica gel 200 mg); Total yield: 38.4 mg (92%); **<sup>1</sup>H NMR (400 MHz, CDCl<sub>3</sub>)** δ 8.07 (d, *J* = 8.3 Hz, 1H), 7.35 – 7.30 (m, 2H), 7.24 – 7.15 (m, 5H), 7.13 – 7.03 (m, 2H), 5.18 (t, *J* = 5.9 Hz, 1H), 4.18 – 4.00 (m, 4H), 1.70 (s, 9H), 1.21 (t, *J* = 7.1 Hz, 3H). **<sup>13</sup>C NMR (100 MHz, CDCl<sub>3</sub>)** δ 166.41, 150.73, 143.15, 136.25, 134.87, 132.60, 130.82, 128.95, 128.27, 128.24, 126.62, 123.91, 122.73, 118.90, 118.13, 115.51, 84.03, 60.69, 40.49, 28.57, 28.43, 14.21. **ESI-MS: calculated [C<sub>26</sub>H<sub>27</sub>NO<sub>4</sub> + Na]<sup>+</sup>: 440.1832, found: 440.1833.** [α]<sup>20</sup><sub>D</sub> = 26.8 (c = 0.96, CH<sub>2</sub>Cl<sub>2</sub>). The product was analyzed by HPLC to determine the enantiomeric excess: 94% ee (CHIRALPAK IA, hexane/*i*-PrOH = 97/3, detector: 254 nm, T = 30 °C, flow rate: 1 mL/min), t<sub>1</sub>(minor) = 5.72 min, t<sub>2</sub>(major) = 7.46 min.

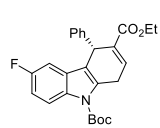
#### **9-(Tert-butyl) 3-ethyl (*S*)-6-methyl-4-phenyl-1,4-dihydro-9H-carbazole-3,9-dicarboxy-**

**late (3b)**



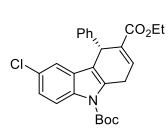
Step 1: 20 h; Step 2: 2 h (Silica gel 200 mg); Total yield: 36.3 mg (84%); **<sup>1</sup>H NMR (400 MHz, CDCl<sub>3</sub>)** δ 7.93 (d, *J* = 8.4 Hz, 1H), 7.36 – 7.30 (m, 2H), 7.24 – 7.17 (m, 3H), 7.14 – 7.08 (m, 1H), 7.05 – 6.97 (m, 2H), 5.16 (t, *J* = 5.8 Hz, 1H), 4.18 – 4.00 (m, 4H), 2.31 (s, 3H), 1.69 (s, 9H), 1.22 (t, *J* = 7.1 Hz, 3H). **<sup>13</sup>C NMR (100 MHz, CDCl<sub>3</sub>)** δ 166.46, 150.78, 143.24, 134.93, 134.45, 132.72, 132.15, 130.89, 128.95, 128.42, 128.28, 126.59, 125.25, 118.86, 117.93, 115.17, 83.85, 60.70, 40.45, 28.62, 28.47, 21.46, 14.23. **ESI-MS:** calculated [C<sub>27</sub>H<sub>29</sub>NO<sub>4</sub>+ Na]<sup>+</sup>: 454.1989, found: 454.1989. [α]<sup>20</sup><sub>D</sub> = 4.8 (c = 0.98, CH<sub>2</sub>Cl<sub>2</sub>). The product was analyzed by HPLC to determine the enantiomeric excess: 92% ee (CHIRALPAK IA, hexane/*i*-PrOH = 97/3, detector: 254 nm, T = 30 °C, flow rate: 1 mL/min), t<sub>1</sub>(minor) = 5.12 min, t<sub>2</sub>(major) = 10.56 min.

**9-(Tert-butyl) 3-ethyl (*S*)-6-fluoro-4-phenyl-1,4-dihydro-9H-carbazole-3,9-dicarboxylate (3c)**



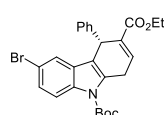
Step 1: 24 h; Step 2: 4 h (Silica gel 400 mg); Total yield: 22.8 mg (52%); **<sup>1</sup>H NMR (400 MHz, CDCl<sub>3</sub>)** δ 8.05 – 7.97 (m, 1H), 7.34 – 7.26 (m, 2H), 7.25 – 7.18 (m, 3H), 7.17 – 7.10 (m, 1H), 6.93 – 6.83 (m, 2H), 5.12 (t, *J* = 5.9 Hz, 1H), 4.18 – 3.99 (m, 4H), 1.70 (s, 9H), 1.21 (t, *J* = 7.1 Hz, 3H). **<sup>13</sup>C NMR (100 MHz, CDCl<sub>3</sub>)** δ 166.31, 159.13 (*J* = 239.3 Hz), 150.46, 142.75, 134.62, 132.61, 132.51, 129.27, 129.18, 128.89, 128.43, 126.84, 117.93 (d, *J* = 3.8 Hz), 116.48 (d, *J* = 8.9 Hz), 111.46 (d, *J* = 24.8 Hz), 104.62 (d, *J* = 23.9 Hz). 84.37, 60.78, 40.46, 28.63, 28.44, 14.22. **<sup>19</sup>F NMR (377 MHz, CDCl<sub>3</sub>)** δ -120.41. **ESI-MS:** calculated [C<sub>26</sub>H<sub>27</sub>FNO<sub>4</sub> + H]<sup>+</sup>: 436.1919, found: 436.1924. [α]<sup>20</sup><sub>D</sub> = 21.3 (c = 1.07, CH<sub>2</sub>Cl<sub>2</sub>). The product was analyzed by HPLC to determine the enantiomeric excess: 91% ee (CHIRALPAK IA, hexane/*i*-PrOH = 98.5/1.5, detector: 254 nm, T = 30 °C, flow rate: 1 mL/min), t<sub>1</sub>(minor) = 7.04 min, t<sub>2</sub>(major) = 9.21 min.

**9-(Tert-butyl) 3-ethyl (*S*)-6-chloro-4-phenyl-1,4-dihydro-9H-carbazole-3,9-dicarboxylate (3d)**

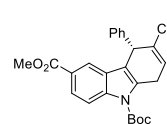


Step 1: 24 h; Step 2: 12 h (Silica gel 400 mg); Total yield: 34.4 mg (76%); **<sup>1</sup>H NMR (400 MHz, CDCl<sub>3</sub>)** δ 7.99 (d, *J* = 8.8 Hz, 1H), 7.34 – 7.27 (m, 2H), 7.26 – 7.17 (m, 4H), 7.17 – 7.10 (m, 2H), 5.13 (t, *J* = 5.8 Hz, 1H), 4.18 – 3.99 (m, 4H), 1.70 (s, 9H), 1.21 (t, *J* = 7.1 Hz, 3H). **<sup>13</sup>C NMR (100 MHz, CDCl<sub>3</sub>)** δ 166.25, 150.36, 142.70, 134.70, 134.53, 132.56, 132.26, 129.45, 128.85, 128.45, 128.32, 126.87, 124.06, 118.49, 117.59, 116.57, 84.55, 60.79, 40.34, 28.57, 28.42, 14.21. **ESI-MS:** calculated [C<sub>26</sub>H<sub>26</sub>ClNO<sub>4</sub> + H]<sup>+</sup>: 452.1623, found: 452.1628. [α]<sup>20</sup><sub>D</sub> = 24.3 (c = 0.97, CH<sub>2</sub>Cl<sub>2</sub>). The product was analyzed by HPLC to determine the enantiomeric excess: 92% ee (CHIRALPAK IA, hexane/*i*-PrOH = 98.5/1.5, detector: 254 nm, T = 30 °C, flow rate: 1 mL/min), t<sub>1</sub>(minor) = 7.00 min, t<sub>2</sub>(major) = 9.44 min.

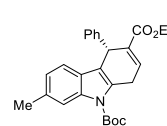
**9-(Tert-butyl) 3-ethyl (*S*)-6-bromo-4-phenyl-1,4-dihydro-9H-carbazole-3,9-dicarboxylate (3e)**


**Step 1:** 24 h; **Step 2:** 16 h (Silica gel 400 mg); Total yield: 30.3 mg (61%); **<sup>1</sup>H NMR (400 MHz, CDCl<sub>3</sub>)** δ 7.95 (d, *J* = 8.8 Hz, 1H), 7.35 (d, *J* = 1.8 Hz, 1H), 7.32 – 7.20 (m, 6H), 7.17 – 7.10 (m, 1H), 5.12 (t, *J* = 5.8 Hz, 1H), 4.21 – 3.99 (m, 4H), 1.70 (s, 9H), 1.21 (t, *J* = 7.1 Hz, 3H). **<sup>13</sup>C NMR (100 MHz, CDCl<sub>3</sub>)** δ 166.24, 150.34, 142.68, 135.08, 134.51, 132.57, 132.13, 129.95, 128.83, 128.46, 126.88, 126.77, 121.52, 117.51, 116.99, 116.09, 84.59, 60.79, 40.31, 28.54, 28.42, 14.21. **ESI-MS:** calculated [C<sub>26</sub>H<sub>26</sub>BrNO<sub>4</sub> + H]<sup>+</sup>: 496.1118, found: 496.1100. [α]<sup>20</sup><sub>D</sub> = -38.3 (c = 1.01, CH<sub>2</sub>Cl<sub>2</sub>). The product was analyzed by HPLC to determine the enantiomeric excess: 97% ee (CHIRALPAK IA, hexane/i-PrOH = 98.5/1.5, detector: 254 nm, T = 30 °C, flow rate: 1 mL/min), t<sub>1</sub>(major) = 9.77 min, t<sub>2</sub>(minor) = 12.54 min.

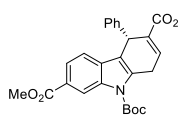
**9-(Tert-butyl) 3-ethyl 6-methyl (S)-4-phenyl-1,4-dihydro-9H-carbazole-3,6,9-tricarboxylate (3f)**


**Step 1:** 24 h; **Step 2:** 12 h (Silica gel 400 mg); Total yield: 23.8 mg (50%); **<sup>1</sup>H NMR (400 MHz, CDCl<sub>3</sub>)** δ 8.12 (d, *J* = 8.8 Hz, 1H), 7.99 (s, 1H), 7.89 (d, *J* = 8.8 Hz, 1H), 7.38 – 7.30 (m, 2H), 7.25 – 7.20 (m, 3H), 7.16 – 7.07 (m, 1H), 5.23 (t, *J* = 5.8 Hz, 1H), 4.19 – 4.02 (m, 4H), 3.88 (s, 3H), 1.71 (s, 9H), 1.22 (t, *J* = 7.1 Hz, 3H). **<sup>13</sup>C NMR (100 MHz, CDCl<sub>3</sub>)** δ 167.51, 166.27, 150.36, 142.85, 139.11, 134.59, 132.65, 132.22, 128.82, 128.43, 128.04, 126.84, 125.39, 124.70, 120.97, 118.67, 115.23, 84.81, 60.81, 52.11, 40.32, 28.58, 28.42, 14.22. **ESI-MS:** calculated [C<sub>28</sub>H<sub>29</sub>NO<sub>6</sub> + H]<sup>+</sup>: 476.2068, found: 476.2068. [α]<sup>20</sup><sub>D</sub> = -49.2 (c = 0.96, CH<sub>2</sub>Cl<sub>2</sub>). The product was analyzed by HPLC to determine the enantiomeric excess: 92% ee (CHIRALPAK IA, hexane/i-PrOH = 90/10, detector: 254 nm, T = 30 °C, flow rate: 1 mL/min), t<sub>1</sub>(minor) = 5.61 min, t<sub>2</sub>(major) = 6.62 min.

**9-(Tert-butyl) 3-ethyl (S)-7-methyl-4-phenyl-1,4-dihydro-9H-carbazole-3,9-dicarboxylate (3g)**


**Step 1:** 24 h; **Step 2:** 0.5 h (Silica gel 200 mg); Total yield: 37.3 mg (86%); **<sup>1</sup>H NMR (400 MHz, CDCl<sub>3</sub>)** δ 7.94 (s, 1H), 7.33 – 7.28 (m, 2H), 7.24 – 7.16 (m, 3H), 7.14 – 7.05 (m, 2H), 6.92 – 6.86 (m, 1H), 5.16 (t, *J* = 6.0 Hz, 1H), 4.20 – 3.97 (m, 4H), 2.39 (s, 3H), 1.70 (s, 9H), 1.21 (t, *J* = 7.1 Hz, 3H). **<sup>13</sup>C NMR (100 MHz, CDCl<sub>3</sub>)** δ 166.47, 150.80, 143.22, 136.74, 134.95, 133.81, 132.60, 129.91, 128.94, 128.26, 126.59, 125.98, 124.07, 118.48, 118.11, 115.92, 83.90, 60.68, 40.55, 28.65, 28.44, 22.10, 14.22. **ESI-MS:** calculated [C<sub>27</sub>H<sub>29</sub>NO<sub>4</sub> + H]<sup>+</sup>: 432.2169, found: 432.2170. [α]<sup>20</sup><sub>D</sub> = 15.0 (c = 1.02, CH<sub>2</sub>Cl<sub>2</sub>). The product was analyzed by HPLC to determine the enantiomeric excess: 95% ee (CHIRALPAK IA, hexane/i-PrOH = 97/3, detector: 254 nm, T = 30 °C, flow rate: 1 mL/min), t<sub>1</sub>(minor) = 5.48 min, t<sub>2</sub>(major) = 8.14 min.

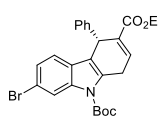
**9-(Tert-butyl) 6-ethyl 2-methyl (S)-5-phenyl-5,8-dihydro-9H-carbazole-2,6,9-tricarboxylate (3h)**



Step 1: 24 h; Step 2: 6 h (Silica gel 400 mg); Total yield: 24.4 mg (51%); **<sup>1</sup>H NMR (400 MHz, CDCl<sub>3</sub>)** δ 8.81 (s, 1H), 7.77 (dd, *J* = 8.2, 1.2 Hz, 1H), 7.34 – 7.29 (m, 2H), 7.27 – 7.19 (m, 4H), 7.15 – 7.07 (m, 1H), 5.20 (t, *J* = 5.8 Hz, 1H), 4.19 – 4.06 (m, 4H), 3.89 (s, 3H), 1.74 (s, 9H), 1.22 (t, *J* = 7.1 Hz, 3H).

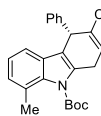
**<sup>13</sup>C NMR (100 MHz, CDCl<sub>3</sub>)** δ 167.84, 166.27, 150.33, 142.80, 135.68, 134.47, 134.28, 132.50, 131.86, 128.90, 128.39, 126.83, 125.51, 124.06, 118.50, 118.21, 117.53, 84.80, 60.82, 52.16, 40.35, 28.56, 28.38, 14.21. **ESI-MS:** calculated [C<sub>28</sub>H<sub>29</sub>NO<sub>6</sub> + H]<sup>+</sup>: 476.2068, found: 476.2083. [α]<sup>20</sup><sub>D</sub> = 15.5 (c = 0.51, CH<sub>2</sub>Cl<sub>2</sub>). The product was analyzed by HPLC to determine the enantiomeric excess: 86% ee (CHIRALPAK IA, hexane/i-PrOH = 95/5, detector: 254 nm, T = 30 °C, flow rate: 1 mL/min), t<sub>1</sub>(minor) = 7.49 min, t<sub>2</sub>(major) = 8.38 min.

### 9-(Tert-butyl) 3-ethyl (S)-7-bromo-4-phenyl-1,4-dihydro-9H-carbazole-3,9-dicarboxylate (3i)



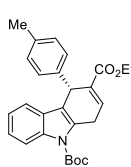
Step 1: 24 h; Step 2: 6 h (Silica gel 200 mg); Total yield: 30.3 mg (61%); **<sup>1</sup>H NMR (400 MHz, CDCl<sub>3</sub>)** δ 8.29 (s, 1H), 7.32 – 7.27 (m, 2H), 7.24 – 7.15 (m, 4H), 7.15 – 7.09 (m, 1H), 7.09 – 7.04 (m, 1H), 5.14 (t, *J* = 5.8 Hz, 1H), 4.20 – 3.97 (m, 4H), 1.71 (s, 9H), 1.21 (t, *J* = 7.1 Hz, 3H). **<sup>13</sup>C NMR (100 MHz, CDCl<sub>3</sub>)** δ 166.29, 150.29, 142.84, 137.00, 134.58, 132.48, 131.37, 128.88, 128.37, 127.06, 126.81, 125.94, 119.93, 118.81, 117.95, 117.68, 84.72, 60.78, 40.38, 28.51, 28.39, 14.22. **ESI-MS:** calculated [C<sub>26</sub>H<sub>26</sub>BrNO<sub>4</sub> + H]<sup>+</sup>: 496.1118, found: 496.1121. [α]<sup>20</sup><sub>D</sub> = -24.8 (c = 0.97, CH<sub>2</sub>Cl<sub>2</sub>). The product was analyzed by HPLC to determine the enantiomeric excess: 91% ee (CHIRALPAK IA, hexane/i-PrOH = 97/3, detector: 254 nm, T = 30 °C, flow rate: 1 mL/min), t<sub>1</sub>(minor) = 5.87 min, t<sub>2</sub>(major) = 7.63 min.

### 9-(Tert-butyl) 3-ethyl (S)-8-methyl-4-phenyl-1,4-dihydro-9H-carbazole-3,9-dicarboxylate (3j)



Step 1: 18 h; Step 2: 6 h (Silica gel 400 mg); Total yield: 23.9 mg (55%); **<sup>1</sup>H NMR (400 MHz, CDCl<sub>3</sub>)** δ 7.33 – 7.28 (m, 2H), 7.24 – 7.17 (m, 3H), 7.13 – 7.06 (m, 2H), 7.00 – 6.95 (m, 2H), 5.17 (t, *J* = 5.9 Hz, 1H), 4.18 – 4.04 (m, 2H), 4.00 – 3.78 (m, 2H), 2.45 (s, 3H), 1.68 (s, 9H), 1.21 (t, *J* = 7.1 Hz, 3H). **<sup>13</sup>C NMR (100 MHz, CDCl<sub>3</sub>)** δ 166.45, 150.35, 143.09, 135.84, 134.33, 133.16, 130.71, 129.23, 129.01, 128.26, 127.06, 126.60, 124.68, 122.90, 117.27, 116.65, 84.01, 77.48, 77.16, 76.84, 60.73, 40.70, 28.25, 27.97, 21.36, 14.22. **ESI-MS:** calculated [C<sub>27</sub>H<sub>29</sub>NO<sub>4</sub> + Na]<sup>+</sup>: 454.1989, found: 454.1993. [α]<sup>20</sup><sub>D</sub> = 21.5 (c = 0.51, CH<sub>2</sub>Cl<sub>2</sub>). The product was analyzed by HPLC to determine the enantiomeric excess: 90% ee (CHIRALPAK IA, hexane/i-PrOH = 97/3, detector: 254 nm, T = 30 °C, flow rate: 1 mL/min), t<sub>1</sub>(major) = 7.25 min, t<sub>2</sub>(minor) = 7.98 min.

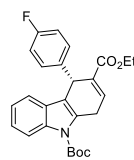
### 9-(Tert-butyl) 3-ethyl (S)-4-(p-tolyl)-1,4-dihydro-9H-carbazole-3,9-dicarboxylate (3k)



Step 1: 24 h; Step 2: 3 h (Silica gel 200 mg); Total yield: 33.2 mg (77%); **<sup>1</sup>H NMR (400 MHz, CDCl<sub>3</sub>)** δ 8.07 (d, *J* = 8.3 Hz, 1H), 7.28 – 7.24 (m, 1H), 7.23 – 7.15 (m, 4H), 7.09 – 7.04 (m, 1H), 7.01 (d, *J* = 7.9 Hz, 2H), 5.15 (t, *J* = 5.8 Hz, 1H), 4.20 – 4.00 (m, 4H), 2.24 (s, 3H), 1.70 (s, 9H), 1.23 (t, *J* = 7.1 Hz, 3H). **<sup>13</sup>C NMR (100 MHz, CDCl<sub>3</sub>)** δ 167.84, 166.27, 150.33, 142.80, 135.68, 134.47, 134.28, 132.50, 131.86, 128.90, 128.39, 126.83, 125.51, 124.06, 118.50, 118.21, 117.53, 84.80, 60.82, 52.16, 40.35, 28.56, 28.38, 14.21. **ESI-MS:** calculated [C<sub>28</sub>H<sub>29</sub>NO<sub>6</sub> + H]<sup>+</sup>: 476.2068, found: 476.2083. [α]<sup>20</sup><sub>D</sub> = 15.5 (c = 0.51, CH<sub>2</sub>Cl<sub>2</sub>). The product was analyzed by HPLC to determine the enantiomeric excess: 86% ee (CHIRALPAK IA, hexane/i-PrOH = 95/5, detector: 254 nm, T = 30 °C, flow rate: 1 mL/min), t<sub>1</sub>(minor) = 7.49 min, t<sub>2</sub>(major) = 8.38 min.

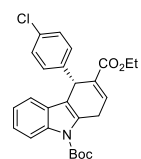
**MHz, CDCl<sub>3</sub>)** δ 166.52, 150.78, 140.13, 136.28, 136.08, 134.70, 132.76, 130.76, 129.02, 128.76, 128.30, 123.90, 122.74, 118.94, 118.34, 115.52, 84.03, 60.71, 40.04, 28.59, 28.47, 21.19, 14.25. **ESI-MS:** calculated [C<sub>27</sub>H<sub>29</sub>NO<sub>4</sub> + H]<sup>+</sup>: 432.2169, found: 432.21625. [α]<sup>20</sup><sub>D</sub>= 11.7 (c = 0.38, CH<sub>2</sub>Cl<sub>2</sub>). The product was analyzed by HPLC to determine the enantiomeric excess: 94% ee (CHIRALPAK IA, hexane/i-PrOH =97/3, detector: 254 nm, T = 30 °C, flow rate: 1 mL/min), t<sub>1</sub>(minor) = 5.47 min, t<sub>2</sub>(major) = 6.64 min.

### 9-(Tert-butyl) 3-ethyl (*S*)-4-(4-fluorophenyl)-1,4-dihydro-9H-carbazole-3,9-dicarboxylate (3l)



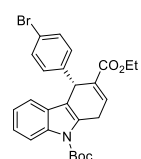
Step 1: 12 h; Step 2: 2 h (Silica gel 200 mg); Total yield: 40.1 mg (92%); **<sup>1</sup>H NMR (400 MHz, CDCl<sub>3</sub>)** δ 8.08 (d, J = 8.3 Hz, 1H), 7.32 – 7.26 (m, 2H), 7.24 – 7.16 (m, 3H), 7.11 – 7.05 (m, 1H), 6.93 – 6.86 (m, 2H), 5.18 (t, J = 5.9 Hz, 1H), 4.24 – 3.94 (m, 4H), 1.71 (s, 9H), 1.23 (t, J = 7.1 Hz, 3H). **<sup>13</sup>C NMR (100 MHz, CDCl<sub>3</sub>)** δ 166.32, 161.60 (J = 244.5 Hz), 150.71, 138.91 (J = 3.0 Hz), 136.26, 134.99, 132.44, 130.91, 130.41 (J = 8.0 Hz), 128.07, 124.04, 122.78, 118.79, 117.84, 115.60, 115.11 (J = 21.4 Hz), 84.17, 60.78, 39.72, 28.52, 28.45, 14.25. **<sup>19</sup>F NMR (376 MHz, CDCl<sub>3</sub>)** δ -116.42. **ESI-MS:** calculated [C<sub>26</sub>H<sub>26</sub>FNO<sub>4</sub> + Na]<sup>+</sup>: 458.1738, found: 458.1746. [α]<sup>20</sup><sub>D</sub>= 27.6 (c = 1.00, CH<sub>2</sub>Cl<sub>2</sub>). The product was analyzed by HPLC to determine the enantiomeric excess: 94% ee (CHIRALPAK IA, hexane/i-PrOH =97/3, detector: 254 nm, T = 30 °C, flow rate: 1 mL/min), t<sub>1</sub>(minor) = 5.58 min, t<sub>2</sub>(major) = 7.38 min.

### 9-(Tert-butyl) 3-ethyl (*S*)-4-(4-chlorophenyl)-1,4-dihydro-9H-carbazole-3,9-dicarboxylate (3m)



Step 1: 12 h; Step 2: 2 h (Silica gel 200 mg); Total yield: 41.3 mg (91%); **<sup>1</sup>H NMR (400 MHz, CDCl<sub>3</sub>)** δ 8.08 (d, J = 8.3 Hz, 1H), 7.28 – 7.16 (m, 7H), 7.11 – 7.03 (m, 1H), 5.16 (t, J = 5.9 Hz, 1H), 4.23 – 4.00 (m, 4H), 1.71 (s, 9H), 1.23 (d, J = 7.1 Hz, 3H). **<sup>13</sup>C NMR (100 MHz, CDCl<sub>3</sub>)** δ 166.22, 150.69, 141.77, 136.25, 135.27, 132.31, 132.17, 130.98, 130.32, 128.47, 127.99, 124.10, 122.82, 118.74, 117.59, 115.61, 84.21, 60.83, 39.88, 28.53, 28.45, 14.26. **ESI-MS:** calculated [C<sub>26</sub>H<sub>26</sub>CINO<sub>4</sub> + Na]<sup>+</sup>: 474.1443, found: 474.1443. [α]<sup>20</sup><sub>D</sub>= 13.5 (c = 1.01, CH<sub>2</sub>Cl<sub>2</sub>). The product was analyzed by HPLC to determine the enantiomeric excess: 94% ee (CHIRALPAK IA, hexane/i-PrOH =97/3, detector: 254 nm, T = 30 °C, flow rate: 1 mL/min), t<sub>1</sub>(minor) = 6.06 min, t<sub>2</sub>(major) = 7.57 min.

### 9-(Tert-butyl) 3-ethyl (*S*)-4-(4-bromophenyl)-1,4-dihydro-9H-carbazole-3,9-dicarboxylate (3n)



Step 1: 18 h; Step 2: 2 h (Silica gel 200 mg); Total yield: 34.6 mg (70%); **<sup>1</sup>H NMR (400 MHz, CDCl<sub>3</sub>)** δ 8.08 (d, J = 8.3 Hz, 1H), 7.36 – 7.30 (m, 2H), 7.26 – 7.15 (m, 5H), 7.11 – 7.03 (m, 1H), 5.16 (t, J = 5.9 Hz, 1H), 4.21 – 4.09 (m, 2H), 4.09 – 4.02 (m, 2H), 1.71 (s, 9H), 1.24 (t, J = 7.1 Hz, 3H). **<sup>13</sup>C NMR (100 MHz, CDCl<sub>3</sub>)** δ 166.21, 150.69, 142.31, 136.25, 135.32, 132.10, 131.42, 130.99, 130.72, 127.98, 124.12, 122.84, 120.48, 118.74, 117.52, 115.62, 84.23, 60.85, 39.96, 28.54, 28.46, 14.27. **ESI-MS:**

**calculated [C<sub>26</sub>H<sub>26</sub>BrNO<sub>4</sub> + H]<sup>+</sup>: 496.1118, found: 496.1111.**  $[\alpha]^{20}_{\text{D}} = 9.0$  ( $c = 1.01$ , CH<sub>2</sub>Cl<sub>2</sub>). The product was analyzed by HPLC to determine the enantiomeric excess: 93% ee (CHIRALPAK IA, hexane/*i*-PrOH = 97/3, detector: 254 nm, T = 30 °C, flow rate: 1 mL/min), t<sub>1</sub>(minor) = 5.73 min, t<sub>2</sub>(major) = 7.02 min.

**9-(Tert-butyl) 3-ethyl (S)-4-(4-(trifluoromethyl)phenyl)-1,4-dihydro-9H-carbazole-3,9-dicarboxylate (3o)**

Step 1: 10 h; Step 2: 2 h (Silica gel 200 mg); Total yield: 38.7 mg (80%); **<sup>1</sup>H NMR (400 MHz, CDCl<sub>3</sub>)** δ 8.09 (d,  $J = 8.3$  Hz, 1H), 7.52 – 7.40 (m, 4H), 7.32 – 7.27 (m, 1H), 7.24 – 7.16 (m, 2H), 7.13 – 7.05 (m, 1H), 5.26 (t,  $J = 5.9$  Hz, 1H), 4.21 – 3.98 (m, 4H), 1.71 (s, 9H), 1.23 (t,  $J = 7.1$  Hz, 3H). **<sup>13</sup>C NMR (100 MHz, CDCl<sub>3</sub>)** δ 166.07, 150.67, 147.35, 136.27, 135.79, 131.88, 131.14, 129.29, 128.88 ( $J = 32.2$  Hz), 127.88, 125.21 ( $J = 3.7$  Hz), 124.30 ( $J = 270.3$  Hz), 124.19, 122.88, 118.62, 117.30, 115.68, 84.32, 60.91, 40.36, 28.59, 28.45, 14.23. **ESI-MS: calculated [C<sub>27</sub>H<sub>26</sub>F<sub>3</sub>NO<sub>4</sub> + H]<sup>+</sup>: 486.1887, found: 486.1896.**  $[\alpha]^{20}_{\text{D}} = 18.8$  ( $c = 1.00$ , CH<sub>2</sub>Cl<sub>2</sub>). The product was analyzed by HPLC to determine the enantiomeric excess: 94% ee (CHIRALPAK IA, hexane/*i*-PrOH = 97/3, detector: 254 nm, T = 30 °C, flow rate: 1 mL/min), t<sub>1</sub>(minor) = 5.67 min, t<sub>2</sub>(major) = 6.86 min.

**9-(Tert-butyl) 3-ethyl (S)-4-(4-(methoxycarbonyl)phenyl)-1,4-dihydro-9H-carbazole-3,9-dicarboxylate (3p)**

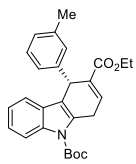
Step 1: 8 h; Step 2: 2 h (Silica gel 200 mg); Total yield: 40.9 mg (86%); **<sup>1</sup>H NMR (400 MHz, CDCl<sub>3</sub>)** δ 8.08 (d,  $J = 8.5$  Hz, 1H), 7.90 (d,  $J = 8.3$  Hz, 2H), 7.41 (d,  $J = 8.3$  Hz, 2H), 7.28 (t,  $J = 3.5$  Hz, 1H), 7.22 – 7.17 (m, 2H), 7.08 – 7.03 (m, 1H), 5.24 (t,  $J = 5.9$  Hz, 1H), 4.19 – 4.03 (m, 4H), 3.85 (s, 3H), 1.71 (s, 9H), 1.19 (d,  $J = 4.9$  Hz, 3H). **<sup>13</sup>C NMR (100 MHz, CDCl<sub>3</sub>)** δ 167.09, 166.15, 150.68, 148.58, 136.24, 135.68, 131.87, 131.03, 129.72, 129.07, 128.59, 127.96, 124.11, 122.83, 118.68, 117.33, 115.61, 84.26, 60.86, 52.10, 40.56, 28.58, 28.45, 14.23. **ESI-MS: calculated [C<sub>28</sub>H<sub>29</sub>NO<sub>6</sub> + H]<sup>+</sup>: 476.2068, found: 476.2063.**  $[\alpha]^{20}_{\text{D}} = 15.2$  ( $c = 1.02$ , CH<sub>2</sub>Cl<sub>2</sub>). The product was analyzed by HPLC to determine the enantiomeric excess: 94% ee (CHIRALPAK IA, hexane/*i*-PrOH = 97/3, detector: 254 nm, T = 30 °C, flow rate: 1 mL/min), t<sub>1</sub>(minor) = 10.97 min, t<sub>2</sub>(major) = 15.22 min.

**9-(Tert-butyl) 3-ethyl (S)-4-(4-cyanophenyl)-1,4-dihydro-9H-carbazole-3,9-dicarboxylate (3q)**

Step 1: 12 h; Step 2: 2 h (Silica gel 200 mg); Total yield: 38.4 mg (87%); **<sup>1</sup>H NMR (400 MHz, CDCl<sub>3</sub>)** δ 8.09 (d,  $J = 8.4$  Hz, 1H), 7.52 (d,  $J = 8.3$  Hz, 2H), 7.45 (d,  $J = 8.3$  Hz, 2H), 7.31 (t,  $J = 3.4$  Hz, 1H), 7.25 – 7.19 (m, 1H), 7.16 – 7.12 (m, 1H), 7.11 – 7.05 (m, 1H), 5.24 (t,  $J = 5.9$  Hz, 1H), 4.20 – 3.99 (m, 4H), 1.71 (s, 9H), 1.23 (t,  $J = 7.1$  Hz, 3H). **<sup>13</sup>C NMR (100 MHz, CDCl<sub>3</sub>)** δ 165.89, 150.60, 148.84, 136.21, 132.23, 131.41, 131.23, 129.79, 127.69, 124.30, 124.08, 122.93, 119.04, 118.42, 116.79, 115.72, 110.54, 84.43, 60.98, 40.62, 28.56, 28.43, 14.24. **ESI-MS: calculated**

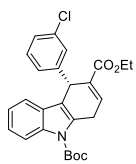
**[C<sub>27</sub>H<sub>26</sub>N<sub>2</sub>O<sub>4</sub> + H]<sup>+</sup>: 443.1965, found: 443.1966.** [α]<sup>20</sup><sub>D</sub> = 8.7 (c = 1.01, CH<sub>2</sub>Cl<sub>2</sub>). The product was analyzed by HPLC to determine the enantiomeric excess: 94% ee (CHIRALPAK IA, hexane/*i*-PrOH = 90/10, detector: 254 nm, T = 30 °C, flow rate: 1 mL/min), t<sub>1</sub>(minor) = 7.03 min, t<sub>2</sub>(major) = 8.21 min.

### 9-(Tert-butyl) 3-ethyl (*S*)-4-(m-tolyl)-1,4-dihydro-9H-carbazole-3,9-dicarboxylate (3r)



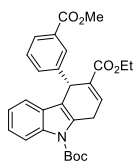
Step 1: 20 h; Step 2: 2 h (Silica gel 200 mg); Total yield: 25.0 mg (58%); **<sup>1</sup>H NMR (400 MHz, CDCl<sub>3</sub>)** δ 8.07 (d, *J* = 8.3 Hz, 1H), 7.29 – 7.15 (m, 4H), 7.13 – 7.03 (m, 3H), 6.92 (d, *J* = 7.2 Hz, 1H), 5.15 (t, *J* = 5.8 Hz, 1H), 4.19 – 4.01 (m, 4H), 2.26 (s, 3H), 1.71 (s, 9H), 1.22 (t, *J* = 7.1 Hz, 3H). **<sup>13</sup>C NMR (100 MHz, CDCl<sub>3</sub>)** δ 166.53, 150.80, 143.02, 137.73, 136.28, 134.79, 132.73, 130.80, 129.56, 128.36, 128.07, 127.47, 126.20, 123.89, 122.75, 118.99, 118.24, 115.51, 84.05, 60.70, 40.46, 28.59, 28.48, 21.62, 14.22. **ESI-MS: calculated [C<sub>27</sub>H<sub>29</sub>NO<sub>4</sub> + Na]<sup>+</sup>: 454.1989, found: 454.2002.** [α]<sup>20</sup><sub>D</sub> = 27.5 (c = 0.94, CH<sub>2</sub>Cl<sub>2</sub>). The product was analyzed by HPLC to determine the enantiomeric excess: 92% ee (CHIRALPAK IA, hexane/*i*-PrOH = 98.5/1.5, detector: 254 nm, T = 30 °C, flow rate: 1 mL/min), t<sub>1</sub>(minor) = 6.35 min, t<sub>2</sub>(major) = 10.35 min.

### 9-(Tert-butyl) 3-ethyl (*S*)-4-(3-chlorophenyl)-1,4-dihydro-9H-carbazole-3,9-dicarboxylate (3s)



Step 1: 12 h; Step 2: 2 h (Silica gel 100 mg); Total yield: 23.5 mg (52%); **<sup>1</sup>H NMR (400 MHz, CDCl<sub>3</sub>)** δ 8.09 (d, *J* = 8.3 Hz, 1H), 7.29 – 7.18 (m, 5H), 7.18 – 7.06 (m, 3H), 5.16 (t, *J* = 5.8 Hz, 1H), 4.21 – 4.02 (m, 4H), 1.71 (s, 9H), 1.24 (t, *J* = 7.1 Hz, 3H). **<sup>13</sup>C NMR (100 MHz, CDCl<sub>3</sub>)** δ 166.18, 150.69, 145.33, 136.29, 135.59, 134.09, 131.99, 131.07, 129.50, 128.99, 128.00, 127.42, 126.96, 124.11, 122.85, 118.73, 117.39, 115.63, 84.25, 60.87, 40.26, 28.57, 28.47, 14.24. **ESI-MS: calculated [C<sub>26</sub>H<sub>26</sub>CINO<sub>4</sub> + H]<sup>+</sup>: 452.1623, found: 452.1616.** [α]<sup>20</sup><sub>D</sub> = 17.4 (c = 1.03, CH<sub>2</sub>Cl<sub>2</sub>). The product was analyzed by HPLC to determine the enantiomeric excess: 92% ee (CHIRALPAK IA, hexane/*i*-PrOH = 97/3, detector: 254 nm, T = 30 °C, flow rate: 1 mL/min), t<sub>1</sub>(minor) = 5.39 min, t<sub>2</sub>(major) = 7.82 min.

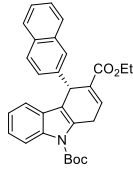
### 9-(Tert-butyl) 3-ethyl (*S*)-4-(3-(methoxycarbonyl)phenyl)-1,4-dihydro-9H-carbazole-3,9-dicarboxylate (3t)



Step 1: 12 h; Step 2: 2 h (Silica gel 100 mg); Total yield: 29.4 mg (62%); **<sup>1</sup>H NMR (400 MHz, CDCl<sub>3</sub>)** δ 8.10 – 8.05 (m, 1H), 8.00 (t, *J* = 1.6 Hz, 1H), 7.85 – 7.78 (m, 1H), 7.57 – 7.51 (m, 1H), 7.34 – 7.26 (m, 2H), 7.22 – 7.15 (m, 2H), 7.09 – 7.02 (m, 1H), 5.26 – 5.22 (m, 1H), 4.19 – 4.05 (m, 4H), 3.87 (s, 3H), 1.71 (s, 9H), 1.22 (t, *J* = 7.1 Hz, 3H). **<sup>13</sup>C NMR (100 MHz, CDCl<sub>3</sub>)** δ 167.22, 166.21, 150.69, 143.76, 136.27, 135.66, 133.75, 132.01, 131.08, 130.19, 130.10, 128.36, 128.05, 128.01, 124.05, 122.80, 118.71, 117.46, 115.60, 84.21, 60.82, 52.16, 40.42, 28.58, 28.45, 14.18. **ESI-MS: calculated [C<sub>28</sub>H<sub>29</sub>NO<sub>6</sub> + Na]<sup>+</sup>: 498.1887, found: 498.1890.** [α]<sup>20</sup><sub>D</sub> = 14.3 (c = 1.01, CH<sub>2</sub>Cl<sub>2</sub>). The product was analyzed by HPLC to determine the enantiomeric excess: 94% ee

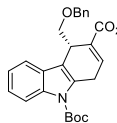
(CHIRALPAK IA, hexane/*i*-PrOH =97/3, detector: 254 nm, T = 30 °C, flow rate: 1 mL/min), t<sub>1</sub>(minor) = 8.06 min, t<sub>2</sub>(major) = 13.97 min.

**9-(Tert-butyl) 3-ethyl (*S*)-4-(naphthalen-2-yl)-1,4-dihydro-9H-carbazole-3,9-dicarboxylate (3u)**



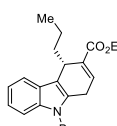
Step 1: 36 h; Step 2: 3 h (Silica gel 200 mg); Total yield: 41.0 mg (88%); **1H NMR (400 MHz, CDCl<sub>3</sub>)** δ 8.06 (d, *J* = 8.3 Hz, 1H), 7.85 (s, 1H), 7.78 (d, *J* = 7.9 Hz, 1H), 7.72 (d, *J* = 7.8 Hz, 1H), 7.67 (d, *J* = 8.5 Hz, 1H), 7.44 – 7.32 (m, 3H), 7.29 – 7.22 (m, 2H), 7.15 (t, *J* = 7.7 Hz, 1H), 7.01 (t, *J* = 7.5 Hz, 1H), 5.37 (t, *J* = 6.0 Hz, 1H), 4.21 – 3.98 (m, 4H), 1.71 (s, 9H), 1.19 (t, *J* = 7.1 Hz, 3H). **13C NMR (100 MHz, CDCl<sub>3</sub>)** δ 166.42, 150.79, 140.58, 136.26, 135.04, 133.48, 132.53, 132.50, 130.96, 128.25, 128.01, 127.93, 127.81, 127.69, 127.13, 125.90, 125.55, 123.96, 122.77, 118.95, 117.97, 115.52, 84.12, 60.74, 40.64, 28.65, 28.47, 14.23. **ESI-MS: calculated [C<sub>30</sub>H<sub>29</sub>NO<sub>4</sub> + Na]<sup>+</sup>: 490.1989, found: 490.1994.** [α]<sup>20</sup><sub>D</sub> = 48.3 (c = 0.99, CH<sub>2</sub>Cl<sub>2</sub>). The product was analyzed by HPLC to determine the enantiomeric excess: 93% ee (CHIRALPAK IA, hexane/*i*-PrOH =97/3, detector: 254 nm, T = 30 °C, flow rate: 1 mL/min), t<sub>1</sub>(minor) = 6.66 min, t<sub>2</sub>(major) = 10.38 min.

**9-(Tert-butyl) 3-ethyl (*S*)-4-((benzyloxy)methyl)-1,4-dihydro-9H-carbazole-3,9-dicarboxylate (3v)**



Step 1: 24 h; Step 2: 2 h (Silica gel 200 mg); Total yield: 30.2 mg (65%); **1H NMR (400 MHz, CDCl<sub>3</sub>)** δ 8.14 (d, *J* = 8.2 Hz, 1H), 7.55 (d, *J* = 7.5 Hz, 1H), 7.28 – 7.17 (m, 6H), 7.14 – 7.07 (m, 2H), 4.38 – 4.31 (m, 3H), 4.23 (q, *J* = 7.1 Hz, 2H), 3.99 – 3.85 (m, 2H), 3.84 – 3.77 (m, 2H), 1.69 (s, 9H), 1.31 (t, *J* = 7.1 Hz, 3H). **13C NMR (100 MHz, CDCl<sub>3</sub>)** δ 166.87, 150.65, 138.59, 137.69, 136.34, 132.35, 130.10, 128.44, 128.20, 123.86, 122.68, 118.85, 116.39, 115.67, 83.92, 73.17, 72.65, 60.78, 35.15, 28.77, 28.44, 14.39. **ESI-MS: calculated [C<sub>28</sub>H<sub>31</sub>NO<sub>5</sub> + Na]<sup>+</sup>: 484.2094, found: 484.2103.** [α]<sup>20</sup><sub>D</sub> = -34.2 (c = 1.15, CH<sub>2</sub>Cl<sub>2</sub>). The product was analyzed by HPLC to determine the enantiomeric excess: 92% ee (CHIRALPAK IA, hexane/*i*-PrOH =97/3, detector: 254 nm, T = 30 °C, flow rate: 1 mL/min), t<sub>1</sub>(major) = 8.15 min, t<sub>2</sub>(minor) = 9.94 min.

**9-(Tert-butyl) 3-ethyl (*S*)-4-propyl-1,4-dihydro-9H-carbazole-3,9-dicarboxylate (3w)**



Step 1: 36 h; Step 2: 4 h (Silica gel 400 mg); Total yield: 28.9 mg (75%); **1H NMR (400 MHz, CDCl<sub>3</sub>)** δ 8.14 (d, *J* = 7.8 Hz, 1H), 7.54 (d, *J* = 7.1 Hz, 1H), 7.32 – 7.23 (m, 3H), 7.20 (s, 1H), 4.36 – 4.20 (m, 3H), 3.97 – 3.72 (m, 2H), 1.95 – 1.80 (m, 2H), 1.69 (s, 9H), 1.36 (t, *J* = 7.0 Hz, 3H), 1.17 – 1.04 (m, 1H), 1.00 – 0.87 (m, 1H), 0.74 (t, *J* = 7.2 Hz, 3H). **13C NMR (100 MHz, CDCl<sub>3</sub>)** δ 166.95, 150.69, 136.55, 136.36, 132.27, 131.83, 128.45, 123.80, 122.67, 118.63, 118.10, 115.70, 83.89, 60.72, 36.08, 33.27, 28.74, 28.45, 17.93, 14.45, 14.35. **ESI-MS: calculated [C<sub>23</sub>H<sub>29</sub>NO<sub>4</sub> + H]<sup>+</sup>: 384.2169, found: 384.2161.** [α]<sup>20</sup><sub>D</sub> = -71.1 (c = 0.39, CH<sub>2</sub>Cl<sub>2</sub>). The product was analyzed by HPLC to determine the enantiomeric excess: 90% ee (CHIRALPAK IA, hexane/*i*-PrOH =99/1, detector: 254 nm, T = 30 °C, flow rate: 1 mL/min), t<sub>1</sub>(minor) = 5.54 min, t<sub>2</sub>(major) = 7.23 min.

**9-(Tert-butyl) 3-ethyl (*S*)-4-(3-ethoxy-3-oxopropyl)-1,4-dihydro-9H-carbazole-3,9-dicarboxylate (3x)**

Step 1: 36 h; Step 2: 4 h (Silica gel 400 mg); Total yield: 30.8 mg (70%); **<sup>1</sup>H NMR (400 MHz, CDCl<sub>3</sub>)** δ 8.14 (d, *J* = 8.0 Hz, 1H), 7.55 (d, *J* = 7.2 Hz, 1H), 7.35 – 7.18 (m, 3H), 4.41 – 4.34 (m, 1H), 4.32 – 4.22 (m, 2H), 3.98 – 3.88 (m, 3H), 3.87 – 3.77 (m, 1H), 2.37 – 2.27 (m, 2H), 2.12 – 2.01 (m, 1H), 1.98 – 1.88 (m, 1H), 1.70 (s, 9H), 1.37 (t, *J* = 7.1 Hz, 3H), 1.12 (t, *J* = 7.1 Hz, 3H). **<sup>13</sup>C NMR (100 MHz, CDCl<sub>3</sub>)** δ 173.65, 166.46, 150.57, 137.70, 136.40, 132.28, 130.99, 127.99, 124.06, 122.86, 118.53, 116.56, 115.75, 84.08, 60.88, 60.30, 32.42, 29.58, 28.71, 28.43, 28.08, 14.42, 14.19. **ESI-MS:** calculated [C<sub>25</sub>H<sub>31</sub>NO<sub>6</sub> + H]<sup>+</sup>: 442.2224, found: 442.2208. [α]<sup>20</sup><sub>D</sub> = -47.5 (c = 0.51, CH<sub>2</sub>Cl<sub>2</sub>). The product was analyzed by HPLC to determine the enantiomeric excess: 81% ee (CHIRALPAK AS-H, hexane/i-PrOH = 97/3, detector: 254 nm, T = 30 °C, flow rate: 1 mL/min), t<sub>1</sub>(major) = 5.74 min, t<sub>2</sub>(minor) = 6.62 min.

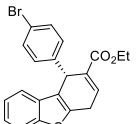
**3-Benzyl 9-(tert-butyl) (*S*)-4-phenyl-1,4-dihydro-9H-carbazole-3,9-dicarboxylate (3y)**

Step 1: 18 h; Step 2: 1.5 h (Silica gel 200 mg); Total yield: 32.9 mg (69%); **<sup>1</sup>H NMR (400 MHz, CDCl<sub>3</sub>)** δ 8.07 (d, *J* = 8.3 Hz, 1H), 7.34 – 7.27 (m, 6H), 7.26 – 7.15 (m, 6H), 7.14 – 7.09 (m, 1H), 7.08 – 7.02 (m, 1H), 5.20 (t, *J* = 5.9 Hz, 1H), 5.10 (dd, *J* = 39.1, 12.4 Hz, 2H), 4.15 – 3.95 (m, 2H), 1.69 (s, 9H). **<sup>13</sup>C NMR (100 MHz, CDCl<sub>3</sub>)** δ 166.25, 150.71, 143.00, 136.26, 136.00, 135.59, 132.38, 130.69, 128.98, 128.60, 128.36, 128.26, 128.23, 128.19, 126.68, 123.95, 122.75, 118.91, 118.08, 115.53, 84.07, 66.57, 40.53, 28.64, 28.45. **ESI-MS:** calculated [C<sub>31</sub>H<sub>29</sub>NO<sub>4</sub> + Na]<sup>+</sup>: 502.1989, found: 502.1987. [α]<sup>20</sup><sub>D</sub> = 24.5 (c = 0.97, CH<sub>2</sub>Cl<sub>2</sub>). The product was analyzed by HPLC to determine the enantiomeric excess: 93% ee (CHIRALPAK IA, hexane/i-PrOH = 97/3, detector: 254 nm, T = 30 °C, flow rate: 1 mL/min), t<sub>1</sub>(minor) = 8.10 min, t<sub>2</sub>(major) = 11.15 min.

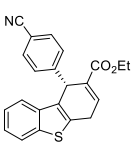
**Di-tert-butyl (*S*)-4-phenyl-1,4-dihydro-9H-carbazole-3,9-dicarboxylate (3z)**

Step 1: 36 h; Step 2: 1.5 h (Silica gel 200 mg); Total yield: 33.7 mg (76%); **<sup>1</sup>H NMR (400 MHz, CDCl<sub>3</sub>)** δ 8.07 (d, *J* = 8.3 Hz, 1H), 7.34 – 7.27 (m, 3H), 7.26 – 7.17 (m, 3H), 7.17 – 7.10 (m, 2H), 7.09 – 7.04 (m, 1H), 5.12 (t, *J* = 6.0 Hz, 1H), 4.12 – 3.93 (m, 2H), 1.70 (s, 9H), 1.36 (s, 9H). **<sup>13</sup>C NMR (100 MHz, CDCl<sub>3</sub>)** δ 165.89, 150.76, 143.28, 136.29, 133.95, 133.89, 130.91, 129.02, 128.35, 128.18, 126.56, 123.85, 122.69, 118.95, 118.12, 115.52, 84.02, 80.92, 40.72, 28.53, 28.46, 28.10. **ESI-MS:** calculated [C<sub>28</sub>H<sub>31</sub>NO<sub>4</sub> + H]<sup>+</sup>: 446.2326, found: 446.2318. [α]<sup>20</sup><sub>D</sub> = 26.9 (c = 2.0, CH<sub>2</sub>Cl<sub>2</sub>). The product was analyzed by HPLC to determine the enantiomeric excess: 92% ee (CHIRALPAK IA, hexane/i-PrOH = 98.5/1.5, detector: 254 nm, T = 30 °C, flow rate: 1 mL/min), t<sub>1</sub>(minor) = 5.32 min, t<sub>2</sub>(major) = 6.60 min.

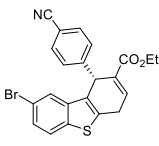
**Ethyl (*R*)-1-(4-bromophenyl)-1,4-dihydrodibenzo[b,d]thiophene-2-carboxylate (6a)**


 Step 1: 48 h; Step 2: 5 h (Silica gel 300 mg); Total yield: 24.4 mg (59%); **<sup>1</sup>H NMR (400 MHz, CDCl<sub>3</sub>)** δ 7.77 – 7.71 (m, 1H), 7.48 – 7.42 (m, 1H), 7.34 – 7.30 (m, 2H), 7.28 – 7.25 (m, 1H), 7.24 – 7.16 (m, 4H), 5.27 (t, *J* = 5.2 Hz, 1H), 4.26 – 4.06 (m, 2H), 4.02 – 3.89 (m, 1H), 3.87 – 3.74 (m, 1H), 1.27 (t, *J* = 7.1 Hz, 3H). **<sup>13</sup>C NMR (100 MHz, CDCl<sub>3</sub>)** δ 166.04, 141.73, 139.23, 137.89, 134.40, 133.13, 132.89, 131.50, 130.77, 130.44, 124.30, 124.28, 122.48, 121.78, 120.62, 60.97, 41.47, 28.07, 14.30. **ESI-MS:** calculated [C<sub>21</sub>H<sub>17</sub>BrN<sub>2</sub>S + H]<sup>+</sup>: 413.0205, found: 413.0213. [α]<sup>20</sup><sub>D</sub> = -36.9 (c = 0.81, CH<sub>2</sub>Cl<sub>2</sub>). The product was analyzed by HPLC to determine the enantiomeric excess: 95% ee (CHIRALPAK IA, hexane/i-PrOH =90/10, detector: 254 nm, T = 30 °C, flow rate: 1 mL/min), t<sub>1</sub>(minor) = 7.53 min, t<sub>2</sub>(major) = 8.22 min.

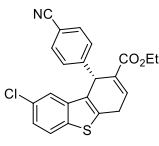
#### Ethyl (*R*)-1-(4-cyanophenyl)-1,4-dihydrodibenzo[b,d]thiophene-2-carboxylate (6b)


 Step 1: 48 h; Step 2: 5 h (Silica gel 300 mg); Total yield: 25.7 mg (72%); **<sup>1</sup>H NMR (400 MHz, CDCl<sub>3</sub>)** δ 7.79 – 7.74 (m, 1H), 7.53 – 7.48 (m, 2H), 7.45 – 7.38 (m, 3H), 7.36 – 7.32 (m, 1H), 7.29 – 7.19 (m, 2H), 5.36 (t, *J* = 5.1 Hz, 1H), 4.25 – 4.08 (m, 2H), 4.03 – 3.94 (m, 1H), 3.91 – 3.78 (m, 1H), 1.26 (t, *J* = 7.1 Hz, 3H). **<sup>13</sup>C NMR (100 MHz, CDCl<sub>3</sub>)** δ 165.76, 148.20, 139.27, 137.64, 135.25, 133.35, 132.50, 132.30, 129.86, 129.69, 124.47, 124.45, 122.62, 121.49, 118.95, 110.68, 61.11, 42.09, 28.12, 14.29. **ESI-MS:** calculated [C<sub>22</sub>H<sub>17</sub>NO<sub>2</sub>S + H]<sup>+</sup>: 360.1053, found: 360.1055. [α]<sup>20</sup><sub>D</sub> = -34.2 (c = 1.15, CH<sub>2</sub>Cl<sub>2</sub>). The product was analyzed by HPLC to determine the enantiomeric excess: 90% ee (CHIRALPAK IA, hexane/i-PrOH =90/10, detector: 254 nm, T = 30 °C, flow rate: 1 mL/min), t<sub>1</sub>(minor) = 15.32 min, t<sub>2</sub>(major) = 18.83 min.

#### Ethyl (*R*)-8-bromo-1-(4-cyanophenyl)-1,4-dihydrodibenzo[b,d]thiophene-2-carboxylate (6c)


 Step 1: 60 h; Step 2: 8 h (Silica gel 500 mg); Total yield: 23.7 mg (54%); **<sup>1</sup>H NMR (400 MHz, CDCl<sub>3</sub>)** δ 7.61 (d, *J* = 8.5 Hz, 1H), 7.56 – 7.50 (m, 3H), 7.41 (d, *J* = 8.3 Hz, 2H), 7.37 – 7.29 (m, 2H), 5.30 (t, *J* = 5.1 Hz, 1H), 4.30 – 4.08 (m, 2H), 4.04 – 3.91 (m, 1H), 3.90 – 3.77 (m, 1H), 1.26 (t, *J* = 7.1 Hz, 3H). **<sup>13</sup>C NMR (100 MHz, CDCl<sub>3</sub>)** δ 165.55, 139.30, 137.86, 135.38, 134.93, 132.45, 132.40, 129.72, 129.15, 127.52, 124.24, 123.91, 118.86, 118.56, 110.95, 61.19, 41.89, 28.09, 14.28. **ESI-MS:** calculated [C<sub>22</sub>H<sub>16</sub>BrNO<sub>2</sub>S + H]<sup>+</sup>: 438.0158, found: 438.0164. [α]<sup>20</sup><sub>D</sub> = -100.3 (c = 0.74, CH<sub>2</sub>Cl<sub>2</sub>). The product was analyzed by HPLC to determine the enantiomeric excess: 91% ee (CHIRALPAK IA, hexane/i-PrOH =90/10, detector: 254 nm, T = 30 °C, flow rate: 1 mL/min), t<sub>1</sub>(minor) = 18.98 min, t<sub>2</sub>(major) = 21.56 min.

#### Ethyl (*R*)-8-chloro-1-(4-cyanophenyl)-1,4-dihydrodibenzo[b,d]thiophene-2-carboxylate (6d)


 Step 1: 60 h; Step 2: 8 h (Silica gel 500 mg); Total yield: 24.2 mg (61%); **<sup>1</sup>H NMR (400 MHz, CDCl<sub>3</sub>)** δ 7.66 (d, *J* = 8.5 Hz, 1H), 7.53 (d, *J* = 8.2 Hz, 2H), 7.42 (d, *J* = 8.2 Hz, 2H), 7.35 (d, *J* = 1.9 Hz, 1H), 7.34 – 7.30 (m, 1H), 7.21 (dd,

*J* = 8.5, 1.9 Hz, 1H), 5.30 (t, *J* = 5.1 Hz, 1H), 4.25 – 4.09 (m, 2H), 4.04 – 3.93 (m, 1H), 3.90 – 3.77 (m, 1H), 1.26 (t, *J* = 7.1 Hz, 3H). **13C NMR** (100 MHz, CDCl<sub>3</sub>) δ 165.45, 147.57, 138.76, 137.24, 135.44, 134.83, 132.34, 132.28, 130.68, 129.63, 129.13, 124.80, 123.48, 121.08, 118.75, 110.83, 61.09, 41.81, 28.02, 14.18. **ESI-MS:** calculated [C<sub>22</sub>H<sub>16</sub>CINO<sub>2</sub>S + H]<sup>+</sup>: 394.0663, found: 394.0667. [α]<sup>20</sup>D = -100.0 (c = 1.01, CH<sub>2</sub>Cl<sub>2</sub>). The product was analyzed by HPLC to determine the enantiomeric excess: 91% ee (CHIRALPAK IA, hexane/*i*-PrOH =90/10, detector: 254 nm, T = 30 °C, flow rate: 1 mL/min), t<sub>1</sub>(minor) = 16.12 min, t<sub>2</sub>(major) = 19.62 min.

### Ethyl (*R*)-7-bromo-1-(4-cyanophenyl)-1,4-dihydrobenzo[b,d]thiophene-2-carboxylate (6e)

Step 1: 60 h; Step 2: 5 h (Silica gel 600 mg); Total yield: 22.5 mg (51%); **1H NMR** (400 MHz, CDCl<sub>3</sub>) δ 7.88 (d, *J* = 1.6 Hz, 1H), 7.51 (d, *J* = 8.2 Hz, 2H), 7.40 (d, *J* = 8.3 Hz, 2H), 7.34 – 7.28 (m, 2H), 7.23 (d, *J* = 8.5 Hz, 1H), 5.31 (t, *J* = 5.2 Hz, 1H), 4.27 – 4.07 (m, 2H), 4.03 – 3.89 (m, 1H), 3.89 – 3.75 (m, 1H), 1.26 (t, *J* = 7.1 Hz, 3H). **13C NMR** (100 MHz, CDCl<sub>3</sub>) δ 165.59, 147.80, 140.74, 136.42, 134.91, 134.03, 132.35, 129.78, 129.48, 127.87, 125.16, 122.53, 118.80, 118.30, 110.89, 61.16, 41.97, 28.01, 14.27. **ESI-MS:** calculated [C<sub>22</sub>H<sub>16</sub>NO<sub>2</sub>S + H]<sup>+</sup>: 438.0158, found: 438.0167. [α]<sup>20</sup>D = -11.8 (c = 0.49, CH<sub>2</sub>Cl<sub>2</sub>). The product was analyzed by HPLC to determine the enantiomeric excess: 94% ee (CHIRALPAK IA, hexane/*i*-PrOH =90/10, detector: 254 nm, T = 30 °C, flow rate: 1 mL/min), t<sub>1</sub>(minor) = 18.73 min, t<sub>2</sub>(major) = 23.81 min.

### Ethyl (*R*)-8-bromo-1-(4-bromophenyl)-1,4-dihydrobenzo[b,d]thiophene-2-carboxylate (6f)

Step 1: 60 h; Step 2: 24 h (Silica gel 600 mg); Total yield: 31.9 mg (65%); **1H NMR** (400 MHz, CDCl<sub>3</sub>) δ 7.61 – 7.52 (m, 2H), 7.37 – 7.29 (m, 3H), 7.25 – 7.23 (m, 1H), 7.19 – 7.14 (m, 2H), 5.21 (t, *J* = 5.1 Hz, 1H), 4.26 – 4.07 (m, 2H), 4.00 – 3.89 (m, 1H), 3.85 – 3.73 (m, 1H), 1.27 (t, *J* = 7.1 Hz, 3H). **13C NMR** (101 MHz, CDCl<sub>3</sub>) δ 165.83, 141.24, 139.57, 137.86, 134.91, 134.07, 133.08, 131.68, 130.61, 129.96, 127.34, 124.52, 123.79, 120.90, 118.45, 61.05, 41.31, 28.06, 14.30. **ESI-MS:** calculated [C<sub>21</sub>H<sub>16</sub>Br<sub>2</sub>O<sub>2</sub>S + H]<sup>+</sup>: 492.9290, found: 492.9296. [α]<sup>20</sup>D = -112.6 (c = 1.00, CH<sub>2</sub>Cl<sub>2</sub>). The product was analyzed by HPLC to determine the enantiomeric excess: 97% ee (CHIRALPAK AD-H, hexane/*i*-PrOH =85/15, detector: 254 nm, T = 30 °C, flow rate: 1 mL/min), t<sub>1</sub>(major) = 8.59 min, t<sub>2</sub>(minor) = 9.49 min.

### Ethyl (*R*)-8-bromo-1-(4-(trifluoromethyl)phenyl)-1,4-dihydrobenzo[b,d]thiophene-2-carboxylate (6g)

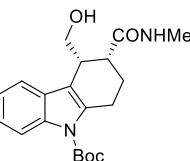
Step 1: 60 h; Step 2: 24 h (Silica gel 600 mg); Total yield: 33.7 mg (70%); **1H NMR** (400 MHz, CDCl<sub>3</sub>) δ 7.61 – 7.54 (m, 2H), 7.49 (d, *J* = 8.2 Hz, 2H), 7.41 (d, *J* = 8.2 Hz, 2H), 7.35 – 7.27 (m, 2H), 5.32 (t, *J* = 5.0 Hz, 1H), 4.28 – 4.07 (m, 2H), 4.05 – 3.92 (m, 1H), 3.89 – 3.75 (m, 1H), 1.26 (t, *J* = 7.1 Hz, 3H). **13C NMR** (100 MHz, CDCl<sub>3</sub>) δ 165.71, 146.27, 139.50, 137.92, 135.19, 134.52, 132.95, 129.74, 129.27

(d,  $J = 32.4$  Hz), 129.23, 127.45, 125.59 (q,  $J = 3.8$  Hz), 124.43, 123.85, 118.54, 61.12, 41.69, 28.13, 14.28.  **$^{19}\text{F}$  NMR (377 MHz,  $\text{CDCl}_3$ )**  $\delta$  -62.45. **ESI-MS:** calculated [ $\text{C}_{22}\text{H}_{16}\text{BrF}_3\text{O}_2\text{S} + \text{H}]^+$ : **481.0079**, found: **481.0090**.  $[\alpha]^{20}\text{D} = -57.1$  ( $c = 0.99$ ,  $\text{CH}_2\text{Cl}_2$ ). The product was analyzed by HPLC to determine the enantiomeric excess: 94% ee (CHIRALPAK AD-H, hexane/*i*-PrOH =85/15, detector: 254 nm, T = 30 °C, flow rate: 1 mL/min),  $t_1$ (minor) = 6.41 min,  $t_2$ (major) = 7.08 min.

#### Ethyl (*R*)-8-chloro-1-phenyl-1,4-dihydrobenzo[b,d]thiophene-2-carboxylate (6h)

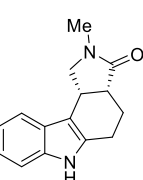
Step 1: 60 h; Step 2: 24 h (Silica gel 600 mg); Total yield: 16.7 mg (45%);  **$^1\text{H}$  NMR (400 MHz,  $\text{CDCl}_3$ )**  $\delta$  7.62 (d,  $J = 8.5$  Hz, 1H), 7.47 (d,  $J = 1.9$  Hz, 1H), 7.32 – 7.27 (m, 2H), 7.26 – 7.10 (m, 5H), 5.24 (t,  $J = 5.1$  Hz, 1H), 4.25 – 4.05 (m, 2H), 4.03 – 3.89 (m, 1H), 3.87 – 3.71 (m, 1H), 1.25 (t,  $J = 7.1$  Hz, 3H).  **$^{13}\text{C}$  NMR (100 MHz,  $\text{CDCl}_3$ )**  $\delta$  166.09, 142.16, 139.43, 137.37, 134.82, 133.67, 130.72, 130.54, 128.94, 128.55, 126.98, 124.55, 123.35, 121.68, 60.92, 41.98, 28.15, 14.27. **ESI-MS:** calculated [ $\text{C}_{21}\text{H}_{17}\text{ClO}_2\text{S} + \text{H}]^+$ : **369.0711**, found: **369.0712**.  $[\alpha]^{20}\text{D} = -109.0$  ( $c = 0.52$ ,  $\text{CH}_2\text{Cl}_2$ ). The product was analyzed by HPLC to determine the enantiomeric excess: 97% ee (CHIRALPAK IA, hexane/*i*-PrOH =90/10, detector: 254 nm, T = 30 °C, flow rate: 1 mL/min),  $t_1$ (minor) = 7.33 min,  $t_2$ (major) = 8.36 min.

#### Tert-butyl(3*R*,4*R*)-4-(hydroxymethyl)-3-(methylcarbamoyl)-1,2,3,4-tetrahydro-9*H*-carbazole-9-carboxylate (7)



**$^1\text{H}$  NMR (400 MHz,  $\text{CDCl}_3$ )**  $\delta$  8.10 (d,  $J = 8.1$  Hz, 1H), 7.47 (d,  $J = 7.3$  Hz, 1H), 7.25 – 7.13 (m, 2H), 6.08 (brs, 1H), 4.01 (dd,  $J = 12.0, 8.1$  Hz, 1H), 3.79 (d,  $J = 10.7$  Hz, 1H), 3.70 (brs, 1H), 3.41 (s, 1H), 3.27 (dd,  $J = 18.4, 5.8$  Hz, 1H), 2.95 – 2.82 (m, 4H), 2.65 – 2.56 (m, 1H), 2.42 – 2.27 (m, 1H), 2.08 – 1.99 (m, 1H), 1.66 (s, 9H).  **$^{13}\text{C}$  NMR (100 MHz,  $\text{CDCl}_3$ )**  $\delta$  177.26, 150.61, 136.11, 135.70, 128.41, 123.89, 122.83, 117.66, 116.02, 115.76, 83.91, 62.69, 44.39, 38.03, 28.40, 26.72, 25.55, 22.34. **ESI-MS:** calculated [ $\text{C}_{20}\text{H}_{26}\text{N}_2\text{O}_4\text{S} + \text{H}]^+$ : **359.1965**, found: **359.1966**. The product was analyzed by HPLC to determine the enantiomeric excess: 92% ee (CHIRALPAK IA, hexane/*i*-PrOH =95/5, detector: 254 nm, T = 30 °C, flow rate: 1 mL/min),  $t_1$ (minor) = 17.88 min,  $t_2$ (major) = 19.27 min.

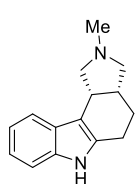
#### (3*aR*,10*cR*)-2-methyl-1,3*a*,4,5,6,10*c*-hexahydropyrrolo[3,4-*c*]carbazol-3(2*H*)-one (8)



**$^1\text{H}$  NMR (400 MHz,  $\text{CDCl}_3$ )**  $\delta$  8.39 (brs, 1H), 7.43 (d,  $J = 7.6$  Hz, 1H), 7.30 (d,  $J = 7.8$  Hz, 1H), 7.12 (m, 2H), 4.62 – 4.36 (m, 2H), 3.89 – 3.76 (m, 1H), 3.22 – 3.08 (m, 1H), 2.96 (s, 3H), 2.92 – 2.80 (m, 1H), 2.70 – 2.57 (m, 1H), 2.41 – 2.27 (m, 1H), 2.10 – 1.95 (m, 1H).  **$^{13}\text{C}$  NMR (100 MHz,  $\text{CDCl}_3$ )**  $\delta$  165.58, 136.06, 135.49, 126.71, 121.58, 119.61, 117.60, 111.03, 107.64, 73.59, 39.37, 34.85, 34.12, 22.31, 19.60. **ESI-MS:** calculated [ $\text{C}_{15}\text{H}_{16}\text{N}_2\text{O} + \text{H}]^+$ : **235.1335**, found: **235.1331**. The product was analyzed by HPLC to determine the enantiomeric excess: 92% ee (CHIRALPAK

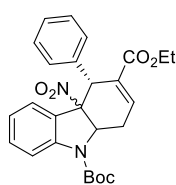
AD-H, hexane/*i*-PrOH =90/10, detector: 254 nm, T = 30 °C, flow rate: 1 mL/min), t<sub>1</sub>(minor) = 7.48min, t<sub>2</sub>(major) = 8.71 min.

**(3a*R*,10*cR*)-2-methyl-1,2,3,3*a*,4,5,6,10*c*-octahydropyrrolo[3,4-*c*]carbazole (9)**



**<sup>1</sup>H NMR (400 MHz, DMSO)** δ 10.66 (s, 1H), 7.40 (d, *J* = 7.6 Hz, 1H), 7.23 (d, *J* = 7.8 Hz, 1H), 7.01 – 6.86 (m, 2H), 3.62 – 3.52 (m, 2H), 3.25 – 3.14 (m, 1H), 2.76 – 2.58 (m, 4H), 2.31 (s, 3H), 2.17 – 2.04 (m, 1H), 1.83 – 1.65 (m, 2H). **<sup>13</sup>C NMR (100 MHz, DMSO)** δ 136.10, 135.00, 126.92, 120.01, 118.10, 117.29, 110.67, 109.71, 61.79, 54.49, 37.08, 35.72, 23.31, 22.69. **ESI-MS:** calculated [C<sub>15</sub>H<sub>18</sub>N<sub>2</sub> + H]<sup>+</sup>: 227.1543, found: 227.1541. The product was analyzed by HPLC to determine the enantiomeric excess: 92% ee (CHIRALPAK AS-H, hexane/*i*-PrOH =70/30, detector: 254 nm, T = 30 °C, flow rate: 1 mL/min), t<sub>1</sub>(major) = 5.49min, t<sub>2</sub>(minor) = 9.67 min.

**9-(Tert-butyl) 3-ethyl (4*R*)-4*a*-nitro-4-phenyl-1,4,4*a*,9*a*-tetrahydro-9*H*-carbazole-3,9-dicarboxylate (10)**



Total yield: 34.6 mg (74%); **<sup>1</sup>H NMR (400 MHz, Acetone)** δ 7.92 – 7.49 (m, 2H), 7.44 (t, *J* = 7.7 Hz, 1H), 7.40 – 7.26 (m, 5H), 7.19 – 7.12 (m, 2H), 5.86 (d, *J* = 8.5 Hz, 1H), 5.45 (s, 1H), 4.16 – 4.03 (m, 2H), 3.74 – 3.49 (m, 1H), 2.70 (d, *J* = 18.6 Hz, 1H), 1.61 (s, 9H), 1.17 (t, *J* = 7.4 Hz, 3H). **<sup>13</sup>C NMR (100 MHz, Acetone)** δ 171.38, 165.60, 140.51, 138.62, 133.33, 131.59, 130.08, 129.90, 129.30, 126.01, 124.73, 116.84, 62.03, 61.02, 59.69, 45.78, 34.27, 28.94, 21.33, 14.98, 14.81. **ESI-MS:** calculated [C<sub>26</sub>H<sub>28</sub>N<sub>2</sub>O<sub>6</sub> + Na]<sup>+</sup>: 487.1845, found: 487.1869. [α]<sup>20</sup><sub>D</sub> = -246.5 (c = 0.45, CH<sub>2</sub>Cl<sub>2</sub>). The product was analyzed by HPLC to determine the enantiomeric excess: 94% ee (CHIRALPAK IA, hexane/*i*-PrOH =99/1, detector: 254 nm, T = 30 °C, flow rate: 1 mL/min), t<sub>1</sub>(major) = 12.93 min, t<sub>2</sub>(minor) = 19.06 min.

**Supplemental References**

- Cheng, Q., Zhang, F., Cai, Y., Guo, Y.-L., and You, S.-L. (2018). Stereodivergent synthesis of tetrahydrofuroindoles through Pd-catalyzed asymmetric dearomatic formal [3+2] cycloaddition. *Angew. Chem. Int. Ed.* **57**, 2134-2138.
- Cheng, Q., Zhang, H.-J., Yue, W.-J., You, S.-L. (2017). Palladium-catalyzed highly stereoselective dearomatic [3 + 2] cycloaddition of nitrobenzofurans. *Chem* **3**, 428-436.
- Tran, Y. S., and Kwon, O. (2007). Phosphine-catalyzed [4 + 2] annulation: synthesis of cyclohexenes. *J. Am. Chem. Soc.* **129**, 12632-12633.